DEVELOPING ANTIMICROBIAL BIOMEDICAL DEVICE SURFACES VIA TUNABLE NITRIC OXIDE RELEASE AND SYNERGY WITH ANTIFOULING INTERFACES

by

MANJYOT KAUR CHUG

(Under the Direction of ELIZABETH J. BRISBOIS)

ABSTRACT

Biomedical devices are often targeted by bacteria leading to biofilm development and device-associated infections. Infections arising from biomedical devices not only exhibit detrimental effects which severely impact the quality of life for patients, but also bar advancements in the healthcare system by significantly increasing the cost of treatment. Each year >1 million people are affected by medical device-associated infections in the United States alone. The complex nature of bacterial biofilm, increasing bacterial resistance to conventional antibiotics, and failure of current hospital regimens to treat infections are one of the several factors that result in a continuous escalation of medical device-associated infections. The antimicrobial efficacy of polymeric medical devices is greatly reliant upon the deterrence of the first step of biofilm formation. This can be attained by preventing the bacteria from attaching to the surface of a medical device. Therefore, strategies that can prevent or eradicate life-threatening infections are urgently needed to thwart the occurrence of bacterial infections. Nitric oxide (NO) is a diatomic gaseous molecule endogenously synthesized by the body via nitric oxide synthase (NOS) enzymes and regulates several important functions such as pathogen invasion, wound healing, and prevention of platelet activation. Various NO donor molecules have been designed by researchers that can be exogenously utilized to emulate the physiological roles of NO in biomaterials and medical device materials. Materials with NO-releasing properties have been

demonstrated to eradicate pathogenic bacteria and inhibit the attachment of viable bacteria on the surface. However, NO-releasing materials have historically faced the challenges of uncontrolled NO release, thermal instability of NO donors during the polymer fabrication process, limited shelf-life at room temperature, and inability to prevent biofouling. This dissertation is focused on developing NO-releasing antibacterial medical devices using additive manufacturing and photosensitivity of NO donors to regulate the NO release from medical device surfaces, combined effect with other active antibacterial drugs such as chlorhexidine to improve efficacy and evaluate synergy with slippery surface technology to prevent biofouling on biomedical devices. These approaches hold great potential to enhance biocompatibility and antimicrobial properties of biomedical surfaces and improve their efficiency in the patient care setting.

INDEX WORDS: Biomedical devices, Antimicrobial, Antifouling, Controlled release, Nitric oxide

DEVELOPING ANTIMICROBIAL BIOMEDICAL DEVICE SURFACES VIA TUNABLE NITRIC OXIDE RELEASE AND SYNERGY WITH ANTIFOULING INTERFACES

by

MANJYOT KAUR CHUG

MSc, Birla Institute of Technology and Science (BITS)-Pilani, Hyderabad, India, 2016

A Dissertation Submitted to the Graduate Faculty of The University of Georgia in Partial Fulfillment of the Requirements for the Degree

DOCTOR OF PHILOSOPHY

ATHENS, GEORGIA

2022

DEVELOPING ANTIMICROBIAL BIOMEDICAL DEVICE SURFACES VIA TUNABLE NITRIC OXIDE RELEASE AND SYNERGY WITH ANTIFOULING INTERFACES

by

MANJYOT KAUR CHUG

Major Professor:	Elizabeth J. Brisbois
Committee:	Hitesh Handa
	Ramana Pidaparti
	Eric Freeman
	Benjamin Brainard

Electronic Version Approved:

Ron Walcott
Vice Provost for Graduate Education and Dean of the Graduate School
The University of Georgia
December 2022

DEDICATION

This dissertation is wholeheartedly dedicated to my family for their unwavering love and support throughout my life.

ACKNOWLEDGEMENTS

The journey of PhD has been a roller coaster from one city to another bringing numerous rides. Words cannot express my gratitude to my mentor Dr. Elizabeth Brisbois who has played a very instrumental role in shaping me as a doctoral student with her invaluable patience and feedback. I am deeply indebted to my committee members – Dr. Hitesh Handa, Dr. Benjamin Brainard, Dr. Eric Freeman, and Dr. Ramana Pidaparti for providing their generous knowledge and expertise. Thanks to all my co-authors for helping me finish the projects. This endeavor would not have been possible without Brisbois and Handa Lab members and colleagues who offered valuable collaborations and support: Patrick Maffe, Dr. Arnab Mondal, Aasma Sapkota, Dr. Vijay Gondil, Dr. Jitendra Pant, Dr. Megan Douglass, Dr. Ryan Devine, Dr. Sama Ghalei, Lori Estes-Bright, Mark Garren, Divine Francis, Lauren Griffin, Rashmi Pandey, Grace Nguyen, Yi Wu, Sarah Wilson, Stephen Thompson, Natalie Crutchfield, Tushita Jain, Dr. Morgan Ashcraft, Vicente Pinon, Tia Shorter, Dr. Ken Gall, Emilio Bachtiar, Dr. Anil Kumar, Dr. Ekrem Ozkan, Corbin Feit, Alexis Rivera, Nick Narwold, Cole Bousquet, Gabrielle Aluisio, and Emma Tharp. It has been a real pleasure working with such an influential and motivating group. I am also grateful to my funding sources NIH, JDRF, UGA, and UCF who supported my research. Lastly, I would be remiss in not mentioning my family and friends, especially my parents, Dr. Gurnam Singh Chugh, and Simran Kaur, Didi, Jiju, Gurnidh, Dr. Ishneet Kaur Banga, Shanti Modi, Dilip Kunderu, Tanmaye Nallan, Shreya Kumar, and other friends and family members for their prayers, unconditional love, motivation, and emotional support. Their confidence in me has kept my spirits high during this journey. I feel extremely fortunate to have so many loving and positive people in my life who supported me during highs and lows helping me grow both personally and professionally.

TABLE OF CONTENTS

LIST OF TABLES

LIST OF FIGURES

Page

CHAPTER 1:

INTRODUCTION - RECENT DEVELOPMENTS IN MULTIFUNCTIONAL ANTIMICROBIAL SURFACES AND APPLICATIONS TOWARDS ADVANCED NITRIC OXIDE BASED BIOMATERIALS

[1] Chug, M. K., & Brisbois, E. J. (2022). Recent Developments in Multifunctional Antimicrobial Surfaces and Applications toward Advanced Nitric Oxide-Based Biomaterials. *ACS Materials Au*, *2*(5), 525-551.

1.1 Medical Device Associated Infections and Challenges with Bacteria

A large population in the world depends on biomedical devices such as stents, catheters, prosthetic joints and meshes, pacemakers, vascular grafts, endotracheal tubes, and orthopedic devices.[1-3] Although medical devices are beneficial to people with various types of diseases and health conditions, the proliferation of bacteria on the surface of these devices is a prevalent global problem.[4] Bacterial pathogens have become a severe threat by causing infectious diseases that lead to high morbidity and mortality worldwide and are the main cause of biomedical device-associated infections such as catheter-related bloodstream infections (CRBSIs), catheter-associated urinary tract infections (CAUTI), and ventilator-associated pneumonia (VAP) (**Figure 1.1**).[2, 5] Approximately 687,000 were affected by a hospital-acquired infection (HAI) in 2015.[6] More than 72,000 patient deaths were caused by HAIs in the United States, out of which >25% are related to implanted medical devices.[7] Infections associated with medical implants often lead to post-surgical complications that require removal and replacement of the infected implant leading to increased healthcare costs to patients and hospitals while increasing the rate of infection.[2] The widespread use of antibiotics has led to the prevalence of drug-resistant bacteria that are more dangerous and life-threatening because they are difficult to treat.[2] The most common pathogenic drug-resistant bacteria in biomedical device-associated infections are methicillin-resistant *Staphylococcus aureus* (MRSA) and vancomycin-resistant *Enterococcus* (VRE) which account for a large number of healthcare-related infections per year, resulting in increased morbidity, risk of mortality, and a severe financial burden.[1] It is estimated by the O'Neill commission that antimicrobial resistance will cost $100 trillion and over 10 million lives will be lost by 2050, making multidrug-resistant bacteria a major problem to the economy and public health.[5] Biomedical device-associated infections occur when planktonic bacterial cells attach to the surface of a biomedical device and form a multilayered biofilm from both Gram-positive and Gram-negative bacteria including *Enterococcus faecalis*, *Staphylococcus aureus*, *Staphylococcus*

epidermidis, *Streptococcus viridans*, *Escherichia coli*, *Klebsiella pneumoniae*, *Proteus mirabilis*, and *Pseudomonas aeruginosa*.[2, 8, 9] Biofilms are formed when planktonic bacteria adhere to an organic or inorganic surface and produce an extracellular polymeric substance (EPS) that is composed of proteins and other extracellular polymers **(Figure 1.2A)**.[2]

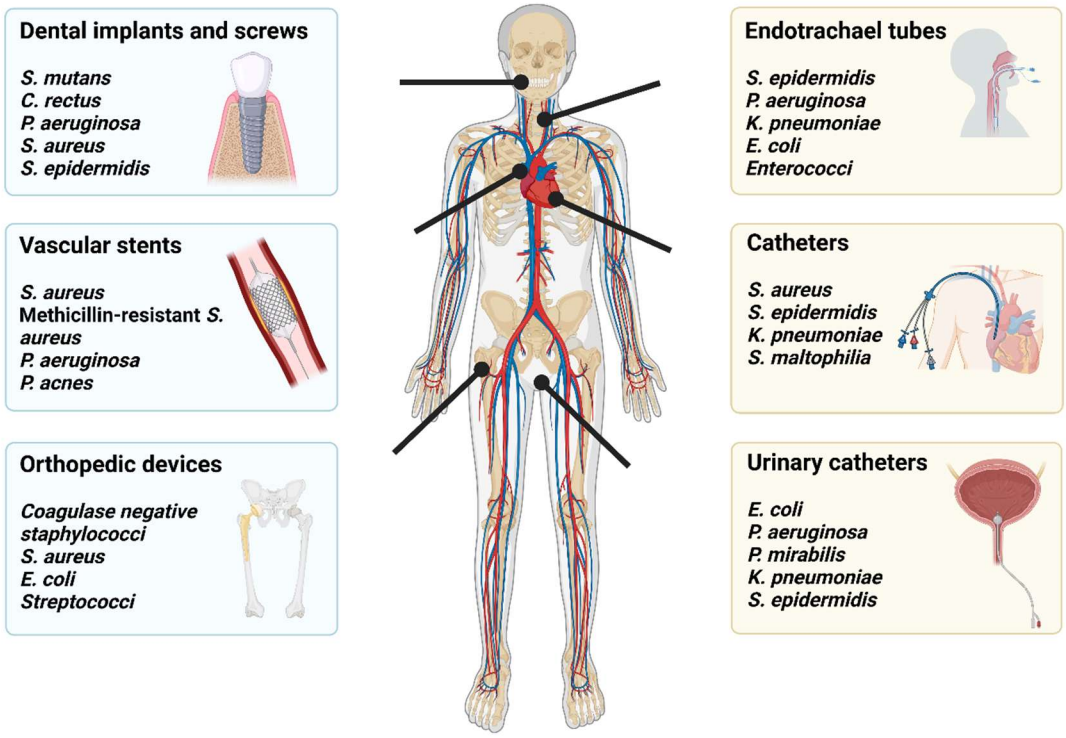

Figure 1.1 Examples of microbial species frequently responsible for causing biomedical device-associated infections that arise from various implantable and indwelling medical devices. This includes both short- and long-term devices including dental implants, endotracheal tubes, vascular and peritoneal catheters, vascular stents, urinary catheters, and fracture fixation devices. The 3 most common infections arising from medical devices include: Catheter Related Blood Stream Infections (CRBSIs), Catheter Associated Urinary Tract Infections (CAUTI), and Ventilator Associated Pneumonia (VAP). These are indicated by yellow boxes on the right.

The formation of biofilm can be considered as bacteria's defense mechanism to survive in a hostile setting and colonize new substrates. The bacteria protected within the EPS matrix largely vary in their genetic composition compared to free-floating planktonic bacteria which makes them resistant to conventional antibiotic agents. These bacterial species deeply embedded in the

biofilm require 1000X more dosage of antibiotic treatment as opposed to free-floating planktonic cells as not all antimicrobial agents can penetrate deeper into the matrix.[10] This high amount of drug increases the issues of antibiotic resistance in bacteria, leads to higher healthcare costs, and can be cytotoxic to other healthy cells or tissues.[11, 12] Dental plaque, upper respiratory tract infections, peritonitis, and urogenital infections are examples of medical conditions that are associated with biofilms and often have an increased resistance to antimicrobial agents.[8] The interface between a medical device and the surrounding physiological environment (e.g., urine, saline, blood, tissues, etc.) offers a suitable environment for the bacteria to attach and proliferate on the surface. The development of biofilm on the device surface is heavily influenced by the physical characteristics of medical device surfaces such as surface roughness, hydrophobicity, surface charge, and bacterial membrane charge appear to govern bacterial adhesion and subsequent biofilm formation.[6, 13] The complexity of biofilm increases with the presence of diverse microbial species, antibiotic resistant genes, virulence factors, etc. which all makes eradication of bacteria in biofilm a very challenging task.

Biofilm infections are difficult to eliminate because the EPS allows bacterial cells to proliferate while providing the necessary environment to protect bacterial colonies from immunologic defense systems, nutrient limitations, and antibacterial agents.[2, 4, 14] Infections can then spread by the detachment of bacterial cells from mature biofilms.[13] Furthermore, the accumulation of biofilms on a surface can impede the function, durability, and usability of medical devices and implants.[4, 15] To solve these issues, significant attempts have been targeted toward creating antibacterial surfaces that can considerably lower the scope of preliminary microbial attachment, and thus prevent the consequent biofilm development. These include generating bactericidal surfaces with an active killing mechanism or by creating an antifouling interface for preventing bacterial adhesion on the device surface **(Figure 1.2B)**.[16] Active antibacterial mechanisms kill bacteria on contact once the bacteria adhere to the surface. Polymers with an active mechanism

are functionalized with cationic biocides, antimicrobial peptides, antibiotics, silver metal or nanoparticles, salts, or antimicrobial agents (see **Table 1.1**).[14, 17] Quaternary ammonium compounds (QACs) are an example of an active agent investigated for antimicrobial coatings. These compounds disrupt the negatively charged bacterial cell surface which leads to microbe death by exerting strong electrostatic interactions with long cationic polymeric chains that penetrate the bacterial cell membrane.[3, 18] Antimicrobial peptides (AMPs) exhibit antimicrobial properties that have been effective against both Gram-positive and Gram-negative bacteria, fungi, viruses, and unicellular protozoa; several AMPs can indirectly promote pathogen clearance by modulating the immune response of the host **(Figure 1.2C)**.[19] Metal-based nanoparticles such as silver nanoparticles (AgNPs) have emerged as a strong approach to developing robust antibacterial surfaces.[20] The relatively smaller size of these particles along with a higher surface-to-volume ratio allows them to create a strong interaction with the outer membrane resulting in significant antibacterial action. Materials with AgNPs exhibit non-specific antibacterial activity as there is no one specific receptor that these particles target. These characteristics make it more difficult for bacteria to develop resistance to the antibacterial mechanisms.[21] In contrast, antifouling coating materials such as polyethylene glycol (PEG), poly(N-vinylpyrrolidone) (PVP), PEG-based copolymers, zwitterionic materials, and biomimetic materials such as polysaccharides, cell membrane mimicking strategies, slippery liquid infused porous surfaces (SLIPs) and topographical patterns on the surface have been reported to reduce or inhibit the biofouling of microbes on biomaterial interfaces (see **Table 1.2**).[17, 22]

Table 1.1 Classification of single antimicrobial surface and their mode of action

Material Classification	Example Compounds	Action
Cationic Biocides	Quaternary ammonium compounds (QACs)	Disrupts microbial membrane through strong electrostatic interactions with the negatively charged bacterial cell surface.

	Chlorhexidine	Disrupts the bacteria cell membrane by binding to the negatively charged cell wall and displacing the stabilizing calcium ions.
Antimicrobial Enzymes	Acylase	Quorum quenching enzyme cleaves the amide bond of acyl-homoserine lactones.
	Lysozyme	A hydrolytic enzyme that can catalyze the hydrolysis of β-(1–4) glycoside bonds between N-acetyl-muramic acid and N-acetyl-glucosamine in the cell wall peptidoglycan layer.
Antimicrobial Peptides (AMPs)	Human beta-defensin 3	Formation of transmembrane pores and inhibition of cell wall formation and other essential parts of bacterial physiology.
	LL-37	
	Dermcidin	
Antibiotics	β-lactams	Disrupts synthesis of peptidoglycan.
	Glycopeptides	Inhibits cell wall synthesis.
	Aminoglycosides	Inhibits protein synthesis through hydrogen bond interactions with the 16S rRNA of the 30S subunit.
	Quinilones	Inhibits DNA replication by inhibiting bacterial DNA gyrase.
	Sulfonamides and trimethoprim	Inhibit folic acid metabolism.
Metals	Ag ions	Penetration of Ag ions into bacterial cells hinders DNA replication. Ag ions bind to proteins with the sulfhydryl group (–SH) which leads to a decrease/loss of enzyme activity.
	Silver nanoparticles (AgNPs)	AgNPs inhibit cell proliferation by causing oxidative stress to damage proteins and nucleic acids through the generation of reactive oxygen species (ROS).
	Copper ions	Generation of reactive oxygen species (ROS) makes Cu ions toxic to microbial cells.
	Copper nanoparticles (CuNPs)	CuNPs kill bacteria by forming stable complexes with vital enzymes inside the cell which impede cellular function.
	Zinc oxide nanoparticles (ZnONPs)	ZnONPs permeate into the cell membrane which damages lipids, carbohydrates, proteins, and DNA through oxidative stress. Vital cellular functions are disrupted by alteration of the cell membrane caused by lipid peroxidation.
Nitric Oxide Donors	*S*-Nitroso-*N*-acetylpenicillamine (SNAP)	Highly reactive with superoxide radical to generate peroxynitrite resulting in

	S-Nitrosoglutathione (GSNO)	cellular oxidative stress. The oxidation causes the modification of protein functionality and DNA strands and damage to cell membranes. Direct nitrosation of cysteine thiols groups in proteins by the NO radical can also readily alter the protein functionality and lead to cell stasis or death.
	N-Diazeniumdiolates	

Table 1.2 Classification of single antifouling surfaces and their mode of action

Material Classification	Example Compounds	Action
Hydrophilic Polymers	Polyethylene glycol (PEG)	Large exclusion volume, chain flexibility, and steric hindrance of hydrated layer reduce protein and bacterial attachment.
	Poly(N-vinylpyrrolidone) (PVP)	Low protein adsorption compared to PEG-modified surfaces.
Zwitterionic Materials	Zwitterionic polymers and polymer brushes	Contains distinct chemical structures of anionic and cationic groups incorporated into the polymer structure that induces functionalities like antifouling abilities that can be controlled by adjusting the polymer charge density, pH sensitivity, and counterion association. Zwitterionic polymer brushes have a strong water association ability that reduces nonspecific protein adsorption, cells, and bacteria.
Biomimetic Materials	Polysaccharides	Polysaccharides are highly hydrophilic and able to form water-storing hydrogels with antifouling properties.
	Cell membranes-inspired materials	Forms a structure that mimics the cell's outer membrane to prevent fouling.
	Slippery liquid-infused porous surfaces (SLIPs)	Uses capillary forces to reduce the surface adsorption and generates a low adhesion interface between material and contacting liquid.
Nano-micro Patterned Surfaces	Nano-micro pillars, square-shaped patterns	Alters total surface area and surface wetness of the substrate. Affects cellular signaling, cell membrane expression, and the function of bacterial flagella.

Polymers with an antifouling mechanism are generally hydrophilic, negatively charged, or have a low surface free energy which reduces protein adsorption and negates the hydrophobic and negatively charged properties of bacteria.[17] PEG is one of the commonly used antifouling materials and it inhibits biofilm formation by resisting protein and polysaccharide adsorption on surfaces due to its high chain mobility, large exclusion volume, and the steric hindrance effect of the highly hydrated layer.[17, 23] Zwitterionic materials are neutrally charged due to an equal amount of positive and negative charges on the same molecule that are used for antifouling applications. Zwitterionic polymers can be formed with low molecular weight polymers that bind water molecules more strongly than PEG resulting in a protective layer that increases the antifouling effect.[22, 24] Slippery liquid infused porous surfaces (SLIPs) are comprised of Food & Drug Administration (FDA) approved silicone oil to mimic the mucus production in the gastrointestinal tract and provide an ultralow fouling surface that prevents protein adsorption and bacterial adhesion.[25] Topographical patterns with nano-microstructures can obstruct the adhesion and interaction of bacteria in their collaborative work of developing EPS and biofilm on surfaces.

1.2 Challenges with Monofunctional Approaches

Many reports have confirmed the limitations of exclusive antibacterial or antifouling coating in hindering biofouling and biofilm formation. Adsorption of proteins, cells, or microorganisms on the surfaces of implanted biomedical devices poses a significant danger to human health.[24] Antifouling surfaces do not kill microorganisms, but instead prevent adhesion through physical mechanisms.[26] Although antibacterial and antifouling mechanisms are effective methods to fight against infections, there are disadvantages to utilizing a single antibacterial or antifouling mechanism. Antifouling coatings can prevent bacterial adhesion on the surface up to a certain degree. However, they do not possess the ability to kill bacteria directly **(Figure 1.3).**[14, 27]

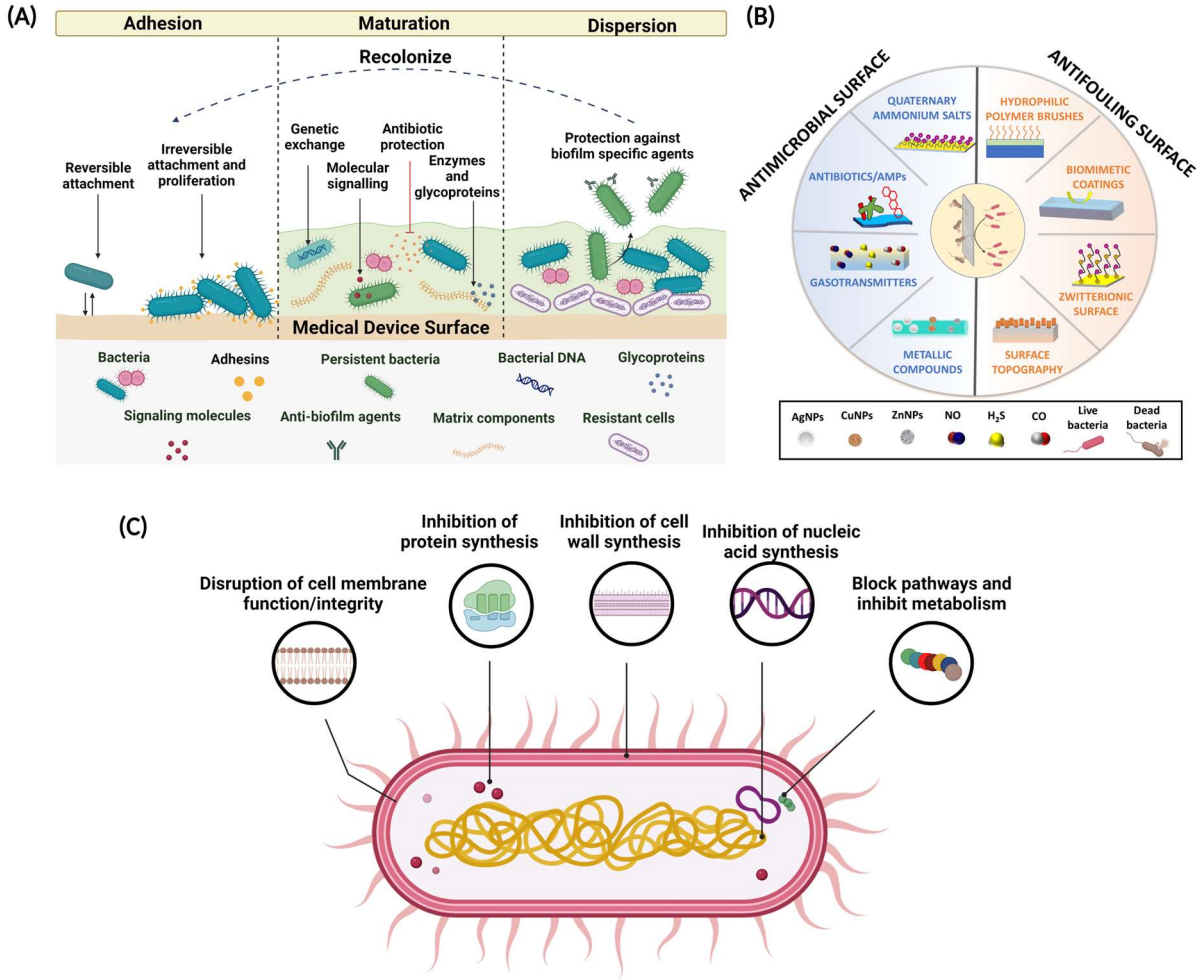

Figure 1.2 (A) Progression of biofilm formation and proliferation on a medical device surface. **(B)** Types of active and passive mechanisms used in the development of biomedical device surfaces. **(C)** The five common active killing mechanisms of antimicrobial biomaterials utilizing agents such as antibiotics, antimicrobial peptides, quaternary ammonium compounds, nitric oxide, and metallic nanoparticles to kill and eradicate bacteria on these surfaces.

Functionalization of a surface with antifouling surface chemistry can also be compromised by the reactive physiological environment, leading to failure of the antifouling mechanisms (e.g., patches of altered chemistry) where bacteria can begin attaching and forming biofilm after prolonged implantation time. To date, not one surface has been reported that can attain 100% prevention of microbial infections in clinical applications.

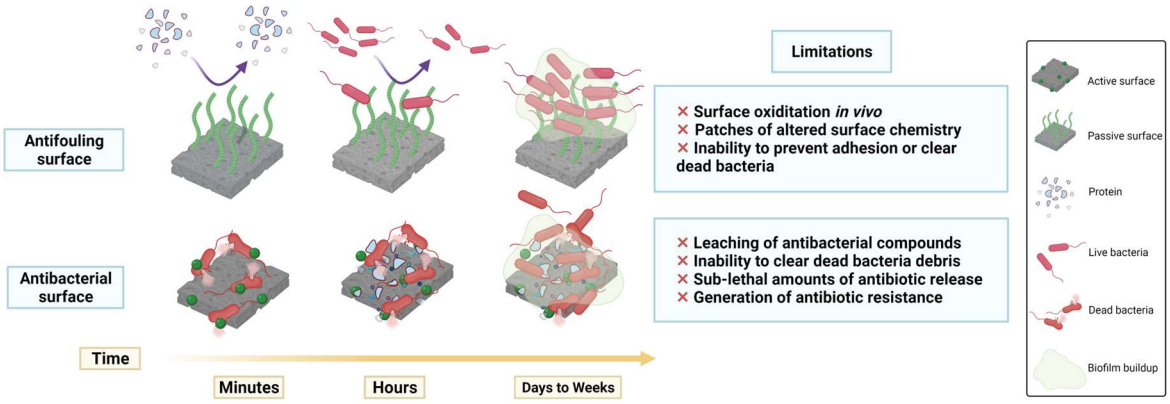

Figure 1.3 Progression of biofilm formation and proliferation on a medical device surface and failure of a singular approach to fully prevent infection on biomaterial surfaces. A passive surface can prevent or reduce the initial attachment of bacteria. However, material chemistry can significantly change upon exposure to the physiological environment which can lead to failure of the antifouling materials chemistry. Ultimately, the bacteria are able to breach the altered surface, colonize and form biofilm. Active surface with contact-based killing succumbs to fouling from dead bacteria debris and proteins. However, the release of active agents from these biomaterials continues to eradicate pathogens until the source of the active agent becomes depleted. Both single-mechanism active and passive surfaces lead to eventual biofilm formation in long-term applications.

While surfaces with active mechanisms can directly kill bacteria, they do not have the ability to release the dead bacteria and other biofoulants accumulated on surfaces. In long-term applications, other live pathogens can use this debris as a substrate to colonize the surface which can conceal the active moieties and reduce the efficacy of the device **(Figure 1.3).**[27] For example, the positively charged nature of QACs reduces antimicrobial efficacy by increasing protein adsorption and the accumulation of dead bacteria on the surface blocking the influence of antibacterial compounds that will lead to biofilm formation.[14] Cytotoxicity from high dose requirements, a narrow antimicrobial spectrum, and implications for propagating multidrug resistance are other potential drawbacks of compounds with a singular active mechanism.[14] Thus, with the great sense of necessity to produce a multi-functionalized material, integration of active surfaces having broad-spectrum antibacterial and antifouling functionalities are widely reported.[28, 29] Materials with the combination of multiple antibacterial mechanisms are expected to show synergy and provide a stronger combined defense against medical device infections.

Over the past few years, surfaces with multiple active components have been integrated into a single biomaterial interface using methods of tethering an active agent with a substrate embedded with an active antibacterial compound, two active antibacterial compounds embedded in the substrate, or light-sensitive compounds added to a conventional antibacterial agent. Many studies in the literature have reported approaches to combine dual active bactericidal surfaces that can help lower the microbial burden on medical devices. Such methods involve combinations of antimicrobial components such as QACs, metal nanoparticles (Cu, Zn, Ag), antibiotic and antimicrobial coated/impregnated materials (chlorhexidine, silver sulfadiazine, rifampicin, gentamicin, etc.)[30-33], and nitric oxide (NO)-releasing therapeutic strategies.[34-37] Some of the materials with dual active strategies that involve combination of two antibiotics have been successfully translated to pre-clinical stages.[31] For instance, indwelling catheters with chlorhexidine and silver sulfadiazine are commercially available and are at present used in patients to combat bacterial infections arising from biomedical devices. However, infections on medical devices are continuing to rise because these surfaces 1) lack antifouling mechanisms to prevent microbial adhesion and 2) the material surface is left vulnerable after the eventual depletion of active antimicrobial agents over time.[38] Therefore, these limitations have motivated researchers to integrate antibacterial (bacteria-killing) and antifouling (bacteria/fouling-resistant) strategies into one substrate with broad-spectrum antimicrobial activity and mechanisms to discourage further bacterial adhesion and biofilm formation on the surface (see **Table 1.3**).

1.3 Antimicrobial Surfaces with Dual Antibacterial and Antifouling Strategy

1.3.1 Hydrophilic Polymer Brush-based Coatings

To lower the bacterial attachment on the device surface, three important surface strategies have been extensively explored in the field of materials engineering to transform the hydrophilicity, hydrophobicity, and charge of the desired material (**Figure 1.4**). The other approaches include altering the surface topography through nano and micro patterns and changing the surface

architecture through the introduction of polymer brushes. These brushes can be tuned by adjusting the thickness, mobility, and density of the brushes on the surface. Chemical modification of surfaces with polymer brushes can enhance the antibacterial properties of materials. Hydrophilic cationic polymer brushes exhibit antifouling properties that influence the adhesion of microorganisms, proteins, and cells to a surface.[39-41] Employing antifouling polymer chains on a surface is a very valuable synthetic approach, as it lets widespread tuning of the surface properties merely by modifying the makeup, functionality, or structural design of the tethered polymer brushes. Regulating the surface-wetting properties, inhibition of non-specific binding of biomolecules, colloidal stabilization, and resistance to fouling are all examples of successful application of polymer brushes. Notably, these polymer brushes can be functionalized on a range of materials with secondary antibacterial functions arising from antibiotics, nanoparticles, peptides, or zwitterion molecules to counteract implant-associated infections. [42-46] These surfaces are of particular significance because they can minimize the selection and propagation of resistant microbes, supporting persistent antibacterial efficacy.

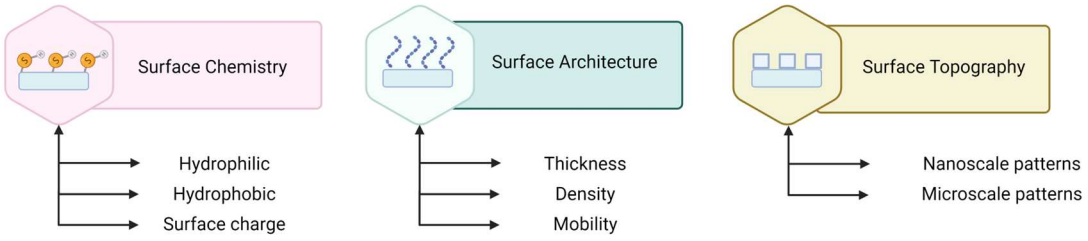

Figure 1.4 Three main surface modification techniques to create an antifouling interface on biomedical materials. This includes surface chemistry, surface architecture and surface topography.

Early studies on the development of dual-functional antimicrobial surfaces involved contact-active antibacterial and antifouling multifunctional coatings containing PEG with anchored antibiotics (penicillin, ampicillin, vancomycin).[47] These coatings could be easily applied on biomedical materials surfaces like PDMS, stainless steel, TiO_2, PTFE, and PP using microwave

plasma and chemical reactions to adjust the surface energy, roughness, and reactivity of the material surface.[48, 49]

Table 1.3 Examples of biomaterials with antimicrobial and antifouling strategies

Antibacterial component	Antifouling component	Target microorganism (s)	Applications	Ref
Gentamicin	Ethylene glycol linker	*S. aureus, E. Coli*	Titanium implant	50
Sulfamethoxazole (SMZ) and trimethoprim (TMP)	PEG	*S. aureus, E. Coli*	Biomedical catheters	51
Quaternized polyethyleneimine	poly(glycidyl methacrylate) brushes	*S. aureus*	Dental implant	121
poly(styrenesulfonate) (PSS), quaternary ammonium, H_2O_2 enzyme	Zwitterionic, novel copolymers (PTMAEMA-co-PSPE) with varied sulfobetaine fractions	*S aureus biofilm*	Urinary catheter	65
Cationic antimicrobial polypeptides	Heterofunctionalized poly(ethylene glycol)	*S. aureus, E. coli, P. aeruginosa*	Surface coatings	122
Rosin acid-derived maleopimaric acid quaternary ammonium cation (MPA-N+)	Allyloxy PEG	*E. coli, S. aureus, and P. aeruginosa*	Biomedical device	14
Chlorination of cysteine sulfurs	Bovine serum albumin/zwitterion	*E. coli*	Surface coating	86
Silver, Magnesium	Pyarogallol	*S. aureus, S. epidermis, E. faecalis, MRSA, P. aeruginosa, E. coli, K. pneumoniae, A. baumannii*	Suction catheters	123
α-aminoisobutyric acid	Lysine	*E. coli, B. subtilis*	Foley catheters	124
Vancomycin	phenylboronic acid polymer brushes	*S. aureus, S. epidermidis*	Contact lens	125
Silver	2-methacryloyloxyethyl phosphorylcholine	*E. coli, E. coli K 1-2*	Catheters, stents, and dialysis equipment.	126
Silver	perfluorodecanethiol	*S. aureus, E. Coli*	Catheters	127

Over the years, this phenomenon became more refined where implant surfaces can be modified with hyperbranched polymers on a pre-functionalized surface and simultaneously be linked to antibiotics. For example, a sequence of hyperbranched polymers comprising gentamicin moieties and PEG linkers was synthesized via a one-pot ring-opening reaction namely GPEG (from gentamicin and poly(ethylene glycol) diglycidyl ether) and GEG (from gentamicin and ethylene glycoldiglycidyl ether).[50] Biomaterial interfaces such as Ti can be functionalized with hyperbranched polymers using polydopamine (PDA) adhesive chemistry. The antibacterial activity of the coated Ti disks (Ti-GEG, Ti-GPEG, Ti-EPEG (antifouling analogue)) was evaluated *in vitro* and *in vivo* mice model against *S. aureus* and *E. coli* that showed a significant reduction in the number of viable cells adhered on the combinational implant surface (Ti-GPEG) demonstrating excellent antibacterial and antifouling properties compared to pristine and individual controls. These characteristics of the dual functionalized Ti disks presented potential clinical applications to reduce implant-related infections.

More recently, an efficient method for developing antibacterial and antifouling coatings on biomedical catheters (BC) via co-deposition of microcrystalline antibacterial drugs sulfamethoxazole (SMZ) and trimethoprim (TMP) combined with PEG immobilization via PDA chemistry was reported.[51] The product, namely BC-PEG-drugs, were effectively studied for their drug loading and releasing capacity in an acetic acid buffer solution (pH 5.5). The surface-modified catheters showed significant antibacterial and antifouling activity in solution and as well as in the zone of inhibition study. Moreover, the drug-loaded coating along with PDA-PEG helped in inhibiting the biofilm formation toward *S. aureus* and *E. coli* for up to 7 d and showed exceptional antibacterial and antifouling abilities in an *in vivo* animal infection model against *S. aureus*. These drug-loaded implant coatings allow on-demand deployment of drug payloads and highlight the advancement of multimodal antibacterial remedies for clinical applications. Dual-function coatings of this kind illustrate great initial bacteria-killing efficacy due to the release of antibiotics and

preserve significant antifouling activity after the depletion of embedded antibiotics because of the surface-immobilized polymer brushes.

However, antimicrobial materials that employ biocide release methods have demonstrated low accomplishment, with their primary disadvantage being the loss of activity as soon as the anti-infective molecules have been released or are no longer released at required dosages. Sublethal amounts of antibiotics have been shown to hasten resistance mechanisms and biofilm development.[52] Therefore, various innovative antimicrobial coatings that can supplant the high doses of traditional antibiotics have strongly influenced the field of surface chemistry. These coatings can be chemically altered to achieve a variety of features without altering the physical aspects of the base material. The fact that antimicrobial coatings can be readily applied to the surface of insertable, or implantable medical devices underscores their importance in inhibiting bacterial adhesion, proliferation, and eventual destruction. In this regard, AgNPs-based compounds have shown the potential to regulate bacterial contaminations. However, safety factors about using AgNPs have been raised due to their toxic nature to mammalian cells.[53, 54] The presence of AgNPs in the proximity of the cell membrane is reported to rise the reactive oxygen species (ROS) to a toxic level. To address the issue of cytotoxicity, the antifouling properties of surface immobilized-PEG have been used in devising a defensive layer to protect the direct contact and uncontrolled release of AgNPs and Ag^{+} ions from a material surface.[55] Literature suggests that, at minimal concentrations, such surfaces lack toxicity towards eukaryotic cells and interestingly are adequate to avert bacteria, including *E. coli, S. Typhimurium, S. aureus,* and *S. pyogenes*. [56-59]

Another strategy is to develop a dual-function technology in which antibacterial gemini quaternary ammonium salt waterborne polyurethanes (GWPU) brushes are placed over an antifouling layer of PEG and carboxyl anion of L-lysine.[60] The bactericidal activity of the upper layer at 4.96% biocidal concentration along with the antifouling features of the sub-layer resulted

in an augmentation of the coated surface which reduced the growth of both Gram-positive and Gram-negative bacteria by > 99%. However, the long-term usage and *in vivo* applicability of coatings comprised of hydrophilic moieties are restricted by their rich hydrophilic surface. Such polymers are prone to quicker release of the antibacterial component and are susceptible to disintegration by established biofilms in long-term *in vivo* applications. To improvise the biocompatibility and stability of these materials, recently a cross-linked double-layered contact-active antibacterial and antifouling waterborne polyurethane using PEG, L-lysine, and Gemini QAS (GQAS) was synthesized.[61] ATR-FTIR confirmed the stability of cross-linked structure for at least 5 months with promising long-term antibacterial and antifouling applications. Moreover, these films exhibited >95% killing efficacy at 2 and 7 d of implantation suggestive of great antibacterial action with diminishing acute inflammatory stage after 90 d of implantation *in vivo*. One major advantage of these release-based coatings is the antibacterial moieties can not only kill the bacteria adhered to the surface, but also eradicate the planktonic bacteria surrounding the medical device before their colonization on the surface (e.g., bacteria present in the lumen of the catheter, saliva, or in the bloodstream). Dual functional surfaces with bactericidal agent release have been explored with agents such as antimicrobial peptides,[45] antibiotics,[62] metallic nanoparticles,[63, 64] enzyme[65], etc. with on-demand release and switchable properties.

While PEG has been studied as a gold standard in antifouling materials, one challenge that has been observed is that it gets oxidized under physiological conditions, which results in the demolition of the hydration layer. Accordingly, the efforts to find substitutes with higher stability have directed efforts towards an exploration of mixed polymer brushes, zwitterionic polymers, side chains, and surface grafts.[39, 66] Neutral, hydrophilic PEG alternatives, such as poly(glycerol) and poly(2-methyl-2-oxazoline), have demonstrated comparable protein resistance to PEG controls and improved oxidative stability on polydopamine modified surfaces.[67-70] Bacterial species consist of negatively charged surfaces due to the presence of ionic carbohydrates,

teichoic acids, and lipopolysaccharides structures. Therefore, antibacterial agents with positively charged surfaces comprising of particles, polymers, and peptides have been developed and extensively investigated for their dual-functional antibacterial behavior against a vast span of bacteria including multi-drug resistant strains.[71-73]

1.3.2 Zwitterion Based Coatings

Many multifunctional antimicrobial surfaces in the literature have been fabricated through the incorporation of bactericidal agents into antifouling materials.[40, 74] Materials with contact-based killing require the bacteria to adhere to the surface for efficient eradication of bacteria. However, the features offered by antifouling qualities restrict this process. To evade this conflict, the antibacterial and antifouling elements need to be spatially or chronologically distinct. To achieve this, PDMS-based silicone catheters with the ability to eradicate UTI pathogens were fabricated using electrostatic layer-by-layer assembly.[65] The coatings comprised of three building blocks, namely, a copolymer in conjunction with zwitterionic/quaternary ammonium side chains for antifouling properties, a derivative of the same polymer with octyl group for potential bactericidal activity, and cellobiose dehydrogenase (CDH), another antibacterial moiety with H_2O_2 releasing capacity. The working of the integrated coatings was initially analyzed on the silicon wafers as model substrates, and later on the predeveloped silicone rubber surface following zeta potential, wettability, and morphological evaluation. The H_2O_2 byproduct of the immobilized CDH enzyme was the primary means of antibacterial activity from the surface-functionalized coating which resulted in a > 60% decline in the viable *S. aureus* attachment. Moreover, the magnitude of the antifouling capacity of the coatings was observed to be reliant on the depth on the surface and remained stable for at least 10 d in water and urine. The controlled release of the antimicrobial moieties from functionalized surfaces can be utilized to lower microbial contamination on devices and prevent the attachment of free-floating bacteria and inhibit biofilm formation.

Recently a novel zwitterionic monomer, 3-(dimethyl(4-vinyl benzyl) ammonio) butanesulfonate (DVBABS), and a polymeric coating that can both destruct bacterial cells and also release the debris of dead cells from the device surface have been synthesized specifically for the anti-biofilm activity.[75] These coatings were formulated via deposition of PDA, following *in situ* synthesis of AgNPs, and ultimately by grafting of polyDVBABS brushes using ARGET-ATRP (activators regenerated by electron transfer for atom transfer radical polymerization). The PDA catechol groups immobilized the AgNPs, which resulted in the killing of bacterial cells, and a shift from water to salt medium caused a reversible structural change of the polyzwitterion, which caused the release of the bacterial cell from the surface. For both *E. coli* and *S. aureus*, the multifunctional coating killed ≥99% of the attached bacteria and then quickly released ≥95% of all the attached bacterial cells. Both functions were found to be preserved over several cycles of killing and release.

A crucial antimicrobial mechanism of QACs requires the cationic chains to infiltrate the membrane of a bacterial cell.[76, 77] This is achieved either by opposite charge attraction and subsequent penetration of the active group leading to the disruption of the phospholipid bilayer or by establishing a charge imbalance that breaks down the transmembrane potential. Membranal integrity of the bacteria cell wall can be compromised upon the transfer of cationic surface charges to active intrinsic cations in the membrane.[78] However, the positively charged QACs are more prone to intensifying the spontaneous protein adsorption in the *in vivo* setting, thus considerably reducing its antimicrobial ability.[79] The surface contaminants of the debris from dead bacteria can conceal the functionalities on the modified surface containing QACs which can increase the possibility of recurring biofilm growth.[80] To overcome this challenge, the antimicrobial activity of QACs has been integrated with that of antifouling properties of hydrophilic polymers. On one hand, zwitterionic polymers can create robust and stable bonding with water molecules through electrostatic interactions, and on the other hand hydrophilic polymers and coatings can help

achieve surface hydration through the formation of hydrogen bonds between the polymer and water molecules. In addition to the surface hydration elements, zwitterionic polymers also tend to exhibit a strong anti-polyelectrolyte effect. In principle, the change in interactions of the polymer can lead to two diverse performances in water and salt solutions. Exposure to water and salt solution can lead to collapsed and stretched conformation of polymer brushes, respectively.[81] From an insightful perspective of composition and shape, the variations of cationic moieties and salt amounts and forms can be used to transform the surface wettability from a highly hydrophobic surface to a highly hydrophilic surface. Such transformation in the material properties has unveiled several research prospects involving the growth of multi-pronged bio-responsive materials that can revoke the shift between kill and release events.[82-84]

1.3.3 Surface Passivation via Protein Coatings

Additional antifouling strategies utilize specific protein interactions to prevent bacterial adhesion and non-specific adsorption of other proteins. A classic example of this method involves the passivation of surfaces with proteins that hinders cell attachment and blocks non-specific protein adsorption. In order to reduce non-specific interactions on polymers, various passivation agents are employed. Out of these, Bovine Serum Albumin (BSA) is most commonly used for surface passivation purposes due to its abundance, low fabrication cost, and a lesser degree of steric hindrance of specific binding proteins. Fabrication of stable protein films with BSA can passivate surfaces and be generated via nanoimprint lithography (NIL).[85] This method comprises a blend of temperature and pressure to generate materials that can substantially preserve the native structure of the protein in aqueous conditions. The coated surface can then be functionalized with various moieties such as chlorinating agents to produce N- or S-chloro species that would slowly release chlorine, providing a strong biocidal activity against uropathogens in addition to antifouling properties.[86] These protein coatings were also combined with nanoparticles as a nano bricks surface modification technique to create thin-film coatings on various substrates

such as dental implant screws for biomedical applications.[87, 88] Such robust approaches can be utilized towards scaling of medical device technology with protein films with an ability to be thermally treated to produce biostable coatings that retain their surface architecture (i.e., hydrophilicity, biodegradability, surface charges, etc.) in an *in vivo* environment.

1.3.4 Surface Topography

Modifications in the surface structure via textured patterns have come out as an advanced method to hamper microbial adhesion, kill bacteria, or sensitize attached microbes on medical implants.[91] These surfaces are inspired by nature where animal and plant surface topographies are employed to transform material with bio-inspired patterns for biofouling control. For example, surface characteristics like nanopillars or spikes have been shown to destruct the bacterial cell membrane, killing them and therefore obstructing bacterial adhesion.[92] Although the exact mechanism behind the bacteria repellence remains unclear, it is believed that nano- and micro-structures radically reduce contact adhesion area, generating improved bactericidal functions in comparison to smooth, solid surfaces. Single bacterial cells that encounter the textured surfaces undergo mechanical stress due to patterns and lower surface area which prevents them from attaching and results in significant distortions in the cell membrane, causing the membrane to rupture.[93, 94] It is also understood that surface patterns comprised of nano-microstructures can disorder nanoscale domains in the bacterial membrane, a critical step of the biofilm development process.[95] Notably, bacteria can switch between planktonic and biofilm states by sensing the topographical patterns around them.[96] Thus, the presence of nano-microstructure on the surface can not only obstruct the adhesion of microorganisms but also prevents the communication between bacteria in their collaborative aim of colonizing the surfaces. Studies have shown that patterns on the surface can hinder flagellar interaction between bacteria and block the release and sensing of small signaling molecules which is responsible for EPS production and biofilm formation.[95]

It is worth noting that bacterial attachment to medical devices and materials is often generalized since bacteria are viewed as immobile, extremely soft, and geometrically defined particles. In reality, bacterial cells are extremely dynamic with a convoluted living system that alter the protein structure in the cell envelope based on surrounding physiochemical circumstances, affecting functions like protein secretion, EPS generation, an extension of flagella, and adhesive molecules such as fimbriae.[97] Moreover, bacterial forms, sizes, growth conditions, and nutrient availability can all influence their interaction with the medical device interface. Therefore, there is no universal set system in terms of the topography of the surface that can prevent all microorganisms from adhering to the surface. Even though the implant at first may be inhospitable for bacterial adhesion, the buildup of a protein-rich conditioning film will ultimately initiate microbial adhesion and biofilm creation. Therefore, these patterned surfaces are primarily effective in delaying the early stage of bacterial biofilm growth when the number of cells is relatively low.[98] As the microbes start to grow and multiply, after a certain period, microorganisms will colonize the surface and initiate biofilm development. Whereas an ideal biomedical implant should possess the ability to not only delay, but also completely prevent the growth of biofilm and associated infections. For this reason, microtopography alone is inadequate and there is a need to develop multifunctional coatings that are both antifouling and antibacterial.

Polymers are widely used in a variety of biomedical applications including short- or long-term indwelling medical devices and implants. By their range of properties, today's polymer-based medical devices are formulated to provide excellent biocompatibility, durability, elevated potency, high-level wear endurance, and processing versatility over a wide range of applications. However, their applications are restricted due to a lack of resistance mechanisms against biofouling and infections. Materials like polymethyl methacrylate (PMMA), polyethylene terephthalate (PET), polyurethane (PU), polydimethylsiloxane (PDMS), titanium, stainless steel, etc. which are widely used in fabricating medical devices such as prosthetic devices, nasoenteral tubes, contact lenses,

indwelling catheters, or orthopedic and dental implants can be functionalized with nanopatterned structures using photolithography, etching, chemical and vapor deposition, electrodeposition, nanoimprinting and other texturing techniques.[99-101] Using Direct Laser Interference Patterning (DLIP), periodic bacteria-repellent microstructures have been produced on a variety of metallic and non-metallic biomedical surfaces with antimicrobial agents.[102] It has been shown that pattern sizes similar to bacterial cell size (1−2 μm) thwart the biofilm formation drastically by isolating the bacterial cells and successively lowering the microbial attachment.[103, 104] This hypothesis is used by several authors to sensitize and eradicate biofilms of *S. aureus* and *P. aeruginosa* with the synergism between micropatterned surfaces and streptomycin antibiotic treatment in the concentration range of 1-4 mg/L.[105] The bacteria-size surface topographic characteristics decrease bacterial adhesion and obstruct the growth of two-dimensional accumulates for the initial few hours.

Recent studies have largely reported the synergistic antibacterial effect of topographical cues and chemical components.[106, 107] The combined effect of chemically modified surface and topography is known to have a greater impact on the adhesion and viability of *P. aeruginosa.*[108] The study consisted of a conducting polymer, polyaniline (PANI), and modified the surface of PET by *in situ* polymerization and microstructured the surface using DLIP. The PANI-modified hydrophilic films decreased the attachment of *P. aeruginosa* by 74% and consecutive biofilm formation by 50%. The presence of microstructure and PANI on the dual-functional PET–PANI film further increased the ability to inhibit bacteria and biofilm formation by 97% and 65%, respectively. Similarly, the antimicrobial properties of inorganic surfaces like copper can be additionally boosted by directed surface functionalization using the same patterning technique.[102] One drawback of DLIP however is that it can induce undesirable chemical variations in the surface of the polymer.[103] Therefore, the validity of the method for the use of the polymeric medical device is still uncertain. Scientists have taken great inspiration from naturally occurring micro- and nano-

topographies with high surface contact to modify biomedical materials that mimic these intricate architectures for their antibacterial and anti-fouling properties. Patterned structures often found on the cicada, dragonfly wings, shark skin, lotus, and rose petals or even liquid infused surfaces possess the ability to inhibit or destroy bacteria.[111, 112]

Evaluation of these surfaces illustrates extensive variants in elemental and conformational traits, suggesting that there is no one specific surface structure that demonstrates bactericidal performance against all types of microorganisms. Nevertheless, complex biological interactions between adsorption and release of protein moieties, cells, and microorganisms on the device interface may be dictated by these designs. For this purpose, high-performance dual-functional coatings that can repel and inactivate bacteria with UV-cross-linkable adhesive material based on shark-skin nanotopography have been developed.[109] This material was loaded with titanium dioxide nanoparticles (TiO_2 NPs) from which shark-skin microstructures can be imprinted on a poly (ethylene terephthalate) (PET) substrate using solvent-assisted soft nanoimprint lithography. Upon exposure to UV-light, TiO_2 NPs can be irradiated where they produce reactive hydroxyl radicals and superoxide ions that can inactivate a variety of microorganisms.[113] The light-activated shark-skin-designed surfaces decreased the attachment of *E. coli* by ~70% compared to the smooth surface films with identical chemical compositions. Even the lowest tested concentration of 10 wt% TiO_2NPs demonstrated > 80% and 95% inactivation of *E. coli* and *S. aureus* within 1 h of UV light exposure. The use of TiO_2 offer superior attributes for biomedical applications compared to other nanoparticles (e.g., Ag, Cu) due to their ability to be loaded into transparent materials and device coatings.[114] This can be beneficial for many medical devices, such as blood-contacting devices where early visual detection of blood clots is imperative.

As per the recent molecular dynamics model report, there is a strong correlation between bacterial adhesion, the physicochemical surface properties, and the design of a medical device, where both the device and bacteria determine the success of the device in terms of antibacterial

activity.[93] Some structures like nanopillars found on surfaces of cicada and dragonfly wings can only impede certain types of bacterial strains.[115, 116] Bactericidal efficacy of the surface is not only influenced by the shape, width, height, and spacing of the structural patterns but also by the cell type and rigidity of the bacterial cell membrane. This might be the reason why rigid Gram-positive bacteria strains including the *S. aureus* bacteria are resistant to nano-patterned surfaces of cicada wings, while Gram-negative may not be affected to a similar extent.[117] To conquer this limitation, engineered surfaces with topographical patterns can be combined with antimicrobial compounds. In this regard, fluorine-loaded hydroxyapatite (FHA) has been widely employed with biomimetic structures for orthopedic and dental applications due to its broad-spectrum antibacterial efficacy against bacteria like *S. aureus*, *E. coli*, and *P. gingivalis.*[118] On the same basis an integrated surface of cicada wing-like nanopillars (diameter ~80 nm) in conjunction with FHA on titanium substrate using electro-chemical additive manufacturing for biomedical applications has been designed.[119] Similarly, dragonfly-wing-based nanopillars made of ZnO/Au on a PDMS (PDMS-ZnO/Au) surface with a dual bactericidal and anti-biofouling activity to reduce the formation of biofilm over a prolonged time have been reported.[110] The superhydrophobic surface of modified PDMS with the ZnO nanopillars produces air pockets for a photocatalytic reaction which is enhanced with the addition of AuNPs. The anti-adhesive and antibacterial PDMS-ZnO/Au surface demonstrated > 99% of bacteria reduction with just 30 min of visible light exposure which can be attributed to ROS generation through photocatalytic reduction of AuNP which results in membranal destruction, protein, and DNA destruction in bacteria.[120]

1.4 Advancements in Nitric Oxide Releasing Multifunctional Biomedical Devices

Conventional approaches for tackling infections associated with medical devices with antibiotic treatments have exhibited decreasing effectiveness as complications with biofilms and resistant bacteria at the material interface become more prevalent. Moreover, these devices can often be affected by other biomedical issues, such as device-induced thrombosis and

inflammation. It is understood that local and systemic microbial infections elevate the threat of thrombosis as much as 20 times and lead to thromboembolic diseases.[128] One main issue that underlines the risk of thrombosis is the degree of inflammation that is triggered by the occurrence of infection, in which a pro-coagulant state can increase inflammation and thrombotic complications.[129] Active antimicrobial surface strategies discussed in the previous sections including antibiotics, metal nanoparticles, and QACs can all effectively tackle bacterial contamination; however, they cannot address other biomedical challenges that occur at biomaterial interfaces (e.g., thrombosis and inflammation). The use of nitric oxide (NO) releasing materials has become a popular strategy to simultaneously overcome the issues arising from the use of biomedical devices, including the issue of biofilm.[130-134] NO is a diatomic free radical, gaseous transmitter molecule that is endogenously produced in the body when L-arginine undergoes enzymatic oxidation in presence of nitric oxide synthases (NOS), resulting in the production of NO and L-citrulline. [135, 136] Healthy endothelial cells generate an NO flux of 0.5–4 × 10^{-10} mol cm^{-2} min^{-1} in the blood vessels which protects against platelet activation and aggregation, and exhibits an anti-proliferative effect on smooth muscle cells (SMCs), and controls vasodilation and blood pressure.[137] Nitric oxide is known to regulate many physiological functions such as neurotransmission, vasodilation, an immune response to infection, wound healing, angiogenesis, and oxygen-free radical generation.[138, 139] Apart from these versatile properties, NO has been also found to possess excellent antimicrobial/bactericidal activity against both Gram-positive and Gram-negative bacteria, including several clinically resistant bacteria strains such as methicillin-resistant *S. aureus* (MRSA).[140-142] The antibacterial activity of NO is governed by multiple mechanisms such as nitrosation of amines and thiols, chemical alteration of DNA, lipid peroxidation, promoting iron depletion in bacteria, and tyrosine nitration.[143-145] Moreover, NO has a very short half-life in the physiological environment which makes its action very rapid due to which bacteria are unable to develop resistance against NO.[146, 147] These properties of NO make

it a superior therapeutic compared to traditional antibiotics or other active antimicrobial agents discussed above.

The multifunctional antimicrobial, anti-thrombotic, and anti-inflammatory properties of NO makes it a promising candidate for the development of various indwelling and blood-contacting biomedical devices with enhanced hemocompatibility and antimicrobial activity. The instability and short biological half-life of NO in aqueous conditions have led to the development of a pharmacologically active class of NO donors, such as nitrates, *N*-diazeniumdiolates (NONOates), and *S*-nitrosothiols (RSNOs), which can be integrated within a variety of medical-grade polymeric devices for prolonged and controlled NO release.[148-152] NONOates are one of the most widely studied NO donating molecules that are synthesized by reacting primary or secondary amines with NO under very high pressure (e.g., 5 atm) and low-temperature environment in basic conditions (**Figure 1.5 a-d**). The NO release from these compounds can be triggered by modulating the pH, light, or enzymes where two moles of NO are released per one mole of a donor.[153-155] *S*-Nitrosothiols (RSNO), another class of commonly investigated NO donating compounds, are endogenously found in the body and can be synthesized by conventional nitrosation of thiol functional group in an acidic environment.[156, 157] RSNOs, can rapidly release NO at physiological conditions and in the presence of various catalysts such as heat, light, metal ions, and enzymes (**Figure 1.5e**). *S*-nitroso-*N*-acetylpenicillamine (SNAP) and *S*-nitrosoglutathione (GSNO) are two commonly used NO donor species studied for biomaterial applications because of their long-term stability and NO release properties apart from ease of synthesis, low cost, and excellent biocompatibility (**Figure 1. 5f-g**).[158]Other RSNOs such as *S*-nitroso-*N*-acetylcysteine (SNACET) (**Figure 1. 5h**) and derivatized molecules such as (*N*-Acetyl-*S*-nitrosopenicillaminyl)-*S*-nitrosopenicillamine (SNAP-SNAP) have also been synthesized and reported.[159, 160]

NO donors can be incorporated into a polymer matrix via solvent impregnation, non-covalent dispersion or blending of the donor in a polymer, or covalently immobilization of the NO donor moiety to the polymer backbone (**Figure 1.6**).

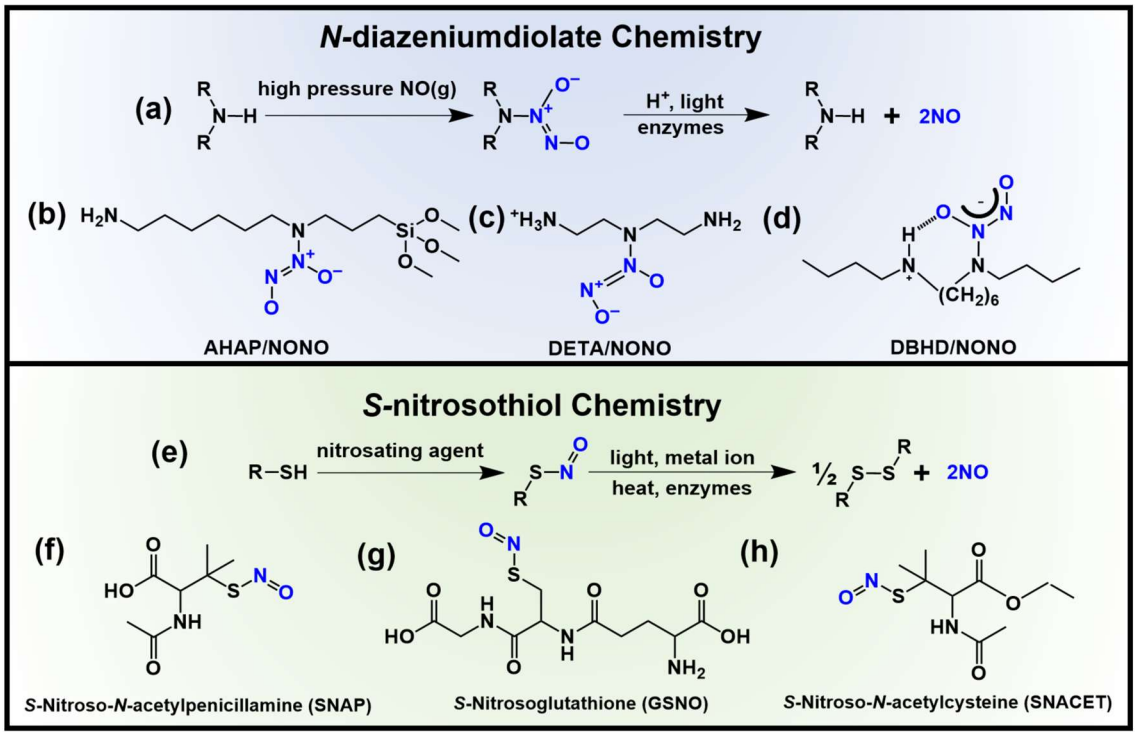

Figure 1.5 (a) Schematic representation of formation and decomposition of (a) *N*-Diazeniumdiolates (NONOates), chemical structure of NONOates donor (b) diazeniumdiolated *N*-(6-Aminohexyl) aminopropyltrimethoxysilane (AHAP/NONOate), (c) diazeniumdiolated diethylenetriamine (DETA/NONOate), (d) diazeniumdiolated dibutylhexanediamine (DBHD/NONOate) (e) Schematic representation of formation and decomposition of *S*-nitrosothiols (RSNOs) , and structure of common RSNO donors, (f) *S*-Nitroso-*N*-acetylpenicillamine (SNAP), (g) *S*-Nitrosoglutathione (GSNO) and (h) *S*-nitroso-*N*-acetylcysteine ethyl ester (SNACET).

NO-releasing materials have historically faced the challenges of attaining controlled NO release and long-term release properties to meet the requirements for various medical device applications. This is one of the challenges that has restricted effective clinical translation of NO-releasing materials to date. Given that the therapeutic levels of NO and its effects can vary significantly in physiological conditions, it is essential to regulate the levels of NO for desired biomedical application.

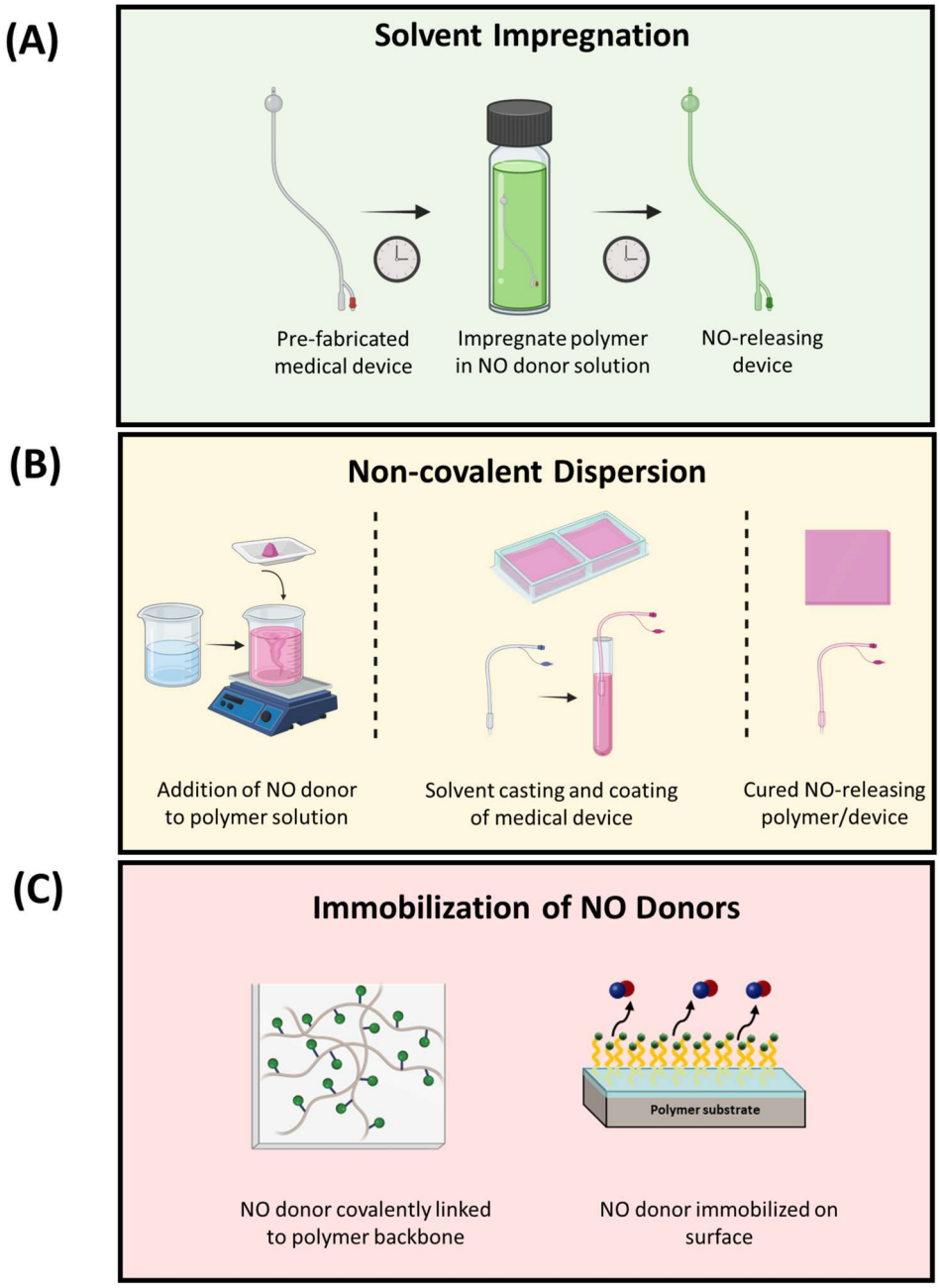

Figure 1.6 Methods to generate NO-releasing/generating materials. This includes (A) solvent impregnation, (B) non-covalent dispersion of NO donors in a polymer solution and solvent casting, and (C) immobilization of NO donors to functionalized polymer substrate.

For example, during the introduction of a medical device implant to the body, the device may need elevated levels of NO to thwart the initial bacterial attachment on the device surface.

Nevertheless, over longer durations, these implanted devices may need reduced levels of NO to maintain a bacteria-free state. The NO release from materials has been determined by a combination of the NO donor chemistry and the material properties. Recent work has utilized approaches that can control the NO release by modulating the polymer properties (water uptake), dip coating with hydrophilic polymer to create a hydration layer and prevent adsorption of biomolecules, coating with low water uptake/hydrophobic polymer, covalent immobilization of NO donors that can control leaching and prolong NO release, or by elevating the levels of NO using catalysts (light, metals, enzymes, etc.).[161-163] The metal-based catalysts can also provide a second active antimicrobial mechanism while helping control the NO release. Similarly, to precisely regulate the dosage and NO delivery time from polymers, the photoresponsive properties of NO donors have been exploited for various biomedical applications (catheter disinfection, inhalation NO therapy, osteosarcoma therapy, etc.).[155, 163-165] Another approach to controlling the location and enabling site-specific NO availability is transnitrosation reactions at thiol moieties, like cysteine, that are immobilized on surfaces providing a localized site for NO at these biointerfaces.[166-169] The specific details of these combinational materials are discussed later in the manuscript.

1.5 NO-Releasing Combinational Surfaces with Dual Antimicrobial Strategies

NO-releasing antimicrobial surfaces are a promising approach to increasing the lifetime and enhancing the biocompatibility of medical devices. Nevertheless, one major issue with these devices is that the levels of NO may decline with time owing to the degradation of the NO donor within the polymer matrix, which restricts the potential of devices to eliminate bacteria over longer durations. Therefore, many efforts in the field have been directed toward combining dual-active antimicrobial approaches (**Figure 1.7**). These strategies are exciting since medical devices with NO and a secondary antimicrobial mechanism will not only help with tackling infection issues at medical device interfaces, but also help overcome other significant challenges with indwelling

medical devices such as thrombosis, inflammation, etc. due to inherent biological properties of NO. Surface modifications of NO-releasing antibacterial polymer coatings are attempted to bestow additional antibacterial properties to synergistically combat bacteria. These techniques involve the incorporation of NO donor along with secondary antibacterial agents such as nanoparticles [170], antibiotics, antimicrobial peptides,[171], and other antiseptic molecules.[172] The reported studies usually contain an NO donor incorporated in the base polymer that is top-coated with a polymer containing secondary active molecules (see **Table 1.4**).

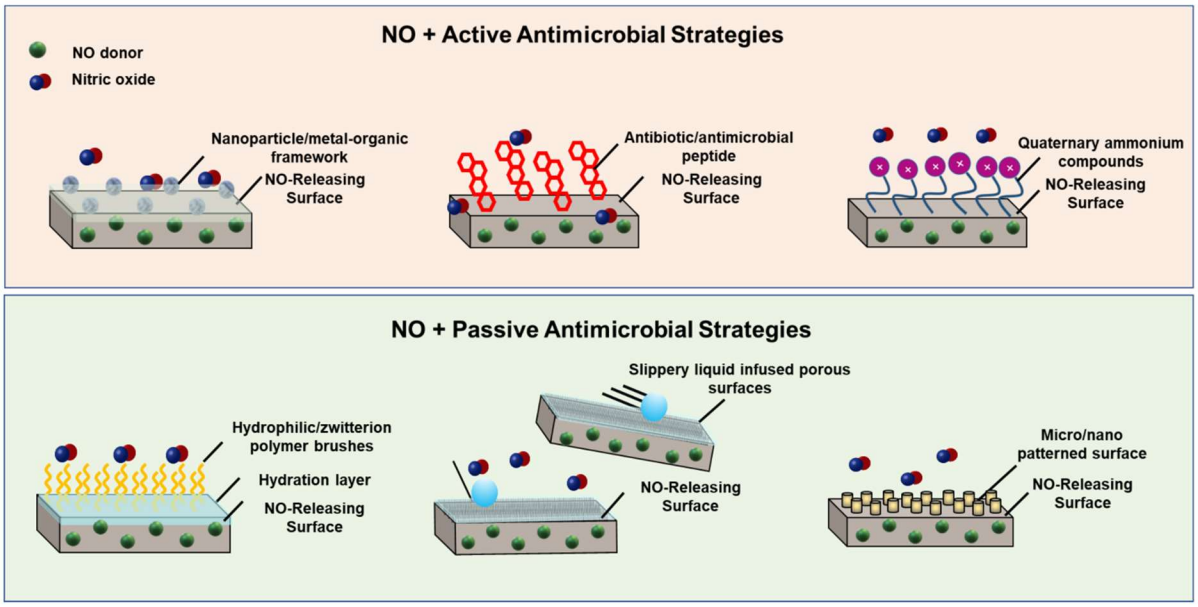

Figure 1.7 Different physical and chemical modification techniques to incorporate multifunctional antibacterial and antifouling surface properties to nitric oxide-releasing materials. These strategies include surfaces with nanoparticles, metallic organic frameworks, antibiotics antimicrobial peptides, and quaternary ammonium compounds for antibacterial action. Antifouling surfaces include hydrophilic/zwitterionic polymer brushes, slippery liquid infused porous surfaces, and surface patterning with micro- and nano-topographies.

Table 1.4 List of NO-releasing medical devices/polymeric surfaces exhibiting dual-action antibacterial behavior.

Strategy	Secondary component	Microorganisms	Material/Device	Ref.
Antibacterial	Formaldehyde	*S. aureus, E. coli*	Micellar nanoparticles	218

Antibacterial	Dihydropyrrolones	*S. aureus, P. aeruginosa*	Fluorinated ethylene propylene surface	[219]
Antibacterial	beta-defensin 2 (BD-2), colistin, gentamicin, chloramphenicol, ciprofloxacin, tetracycline	*P. aeruginosa*	Catheter	[190]
Antibacterial	Tobramycin, Meropenem, Colistin, Ciprofloxacin, Ceftazidime, Aztreonam,	*S. aureus, P. aeruginosa, MRSA, Burkholderia cepacia complex.* Clinical resistant- *K. pneumoniae* and *P. aeruginosa*	Chitosan oligosaccharides	[188]
Antibacterial	Cu NPs	*S. aureus, P. aeruginosa*	PU composites	[170]
Antibacterial	Cu NPs	*S. aureus, P. aeruginosa*	PVC tubing	[177]
Antibacterial	Ag^{+}	*S. aureus, P. aeruginosa*	Xerogel	[179]
Antibacterial	AgNPs	*S. aureus, E. coli, S. mutans*	Alginate NPs	[220]
Antibacterial	Benzophenone-based quaternary ammonium	*S. aureus, P. aeruginosa*	PU composites	[196]
Antibacterial	Selenium	*S. aureus, E. coli*	PU composites	[176]
Antibacterial	Chlorhexidine	*S. aureus, E. coli*	Silicone rubber	[172]
Antibacterial	Nisin	*S. aureus, E. coli*	Silicone rubber	[171]
Antibacterial	Heparin	*S. aureus*	Silicone rubber	[221]
Antibacterial	Quaternary ammonium epoxides	*S. aureus, P. aeruginosa*	Functionalized silica nanoparticles	[222]
Antibacterial	Quaternary ammonium	*S. aureus, P. aeruginosa*	Poly(amidoamine) (PAMAM) dendrimers	[194]
Antibacterial	Oligoethylene glycol, hydrophobic Ethylhexyl, cationic primary amine-containing antimicrobial polymer	*P. aeruginosa*	Amphiphilic statistical ternary copolymer	[132]
Antibacterial	Amphotericin B	*S. aureus, E. coli, C. albicans*	Polydimethylsiloxane	[192]
Antifouling	Ordered submicron pillar	*S. aureus, P. aeruginosa, S.*	PU surface	[215]

	topographical surface	*epidermidis, E. coli*		
Antifouling	Ordered submicron pillar topographical surface	*S. epidermidis*	PU surface	[217]
Antifouling	Silicone Oil	*S. aureus, P. aeruginosa*	Silicone rubber tubing	[207]
Antifouling	Silicone oil	*S. aureus*	Silicon Foley catheter	[209]
Antifouling	Silicone oil	*S. aureus, S. epidermidis*	Insulin cannula	[25]
Antifouling	BPMPC	*S. aureus*	PU composites	[212]
Antifouling	BPMPC	*S. aureus*	Vascular catheters	[213]
Antifouling	Tecophillic SP60D60, hydrophilic, antifouling polymer	*S. aureus*	PU coatings	[161]
Antifouling	Hydrophobin SC3	*S. aureus*	PU-PDMS composites	[191]
Antifouling	PDMS	*S. aureus*	PDMS surface	[200]

1.5.1 NO-Releasing Surface with Metal Nanoparticles

The advantage of having antibacterial nanoparticles as a secondary active mechanism serves a dual purpose with NO-releasing materials. Metal nanoparticles are known to catalyze the NO release from *S*-nitrosothiol-based NO donor compounds due to their ability to break the S-NO bond of the donor. Metals like copper have been demonstrated to facilitate RSNO decomposition via Cu^{+} interaction thereby leading to NO release from the donor.[156, 173] In one example, NO-releasing biocompatible polyurethane composites can be generated by incorporating 10 wt% of SNAP into the CarboSil-20 80A, a commercially available biomedical grade polymer followed by a top coating of 1, 3, or 5 wt % Cu-NPs. Here, the SNAP molecule

worked as NO-releasing (NOrel) material whereas, Cu-NPs worked as NO generating (NOgen) material.[170] The topcoat of Cu-NPs not only helped in the enhancement of the NO release but also improved the overall antimicrobial activity via the oligodynamic effect of Cu.[174] The NO flux for the SNAP-CarboSil composites without Cu-NP coatings after 3 h was found to be 1.32 ± 0.6 × 10^{-10} mol min^{-1} cm^{-2}, whereas, with 1, 3, and 5 wt% Cu-NPs coatings, it was observed to be 4.48 ± 0.5 × 10^{-10}, 4.84 ± 0.3 × 10^{-10} and 11.7 ± 3.6 × 10^{-10} mol min^{-1} cm^{-2}, respectively. While the Cu-NPs only controls exhibited some antimicrobial effects, the 3% Cu-SNAP composites exhibited a significant reduction (up to 99.8%) in both Gram-positive *S. aureus* and Gram-negative *P. aeruginosa* compared to the controls. Various other studies have shown the use of nanoparticles as a catalyst and a means to generate NO using zinc, copper, and selenium to enhance the antibacterial efficacy with a variety of NO donors.[175] [176, 177] The combination of CuNPs and NO has been shown to increase antimicrobial effects and blood-compatibility for short-term extracorporeal circulation (ECC) applications.[177] Combinational approaches involving metal nanoparticles can be extremely advantageous for the catalytic release of NO from medical-grade polymers. The innate bactericidal efficacy and ability to interact with endogenous RSNOs in blood makes CuNPs superior compared to other types of metallic nanoparticles. Similarly, the broad-spectrum antimicrobial properties of NO have been combined with ZnNPs for sterilizing hub regions of tunnel dialysis catheters.[178] Meyerhoff and group developed a novel NO-releasing insert for hemodialysis catheter hub disinfection, where the ZnNPs combined with GSNO significantly increased the NO flux that demonstrated superior antimicrobial activity in a full-length catheter implanted in 14-d *in vivo* sheep model as compared to clinically used chlorhexidine impregnated caps. Other literature has reported the potential for the synergistic killing of NO with Ag which also been explored against infection-causing pathogens for biomedical applications. [179]

While metal nanoparticles can trigger higher levels of NO surface flux, they also have the potential to generate a consequent cytotoxic effect from the leaching of these particles.[180] The

undesired leaching can harm the neighboring cells and healthy tissues leading to inflammatory reactions in the body. To overcome the challenge of metal leaching, copper-based metal-organic frameworks (MOFs) have been reported to alleviate $Cu^{2+/1+}$ via coordination with extended catalytic operation as opposed to their salt or nanoparticle counterparts. The use of MOFs in NO-releasing polymeric composites with NO donor compounds was demonstrated by creating a multifunctional triple-layered composite scaffold with CuBTTri and SNAP.[181] The NO release levels from the catalyzed SNAP decay could be finely-tubed by varying the concentration of CuBTTri. These combinational NO-MOF surfaces demonstrated 2.74 and 1.23-log reduction in adhered methicillin-resistant *S. aureus* and *E. coli*, respectively.[181] Although, these surfaces showed improved antibacterial properties compared to the individual NO or MOF control surfaces, the practical use of MOF-containing materials has been restricted due to high production rates, inadequate selectivity, minimal function, and complexities in recycling/regeneration.[182] Similar studies have been reported consisting of a combination of NO and nanocomposite polyvinylidene fluoride (PVDF) membrane or other light-activated antibacterial nanomolecules.[183-186] These metal-based surfaces can be irradiated with a light source taking advantage of photocatalytic activity to increase the therapeutic efficacy of NO-releasing surfaces. Readers are directed to other thorough review articles for more information on NO-releasing photo-activable materials for antibiofilm applications.[187]

1.5.2 NO-Releasing Surfaces with Antibiotics, Antiseptics, or Antimicrobial Peptides

Many studies in the past have reported the efficiency of NO-releasing materials in eradicating viable bacteria that can maintain a biofilm-free state for an extended period of time.[37, 159] It has been demonstrated that NO can increase the susceptibility of multiple classes of antibiotics in drug-resistant bacteria, while simultaneously slowing down the resistance process.[188] This can be attributed to the augmented membrane permeability in bacteria caused by reactive oxygen and nitrogen species generated by exogenous delivery of NO. It is hypothesized that an increase in

membrane permeability driven by NO can result in better action of antibiotics in bacteria. For this reason, scientists have attempted to either modify the NO-releasing surface with broad-spectrum antibiotics[189] or improve the antibacterial properties of NO by co-delivery/subsequent delivery of antibiotics after NO treatment.[189, 190] The Schoenfisch group has studied the combined effects of NO with various antibiotics in chitosan oligosaccharides.[188] Their study confirmed that most combinations of NO and antibiotics were synergistic or additive, without any antagonism, demonstrating the synergy of the approaches and advantages of their combination.[188] These strategies can prove superior against antibiotic-resistant pathogens such as *P. aeruginosa* which have lower permeability to conventional antibiotics, presence of efflux pumps, and production of enzymes that can chemically alter the expression and deactivate the action of antibiotics.

Despite the excellent broad-spectrum antimicrobial, anti-thrombotic, and anti-inflammatory properties of NO, the commercialization of NO-releasing materials has not been achieved to date. Hence, approaches that involve other clinically available antimicrobial catheter materials have also been combined with NO-releasing properties to create a multifunctional medical device interface for a greater level of microbial eradication. Recently, a method to modify silicone rubber medical device interfaces with the incorporation of the NO-donor SNAP and a commonly used broad-spectrum antiseptic chlorhexidine (CHXD) was reported.[172] The antiseptic CHXD was top-coated on the SNAP-loaded surface at various concentrations. The CHXD was homogeneously dispersed on the surface of the films and its mechanism of action is that it can kill pathogens upon contact, thereby preventing biofilm formation on the surfaces. The dual-active SNAP-CHXD surfaces demonstrated the highest reduction in viable *S. aureus* and *E. coli* bacteria with > 3-log reduction on the surface of the films with up to 4 weeks of physiologically relevant levels of NO.[172] A similar methodology has been used by other groups that immobilize hydrophobin and Amphotericin-B on NO-releasing surfaces for bacterial and fungal eradication.[191, 192] The fate of the medical device is highly dependent on the initial timepoints of implantation or insertion where prevention of microbial adhesion on the surface is determined to

be very crucial. The synergy of multiple antimicrobial interfaces can radically reduce the attachment of viable bacterial cells on the surfaces. The successive levels of NO release from the surface can then persistently offer antibacterial action against clinical pathogens and help maintain a biofilm-free state.

1.5.3 NO Releasing Surfaces with Quaternary Ammonium Compounds

Ionic compounds such as quaternary ammonium, phosphonium, phosphonic acid, and sulfonic acid are well-known groups of organic compounds for their antimicrobial activities. When these charged molecules are combined with the NO donors, the antimicrobial effect of the materials increases significantly.[193] Since long chains of alkyl on the QACs have been shown to increase the penetration of molecules into the bacterial cell membrane, NO-releasing QAC-functionalized generation 1 (G1) and generation 4 (G4) poly(amidoamine) (PAMAM) dendrimers using NONOate form of NO donors have also been reported.[194] Modification of QAC dendrimer scaffolds with NO release capabilities resulted in increased bactericidal efficacy against both Gram-positive and -negative bacteria compared to the QAC-modified dendrimers alone.[194, 195] The NO payload in these materials can be tuned by regulating the polarity of the charging solvent used in NONOate synthesis reaction (i.e., by increasing the ratio of tetrahydrofuran to methanol with increasing alkyl chain length). However, the stability of polymers with NONOates during shelf-life storage and with various hospital sterilization methods is yet to be evaluated. To overcome this, a combination of RSNO and QA was synthesized that demonstrated superior bactericidal effect by permanent photo-crosslinking and surface immobilization of benzophenone-based quaternary ammonium antimicrobial (BPAM) on a CarboSil based polymeric composite with SNAP embedded as an NO donor.[196] SNAP has the capacity to crystallize in the polymer matrix and be triggered via heat, light, or metal ions. The crystallinity of the donor in the polymer matrix increases its lifetime in the RSNO-loaded polymers up to 8 months of storage at room temperature.[197] Owing to its excellent storage capacity, a dual functional polyurethane polymer

CarboSil 20 80A was loaded with NO donor SNAP followed by top coating with surface-immobilized BPAM molecule. BPAM exhibits instant contact killing and high biocidal activity against both Gram-positive and Gram-negative bacteria along with rapid surface attachment (within 1 min) to the polymer with mild UV irradiation and good mechanical durability.[196]

1.6 NO-releasing Combinational Surfaces with Antimicrobial and Antifouling Strategies

A second potential limitation of NO-releasing polymers, and motivation for their combination with antifouling strategies, is they have been shown to promote surface fouling via blood protein adsorption.[198] As previously mentioned, such non-specific adsorption of physiological protein often becomes a substrate for bacteria attachment which adversely influences the performance of NO-releasing materials. Although the adsorption of protein on the surface does not affect the activity of NO release from polymers[176], it can increase surface fouling arising from dead bacterial debris. Therefore, a secondary antifouling mechanism that eliminates the fouling on the NO-releasing device surface that encounters bodily fluids, while actively killing bacteria via NO is one of the newest and most promising directions in this field of research. The antifouling approaches applied to NO-releasing materials include texturing of the polymer surface, liquid-infused slippery surfaces, conjugation of NO donors on polymeric brushes, NO impregnated/incorporated surfaces with zwitterionic, superhydrophobic, and even hydrophilic topcoats.[25, 199]

1.6.1 NO Releasing Hydrophilic and Hydrophobic Antifouling Surface

Hydrophilic coating materials due to their intrinsic antifouling property play a crucial role in combating microbial growth on the surface. When a hydrophilic surface comes in contact with bodily fluid, a hydration layer is formed on the surface which inhibits the attachment of non-specific hydrophobic proteins. Further, the combination of NO donating materials and antifouling surface exhibits a synergistic antimicrobial effect. This method was demonstrated using a polyurethane coating with antibacterial and antifouling properties using CarboSil 2080A polymer and SNAP as

NO donor [161]. The developed CarboSil-SNAP composite was top coated with Tecophillic SP60D60, a commercially available hydrophilic, antifouling polymer with a contact angle of ca. 51°. The fabricated coating showed a sustained NO release and a synergistic effect in the reduction of up to 96% of *S. aureus* viable cell count compared to the control samples. A biomimetic surface coating on NO-releasing polymers was also evaluated for antimicrobial applications. This methodology included solvent impregnation of SNAP in CarboSil and PDMS polymer, followed by a topcoat of hydrophobin SC3 (SC3), a self-assembling amphiphilic protein.[191] The top-coated SC3 led to a β-sheet formation on the CarboSil surface that induced hydrophilicity resulting in a ca. 30% reduction in the contact angle (from 107° to 76° for SC3-SNAP-CarboSil). The change in surface wetting also resulted in a tenfold drop in the fibrinogen adsorption on SC3 top-coated polymer samples when compared to non-SC3-coated samples. The SC3 top-coated SNAP-PDMS polymer samples demonstrated superior bactericidal property with a ca. 79% reduction in viable *S. aureus*. However, one of the major constraints with using polymers for top-coating the substrates is the potential for untimely polymer degradation which can lead to an increase in surface roughness or a non-homogenous top-coat layer, which can defeat the purpose of having an antifouling interface.

Surface immobilization of NO donors has greatly impacted the field, and a major advantage of combining antibacterial and antifouling strategies is accomplishing the long-term function of medical devices. The presence of an antifouling interface has been understood to prolong the life of NO-releasing materials even after the total NO payload is exhausted in the polymer matrix. This was exemplified with a triple-action (protein, platelet, and bacteria repellent) coating called surface-immobilized *S*-nitroso-*N*-acetylpenicillamine (SIM-S) on a PDMS polymer surface to combat infection.[200] The modified PDMS polymers released NO at physiologically relevant levels for up to 4 weeks, resulting in a 99.99% (~4 log) reduction in viable *S. aureus* over 24 h. The functionalized polymer surfaces revealed non-fouling nature and significantly reduced protein

adhesion by ca. 65% when compared to unmodified PDMS. The antifouling capability of the material surface was preserved despite the complete depletion of NO payload within the polymer because of the surface-immobilized NAP degradation product.

Similarly, using the mussel adhesive chemistry via polydopamine (PDA) immobilization of polytetrafluoroethylene (PTFE) particles on the SNAP-loaded NO-releasing polymer composite surface was recently reported.[201] The PTFE coating on the NO-releasing surface decreases the surface wettability of the polymer making it highly hydrophobic. On very hydrophobic surfaces like PTFE coating, air-water interfaces, or the presence of interfacial nanobubbles can significantly reduce the contact of bacteria with the surface. Therefore, together the PTFE coating is known to passively lower the degree of bacterial attachment to the surface of the polymer, and the presence of active NO release is expected to eradicate bacteria that were able to adhere to the surface. The combination of these two interfaces was shown to reduce 99.3% and 99.1% of viable *S. aureus* and *E. coli* bacteria on the surface, respectively.

Despite integrating multiple mechanisms in a single medical device, NO-releasing materials suffer from limitations such as a lower range of NO release levels, leaching of NO donors from polymer, and clinical/commercial translatability. Many approaches reported in the literature need to be scalable, easy to manufacture, and ready for the regulatory pathway for effective clinical translation. From a broader perspective, blood-contacting devices frequently face the problem of clotting which is often linked with device-associated infection. One major advantage of NO-releasing devices is their diverse role in various biological pathways. Combinational surfaces with NO-releasing properties are superior to other surfaces due to the multiple roles of NO (vasodilation, platelet activation, inflammation, pathogen elimination, etc.). To demonstrate this, Hou et al. reported a NO-releasing catheter with uniform high-density precision diblock copolymer brushes (termed H(N)-*b*-S) consisting of a surface block of antifouling poly(sulfobetaine methacrylate) with a subsurface block of antibacterial RSNO-modified poly(hydroxyethyl

methacrylate).[202] Using a novel catheter modification technique of ozone-initiated surface reversible addition-fragmentation chain-transfer (ozone-surface-RAFT) block copolymerization, both the inner and outer surface of a slender polyurethane (PU) catheter were altered. These dual-functional NO-releasing catheters exhibited 99.99% biofilm reduction of various Gram-positive and Gram-negative bacteria as compared to <90% antibacterial activity of commercial silver catheter in a murine subcutaneous infection model. In a long-term study, these modified catheters exhibited >99.99% reduction in MRSA bacteria in a 5-d implantation study in a porcine central venous catheter infection model. In addition, the combination of NO and polymer brushes demonstrated excellent antithrombogenicity and biocompatibility. More importantly, this study presented a technique to design a flow reactor to scale up the H(N)-*b*-S coating procedure to modify clinically relevant size catheter (30 cm long). Overcoming these challenges in scaling up the synthesis of material design along with the combination of secondary antimicrobial approach is expected to significantly enhance the translatability of NO-releasing materials for clinical applications.

1.6.2 Liquid-Infused Nitric Oxide-Releasing (LINORel) Surface

Although the impregnation of NO donor does solve the issue of treating the bacterial infection, it does not completely resolve the issue of fouling from proteins of dead bacteria. When it comes to designing biocompatible coatings, material scientists are often drawn toward biomimetics to explore and construct materials inspired by natural phenomena. Strategies to mitigate the bacterial colonization on the device surfaces are urgently needed that are equipped with synergistic elements like surface chemistry and surface roughness that are unfavorable for bacterial attachment. Keeping this in mind, there has been tremendous growth in the development of Slippery liquid-infused porous surfaces (SLIPS).[204, 205] These surfaces are a new class of antifouling materials and are an inspiration from the gastrointestinal tract that takes the advantage of van der Waals and capillary forces between fouling liquid and infused polymer.

Together these forces generate an atmosphere in which they actively favor the infusing liquid as opposed to the fouling fluid resulting in a continuous infused surface. The SLIPs materials provide an antifouling approach to resist the adhesion of pathogenic microorganisms and protein without affecting the NO release which can be achieved by infusing the polymer with biocompatible silicone oil (Si oil).[206]

Nitric oxide-releasing medical devices made of silicone rubber polymer have shown promising ability to be infused with Si oil for creating an antimicrobial and antifouling interface.[25, 203, 207, 208] Such surfaces can be impregnated with NO donor, SNAP, and then later infused with silicone oil to generate the antifouling surfaces. Reports suggest that the infusion of Si oil not only improved the controlled release of NO, but also reduced the leaching of SNAP while maintaining the ultra-low fouling property of liquid-infused silicone tubing surface.[207] Further, the Liquid-Infused Nitric Oxide-Releasing (LINORel) surface exhibited 99% and 88% reduction in viable cell adhesion of *S. aureus* and *P. aeruginosa* respectively over 7 days in a CDC bioreactor environment.[207] Moreover, the fabricated NO-releasing non-fouling surface was also found to be non-cytotoxic toward mammalian fibroblast cells. A similar methodology was reported with other SR-based medical devices for the use of urinary catheters and insulin cannula with long-term NO release, reduced SNAP leaching, and protein fouling in addition to excellent antibacterial, antifouling, and biocompatible properties. [25, 203, 209] This is a simple and promising approach to generate LINORel on prefabricated medical devices and therefore holds huge potential in clinical translation. Recently, a novel method to generate NO-releasing Si oil with proactive antibacterial properties was reported that involved covalently immobilizing NO donor to Si oil or generating NO-releasing Si oil by nitrosating the thiolated Si oils.[210, 211] Such oils can be infused on the PDMS surface that often used for biomedical device applications to create an antibacterial interface. NO release from these surfaces can be controlled by modulating the NO-payload based on the type

of application. These studies confirmed the ability to tune the NO surface flux by altering the percent thiol conversion to NO moiety in the NO-releasing Si oil.[210]

1.6.3 NO-releasing Surface with Zwitterionic Properties

To augment the efficacy of NO-releasing surfaces, antifouling zwitterionic-based compounds have been employed. To explore the covalent grafting of zwitterionic polymers to various substrates ranging from hydrophilic to hydrophobic, benzophenone (BP) chromophore, a photo-active tethering reagent was incorporated into the polymeric backbone.[212] The covalent grafting of the synthesized antifouling zwitterionic terpolymer, 2-methacryloyloxyethyl phosphorylcholine-co-butyl methacrylateco-benzophenone (BPMPC) to SNAP incorporated CarboSil through rapid UV-cross-linking resulted in a stable hydrophilic coating (contact angle ~50°) with the antimicrobial ability and excellent antifouling properties. The developed zwitterionic coating material showed a significant reduction (ca. 84−93%) of protein adhesion compared to the control samples. A similar trend was observed for SNAP incorporated CarboSil composite with BPMPC topcoat which also exhibited a 99% reduction of viable *S. aureus* when compared to control samples. Facile treatment of phosphorylcholine-based polyzwitterion and its covalent attachment to a hydrophobic CarboSil polymer also inspired the fabrication of antimicrobial, anti-inflammatory, and antithrombotic vascular catheters.[213] The SNAP-BPMPC catheters released NO above physiological levels for over 1 week. The SNAP-BPMPC catheters exhibited a significant reduction in viable *S. aureus* (97%) after 7 d in a CDC bioreactor environment. The SNAP-BPMPC catheters also demonstrated excellent hemocompatibility in an *in vivo* rabbit model over a 7-d period.

1.6.4 NO-Releasing Surface with Topographical Patterns

Nano- or micro-topographies in combination with NO release have been demonstrated to be useful methodologies to prevent and manage bacterial attachment and biofilm development

on a polymeric substrate. While the patterns can inhibit bacterial attachment in the initial timepoints, NO with biocidal properties can actively kill the bacteria and disperse the biofilms over longer durations.[214, 215] These strategies can inhibit medical device-related infections with no known antibiotic resistance. When the NO-releasing materials are incorporated into the physically modified surfaces, it exhibits an enhanced dual functioning antimicrobial property with reduced foreign body response.[214-216] This phenomenon was verified with a textured polyurethane-based film containing SNAP as the NO-releasing material in the sublayer and an ordered submicron pillar topographies at the top surface.[217] A series of SNAP-textured films with CarboSil 20 80A polyurethane, in which the middle layer of PU was doped with 5 wt%, 10 wt%, and 15 wt% SNAP, and the top surface layer was textured with patterns of 400/400 nm or 500/500 nm using a soft lithography two-stage replication molding technique. The hydrophobicity of PU was seen to increase due to surface texturing (water contact angle changed from 91° to 139°). The NO release rate, reduction in bacterial adhesion, and biofilm formation were in correlation and directly proportional to SNAP concentration in the sublayer. A synergistic effect on the inhibition of *S. epidermidis* bacterial adhesion was observed due to the combination of NO release and surface texturing. Biomimetic SNAP textured CarboSil PU surface containing 15 wt% SNAP and the 500/500 nm pattern surface texture reduced the bacterial adhesion by 88% and inhibited biofilm formation for at least 28 d. However, one disadvantage of the repeated spin-coating process was that depositing the SNAP-polymer solution onto a dried SNAP-polymer surface can cause re-dissolution and re-crystallization of the NO donor, instigating untimely degradation during the fabrication method. To reduce the loss of activity, a new method that utilized the impregnation of SNAP on a textured polymer surface was recently reported.[215] The 700/700/300 nm surface texture alone reduced the surface-bound bacteria counts by 49%, 28%, 52%, and 27% for *P. aeruginosa*, *S. aureus*, *S. epidermidis*, and *E. coli*, respectively, after only 1 h of incubation. However, the 15 wt% SNAP impregnated samples in the 700/700/300 nm textured surface, reduced the degree of bacterial adhesion with 88%, 61%, 85%, and 85% inhibition rates, for the

same four bacteria strains over the 1 h test period corroborating the synergistic effect of SNAP and the textured surface towards the reduction of bacterial adhesion to the polymer surface.

1.7 Summary

The recent progress in biomaterials science and biomedical engineering has led to the development of robust dual-function antibacterial surfaces. These materials contain dual antimicrobial strategies combined into one system with either two active antimicrobial actions (active-active) or an antimicrobial combined with antifouling actions (active-passive). The literature research done in this review confirms that the recent developments made in producing dual-functional surfaces can synergistically enhance the antibacterial effect of other antibacterial agents such as antibiotics, metal nanoparticles, or nitric oxide, showing an effective antibacterial therapy compared to traditional monofunctional surfaces. While active-active approaches might be better suited for shorter-term device applications since their antimicrobial reservoir will become depleted over time, the active-passive approaches have the advantage of initial active antimicrobials to fight initial infection while the passive moieties can continue protecting the surface longer (provided that the antifouling chemistry is stable). This can be a crucial issue in medical devices with long-term implantation, such as heart valves, that can get seriously infected years after the surgery which might necessitate a long-term solution. Ultimately the specific material requirements have to be considered for the final medical device application since not all dual-functional materials may be the best approach to addressing infection challenges universally for all medical device applications. For example, the anti-adhesive/antifouling materials approaches may have limitations in orthopedic applications because it is a significant challenge to fabricate an implant that inhibits bacterial colonization and concomitantly promotes osteoblast adhesion. Combinational surfaces with such mechanisms might, however, prove beneficial for urinary and intravascular catheters that do not require such prerequisites. In fact, vascular catheters require the inhibition of platelets and plasma proteins (albumin, fibrinogen,

fibronectin, etc.) attachment on the device surface. It is understood that the adsorption of proteins can trigger platelet activation and blood-clotting which is highly undesirable for blood-contacting devices. Similarly, the microenvironment of the urinary catheter implant site may contain proteins and electrolytes which may accumulate over time and negatively impact the function of the urinary catheter. Therefore, having a combinational surface with both antimicrobial and antifouling strategies can significantly prevent the adhesion of biomolecules in addition to actively eradicating bacteria which can all improve the function and lifetime of the device.

Strategies involving metal nanoparticles, antibiotics, or QAC integrated with antifouling mechanisms like polymer brushes, and topographies have been seen to exhibit promising activity in the initial microbe exposure time points. However, the success rate of these medical devices *in vivo* for long-term applications has been limited due to other underlying biological issues associated with medical devices (eg., thrombosis and inflammation). Since medical-device-related infection is a complex series of steps, many of these materials still lack the universal properties needed to prevent biofilm on the device surface. Moreover, most contact-killing biocides have a higher probability of failing against superbugs with multidrug resistance. To overcome these problems, nitric oxide (NO)-releasing polymers have been extensively explored in the field of biomedical engineering for their therapeutic efficiency. These materials have not only exhibited synergistic effects when combined with other antimicrobial/antifouling strategies against clinically resistant bacterial strains but also demonstrated the ability to address multiple biocompatibility challenges including thrombosis and inflammation, without any reported cytotoxicity or resistance concerns. Furthermore, NO-releasing materials alone have been promising in both short- and long-term animal models;[162, 223] however, a potential limitation with other dual-functional materials reported in the literature is that similar animal studies have not yet been conducted. Even with significant growth in the development of antimicrobial surfaces with multiple functionalities in the literature, to date, not many platforms have accomplished clinical

translational success. This can possibly be related to the functions and properties of multifunctional biomedical devices in long-term applications and severe gaps in meeting the requirements of translational research. There is also no comprehensive evidence in the studies reviewed detailing how the dual functional materials would affect the resistance mechanisms in the biofilm-forming pathogens. Therefore, future studies with dual functionality should consider studying the long-term cytotoxic effects, biocompatibility, and bacterial resistance of the developed material primarily for *in vivo* applications in clinically applicable models (e.g., specific medical device applications).

All the bactericidal agents have their respective disadvantages relating to their shelf-life stability, limited advancement to *in vivo* application, long-term effectiveness, biocompatibility, cost, and ease of synthesis. Moreover, as seen with the topographical designs, not all structures are effective against all types of bacteria and more importantly, these surfaces have not been tested in long-term animal models. Many of these approaches need to be scalable for clinically relevant size medical devices, easy to manufacture, and well prepared for the regulatory pathway in order to be translated to clinical use in patients. Although some materials reported in literature might seem promising with small-scale *in vitro* studies, the translatability of some material designs remains a challenge. Since the biological microenvironments are known to be considerably complex, it is imperative to evaluate the dual functional biomedical materials and devices discussed here for their antimicrobial performance in end-use medical device applications.

1.8 Statement of Dissertation Research

NO-releasing materials have encountered difficulties in clinical translation of materials due to uncontrolled NO release, heat sensitivity of NO donors during the polymer extrusion process, restricted shelf-life stability, and inability to thwart fouling on materials. The key goal of this dissertation was to solve these significant challenges by developing NO-releasing antibacterial medical devices that can control the NO release from biomedical materials, augment stability at

room temperature, and prevent biofouling on biomedical device surface. This dissertation was prepared using a manuscript-style format, where every chapter is taken from articles that have already been published in peer-reviewed scientific journals or currently being prepared for submission. The introductory Chapter 1 also has parts derived from a review article that is published in the journal *ACS Materials Au* and featured as a cover.[224]

In the first approach, the synergy of NO-releasing materials with other active or passive strategies was explored. The combination of active-passive strategy is presented in Chapter 2 where NO-releasing active surface was combined with a passive antifouling strategy with the ability to reduce biofouling on insulin cannula surfaces. Insulin cannula developed in this study provided continuous NO release and an antifouling interface for > 14 d which also exhibited a significant reduction in protein and bacterial adhesion. This method of developing dual function nitric oxide-releasing and antifouling surface for subcutaneous insulin infusion cannulas applications carries promising ability to decrease the rate of infection and inflammation related to insulin pump delivery systems. This work has been published in the journal *ACS Applied Bio Materials*.[25]

Chapter 3 presents an active-active approach where NO-releasing silicone rubber polymer was top-coated with a broad-spectrum antiseptic called chlorhexidine (CHXD) to elevate the antibacterial and biocompatible properties of NO-releasing materials. The dual-active NO-CHXD films were able to significantly lower *E. coli* and *S. aureus* bacteria (> 3-log reduction) adhesion on the surface of films compared to unmodified and single controls with no explicit toxicity towards mouse fibroblast cells. This work has been published in the *Journal of Biomedical Materials Research Part A* and featured as a cover for the journal.[172]

In the second approach, a method to tune NO release via additive manufacturing and light has been presented. Chapter 4 utilizes additive manufacturing to custom fabricate polymeric devices and presents methodology to incorporate NO donor chemistry in 3D-printed polymers.

Tuning the surface porosities can result in tunable NO donor loading and NO release. All the NO-releasing films studied demonstrated >99% prevention of viable *S. aureus* bacteria on the surface as compared to unmodified control films exhibiting the potential for incorporating NO-donors in 3D-printed medical devices such as 3D-scaffolds, catheters, etc. This work has been published in the journal *Biomaterials Science*.[37]

Similarly, light is known to catalyse NO release from RSNO forms of NO donors. In Chapter 5, the photocatalytic property of SNAP was used to design a disposable catheter disinfection insert (DCDI) which involved SNAP-impregnated silicone rubber tubing mounted on a side glowing fiber optic. NO release from DCDI can be regulated real-time using a simple smartphone application where both light wavelength and intensity can be modulated to achieve different levels of NO. The thin and flexible nature of DCDI can be used to disinfect various types of catheters such as vascular, hemodialysis, urinary etc. Results from the study showed that DCDI can inhibit >99% of viable bacterial adhesion on surface and exterminate 97% of pre-colonized bacteria on catheter devices. This work has been published in the *Journal of Controlled Release* and featured as a cover for the journal.[163]

Together, data acquired from these newly designed NO-releasing surfaces highlights the capacity of tuning the NO release via surface porosity or photolytic degradation of NO donor to modulate NO release in real-time. Additionally, the combination of other active (antimicrobial) and passive (antifouling) approaches with NO-releasing materials can help in the fabrication of advanced medical device surfaces with superior antimicrobial and antifouling properties. The surface strategies demonstrated in this dissertation can be the next generation biocompatible solution for combating medical device-associated infections.

1.9 References

1. Zhou, C.; Song, H.; Zhang, F.; Liu, J.; Li, J.; Liu, B.; Liang, J., A Facile Method To Fabricate An Antimicrobial Coating Based On Poly(1-Vinyl-3-Allylimidazolium Iodide) (Pavi) And Poly(Ethylene Glycol) Dimethyl Acrylate (Pegdma). *Polymer Bulletin* **2018,** *76* (10), 5433-5449.

2. Zhao, Y. Q.; Sun, Y.; Zhang, Y.; Ding, X.; Zhao, N.; Yu, B.; Zhao, H.; Duan, S.; Xu, F. J., Well-Defined Gold Nanorod/Polymer Hybrid Coating With Inherent Antifouling And Photothermal Bactericidal Properties For Treating An Infected Hernia. *ACS Nano* **2020,** *14* (2), 2265-2275.

3. Neoh, K. G.; Li, M.; Kang, E. T.; Chiong, E.; Tambyah, P. A., Surface Modification Strategies For Combating Catheter-Related Complications: Recent Advances And Challenges. *J Mater Chem B* **2017,** *5* (11), 2045-2067.

4. Ghasemlou, M.; Daver, F.; Ivanova, E. P.; Rhim, J. W.; Adhikari, B., Switchable Dual-Function And Bioresponsive Materials To Control Bacterial Infections. *ACS Appl Mater Interfaces* **2019,** *11* (26), 22897-22914.

5. Zhang, N.; Ma, S., Recent Development Of Membrane-Active Molecules As Antibacterial Agents. *Eur J Med Chem* **2019,** *184*, 111743.

6. De-La-Pinta, I.; Cobos, M.; Ibarretxe, J.; Montoya, E.; Eraso, E.; Guraya, T.; Quindos, G., Effect Of Biomaterials Hydrophobicity And Roughness On Biofilm Development. *J Mater Sci Mater Med* **2019,** *30* (7), 77.

7. Zander, Z. K.; Becker, M. L., Antimicrobial And Antifouling Strategies For Polymeric Medical Devices. *ACS Macro Letters* **2017,** *7* (1), 16-25.

8. Petrachi, T.; Resca, E.; Piccinno, M. S.; Biagi, F.; Strusi, V.; Dominici, M.; Veronesi, E., An Alternative Approach To Investigate Biofilm In Medical Devices: A Feasibility Study. *Int J Environ Res Public Health* **2017,** *14* (12).

9. Khatoon, Z.; Mctiernan, C. D.; Suuronen, E. J.; Mah, T. F.; Alarcon, E. I., Bacterial Biofilm Formation On Implantable Devices And Approaches To Its Treatment And Prevention. *Heliyon* **2018,** *4* (12), E01067.

10. Rasmussen, T. B.; Givskov, M., Quorum-Sensing Inhibitors As Anti-Pathogenic Drugs. *Int. J. Med. Microbiol.***2006,** *296* (2-3), 149-161.

11. Stewart, P. S.; William Costerton, J., Antibiotic Resistance Of Bacteria In Biofilms. *The Lancet* **2001,** *358* (9276), 135-138.

12. Dincer, S.; Uslu, F. M.; Delik, A., *Bacterial Biofilms*, Intechopen: **2020**, Pp. 1–14.

13. Ramasamy, M.; Lee, J., Recent Nanotechnology Approaches For Prevention And Treatment Of Biofilm-Associated Infections On Medical Devices. *Biomed Res Int* **2016,** *2016*, 1851242.

14. Li, Z.; Yang, X.; Liu, H.; Yang, X.; Shan, Y.; Xu, X.; Shang, S.; Song, Z., Dual-Functional Antimicrobial Coating Based On A Quaternary Ammonium Salt From Rosin Acid With In Vitro And In Vivo Antimicrobial And Antifouling Properties. *Chem. Eng. J.* **2019,** *374*, 564-575.

15. Xu, T.; Zhang, J.; Zhu, Y.; Zhao, W.; Pan, C.; Ma, H.; Zhang, L., A Poly(Hydroxyethyl Methacrylate)-Ag Nanoparticle Porous Hydrogel For Simultaneous In Vivo Prevention Of The Foreign-Body Reaction And Bacterial Infection. *Nanotechnology* **2018,** *29* (39), 395101.

16. Dumée, L. F.; He, L.; King, P. C.; Le Moing, M.; Güller, I.; Duke, M.; Hodgson, P. D.; Gray, S.; Poole, A. J.; Kong, L., Towards Integrated Anti-Microbial Capabilities: Novel Bio-Fouling Resistant Membranes By High Velocity Embedment Of Silver Particles. *Journal Of Membrane Science* **2015,** *475*, 552-561.

17. Huang, K. S.; Yang, C. H.; Huang, S. L.; Chen, C. Y.; Lu, Y. Y.; Lin, Y. S., Recent Advances In Antimicrobial Polymers: A Mini-Review. *Int J Mol Sci* **2016,** *17* (9).

18. Peng, L.; Chang, L.; Si, M.; Lin, J.; Wei, Y.; Wang, S.; Liu, H.; Han, B.; Jiang, L., Hydrogel-Coated Dental Device With Adhesion-Inhibiting And Colony-Suppressing Properties. *ACS Appl Mater Interfaces* **2020,** *12* (8), 9718-9725.

19. Mahlapuu, M.; Hakansson, J.; Ringstad, L.; Bjorn, C., Antimicrobial Peptides: An Emerging Category Of Therapeutic Agents. *Front Cell Infect Microbiol* **2016,** *6*, 194.

20. Ghilini, F.; Rodríguez González, M. C.; Minan, A. G.; Pissinis, D.; Creus, A. H. N.; Salvarezza, R. C.; Schilardi, P. L., Highly Stabilized Nanoparticles On Poly-L-Lysine-Coated Oxidized Metals: A Versatile Platform With Enhanced Antimicrobial Activity. *ACS Appl. Mater. Interfaces* **2018,** *10* (28), 23657-23666.

21. Sánchez-López, E.; Gomes, D.; Esteruelas, G.; Bonilla, L.; Lopez-Machado, A. L.; Galindo, R.; Cano, A.; Espina, M.; Ettcheto, M.; Camins, A., Metal-Based Nanoparticles As Antimicrobial Agents: An Overview. *Nanomaterials* **2020,** *10* (2), 292.

22. Li, Y.; Xu, Y.; Fleischer, C. C.; Huang, J.; Lin, R.; Yang, L.; Mao, H., Impact Of Anti-Biofouling Surface Coatings On The Properties Of Nanomaterials And Their Biomedical Applications. *J Mater Chem B* **2018,** *6* (1), 9-24.

23. Rodriguez-Contreras, A.; Marques-Calvo, M. S.; Gil, F. J.; Manero, J. M., Modification Of Titanium Surfaces By Adding Antibiotic-Loaded Phb Spheres And Peg For Biomedical Applications. *J Mater Sci Mater Med* **2016,** *27* (8), 124.

24. Liu, S.; Guo, W., Anti-Biofouling And Healable Materials: Preparation, Mechanisms, And Biomedical Applications. *Adv. Func. Mater.* **2018,** *28* (41).

25. Chug, M. K.; Feit, C.; Brisbois, E. J., Increasing The Lifetime Of Insulin Cannula With Antifouling And Nitric Oxide Releasing Properties. *ACS Appl. Bio. Mat.* **2019**, *2*(12), Pp.5965-5975.

26. Mora-Boza, A.; Aparicio, F. J.; Alcaire, M.; López-Santos, C.; Espinós, J. P.; Torres-Lagares, D.; Borrás, A.; Barranco, A., Multifunctional Antimicrobial Chlorhexidine Polymers By Remote Plasma Assisted Vacuum Deposition. *Frontiers Of Chemical Science And Engineering* **2019,** *13* (2), 330-339.

27. Gao, K.; Su, Y.; Zhou, L.; He, M.; Zhang, R.; Liu, Y.; Jiang, Z., Creation Of Active-Passive Integrated Mechanisms On Membrane Surfaces For Superior Antifouling And Antibacterial Properties. *Journal Of Membrane Science* **2018,** *548*, 621-631.

28. Wang, L.-S.; Gopalakrishnan, S.; Luther, D. C.; Rotello, V. M., Protein-Based Films As Antifouling And Drug-Eluting Antimicrobial Coatings For Medical Implants. *ACS Appl. Mater. Interfaces* **2021,** *13* (40), 48301-48307.

29. Khlyustova, A.; Kirsch, M.; Ma, X.; Cheng, Y.; Yang, R., Surfaces With Antifouling-Antimicrobial Dual Function Via Immobilization Of Lysozyme On Zwitterionic Polymer Thin Films. *J. Mater. Chem. B* **2022,** *10* (14), 2728-2739.

30. Salim, N.; Silikas, N.; Satterthwaite, J.; Moore, C.; Ramage, G.; Rautemaa, R., Chlorhexidine-Impregnated Pem/Thfm Polymer Exhibits Superior Activity To Fluconazole-Impregnated Polymer Against Candida Albicans Biofilm Formation. *Int. J. Antimicrob. Agents* **2013,** *41* (2), 193-196.

31. Wassil, S. K.; Crill, C. M.; Phelps, S. J., Antimicrobial Impregnated Catheters In The Prevention Of Catheter-Related Bloodstream Infection In Hospitalized Patients. *J. Pediatric Pharmacol. Therap.* **2007,** *12* (2), 77-90.

32. Belfield, K.; Chen, X.; Smith, E. F.; Ashraf, W.; Bayston, R., An Antimicrobial Impregnated Urinary Catheter That Reduces Mineral Encrustation And Prevents Colonisation By Multi-Drug Resistant Organisms For Up To 12 Weeks. *Acta Biomater.* **2019,** *90*, 157-168.

33. Liu, H.; Shukla, S.; Vera-González, N.; Tharmalingam, N.; Mylonakis, E.; Fuchs, B. B.; Shukla, A., Auranofin Releasing Antibacterial And Antibiofilm Polyurethane Intravascular Catheter Coatings. *Frontiers In Cellular And Infection Microbiology* **2019,** *9*, 37.

34. Liedberg D, L. T., Silver Alloy Coated Catherters Reduce Catheter-Associated Bacteriuria. *Bju International* **1990,** *65* (4), 379-381.

35. Redfern, J.; Geerts, L.; Seo, J. W.; Verran, J.; Tosheva, L.; Wee, L. H., Toxicity And Antimicrobial Properties Of Zno@ Zif-8 Embedded Silicone Against Planktonic And Biofilm Catheter-Associated Pathogens. *ACS Appl Nano Mater.* **2018,** *1* (4), 1657-1665.

36. Feit, C.; Chug, M. K.; Brisbois, E. J., Development Of S-Nitroso-N-Acetylpenicillamine (Snap) Impregnated Medical Grade Polyvinyl Chloride For Antimicrobial Medical Device Interfaces. *ACS Appl Bio Mater.* **2019**, *2*(10), 4335-4345.

37. Chug, M. K.; Bachtiar, E.; Narwold, N.; Gall, K.; Brisbois, E. J., Tailoring Nitric Oxide Release With Additive Manufacturing To Create Antimicrobial Surfaces. *Biomater. Sci.* **2021**, *9*(8), Pp.3100-3111.

38. Wang, H.; Tong, H.; Liu, H.; Wang, Y.; Wang, R.; Gao, H.; Yu, P.; Lv, Y.; Chen, S.; Wang, G., Effectiveness Of Antimicrobial-Coated Central Venous Catheters For Preventing Catheter-Related Blood-Stream Infections With The Implementation Of Bundles: A Systematic Review And Network Meta-Analysis. *Annals Of Intensive Care* **2018,** *8* (1), 1-12.

39. Fu, Y.; Yang, Y.; Xiao, S.; Zhang, L.; Huang, L.; Chen, F.; Fan, P.; Zhong, M.; Tan, J.; Yang, J., Mixed Polymer Brushes With Integrated Antibacterial And Antifouling Properties. *Prog. Org. Coat.* **2019,** *130*, 75-82.

40. Li, P.; Ding, Z.; Yin, Y.; Yu, X.; Yuan, Y.; Brió, M.; De Beer, S.; Vancso, G. J.; Yu, Y.; Zhang, S., Cu2+-Doping Of Polyanionic Brushes: A Facile Route To Prepare Implant Coatings With Both Antifouling And Antibacterial Properties. *Eur. Polym. J.* **2020**, 109845.

41. He, Y.; Wan, X.; Lin, W.; Li, J.; Li, Z.; Luo, F.; Li, J.; Tan, H.; Fu, Q., The Synergistic Effect Of Hierarchical Structure And Alkyl Chain Length On The Antifouling And Bactericidal Properties Of Cationic/Zwitterionic Block Polymer Brushes. *Biomater. Sci.* **2020,** *8* (24), 6890-6902.

42. Gao, Q.; Li, P.; Zhao, H.; Chen, Y.; Jiang, L.; Ma, P. X., Methacrylate-Ended Polypeptides And Polypeptoids For Antimicrobial And Antifouling Coatings. *Poly. Chem.* **2017,** *8* (41), 6386-6397.

43. Rodríguez-Contreras, A.; Marqués-Calvo, M. S.; Gil, F. J.; Manero, J. M., Modification Of Titanium Surfaces By Adding Antibiotic-Loaded Phb Spheres And Peg For Biomedical Applications. *J. Mater Sci: Mater Med.* **2016,** *27* (8), 124.

44. Rahaman, M. S.; Thérien-Aubin, H.; Ben-Sasson, M.; Ober, C. K.; Nielsen, M.; Elimelech, M., Control Of Biofouling On Reverse Osmosis Polyamide Membranes Modified With Biocidal Nanoparticles And Antifouling Polymer Brushes. *J. Mater. Chem. B* **2014,** *2* (12), 1724-1732.

45. Zhang, X.Y.; Zhao, Y.Q.; Zhang, Y.; Wang, A.; Ding, X.; Li, Y.; Duan, S.; Ding, X.; Xu, F.J., Antimicrobial Peptide-Conjugated Hierarchical Antifouling Polymer Brushes For Functionalized Catheter Surfaces. *Biomacromolecules* **2019,** *20* (11), 4171-4179.

46. Wang, Y.; Wu, J.; Zhang, D.; Chen, F.; Fan, P.; Zhong, M.; Xiao, S.; Chang, Y.; Gong, X.; Yang, J., Design Of Salt-Responsive And Regenerative Antibacterial Polymer Brushes With Integrated Bacterial Resistance, Killing, And Release Properties. *J. Mater. Chem. B* **2019,** *7* (38), 5762-5774.

47. Stebbins, N. D.; Ouimet, M. A.; Uhrich, K. E., Antibiotic-Containing Polymers For Localized, Sustained Drug Delivery. *Advanced Drug Delivery Reviews* **2014,** *78*, 77-87.

48. Aumsuwan, N.; Heinhorst, S.; Urban, M. W., Antibacterial Surfaces On Expanded Polytetrafluoroethylene; Penicillin Attachment. *Biomacromolecules* **2007,** *8* (2), 713-718.

49. Aumsuwan, N.; Heinhorst, S.; Urban, M. W., The Effectiveness Of Antibiotic Activity Of Penicillin Attached To Expanded Poly (Tetrafluoroethylene)(Eptfe) Surfaces: A Quantitative Assessment. *Biomacromolecules* **2007,** *8* (11), 3525-3530.

50. Zeng, Q.; Zhu, Y.; Yu, B.; Sun, Y.; Ding, X.; Xu, C.; Wu, Y.-W.; Tang, Z.; Xu, F.J., Antimicrobial And Antifouling Polymeric Agents For Surface Functionalization Of Medical Implants. *Biomacromolecules* **2018,** *19* (7), 2805-2811.

51. Yu, M.; Ding, X.; Zhu, Y.; Wu, S.; Ding, X.; Li, Y.; Yu, B.; Xu, F.J., Facile Surface Multi-Functionalization Of Biomedical Catheters With Dual-Microcrystalline Broad-Spectrum

Antibacterial Drugs And Antifouling Poly(Ethylene Glycol) For Effective Inhibition Of Bacterial Infections. *ACS Appl. Bio. Mat.* **2019,** *2* (3), 1348-1356.

52. Bernier, S. P.; Surette, M. G., Concentration-Dependent Activity Of Antibiotics In Natural Environments. *Front Microbiol.* **2013,** *4*, 20.

53. Kim, Y.S, S. M., Park Jd, Et Al., Subchronic Oral Toxicity Of Silver Nanoparticles. *Particle And Fibre Toxicology* **2010,** (7), 20.

54. Zhang, T.; Wang, L.; Chen, Q.; Chen, C., Cytotoxic Potential Of Silver Nanoparticles. *Yonsei Medical Journal* **2014,** *55* (2), 283-291.

55. Karademir, F.; Ayhan, F., Antimicrobial Surface Functionality Of Peg Coated And Agnps Immobilized Extracorporeal Biomaterials. **2021**,12 (1), 1039-1052.

56. Ragaseema, V.; Unnikrishnan, S.; Krishnan, V. K.; Krishnan, L. K., The Antithrombotic And Antimicrobial Properties Of Peg-Protected Silver Nanoparticle Coated Surfaces. *Biomaterials* **2012,** *33* (11), 3083-3092.

57. Nie, C.; Yang, Y.; Cheng, C.; Ma, L.; Deng, J.; Wang, L.; Zhao, C., Bioinspired And Biocompatible Carbon Nanotube-Ag Nanohybrid Coatings For Robust Antibacterial Applications. *Acta Biomater.* **2017,** *51*, 479-494.

58. Chaudhari, A. A.; Jasper, S. L.; Dosunmu, E.; Miller, M. E.; Arnold, R. D.; Singh, S. R.; Pillai, S., Novel Pegylated Silver Coated Carbon Nanotubes Kill Salmonella But They Are Non-Toxic To Eukaryotic Cells. *Journal Of Nanobiotechnology* **2015,** *13* (1), 23.

59. Chaudhari, A. A.; Deb Nath, S.; Kate, K.; Dennis, V.; Singh, S. R.; Owen, D. R.; Palazzo, C.; Arnold, R. D.; Miller, M. E.; Pillai, S. R., A Novel Covalent Approach To Bio-Conjugate Silver Coated Single Walled Carbon Nanotubes With Antimicrobial Peptide. *Journal Of Nanobiotechnology* **2016,** *14* (1), 58.

60. He, W.; Zhang, Y.; Li, J.; Gao, Y.; Luo, F.; Tan, H.; Wang, K.; Fu, Q., A Novel Surface Structure Consisting Of Contact-Active Antibacterial Upper-Layer And Antifouling Sub-Layer Derived From Gemini Quaternary Ammonium Salt Polyurethanes. *Sci. Rep.* **2016,** *6*, 32140.

61. Zhang, Y.; He, X.; Ding, M.; He, W.; Li, J.; Li, J.; Tan, H., Antibacterial And Biocompatible Cross-Linked Waterborne Polyurethanes Containing Gemini Quaternary Ammonium Salts. *Biomacromolecules* **2018,** *19* (2), 279-287.

62. Xu, Q.; Li, X.; Jin, Y.; Sun, L.; Ding, X.; Liang, L.; Wang, L.; Nan, K.; Ji, J.; Chen, H., Bacterial Self-Defense Antibiotics Release From Organic–Inorganic Hybrid Multilayer Films For Long-Term Anti-Adhesion And Biofilm Inhibition Properties. *Nanoscale* **2017,** *9* (48), 19245-19254.

63. Lee, J.; Yoo, J.; Kim, J.; Jang, Y.; Shin, K.; Ha, E.; Ryu, S.; Kim, B.-G.; Wooh, S.; Char, K., Development Of Multimodal Antibacterial Surfaces Using Porous Amine-Reactive Films Incorporating Lubricant And Silver Nanoparticles. *ACS Appl. Mater. Interfaces* **2019,** *11* (6), 6550-6560.

64. Cabana, S.; Lecona-Vargas, C. S.; Meléndez-Ortiz, H. I.; Contreras-García, A.; Barbosa, S.; Taboada, P.; Magarinos, B.; Bucio, E.; Concheiro, A.; Alvarez-Lorenzo, C., Silicone Rubber Films Functionalized With Poly (Acrylic Acid) Nanobrushes For Immobilization Of Gold Nanoparticles And Photothermal Therapy. *J. Drug Delivery Sci. Technol.* **2017,** *42*, 245-254.

65. Vaterrodt, A.; Thallinger, B.; Daumann, K.; Koch, D.; Guebitz, G. M.; Ulbricht, M., Antifouling And Antibacterial Multifunctional Polyzwitterion/Enzyme Coating On Silicone Catheter Material Prepared By Electrostatic Layer-By-Layer Assembly. *Langmuir* **2016,** *32* (5), 1347-1359.

66. Shevtsova, T.; Cavallaro, G.; Lazzara, G.; Milioto, S.; Donchak, V.; Harhay, K.; Korolko, S.; Budkowski, A.; Stetsyshyn, Y., Temperature-Responsive Hybrid Nanomaterials Based On Modified Halloysite Nanotubes Uploaded With Silver Nanoparticles. *Colloids Surf., A* **2022,** *641*, 128525.

67. Li, P.; Ding, Z.; Yin, Y.; Yu, X.; Yuan, Y.; Pérez, M. B.; De Beer, S.; Vancso, G. J.; Yu, Y.; Zhang, S., Cu2+-Doping Of Polyanionic Brushes: A Facile Route To Prepare Implant Coatings With Both Antifouling And Antibacterial Properties. *Eur. Polym. J.* **2020,** *134*, 109845.

68. Kulka, M. W., *Mussel-Inspired Polyglycerol Coatings For The Prevention Of Biomaterial-Related Fouling*. Freie Universitaet Berlin (Germany): 2020.

69. Pelosi, C.; Tinè, M. R.; Wurm, F. R., Main-Chain Water-Soluble Polyphosphoesters: Multi-Functional Polymers As Degradable Peg-Alternatives For Biomedical Applications. *Eur. Polym. J.* **2020,** *141*, 110079.

70. Svoboda, J.; Sedláček, O. E.; Riedel, T. S.; Hrubý, M.; Pop-Georgievski, O., Poly (2-Oxazoline) S One-Pot Polymerization And Surface Coating: From Synthesis To Antifouling Properties Out-Performing Poly (Ethylene Oxide). *Biomacromolecules* **2019,** *20* (9), 3453-3463.

71. Liu, F.; Qu, W.; Zhang, J.; Liu, J.; Zhu, Q.; Yue, T.; Xu, X.; Ma, N.; Ma, J.; Sun, Y., Cationic Alternating Polypeptide Fixed On Polyurethane At Multiple Sites For Excellent Antibacterial And Antifouling Properties. *Langmuir* **2021,** *37* (36), 10657-10667.

72. Chen, C.; Li, Z.; Li, X.; Kuang, C.; Liu, X.; Song, Z.; Liu, H.; Shan, Y., Dual-Functional Antimicrobial Coating Based On The Combination Of Zwitterionic And Quaternary Ammonium Cation From Rosin Acid. *Composites, Part B* **2022**, 109623.

73. Sun, W.; Liu, J.; Hao, Q.; Lu, K.; Wu, Z.; Chen, H., A Novel Y-Shaped Photoiniferter Used For The Construction Of Polydimethylsiloxane Surfaces With Antibacterial And Antifouling Properties. *J. Mater. Chem. B* **2022,** *10* (2), 262-270.

74. Ahmadabadi, H. Y.; Yu, K.; Kizhakkedathu, J. N., Surface Modification Approaches For Prevention Of Implant Associated Infections. *Colloids Surf., B* **2020**, 111116.

75. Liang, B.; Jia, E.; Yuan, X.; Zhang, G.; Su, Z., Salt-Responsive Polyzwitterion Brushes Conjugated With Silver Nanoparticles: Preparation And Dual Antimicrobial/Release Properties. *Chem. Eng. J.* **2020,** *401*, 126114.

76. Minbiole, K. P.; Jennings, M. C.; Ator, L. E.; Black, J. W.; Grenier, M. C.; Ladow, J. E.; Caran, K. L.; Seifert, K.; Wuest, W. M., From Antimicrobial Activity To Mechanism Of Resistance: The Multifaceted Role Of Simple Quaternary Ammonium Compounds In Bacterial Eradication. *Tetrahedron* **2016,** *72* (25), 3559-3566.

77. Elena, P.; Miri, K., Formation Of Contact Active Antimicrobial Surfaces By Covalent Grafting Of Quaternary Ammonium Compounds. *Colloids Surf., B* **2018,** *169*, 195-205.

78. Murata, H.; Koepsel, R. R.; Matyjaszewski, K.; Russell, A. J., Permanent, Non-Leaching Antibacterial Surfaces—2: How High Density Cationic Surfaces Kill Bacterial Cells. *Biomaterials* **2007,** *28* (32), 4870-4879.

79. Imazato, S., Bio-Active Restorative Materials With Antibacterial Effects: New Dimension Of Innovation In Restorative Dentistry. *Dent. Mater. J.* **2009,** *28* (1), 11-19.

80. Klibanov, A. M., Permanently Microbicidal Materials Coatings. *J. Mater. Chem.* **2007,** *17* (24), 2479-2482.

81. Xiao, S.; Zhang, Y.; Shen, M.; Chen, F.; Fan, P.; Zhong, M.; Ren, B.; Yang, J.; Zheng, J., Structural Dependence Of Salt-Responsive Polyzwitterionic Brushes With An Anti-Polyelectrolyte Effect. *Langmuir* **2018,** *34* (1), 97-105.

82. Yu, H.; Liu, L.; Yang, H.; Zhou, R.; Che, C.; Li, X.; Li, C.; Luan, S.; Yin, J.; Shi, H., Water-Insoluble Polymeric Guanidine Derivative And Application In The Preparation Of Antibacterial Coating Of Catheter. *ACS Appl. Mater. Interfaces* **2018,** *10* (45), 39257-39267.

83. Zhi, Z.; Su, Y.; Xi, Y.; Tian, L.; Xu, M.; Wang, Q.; Padidan, S.; Li, P.; Huang, W., Dual-Functional Polyethylene Glycol-B-Polyhexanide Surface Coating With In Vitro And In Vivo Antimicrobial And Antifouling Activities. *ACS Appl. Mater. Interfaces* **2017,** *9* (12), 10383-10397.

84. Su, Y.; Zhi, Z.; Gao, Q.; Xie, M.; Yu, M.; Lei, B.; Li, P.; Ma, P. X., Autoclaving-Derived Surface Coating With In Vitro And In Vivo Antimicrobial And Antibiofilm Efficacies. *Adv. Healthcare Mater.* **2017,** *6* (6), 1601173.

85. Jeoung, E.; Duncan, B.; Wang, L. S.; Saha, K.; Subramani, C.; Wang, P.; Yeh, Y. C.; Kushida, T.; Engel, Y.; Barnes, M. D., Fabrication Of Robust Protein Films Using Nanoimprint Lithography. *Adv. Mater.* **2015,** *27* (40), 6251-6255.

86. Wang, L.-S.; Gupta, A.; Duncan, B.; Ramanathan, R.; Yazdani, M.; Rotello, V. M., Biocidal And Antifouling Chlorinated Protein Films. *ACS Biomater. Sci. Eng.* **2016,** *2* (11), 1862-1866.

87. Wang, L.S.; Gopalakrishnan, S.; Rotello, V. M., Tailored Functional Surfaces Using Nanoparticle And Protein "Nanobrick" Coatings. *Langmuir* **2019,** *35* (34), 10993-11006.

88. Wang, L.S.; Gopalakrishnan, S.; Lee, Y.W.; Zhu, J.; Nonnenmann, S. S.; Rotello, V. M., Translation Of Protein Charge And Hydrophilicity To Materials Surface Properties Using Thermal Treatment In Fluorous Media. *Mater. Horiz* **2018,** *5* (2), 268-274.

89. Fan, Y.J.; Pham, M. T.; Huang, C.J., Development Of Antimicrobial And Antifouling Universal Coating Via Rapid Deposition Of Polydopamine And Zwitterionization. *Langmuir* **2018,** *35* (5), 1642-1651.

90. Zhang, C.; Huang, J.; Lan, X.; Qi, H.; Fan, D.; Zhang, L., Synergy Of Bioinspired Chimeric Protein And Silver Nanoparticles For Fabricating "Kill-Release" Antibacterial Coating. *Applied Surface Science* **2021,** *557*, 149799.

91. Cheng, Y.; Feng, G.; Moraru, C. I., Micro-And Nanotopography Sensitive Bacterial Attachment Mechanisms: A Review. *Front Microbiol.* **2019,** *10*, 191.

92. Modaresifar, K.; Azizian, S.; Ganjian, M.; Fratila-Apachitei, L. E.; Zadpoor, A. A., Bactericidal Effects Of Nanopatterns: A Systematic Review. *Acta Biomater.* **2019,** *83*, 29-36.

93. Lazzini, G.; Lutey, A.; Romoli, L.; Fuso, F., Molecular Dynamics Model For The Antibactericity Of Textured Surfaces. *Colloids Surf., B* **2020**, 111504.

94. Ge, X.; Ren, C.; Ding, Y.; Chen, G.; Lu, X.; Wang, K.; Ren, F.; Yang, M.; Wang, Z.; Li, J., Micro/Nano-Structured Tio2 Surface With Dual-Functional Antibacterial Effects For Biomedical Applications. *Bioact. Mater.* **2019,** *4*, 346-357.

95. Díaz, C.; Schilardi, P.; Salvarezza, R.; De Mele, M. F. L., Have Flagella A Preferred Orientation During Early Stages Of Biofilm Formation?: Afm Study Using Patterned Substrates. *Colloids Surf., B* **2011,** *82* (2), 536-542.

96. Hou, S.; Gu, H.; Smith, C.; Ren, D., Microtopographic Patterns Affect Escherichia Coli Biofilm Formation On Poly (Dimethylsiloxane) Surfaces. *Langmuir* **2011,** *27* (6), 2686-2691.

97. Chen, M.; Cai, Y.; Li, G.; Zhao, H.; An, T., The Stress Response Mechanisms Of Biofilm Formation Under Sub-Lethal Photocatalysis. *Appl. Catal., B* **2022,** *307*, 121200.

98. Cao, Y.; Jana, S.; Bowen, L.; Tan, X.; Liu, H.; Rostami, N.; Brown, J.; Jakubovics, N. S.; Chen, J., Hierarchical Rose Petal Surfaces Delay The Early-Stage Bacterial Biofilm Growth. *Langmuir* **2019,** *35* (45), 14670-14680.

99. Jaggessar, A.; Shahali, H.; Mathew, A.; Yarlagadda, P. K., Bio-Mimicking Nano And Micro-Structured Surface Fabrication For Antibacterial Properties In Medical Implants. *J. Nanobiotechnol.* **2017,** *15* (1), 64.

100. Bing, W.; Cai, Y.; Jin, H.; Tian, L.; Tian, L.; Yin, Y.; Teng, Y.; Wang, P.; Hou, Z.; Bai, X., An Antiadhesion And Antibacterial Platform Based On Parylene F Coatings. *Prog. Org. Coat.* **2020**, 106021.

101. Li, S.; Liu, Y.; Tian, Z.; Liu, X.; Han, Z.; Ren, L., Biomimetic Superhydrophobic And Antibacterial Stainless-Steel Mesh Via Double-Potentiostatic Electrodeposition And Modification. *Surf. Coat. Technol.* **2020,** *403*, 126355.

102. Müller, D. W.; Lößlein, S.; Terriac, E.; Brix, K.; Siems, K.; Moeller, R.; Kautenburger, R.; Mücklich, F., Increasing Antibacterial Efficiency Of Cu Surfaces By Targeted Surface Functionalization Via Ultrashort Pulsed Direct Laser Interference Patterning. *Adv. Mater. Interfaces* **2020**, 8(5), 2001656.

103. Cuello, E. A.; Mulko, L. E.; Barbero, C. A.; Acevedo, D. F.; Yslas, E. I., Development Of Micropatterning Polyimide Films For Enhanced Antifouling And Antibacterial Properties. *Colloids Surf., B* **2020,** *188*, 110801.

104. Díaz, C.; Schilardi, P.; Salvarezza, R.; Fernández Lorenzo De Mele, M., Nano/Microscale Order Affects The Early Stages Of Biofilm Formation On Metal Surfaces. *Langmuir* **2007,** *23* (22), 11206-11210.

105. Díaz, C.; Miñán, A.; Schilardi, P.; De Mele, M. F. L., Synergistic Antimicrobial Effect Against Early Biofilm Formation: Micropatterned Surface Plus Antibiotic Treatment. *Int. J. Antimicrob. Agents* **2012,** *40* (3), 221-226.

106. Li, Y. Q.; Zhu, B.; Li, Y.; Leow, W. R.; Goh, R.; Ma, B.; Fong, E.; Tang, M.; Chen, X., A Synergistic Capture Strategy For Enhanced Detection And Elimination Of Bacteria. *Angew. Chem., Int. Ed.* **2014,** *53* (23), 5837-5841.

107. Gao, Q.; Feng, T.; Huang, D.; Liu, P.; Lin, P.; Wu, Y.; Ye, Z.; Ji, J.; Li, P.; Huang, W., Antibacterial And Hydroxyapatite-Forming Coating For Biomedical Implants Based On Polypeptide-Functionalized Titania Nanospikes. *Biomater. Sci.* **2020,** *8* (1), 278-289.

108. Gallarato, L. A.; Mulko, L. E.; Dardanelli, M. S.; Barbero, C. A.; Acevedo, D. F.; Yslas, E. I., Synergistic Effect Of Polyaniline Coverage And Surface Microstructure On The Inhibition Of Pseudomonas Aeruginosa Biofilm Formation. *Colloids Surf., B* **2017,** *150*, 1-7.

109. Dundar Arisoy, F.; Kolewe, K. W.; Homyak, B.; Kurtz, I. S.; Schiffman, J. D.; Watkins, J. J., Bioinspired Photocatalytic Shark-Skin Surfaces With Antibacterial And Antifouling Activity Via Nanoimprint Lithography. *ACS Appl. Mater. Interfaces* **2018,** *10* (23), 20055-20063.

110. Tang, Y.; Sun, H.; Qin, Z.; Yin, S.; Tian, L.; Liu, Z., Bioinspired Photocatalytic Zno/Au Nanopillar-Modified Surface For Enhanced Antibacterial And Antiadhesive Property. *Chem. Eng. J.* **2020**, 125575.

111. Khalid, S.; Gao, A.; Wang, G.; Chu, P. K.; Wang, H., Tuning Surface Topographies On Biomaterials To Control Bacterial Infection. *Biomater. Sci.* **2020,** *8* (24), 6840-6857.

112. Wang, J.; Wu, B.; Dhyani, A.; Repetto, T.; Gayle, A. J.; Cho, T. H.; Dasgupta, N. P.; Tuteja, A., Durable Liquid-And Solid-Repellent Elastomeric Coatings Infused With Partially Crosslinked Lubricants. *ACS Appl. Mater. Interfaces* **2022**, 14 (19), 22466–22475

113. Ripolles-Avila, C.; Martinez-Garcia, M.; Hascoët, A.-S.; Rodríguez-Jerez, J. J., Bactericidal Efficacy Of Uv Activated Tio2 Nanoparticles Against Gram-Positive And Gram-Negative Bacteria On Suspension. *Cyta-Journal Of Food* **2019,** *17* (1), 408-418.

114. Won, Y.; Schwartzenberg, K.; Gray, K. A., Tio2-Based Transparent Coatings Create Self-Cleaning Surfaces. *Chemosphere* **2018,** *208*, 899-906.

115. Ye, J.; Deng, J.; Chen, Y.; Yang, T.; Zhu, Y.; Wu, C.; Wu, T.; Jia, J.; Cheng, X.; Wang, X., Cicada And Catkin Inspired Dual Biomimetic Antibacterial Structure For The Surface Modification Of Implant Material. *Biomater. Sci.* **2019,** *7* (7), 2826-2832.

116. Bhadra, C. M.; Khanh Truong, V.; Pham, V. T.; Al Kobaisi, M.; Seniutinas, G.; Wang, J. Y.; Juodkazis, S.; Crawford, R. J.; Ivanova, E. P., Antibacterial Titanium Nano-Patterned Arrays Inspired By Dragonfly Wings. *Sci. Rep.* **2015,** *5* (1), 1-12.

117. Hasan, J.; Webb, H. K.; Truong, V. K.; Pogodin, S.; Baulin, V. A.; Watson, G. S.; Watson, J. A.; Crawford, R. J.; Ivanova, E. P., Selective Bactericidal Activity Of Nanopatterned Superhydrophobic Cicada Psaltoda Claripennis Wing Surfaces. *Appl. Microbiol. Biotechnol.* **2013,** *97* (20), 9257-9262.

118. Ge, X.; Leng, Y.; Bao, C.; Xu, S. L.; Wang, R.; Ren, F., Antibacterial Coatings Of Fluoridated Hydroxyapatite For Percutaneous Implants. *J. Biomed. Mater. Res. A* **2010,** *95* (2), 588-599.

119. Ge, X.; Zhao, J.; Esmeryan, K. D.; Lu, X.; Li, Z.; Wang, K.; Ren, F.; Wang, Q.; Wang, M.; Qian, B., Cicada-Inspired Fluoridated Hydroxyapatite Nanostructured Surfaces Synthesized By Electrochemical Additive Manufacturing. *Mater. Des.* **2020**, 108790.

120. He, W.; Kim, H.-K.; Wamer, W. G.; Melka, D.; Callahan, J. H.; Yin, J.-J., Photogenerated Charge Carriers And Reactive Oxygen Species In Zno/Au Hybrid Nanostructures With Enhanced Photocatalytic And Antibacterial Activity. *J. Am. Chem. Soc.* **2014,** *136* (2), 750-757.

121. Sun, Y.; Zhao, Y.Q.; Zeng, Q.; Wu, Y.-W.; Hu, Y.; Duan, S.; Tang, Z.; Xu, F.-J., Dual-Functional Implants With Antibacterial And Osteointegration-Promoting Performances. *ACS Appl. Mater. Interfaces* **2019,** *11* (40), 36449-36457.

122. Gao, Q.; Yu, M.; Su, Y.; Xie, M.; Zhao, X.; Li, P.; Ma, P. X., Rationally Designed Dual Functional Block Copolymers For Bottlebrush-Like Coatings: In Vitro And In Vivo Antimicrobial, Antibiofilm, And Antifouling Properties. *Acta Biomater.* **2017,** *51*, 112-124.

123. Balne, P. K.; Harini, S.; Dhand, C.; Dwivedi, N.; Chalasani, M. L. S.; Verma, N. K.; Barathi, V. A.; Beuerman, R.; Agrawal, R.; Lakshminarayanan, R., Surface Characteristics And Antimicrobial Properties Of Modified Catheter Surfaces By Polypyrogallol And Metal Ions. *Mater. Sci. Eng. C* **2018,** *90*, 673-684.

124. Patel, K.; Kushwaha, P.; Kumar, S.; Kumar, R., Lysine And A-Aminoisobutyric Acid Conjugated Bioinspired Polydopamine Surfaces For The Enhanced Antibacterial Performance Of The Foley Catheter. *ACS Appl. Bio. Mat.* **2019**, 2 (12), 5799–5809.

125. Guo, Y.; Qian, S.; Wang, L.; Zeng, J.; Miao, R.; Meng, Y.; Jin, Y.; Chen, H.; Wang, B., Reversible Antibiotic Loading And Ph-Responsive Release From Polymer Brushes On Contact Lenses For Therapy And Prevention Of Corneal Infections. *J. Mater. Chem. B* **2020,** *8* (44), 10087-10092.

126. Fuchs, A. V.; Ritz, S.; Pütz, S.; Mailänder, V.; Landfester, K.; Ziener, U., Bioinspired Phosphorylcholine Containing Polymer Films With Silver Nanoparticles Combining Antifouling And Antibacterial Properties. *Biomater. Sci.* **2013,** *1* (5), 470-477.

127. Xu, D.; Su, Y.; Zhao, L.; Meng, F.; Liu, C.; Guan, Y.; Zhang, J.; Luo, J., Antibacterial And Antifouling Properties Of A Polyurethane Surface Modified With Perfluoroalkyl And Silver Nanoparticles. *J. Biomed. Mater. Res.* **2016**, *105*(2), 531-538.

128. Smeeth, L.; Cook, C.; Thomas, S.; Hall, A. J.; Hubbard, R.; Vallance, P., Risk Of Deep Vein Thrombosis And Pulmonary Embolism After Acute Infection In A Community Setting. *The Lancet* **2006,** *367* (9516), 1075-1079.

129. Beristain-Covarrubias, N.; Perez-Toledo, M.; Thomas, M. R.; Henderson, I. R.; Watson, S. P.; Cunningham, A. F., Understanding Infection-Induced Thrombosis: Lessons Learned From Animal Models. *Front. Immunol.* **2019**, 2569.

130. Barraud, N.; Hassett, D. J.; Hwang, S.-H.; Rice, S. A.; Kjelleberg, S.; Webb, J. S., Involvement Of Nitric Oxide In Biofilm Dispersal Of Pseudomonas Aeruginosa. *J. Bacteriol.* **2006,** *188* (21), 7344-7353.

131. Barraud, N.; J Kelso, M.; A Rice, S.; Kjelleberg, S., Nitric Oxide: A Key Mediator Of Biofilm Dispersal With Applications In Infectious Diseases. *Curr. Pharm. Des.* **2015,** *21* (1), 31-42.

132. Namivandi-Zangeneh, R.; Sadrearhami, Z.; Bagheri, A.; Sauvage-Nguyen, M.; Ho, K. K. K.; Kumar, N.; Wong, E. H.; Boyer, C., Nitric Oxide-Loaded Antimicrobial Polymer For The Synergistic Eradication Of Bacterial Biofilm. *ACS Macro Letters* **2018,** *7* (5), 592-597.

133. Ashcraft, M.; Douglass, M.; Chen, Y.; Handa, H., Combination Strategies For Antithrombotic Biomaterials: An Emerging Trend Towards Hemocompatibility. *Biomater. Sci.* **2021,** *9* (7), 2413-2423.

134. Evans, C., Nitric Oxide: What Role Does It Play In Inflammation And Tissue Destruction? *Agents Actions Suppl.* **1995,** *47*, 107-116.

135. Ignarro, L. J., Nitric Oxide: Biology And Pathobiology. *Academic Press:* 2000.

136. Butler, A. R.; Nicholson, R., *Life, Death And Nitric Oxide*. Royal Society Of Chemistry: 2003; Vol. 33.

137. Vaughn, M. W.; Kuo, L.; Liao, J. C., Estimation Of Nitric Oxide Production And Reactionrates In Tissue By Use Of A Mathematical Model. *Am. J. Physiol.: Heart Circ. Physiol.* **1998,** *274* (6), H2163-H2176.

138. Carpenter, A. W.; Schoenfisch, M. H., Nitric Oxide Release: Part Ii. Therapeutic Applications. *Chem. Soc. Rev.* **2012,** *41* (10), 3742-3752.

139. Qian, Y.; Kumar, R.; Chug, M. K.; Massoumi, H.; Brisbois, E. J., Therapeutic Delivery Of Nitric Oxide Utilizing Saccharide-Based Materials. *ACS Appl. Mater. Interfaces* **2021,** *13* (44), 52250-52273.

140. Nathan, C. F.; Hibbs Jr, J. B., Role Of Nitric Oxide Synthesis In Macrophage Antimicrobial Activity. *Current Opin. Immunol.* **1991,** *3* (1), 65-70.

141. Jones, M. L.; Ganopolsky, J. G.; Labbé, A.; Wahl, C.; Prakash, S., Antimicrobial Properties Of Nitric Oxide And Its Application In Antimicrobial Formulations And Medical Devices. *Appl. Microbiol. Biotechnol.* **2010,** *88* (2), 401-407.

142. Massoumi, H.; Kumar, R.; Chug, M. K.; Qian, Y.; Brisbois, E. J., Nitric Oxide Release And Antibacterial Efficacy Analyses Of S-Nitroso-N-Acetyl-Penicillamine Conjugated To Titanium Dioxide Nanoparticles. *ACS Appl. Bio. Mat.* **2022,** *5* (5), 2285-2295.

143. Deupree, S. M.; Schoenfisch, M. H., Morphological Analysis Of The Antimicrobial Action Of Nitric Oxide On Gram-Negative Pathogens Using Atomic Force Microscopy. *Acta Biomater.* **2009,** *5* (5), 1405-1415.

144. Gao, Q.; Zhang, X.; Yin, W.; Ma, D.; Xie, C.; Zheng, L.; Dong, X.; Mei, L.; Yu, J.; Wang, C., Functionalized Mos2 Nanovehicle With Near-Infrared Laser-Mediated Nitric Oxide Release And Photothermal Activities For Advanced Bacteria-Infected Wound Therapy. *Small* **2018,** *14* (45), 1802290.

145. Rong, F.; Tang, Y.; Wang, T.; Feng, T.; Song, J.; Li, P.; Huang, W., Nitric Oxide-Releasing Polymeric Materials For Antimicrobial Applications: A Review. *Antioxidants* **2019,** *8* (11), 556.

146. Fang, F. C., Perspectives Series: Host/Pathogen Interactions. Mechanisms Of Nitric Oxide-Related Antimicrobial Activity. *J. Clin. Invest.* **1997,** *99* (12), 2818-2825.

147. Privett, B. J.; Broadnax, A. D.; Bauman, S. J.; Riccio, D. A.; Schoenfisch, M. H., Examination Of Bacterial Resistance To Exogenous Nitric Oxide. *Nitric Oxide* **2012,** *26* (3), 169-173.

148. Wang, P. G.; Xian, M.; Tang, X.; Wu, X.; Wen, Z.; Cai, T.; Janczuk, A. J., Nitric Oxide Donors: Chemical Activities And Biological Applications. *Chem. Rev.* **2002,** *102* (4), 1091-1134.

149. Yang, T.; Zelikin, A. N.; Chandrawati, R., Progress And Promise Of Nitric Oxide-Releasing Platforms. *Adv. Sci.* **2018,** *5* (6), 1701043.

150. Yang, L.; Feura, E. S.; Ahonen, M. J. R.; Schoenfisch, M. H., Nitric Oxide–Releasing Macromolecular Scaffolds For Antibacterial Applications. *Adv. Healthcare Mater.* **2018,** *7* (13), 1800155.

151. Brisbois, E. J.; Handa, H.; Major, T. C.; Bartlett, R. H.; Meyerhoff, M. E., Long-Term Nitric Oxide Release And Elevated Temperature Stability With S-Nitroso-N-Acetylpenicillamine (Snap)-Doped Elast-Eon E2as Polymer. *Biomaterials* **2013,** *34* (28), 6957-6966.

152. Hopkins, S. P.; Pant, J.; Goudie, M. J.; Schmiedt, C.; Handa, H., Achieving Long-Term Biocompatible Silicone Via Covalently Immobilized S-Nitroso-N-Acetylpenicillamine (Snap) That Exhibits 4 Months Of Sustained Nitric Oxide Release. *ACS Appl. Mater. Interfaces* **2018**, 10 (32), pp. 27316-27325.

153. Yang, L.; Wang, X.; Suchyta, D. J.; Schoenfisch, M. H., Antibacterial Activity Of Nitric Oxide-Releasing Hyperbranched Polyamidoamines. *Bioconjugate Chem.* **2018,** *29* (1), 35-43.

154. Nablo, B. J.; Schoenfisch, M. H., Antibacterial Properties Of Nitric Oxide–Releasing Sol-Gels. *Biomed. Mater. Res., Part A* **2003,** *67* (4), 1276-1283.

155. Srinivasan, A.; Kebede, N.; Saavedra, J. E.; Nikolaitchik, A. V.; Brady, D. A.; Yourd, E.; Davies, K. M.; Keefer, L. K.; Toscano, J. P., Chemistry Of The Diazeniumdiolates. 3. Photoreactivity. *J. Am. Chem. Soc.* **2001,** *123* (23), 5465-5472.

156. Williams, D. L. H., The Chemistry Of S-Nitrosothiols. *Acc. Chem. Res.* **1999,** *32* (10), 869-876.

157. Al-Sa'doni, H.; Ferro, A., S-Nitrosothiols: A Class Of Nitric Oxide-Donor Drugs. *Clinic. Sci.* **2000,** *98* (5), 507-520.

158. Melvin, A. C.; Jones, W. M.; Lutzke, A.; Allison, C. L.; Reynolds, M. M., S-Nitrosoglutathione Exhibits Greater Stability Than S-Nitroso-N-Acetylpenicillamine Under Common Laboratory Conditions: A Comparative Stability Study. *Nitric Oxide* **2019,** *92*, 18-25.

159. Kumar, R.; Massoumi, H.; Chug, M. K.; Brisbois, E. J., S-Nitroso-N-Acetyl-L-Cysteine Ethyl Ester (Snacet) Catheter Lock Solution To Reduce Catheter-Associated Infections. *ACS Appl. Mater. Interfaces* **2021**, *13*(22), 25813-25824.

160. Kumar, R.; Chug, M. K.; Brisbois, E. J., Long-Term Storage Stability And Nitric Oxide Release Behavior Of (N-Acetyl-S-Nitrosopenicillaminyl)-S-Nitrosopenicillamine-Incorporated Silicone Rubber Coatings. *ACS Appl. Mater. Interfaces* **2022**, 14 (27), 30595–30606

161. Singha, P.; Pant, J.; Goudie, M. J.; Workman, C. D.; Handa, H., Enhanced Antibacterial Efficacy Of Nitric Oxide Releasing Thermoplastic Polyurethanes With Antifouling Hydrophilic Topcoats. *Biomater. Sci.* **2017,** *5* (7), 1246-1255.

162. Brisbois, E. J.; Bayliss, J.; Wu, J.; Major, T. C.; Xi, C.; Wang, S. C.; Bartlett, R. H.; Handa, H.; Meyerhoff, M. E., Optimized Polymeric Film-Based Nitric Oxide Delivery Inhibits Bacterial Growth In A Mouse Burn Wound Model. *Acta Biomater.* **2014,** *10* (10), 4136-4142.

163. Chug, M. K.; Brisbois, E., Smartphone Compatible Nitric Oxide Releasing Insert To Prevent Catheter-Associated Infections. *J. Control. Release* **2022**, S0168-3659 (22) 00385.

164. Lautner, G.; Stringer, B.; Brisbois, E. J.; Meyerhoff, M. E.; Schwendeman, S. P., Controlled Light-Induced Gas Phase Nitric Oxide Release From S-Nitrosothiol-Doped Silicone Rubber Films. *Nitric Oxide* **2019**, 2019, 86, 31-37.

165. Shi, Q.; Lu, Y.; Zhang, G.; Yang, X.; Li, R.; Zhang, G.; Guo, X.; Song, J.; Ding, Q., Multifunctional Mesoporous Silica Nanoparticles For Ph-Response And Photothermy Enhanced Osteosarcoma Therapy. *Colloids Surf., B* **2022**, 112615.

166. Duan, X.; Lewis, R. S., Improved Haemocompatibility Of Cysteine-Modified Polymers Via Endogenous Nitric Oxide. *Biomaterials* **2002,** *23* (4), 1197-1203.

167. Gappa-Fahlenkamp, H.; Duan, X.; Lewis, R., Analysis Of Immobilized L-Cysteine On Polymers. *Biomed. Mater. Res., Part A* **2004,** *71* (3), 519-527.

168. Muthuvijayan, V.; Gu, J.; Lewis, R. S., Analysis Of Functionalized Polyethylene Terephthalate With Immobilized Ntpdase And Cysteine. *Acta Biomater.* **2009,** *5* (9), 3382-3393.

169. Ramachandran, B.; Muthuvijayan, V., Cysteine Immobilisation On The Polyethylene Terephthalate Surfaces And Its Effect On The Haemocompatibility. *Sci. Rep.* **2019,** *9* (1), 1-12.

170. Pant, J.; Goudie, M. J.; Hopkins, S. P.; Brisbois, E. J.; Handa, H., Tunable Nitric Oxide Release From S-Nitroso-N-Acetylpenicillamine Via Catalytic Copper Nanoparticles For Biomedical Applications. *ACS Appl. Mater. Interfaces* **2017,** *9* (18), 15254-15264.

171. Mondal, A.; Singha, P.; Douglass, M.; Estes, L.; Garren, M.; Griffin, L.; Kumar, A.; Handa, H., A Synergistic New Approach Toward Enhanced Antibacterial Efficacy Via Antimicrobial Peptide Immobilization On A Nitric Oxide-Releasing Surface. *ACS Appl. Mater. Interfaces* **2021,** *13* (37), 43892-43903.

172. Chug, M. K.; Massoumi, H.; Wu, Y.; Brisbois, E. J., Prevention Of Medical Device Infections Via Multi-Action Nitric Oxide And Chlorhexidine Diacetate Releasing Medical Grade Silicone Biointerfaces. *J. Biomed. Mater. Res. A* **2022,** *110* (6), 1263-1277.

173. Williams, D. L. H., The Mechanism Of Nitric Oxide Formation From S-Nitrosothiols (Thionitrites). *Chem. Comm.* **1996,** (10), 1085-1091.

174. Mazia, D.; Mullins, L. J., Radioactive Copper And The Mechanism Of Oligodynamic Action. *Nature* **1941,** *147* (3734), 642-642.

175. Singha, P.; Workman, C. D.; Pant, J.; Hopkins, S. P.; Handa, H., Zinc-Oxide Nanoparticles Act Catalytically And Synergistically With Nitric Oxide Donors To Enhance Antimicrobial Efficacy. *J. Biomed. Mater. Res. A* **2019**, *107*(7), 1425-1433.

176. Mondal, A.; Douglass, M.; Hopkins, S. P.; Singha, P.; Tran, M.; Handa, H.; Brisbois, E. J., Multifunctional S-Nitroso-N-Acetylpenicillamine Incorporated Medical Grade Polymer With Selenium Interface For Biomedical Applications. *ACS Appl. Mater. Interfaces* **2019**, *11*(38), Pp.34652-34662.

177. Douglass, M. E.; Goudie, M. J.; Pant, J.; Singha, P.; Hopkins, S.; Devine, R.; Schmiedt, C. W.; Handa, H., Catalyzed Nitric Oxide Release Via Cu Nanoparticles Leads To An Increase In

Antimicrobial Effects And Hemocompatibility For Short-Term Extracorporeal Circulation. *ACS Appl. Bio. Mat.* **2019**, *2*(6), Pp.2539-2548.

178. Doverspike, J. C.; Mack, S. J.; Luo, A.; Stringer, B.; Reno, S.; Cornell, M. S.; Rojas-Pena, A.; Wu, J.; Xi, C.; Yevzlin, A., Nitric Oxide-Releasing Insert For Disinfecting The Hub Region Of Tunnel Dialysis Catheters. *ACS Appl. Mater. Interfaces* **2020,** *12* (40), 44475-44484.

179. Storm, W. L.; Johnson, J. A.; Worley, B. V.; Slomberg, D. L.; Schoenfisch, M. H., Dual Action Antimicrobial Surfaces Via Combined Nitric Oxide And Silver Release. *J. Biomed. Mater. Res. A* **2015,** *103* (6), 1974-1984.

180. Wo, Y.; Brisbois, E. J.; Bartlett, R. H.; Meyerhoff, M. E., Recent Advances In Thromboresistant And Antimicrobial Polymers For Biomedical Applications: Just Say Yes To Nitric Oxide (No). *Biomater. Sci.* **2016,** *4* (8), 1161-1183.

181. Garren, M.; Maffe, P.; Melvin, A.; Griffin, L.; Wilson, S.; Douglass, M.; Reynolds, M.; Handa, H., Surface-Catalyzed Nitric Oxide Release Via A Metal Organic Framework Enhances Antibacterial Surface Effects. *ACS Appl. Mater. Interfaces* **2021,** *13* (48), 56931-56943.

182. Vikrant, K.; Kumar, V.; Kim, K.-H.; Kukkar, D., Metal–Organic Frameworks (Mofs): Potential And Challenges For Capture And Abatement Of Ammonia. *J. Mater. Chem. A* **2017,** *5* (44), 22877-22896.

183. Sun, J.; Fan, Y.; Ye, W.; Tian, L.; Niu, S.; Ming, W.; Zhao, J.; Ren, L., Near-Infrared Light Triggered Photodynamic And Nitric Oxide Synergistic Antibacterial Nanocomposite Membrane. *Chem. Eng. J.* **2021,** *417*, 128049.

184. Tang, Y.; Wang, T.; Feng, J.; Rong, F.; Wang, K.; Li, P.; Huang, W., Photoactivatable Nitric Oxide-Releasing Gold Nanocages For Enhanced Hyperthermia Treatment Of Biofilm-Associated Infections. *ACS Appl. Mater. Interfaces* **2021,** *13* (43), 50668-50681.

185. Hu, D.; Deng, Y.; Jia, F.; Jin, Q.; Ji, J., Surface Charge Switchable Supramolecular Nanocarriers For Nitric Oxide Synergistic Photodynamic Eradication Of Biofilms. *ACS Nano* **2019,** *14* (1), 347-359.

186. Liang, Z.; Liu, W.; Wang, Z.; Zheng, P.; Liu, W.; Zhao, J.; Zhong, Y.; Zhang, Y.; Lin, J.; Xue, W., Near-Infrared Laser-Controlled Nitric Oxide-Releasing Gold Nanostar/Hollow Polydopamine Janus Nanoparticles For Synergistic Elimination Of Methicillin-Resistant Staphylococcus Aureus And Wound Healing. *Acta Biomater.* **2022,** *143*, 428-444.

187. Poh, W. H.; Rice, S. A., Recent Developments In Nitric Oxide Donors And Delivery For Antimicrobial And Anti-Biofilm Applications. *Molecules* **2022,** *27* (3), 674.

188. Rouillard, K. R.; Novak, O. P.; Pistiolis, A. M.; Yang, L.; Ahonen, M. J.; Mcdonald, R. A.; Schoenfisch, M. H., Exogenous Nitric Oxide Improves Antibiotic Susceptibility In Resistant Bacteria. *ACS Infectious Diseases* **2020**, *7*(1), Pp.23-33.

189. Nguyen, T.-K.; Selvanayagam, R.; Ho, K. K.; Chen, R.; Kutty, S. K.; Rice, S. A.; Kumar, N.; Barraud, N.; Duong, H. T.; Boyer, C., Co-Delivery Of Nitric Oxide And Antibiotic Using Polymeric Nanoparticles. *Chemical Science* **2016,** *7* (2), 1016-1027.

190. Ren, H.; Wu, J.; Colletta, A.; Meyerhoff, M. E.; Xi, C., Efficient Eradication Of Mature Pseudomonas Aeruginosa Biofilm Via Controlled Delivery Of Nitric Oxide Combined With Antimicrobial Peptide And Antibiotics. *Front Microbiol.* **2016,** *7* (1260).

191. Devine, R.; Singha, P.; Handa, H., Versatile Biomimetic Medical Device Surface: Hydrophobin Coated, Nitric Oxide-Releasing Polymer For Antimicrobial And Hemocompatible Applications. *Biomater. Sci* **2019,** *7* (8), 3438-3449.

192. Devine, R.; Douglass, M.; Ashcraft, M.; Tayag, N.; Handa, H., Development Of Novel Amphotericin B-Immobilized Nitric Oxide-Releasing Platform For The Prevention Of Broad-Spectrum Infections And Thrombosis. *ACS Appl. Mater. Interfaces* **2021,** *13* (17), 19613-19624.

193. Lu, Y.; Slomberg, D. L.; Shah, A.; Schoenfisch, M. H., Nitric Oxide-Releasing Amphiphilic Poly (Amidoamine)(Pamam) Dendrimers As Antibacterial Agents. *Biomacromolecules* **2013,** *14* (10), 3589-3598.

194. Worley, B. V.; Slomberg, D. L.; Schoenfisch, M. H., Nitric Oxide-Releasing Quaternary Ammonium-Modified Poly (Amidoamine) Dendrimers As Dual Action Antibacterial Agents. *Bioconjugate Chem.* **2014,** *25* (5), 918-927.

195. Worley, B. V.; Schilly, K. M.; Schoenfisch, M. H., Anti-Biofilm Efficacy Of Dual-Action Nitric Oxide-Releasing Alkyl Chain Modified Poly (Amidoamine) Dendrimers. *Mol. Pharmaceutics* **2015,** *12* (5), 1573-1583.

196. Pant, J.; Gao, J.; Goudie, M. J.; Hopkins, S. P.; Locklin, J.; Handa, H., A Multi-Defense Strategy: Enhancing Bactericidal Activity Of A Medical Grade Polymer With A Nitric Oxide Donor And Surface-Immobilized Quaternary Ammonium Compound. *Acta Biomater.* **2017,** *58*, 421-431.

197. Wo, Y.; Li, Z.; Brisbois, E. J.; Colletta, A.; Wu, J.; Major, T. C.; Xi, C.; Bartlett, R. H.; Matzger, A. J.; Meyerhoff, M. E., Origin Of Long-Term Storage Stability And Nitric Oxide Release Behavior Of Carbosil Polymer Doped With S-Nitroso-N-Acetyl-D-Penicillamine. *ACS Appl. Mater. Interfaces* **2015,** *7* (40), 22218-22227.

198. Lantvit, S. M.; Barrett, B. J.; Reynolds, M. M., Nitric Oxide Releasing Material Adsorbs More Fibrinogen. *J. Biomed. Mater. Res. A* **2013,** (11), 3201.

199. Storm, W. L.; Youn, J.; Reighard, K. P.; Worley, B. V.; Lodaya, H. M.; Shin, J. H.; Schoenfisch, M. H., Superhydrophobic Nitric Oxide-Releasing Xerogels. *Acta Biomater.* **2014,** *10* (8), 3442-3448.

200. Goudie, M. J.; Singha, P.; Hopkins, S. P.; Brisbois, E. J.; Handa, H., Active Release Of An Antimicrobial And Antiplatelet Agent From A Nonfouling Surface Modification. *ACS Appl. Mater. Interfaces.***2019,** *11* (4), 4523-4530.

201. Mondal, A.; Devine, R.; Estes, L.; Manuel, J.; Singha, P.; Mancha, J.; Palmer, M.; Handa, H., Highly Hydrophobic Polytetrafluoroethylene Particle Immobilization Via Polydopamine Anchor Layer On Nitric Oxide Releasing Polymer For Biomedical Applications. *J. Colloid Interface Sci.* **2021,** *585*, 716-728.

202. Hou, Z.; Wu, Y.; Xu, C.; Reghu, S.; Shang, Z.; Chen, J.; Pranantyo, D.; Marimuth, K.; De, P. P.; Ng, O. T., Precisely Structured Nitric-Oxide-Releasing Copolymer Brush Defeats Broad-Spectrum Catheter-Associated Biofilm Infections In Vivo. *ACS Centr. Sci.* **2020,** *6* (11), 2031-2045.

203. Douglass, M.; Hopkins, S.; Chug, M. K.; Kim, G.; Garren, M. R.; Ashcraft, M.; Nguyen, D. T.; Tayag, N.; Handa, H.; Brisbois, E. J., Reduction In Foreign Body Response And Improved Antimicrobial Efficacy Via Silicone-Oil-Infused Nitric-Oxide-Releasing Medical-Grade Cannulas. *ACS Appl. Mater. Interfaces* **2021,** *13* (44), 52425-52434.

204. Manna, U.; Raman, N.; Welsh, M. A.; Zayas-Gonzalez, Y. M.; Blackwell, H. E.; Palecek, S. P.; Lynn, D. M., Slippery Liquid-Infused Porous Surfaces That Prevent Microbial Surface Fouling And Kill Non-Adherent Pathogens In Surrounding Media: A Controlled Release Approach. *Adv. Func. Mater.* **2016,** *26* (21), 3599-3611.

205. Manna, U.; Lynn, D. M., Fabrication Of Liquid-Infused Surfaces Using Reactive Polymer Multilayers: Principles For Manipulating The Behaviors And Mobilities Of Aqueous Fluids On Slippery Liquid Interfaces. *Adv. Mater.* **2015,** *27* (19), 3007-3012.

206. Wong, T.-S.; Kang, S. H.; Tang, S. K.; Smythe, E. J.; Hatton, B. D.; Grinthal, A.; Aizenberg, J., Bioinspired Self-Repairing Slippery Surfaces With Pressure-Stable Omniphobicity. *Nature* **2011,** *477* (7365), 443-447.

207. Goudie, M. J.; Pant, J.; Handa, H., Liquid-Infused Nitric Oxide-Releasing (Linorel) Silicone For Decreased Fouling, Thrombosis, And Infection Of Medical Devices. *Sci. Rep.* **2017,** *7* (1), 13623.

208. Massoumi, H.; Chug, M. K.; Nguyen, G. H.; Brisbois, E. J., A Multidisciplinary Experiment To Characterize Antifouling Biocompatible Interfaces Via Quantification Of Surface Protein Adsorption. *J. Chem. Educ.* **2022**, 99 (7), 2667–2676.

209. Homeyer, K. H.; Singha, P.; Goudie, M. J.; Handa, H., S-Nitroso-N-Acetylpenicillamine Impregnated Endotracheal Tubes For Prevention Of Ventilator-Associated Pneumonia. *Biotechnol. Bioeng.* **2020**, 117(7), 2237-2246.

210. Qian, Y.; Chug, M. K.; Massoumi, H.; Brisbois, E. J., S-Nitroso-N-Acetylpenicillamine Grafted Silicone Oil For Antibacterial Interface Applications. *Mater. Adv.* **2022,** *3*(15), 6270-6279.

211. Yun Qian, Chug, M.K., And Elizabeth J. Brisbois, Nitric Oxide-Releasing Silicone Oil With Tunable Payload For Antibacterial Applications. *ACS Appl Bio Mater.* **2022,** *5*(7), 3396-3404.

212. Liu, Q.; Singha, P.; Handa, H.; Locklin, J., Covalent Grafting Of Antifouling Phosphorylcholine-Based Copolymers With Antimicrobial Nitric Oxide Releasing Polymers To Enhance Infection-Resistant Properties Of Medical Device Coatings. *Langmuir* **2017,** *33* (45), 13105-13113.

213. Singha, P.; Goudie, M. J.; Liu, Q.; Hopkins, S.; Brown, N.; Schmiedt, C. W.; Locklin, J.; Handa, H., Multipronged Approach To Combat Catheter-Associated Infections And Thrombosis By Combining Nitric Oxide And A Polyzwitterion: A 7 Day In Vivo Study In A Rabbit Model. *ACS Appl. Mater. Interfaces.***2020,** *12* (8), 9070-9079.

214. Xu, L.-C.; Meyerhoff, M. E.; Siedlecki, C. A., Blood Coagulation Response And Bacterial Adhesion To Biomimetic Polyurethane Biomaterials Prepared With Surface Texturing And Nitric Oxide Release. *Acta Biomater.* **2019,** *84*, 77-87.

215. Wo, Y.; Xu, L.-C.; Li, Z.; Matzger, A. J.; Meyerhoff, M. E.; Siedlecki, C. A., Antimicrobial Nitric Oxide Releasing Surfaces Based On S-Nitroso-N-Acetylpenicillamine Impregnated Polymers Combined With Submicron-Textured Surface Topography. *Biomater. Sci* **2017,** *5* (7), 1265-1278.

216. Malone-Povolny, M. J.; Bradshaw, T. M.; Merricks, E. P.; Long, C. T.; Nichols, T. C.; Schoenfisch, M. H., Combination Of Nitric Oxide Release And Surface Texture For Mitigating The Foreign Body Response. *ACS Biomater. Sci. Eng.* **2021,** *7* (6), 2444-2452.

217. Xu, L. C.; Wo, Y.; Meyerhoff, M. E.; Siedlecki, C. A., Inhibition Of Bacterial Adhesion And Biofilm Formation By Dual Functional Textured And Nitric Oxide Releasing Surfaces. *Acta Biomater.* **2017,** *51*, 53-65.

218. Duan, Y.; He, K.; Zhang, G.; Hu, J., Photoresponsive Micelles Enabling Codelivery Of Nitric Oxide And Formaldehyde For Combinatorial Antibacterial Applications. *Biomacromolecules* **2021,** *22* (5), 2160-2170.

219. Taunk, A.; Chen, R.; Iskander, G.; Ho, K. K.; Black, D. S.; Willcox, M. D.; Kumar, N., Dual-Action Biomaterial Surfaces With Quorum Sensing Inhibitor And Nitric Oxide To Reduce Bacterial Colonization. *ACS Biomater. Sci. Eng.* **2018,** *4* (12), 4174-4182.

220. Urzedo, A. L.; Goncalves, M. C.; Nascimento, M. H.; Lombello, C. B.; Nakazato, G.; Seabra, A. B., Multifunctional Alginate Nanoparticles Containing Nitric Oxide Donor And Silver Nanoparticles For Biomedical Applications. *Mater. Sci. Eng. C* **2020,** *112*, 110933.

221. Devine, R.; Goudie, M. J.; Singha, P.; Schmiedt, C.; Douglass, M.; Brisbois, E. J.; Handa, H., Mimicking The Endothelium: Dual Action Heparinized Nitric Oxide Releasing Surface. *ACS Appl. Mater. Interfaces* **2020,** *12* (18), 20158-20171.

222. Carpenter, A. W.; Worley, B. V.; Slomberg, D. L.; Schoenfisch, M. H., Dual Action Antimicrobials: Nitric Oxide Release From Quaternary Ammonium-Functionalized Silica Nanoparticles. *Biomacromolecules* **2012,** *13* (10), 3334-3342.

223. Brisbois, E. J.; Davis, R. P.; Jones, A. M.; Major, T. C.; Bartlett, R. H.; Meyerhoff, M. E.; Handa, H., Reduction In Thrombosis And Bacterial Adhesion With 7 Day Implantation Of S-Nitroso-N-Acetylpenicillamine (Snap)-Doped Elast-Eon E2as Catheters In Sheep. *J. Mater. Chem. B* **2015,** *3* (8), 1639-1645.

224. Chug, M. K., & Brisbois, E. J. (2022). Recent Developments in Multifunctional Antimicrobial Surfaces and Applications toward Advanced Nitric Oxide-Based Biomaterials. *ACS Materials Au*, *2*(5), 525-551.

CHAPTER 2:

INCREASING THE LIFETIME OF INSULIN CANNULA WITH ANTIFOULING AND NITRIC OXIDE RELEASING PROPERTIES

Chug, M. K., Feit, C., & Brisbois, E. J. (2019). Increasing The Lifetime of Insulin Cannula With Antifouling And Nitric Oxide-Releasing Properties. *ACS Applied Bio Materials*, *2*(12), 5965-5975.

2.1 Abstract

Many Type 1 diabetes patients utilize insulin pumps, which rely on a small subcutaneous insulin infusion cannula. However, insulin cannulas still suffer from infection and inflammation, which impacts the wear time of the insulin cannula, reduces the efficiency of insulin infusion, and requires frequent rotation of the insulin infusion site. Infection and inflammation of continuous insulin infusion pump therapy are growing issues and are estimated to cost billions of dollars globally each year. This study aims to develop a potent antibacterial and antifouling insulin cannula with a synergistic effect of bioinspired polymers, integrating antifouling Slippery, Liquid-Infused Porous Surface (SLIPs) technology with an active nitric oxide (NO) releasing polymer. The cannulas were developed by impregnating the NO donor molecule *S*-nitroso-*N*-acetylpenicillamine (SNAP) and silicone oil (Si) in commercial medical-grade silicone rubber tubing (SR-SNAP-Si) via a solvent impregnation process. The efficiency of the SR-SNAP-Si to reduce protein adsorption and provide antibacterial properties against *Staphylococcus aureus* and *Staphylococcus epidermidis* were studied using *in vitro* bioassays. The SR-SNAP-Si cannula released NO for > 14 d at physiological levels and were stable during storage for 30 d at room temperature. Scanning electron microscopy images revealed no observable changes to the material surface after the solvent impregnation process. The infusion of silicone oil significantly reduced the protein adsorption on the cannula by 66.40% and the NO release reduced the viable bacterial cell adhesion of *S. epidermidis* and *S. aureus* after 24 h by 94.89% and 99.77%, respectively, as compared to SR controls. This insulin cannula provided continuous NO release and an antifouling interface for > 14 d and exhibited a significant reduction in protein and bacterial adhesion. This method of developing dual-function nitric oxide-releasing and antifouling surfaces for subcutaneous insulin infusion cannulas holds great potential to reduce infection and inflammation associated with insulin pump delivery systems.

Keywords: Diabetes, Insulin pump therapy, Insulin cannula, Nitric oxide, Antibacterial, Antifouling

2.2 Introduction

Diabetes Mellitus is a global epidemic where 30 million people are affected and an additional 84 million people have been diagnosed with prediabetes in the U.S alone.[1] The continuous elevation in the incidence of diabetes directly correlates to the amplified medical and financial burden. According to a 2017 report by the American Diabetes Association, the annual medical cost associated with diabetes is $237 billion.[2] In healthy people the insulin hormone helps metabolize blood glucose that is absorbed by cells. However, in Type 1 diabetes, the beta cells in the pancreas fail to produce adequate amounts of insulin, thus causing a rise in blood glucose levels. Several management devices have been developed to better manage diabetes care. To achieve good glycemic control, all Type 1 and some Type 2 diabetes patients utilize different modes of insulin delivery for treatment of diabetes, such as insulin syringes, insulin pens, or insulin pumps.

One critical device in diabetes care is the Continuous Subcutaneous Insulin Infusion Pump (CSII, **Figure 2.1**). The insulin pump contains the insulin hormone stored in a replaceable reservoir. Insulin travels at a controlled rate through a thin plastic tubing to the subcutaneous insulin cannula. The infusion of insulin triggers the uptake of blood glucose by the cells of the body (e.g., muscle cells). The closed-loop structure of an insulin infusion pump is devised to emulate the role of the pancreas that can provide balanced dosages of insulin hormone to maintain the concentration of glucose in the bloodstream. The cannula is inserted subcutaneously with the help of a needle and is held in place by a small adhesive patch that is adhered to the skin. Insulin infusion pump therapy has been proven to be an extremely effective treatment for Type 1 diabetes and has been used in more than 400,000 patients globally.[3, 4] Normally, the insulin pump therapy is self-administered in order to give more flexibility, control, and accuracy of insulin dosage, and reduces the number of episodes of hypoglycemia compared to regular insulin syringes.[5]

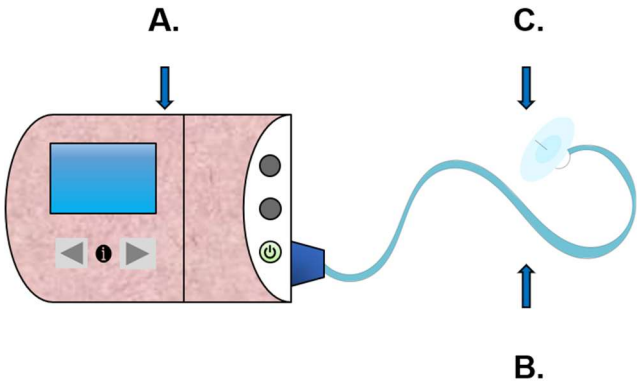

Figure 2.1 Schematic of a continuous insulin infusion pump (A) Insulin is stored inside a tiny cassette in the interior of the pump. (B) At a controlled flowrate, insulin flows into the body through an elastic tubing that ends with a tiny "cannula" inserted in the subcutaneous tissue. (C) The cannula is held in place by an "infusion set", a small adhesive patch adhered to the skin.

The current commercial insulin cannulas are predominately either stainless-steel or Teflon cannulas. However, the wear time of these cannulas is relatively short (2-3 days) due to hindrances caused by two major issues, namely infection and inflammation (foreign body response) that limit their long-term usage.[6] Reports suggest that ~36% of insulin pump users have infection or inflammation at the infusion site and insulin infusion sets have a 65% failure rate after 7 d of implantation.[7-9] The long-term effects of repeated cannula insertion and foreign body response lead to the formation of scar tissue, which limits the availability of insulin infusion sites until the tissue is healed.[10] Bacterial strains such as *Staphylococcus aureus* and *Staphylococcus epidermidis* are the two most prevalent opportunistic pathogens found on various subcutaneous catheters.[11] The skin around the site of cannula insertion is sterilized using an antibacterial agent solution in order to avoid risks of bacterial infections during self-administration of the insulin cannula. However, infections remain prevalent due to the introduction of bacteria and biofilms adhered to the cannula surface. Biofilms are highly resistant to many classes of antibiotics and host defense mechanisms (immune response).[11] Formation of microbial biofilm is facilitated by multifaceted progressive stages involving bacterial cell attachment on an organic or inorganic surface, cell-to-cell communication, microcolony development, and finally the creation of a

confluent matured biofilm.[12] The confluent biofilm is secured by an extracellular polymeric substance, a slimy protective layer, which averts the immune defense by preventing white blood cells and antibiotics from penetrating the biofilm matrix and killing the bacteria. In addition, the attachment of *S. epidermidis* is mediated by a polysaccharide intercellular adhesion (PIA) antigen in preliminary attachment on the polymer substrate, which further guards the constantly dividing bacterial cells from being phagocytosed by polymorphonuclear leukocytes, eventually leading to either systemic or chronic infections related to the indwelling medical devices.[13] Furthermore, the extracellular nuclease enzymes synthesized by *S. aureus* make them resistant to neutrophil extracellular traps (NET), consequently shielding the biofilm from NET-based killing.[14] Therefore, the American Diabetic Association (ADA) recommends replacing the cannula and rotating the infusion site every 2-3 days to avoid the potential encapsulation, infections, and inflammation that can occur from the long-term usage of the insulin cannula.[15]

Considering the problems associated with the current insulin cannulas, there have been efforts toward developing insulin cannula with a variety of antimicrobial coatings. For example, Jamal et al. have developed an insulin cannula with a synergistic antibacterial effect of gentian violet and chlorhexidine.[16] However, these cannulas do not have a mechanism to prevent foreign body response that can lead to local inflammation and encapsulation on the cannula. Elevated doses of the antibiotics are required to penetrate the biofilm, which can lead to the development of bacterial strains with antibiotic-resistant genes overtime leaving the most effective antibiotics futile.[17] Furthermore, these cannulas do not address the biofouling on the cannula surface. Protein adsorption is the first response to the implanted cannula, which leads to the activation of phagocytic immune cells.[18] The activated neutrophils and macrophages sense the presence of the foreign body (implant) and release inflammatory cytokines causing localized inflammation at the site of insertion.[19] The cascade of reactions at the cannula insertion site also leads to encapsulation on the cannula, which then limits the diffusion of insulin to the bloodstream.

Therefore, it is important to have an insulin cannula that not only exhibits antimicrobial properties, but also possesses antifouling and anti-inflammatory properties.

Inspired by the mucus production in the gastrointestinal tract, material scientists have developed slippery, liquid-infused porous surfaces (SLIPs) with an ability to engender ultra-low fouling surfaces that are impervious to protein adsorption and bacterial adhesion using FDA-approved silicone oil (Si).[20] These slippery surfaces have been integrated with several common biomedical devices and have been shown to exhibit improved biocompatibility and reduced biofouling on the device surface.[21, 22] Silicone oil-infused medical polymers have been shown to be non-toxic to healthy tissues in humans near the implant site, making it favorable for infusion of SLIPs materials.[21] Silicone rubber, an elastomer, has been widely utilized in antifouling SLIPs interfaces due to its ability to absorb Si. Although SLIPs can passively decrease bacterial and protein adhesion, they do not actively exhibit any bactericidal effects against bacteria that may adhere to a surface, which may lead to microbial proliferation and eventually biofilm formation.

One tactic to improve the biocompatibility of therapeutic polymer devices is to incorporate nitric oxide (NO) donors within the polymer matrix. Nitric oxide was discovered as an endogenous gas molecule synthesized by the body via nitric oxide synthase (NOS) enzymes that converts L-arginine into citrulline and NO.[23, 24] Nitric oxide released from the polymer matrices can mimic endogenous NO release, such as endothelial cells that release NO at a surface flux of 0.5 - 4 x 10^{-10} mol cm^{-2} min^{-1}, to prevent platelet activation and adhesion.[25] Phagocytic cells, like macrophages, produce NO via inducible nitric oxide synthase (iNOS) at > 1 μM NO that acts as a bactericidal agent and promote the dispersion of biofilms.[26] Additionally, NO has been shown to mitigate the inflammatory reaction and platelet activation.[27, 28] In recent years there has been tremendous interest in developing NO-releasing polymers to exogenously emulate natural immune responses. Nitric oxide is a gaseous radical and has a very short half-life (seconds).[29]

To mimic the physiological release of NO, various NO donors such as *N*-diazeniumdiolates and *S*-nitrosothiols have been synthesized and incorporated into polymeric materials for localized delivery of NO.[30] Nitric oxide donors incorporated in polymeric materials have been fruitful in enhancing wound healing and angiogenesis in diabetic wound animal models, which verify that the activity of exogenously delivered NO is preserved even in the diseased condition like diabetes.[31, 32] In this study, *S*-nitroso-*N*-acetylpenicillamine (SNAP, **Figure 2.2A**), a NO donor molecule, was impregnated into a medical-grade silicone rubber cannula tubing as a promising

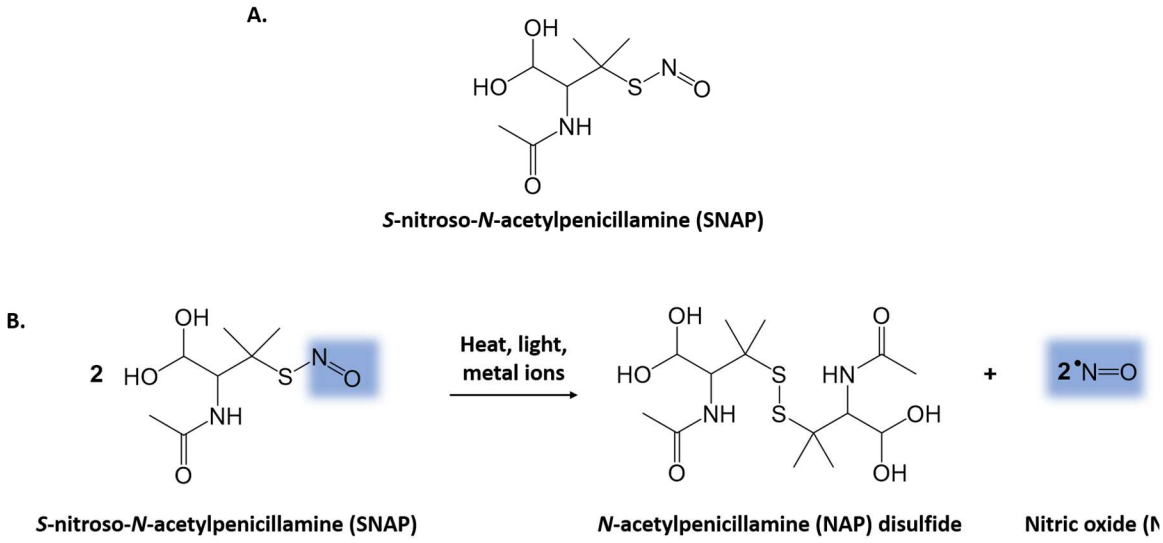

Figure 2.2 (A) Chemical structure of the NO donor *S*-nitroso-*N*-acetylpenicillamine (SNAP), (B) Formation of nitric oxide from the decomposition of SNAP. When 2 molecules of SNAP are triggered by the stimuli of heat, light, or metal ions, the *S*-nitrosothiol bond of SNAP is cleaved, and a resultant two molecules of NO and NAP disulfide are formed. The structure of NAP is sustained by the formation of disulfide bond between NAP molecules.

solution to prevent device infection. S-nitroso-*N*-acetylpenicillamine (SNAP) is one of the most commonly studied NO donors and it has been reported that incorporation/impregnation of SNAP into various polymers, like polyurethanes and silicone elastomers, gives sustained and controlled NO release.[33-36] It is well understood that SNAP is stabilized in the polymer matrix by forming internal hydrogen bonding, which prolongs the NO release for days to months.[37] Moreover, the approach of impregnating the SNAP via solvent swelling process can overcome the thermal degradation of the NO donor molecule during the polymer extrusion process.[38] *S*-nitroso-*N*-

acetylpenicillamine is a stable, cost-effective, and easy to synthesize NO donor with low cytotoxicity and can release NO at physiological conditions. When SNAP is stimulated by heat, light, or metal ions (e.g., Cu^{+}) the *S*-nitrosothiol bond is cleaved and results in the formation of *N*-acetyl-*D*-penicillamine (NAP) disulfide and NO (**Figure 2.2B**). The parent thiol, NAP, and its eventual degraded product, penicillamine, are FDA approved and have been used in treating heavy metal contamination in diseased conditions like Wilson's disease.[39-42] Numerous studies in the field of biomaterials have incorporated NO donors in silicone catheters to integrate the antibacterial properties of NO with the polymers.[21, 34, 43-46] A robust method to develop a new generation of insulin infusion cannula with a combination of NO release and liquid-infused silicone oil in a silicone cannula tubing material is presented with the aim to prolong the indwelling lifetime of insulin cannula by preventing the bacterial infection, foreign body response, and biofouling. The cannula fabrication, surface morphology, lifetime of the antifouling liquid-infused surface property, SNAP leaching, NO release kinetics, and shelf-life were evaluated. Finally, the biocompatibility of the cannula was tested for fibrinogen protein adsorption and the reduction of viable infectious pathogens *Staphylococcus aureus* and *Staphylococcus epidermidis* using *in vitro* bioassays.

2.3 Materials and Methods

2.3.1 Materials

N-Acetyl-*D*-penicillamine (NAP), sodium nitrite, *L*-cysteine, sodium chloride, potassium chloride, sodium phosphate dibasic, potassium phosphate monobasic, copper (II) chloride, ethylenediaminetetraacetic acid (EDTA), tetrahydrofuran (THF), silicone oil with 10 cSt viscosity and sterile phosphate buffer saline powder with 0.01 M, pH 7.4, containing 0.138 M NaCl, 2.7 mM KCl, were purchased from Sigma Aldrich (St. Louis, MO). Methanol, hydrochloric acid, and sulfuric acid were obtained from Fisher Scientific (Hampton, NH). Helixmark® silicone tubing-silastic material (60-011-05) was purchased from VWR (Radnor, PA). All aqueous solutions were

prepared using deionized water. Phosphate buffer saline (PBS) 0.01M with 100 μM EDTA was used for all material characterization and NO analyzer studies. FITC-Fibrinogen (13 mg mL^{-1}) was purchased from Molecular Innovations (Novi, MI). The bacterial strains *Staphylococcus epidermidis* (ATCC 35984) and *Staphylococcus aureus* (ATCC 6538) were obtained from American Type Culture Collection (ATCC). All the buffers and media were sterilized in an autoclave at 121 °C, 100 kPa (15 psi) above atmospheric pressure for 20 minutes before the biocompatibility experiments.

2.3.2 *S*-nitroso-*N*-acetylpenicillamine Synthesis

S-nitroso-*N*-acetylpenicillamine was synthesized using a modified version of a previously described protocol.[47] An equimolar ratio of NAP and sodium nitrite were dissolved into 2 parts of water and 3 parts of methanol. Next, 1 M of H_2SO_4 and 1 M HCl were added to the above mixture and the reaction was stirred for 10 min. The reaction vessel was protected from light, blown with gentle air, and cooled in an ice bath for 8 h. The reaction mixture was filtered, and washed with ice-cold DI water, and precipitated SNAP crystals were collected into a Buchner funnel using suction filtration. Finally, the collected SNAP crystals were dried overnight in a vacuum desiccator by keeping the crystals protected from light. The purity of SNAP crystals (> 90%) was confirmed using the NOA and UV-vis calibration curve.

2.3.3 Preparation of Antifouling Liquid-Infused and Nitric Oxide Releasing Insulin Cannula

All the experiments were performed using HelixMark® silastic silicone cannula tubing (60-011-05) with a length of ~ 2 cm, I.D. of 2.16 mm, and O.D. of 1.02 mm. Cannulas were fabricated by a SNAP impregnation method.[48] Sections of original silicone rubber (SR) tubing were swelled in SNAP-THF solution (125 mg mL^{-1}) for 24 h. The resultant SNAP-impregnated SR (SR-SNAP) cannulas were briefly rinsed and dried overnight in a vacuum desiccator. To develop the

antifouling surface, SR-SNAP were soaked in 10 cSt silicone oil for 24 h, resulting in the SR-SNAP-Si. Samples were always shielded from light.

2.3.4 Characterization of the Cannula Surface and Antifouling Properties

2.3.4.1 Characterization of Surface Morphology using Scanning Electron Microscopy

Scanning electron microscopy (SEM) images were recorded using a JEOL JSM-6480 Scanning Electron Microscope at a magnification of 100x at 15.0 kV. Samples were mounted onto stubs using double-sided carbon tape and gold-sputtered for 180 s before imaging. The original SR cannula surface is smooth and scanning electron microscopy images of the original SR cannula, after SNAP loading, and after infusion of Si were recorded to evaluate the surface properties throughout the fabrication process.

2.3.4.2 Evaluation of Sliding Angle and Lifetime of Antifouling Properties

The SR and SR-SNAP-Si cannula samples were cut longitudinally and mounted onto a glass slide to create a flat surface. A sliding stage fitted with a digital protractor was used to measure the sliding angle of a 10 µL droplet of water on the cannula surface. Before each measurement, each sample was gently washed with DI H_2O to remove contaminants from the surface. A 10 µL droplet of water was pipetted onto the cannula surface at randomly selected positions. The angle of the stage was slowly increased, and the angle was recorded once the sliding of the droplet was observed. The sliding angle of each sample was recorded at at least 3 positions at various timepoints over the period of 21 d. After each measurement, samples were incubated in fresh PBS buffer at 37 °C.

2.3.4.3 Determining the Biocompatibility of Insulin Cannula via Fibrinogen Adsorption *In Vitro*

The quantification of fibrinogen adsorbed on the cannula was performed using a revised version of a previously reported protocol.[49] Human fibrinogen conjugated with FITC (Fg-FITC, 13 mg mL^{-1}, Molecular Innovations) was diluted with DI water to 2 mg mL^{-1} concentration. First, the SR, SR-Si, SR-SNAP, and SR-SNAP-Si were incubated with phosphate buffer (PB) at 37 °C for 30 min in a black flat bottom 96-well plate. Next, the protein solution was added to the wells with cannulas (2 mg mL^{-1},100 µL).[21, 49] The protein solution was exposed to the cannulas for 2 h at 37 °C to emulate the physiological conditions. After the incubation, the wells were infinitely diluted using phosphate buffer to remove the discrepancies occurring from the unadhered or free-floating protein structures. The fluorescence intensities of the samples were recorded using a fluorescence plate reader (Synergy 2, Biotek, Winooski, VT) at 485 nm (excitation) and 528 nm (emission) with top read at 50%. Human fibrinogen adsorption to blank polypropylene wells was used as an internal control to normalize the fluorescence signals. To obtain the qualitative results, all the samples were imaged under Keyence Fluorescence Microscope BZ-X800.

2.3.5 Characterization of SNAP-impregnated Insulin Cannula for Enhanced NO-releasing Properties

2.3.5.1 Determination of SNAP Impregnation in Insulin Cannula

The mass of each sample (SR-SNAP-Si) was recorded by an analytical balance (Mettler Toledo™ XS105DU, Columbus, OH). The samples were soaked in THF for 24 h at room temperature, protected from light, to extract all the impregnated SNAP from the cannula tubing. After 24 h, the soaking buffer was analyzed by UV-vis spectroscopy (Cary 60, Agilent Technologies) to measure the mg SNAP leached from the SR-SNAP-Si. The molar absorptivity of SNAP in THF at 22 °C was determined to be 909 M^{-1} cm^{-1} at 340 nm. Each cannula sample was clear after incubation in the THF, indicating all SNAP had been extracted into the THF

solution. After Si infusion in the SR-SNAP, an absorbance-based extraction method was used to quantify the wt% SNAP impregnated in the cannula. Each sample was soaked in THF to extract all the SNAP from the cannula.

2.3.5.2 Nitric Oxide Release

The real-time NO release from the cannula was quantified by a gold standard chemiluminescence method using a Zysense chemiluminescence Nitric Oxide Analyzer (NOA) 280i (Frederick, CO). To quantify the NO release, a 2 cm section of SR-SNAP-Si cannula was placed in 4 mL of PBS buffer with EDTA pH 7.4 in the NOA sample cell and incubated at a physiological temperature of 37 °C. The cell pressure of the NOA cell was maintained at 9.8 Torr with an oxygen pressure of 6.7 psi. Prior to the sample analysis, an initial 2-point calibration of the NOA was first performed with zero NO gas (baseline) and later with the known 46.6 ppm of NO gas. Nitric oxide released from the sample via a stimulus of physiological conditions (pH 7.4, 37 °C) was detected in the chemiluminescence detector yielding the corresponding ppm/ppb of NO released, which was normalized with the surface area of samples to obtain the flux values with mol cm^{-2} min^{-1}. Samples were throughout incubated in PBS at 37 °C and the NO release was quantified at various time points during the 21 d of the experiment. Fresh PBS was regularly replaced during the incubation of the samples to avoid the saturation of leached SNAP or infused Si.

2.3.5.3 Shelf-Life of Insulin Cannula at Room Temperature

To examine the shelf-life of the SR-SNAP-Si insulin cannula, small portions of the SR-SNAP were divided into two categories. One set was infused with the Si and then stored in dark at room temperature for 30 d. The second set was stored without the Si infusion in the same conditions. This step was done to evaluate any influence of Si on NO stability during storage. The

cannulas stored without liquid infusion were infused with Si before NO release testing using the chemiluminescence NO Analyzer.

2.3.5.4 Determination of SNAP Leaching from SNAP-Impregnated Cannula

The amount of SNAP leached from SNAP-SR and SNAP-SR-Si cannula was determined by a UV-vis spectrophotometer. The surface area of SR-SNAP and SR-SNAP-Si was recorded to normalize the SNAP leaching of each cannula. Each sample was incubated in 10 mM PBS, pH 7.4, with 100 μM EDTA at 37 °C for 7 d. The incubation buffer was analyzed for SNAP concentration each day over a 7-d period. The amount of SNAP leached per surface area of the cannula was detected by UV-vis spectroscopy. The molar absorptivity of SNAP in 10 mM PBS, pH 7.4, with 100 μM EDTA at 37 °C was determined as 1072 M^{-1} cm^{-1} at 340 nm. The soaking buffer was replenished with fresh buffer after each measurement and incubated at 37 °C. The absorbance of the buffer was measured each day using UV-vis spectroscopy.

2.3.6 Evaluating the Antibacterial Efficacy of Insulin Cannula with an *In Vitro* 24 h Bacterial Adhesion Assay

The potential of the insulin cannula to thwart bacterial cell attachment and growth on the cannula surface was tested *in vitro* against two common gram-positive pathogens *Staphylococcus epidermidis* (ATCC 35984) and *Staphylococcus aureus* (ATCC 6538) for using 24 h bacterial adhesion assays. Since these pathogens are commonly found on the human skin, their presence and lack of sterility while inserting the cannula can increase the likelihood of bacterial adhesion and biofilm formation on the cannula leading to infections, thereby impacting the wear time of the cannula.

The antibacterial activity of the cannula was examined in terms of viable bacterial adhesion on the cannula surface. A single isolated colony of the bacterial strain was incubated overnight in LB medium for 15 h at 120 rpm at 37 °C. The optical density (O.D.) was measured

at 600nm (OD_{600}) using a UV-vis spectrophotometer. All samples (SR, SR-Si, SR-SNAP, and SR-SNAP-Si; n ≥ 3 each) were sterilized with UV irradiation under a Biosafety Cabinet (BSC). Cannulas were exposed to the bacterial solution with the final OD_{600} of bacteria ranging between 10^6 – 10^8 CFU mL^{-1} for 24 h at 120 rpm at 37 °C to maintain the chronic infection conditions. After 24 h, samples were gently rinsed with PBS to eliminate any loosely bound bacteria. The cannulas were then transferred to a fresh tube with sterile PBS and homogenized for 60 s using an OmniTip THb tissue homogenizer (Omni International, Inc.), followed by 60 s of vortexing to detach the adhered bacterial cells from the cannula into the PBS solution.

The bacterial cells collected in the PBS buffer were serially diluted (10^{-1} to 10^{-4}) and 30 µL of bacterial culture was spread onto an LB agar plate using a sterile L-shape spreader. The plates were incubated overnight at 37 °C and viable colonies were counted to calculate the antibacterial activity of the test cannula (C_{Test}) compared to the SR control cannula ($C_{Control}$) using Equation 2.1 and presented as CFU cm^{-2}.

$$\%\ Bacterial\ reduction = \frac{C_{Control} - C_{Test}}{C_{Control}}\ x\ 100 \quad \textbf{(Equation 2.1)}$$

2.3.7 Statistical Analysis

All the data were performed with a sample size n ≥ 3. Data are reported as mean ± standard error of mean. Dixon's Q-test was performed on the data points to identify any outliers. Statistical significance was determined using a two-tailed Student's *t*-test with a hypothesis of unequal variance and α = 0.05 to show the significance of the results.

2.4 Results

2.4.1 Antifouling Liquid-Infused and Nitric Oxide Releasing Insulin Cannula

In this study, SR cannula that exhibits NO release via SNAP impregnation and antifouling surface properties via Si oil infusion were investigated. This new generation of insulin cannula is

green in color due to the presence of SNAP (**Figure 2.3A**). The excellent swelling capacity of the silicone polymer in THF solvent enabled homogenous impregnation of SNAP.[34] The SR-SNAP cannulas were infused with Si for 24 h to develop the antifouling surface (SR-SNAP-Si). Silicone oil provided the antifouling surface to reduce protein and bacterial adhesion and assisted in the controlled release of NO by restricting the hydration of the SR. The final SR-SNAP-Si cannula can then be attached to an insulin infusion set for subcutaneous delivery of insulin (**Figure 2.3B**).

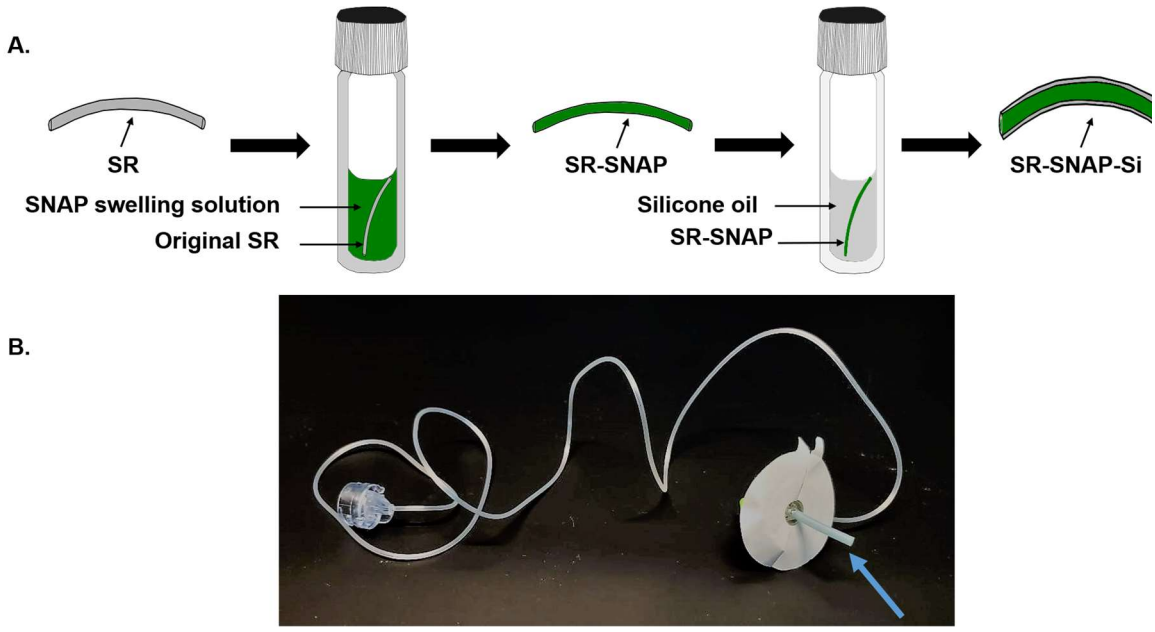

Figure 2.3 (A) Methodology for the fabrication of SR-SNAP-Si insulin cannulas. Silicone rubber (SR) cannula tubing is soaked in SNAP-THF mixture for 24 h to develop an antibacterial and anti-inflammatory surface (SR-SNAP), followed by 24 h of soaking in silicone oil to generate an antifouling surface. (B) The resultant SR-SNAP-Si cannulas (indicated by the blue arrow) can then be attached to the insulin infusion pump set, which will deliver insulin to the body. The insulin cannula is inserted into the body subcutaneously with the help of a small needle and held in place by an adhesive patch adhered to the skin.

2.4.2 Characterization of Cannula Surface through SEM Imaging

The scanning electron microscopy images of the original SR cannula, SNAP-impregnated cannula only, Si oil-infused cannula only, and combined SR-SNAP-Si cannula, were used to evaluate the surface properties throughout the fabrication process (**Figure 2.4)**. The images show no observable changes to the surface, which indicated that the SNAP impregnation and Si

infusion of the SR cannula do not significantly alter the surface properties. These findings are consistent with previous literature that report no significant changes to surface morphology after SNAP impregnation or Si swelling.[34]

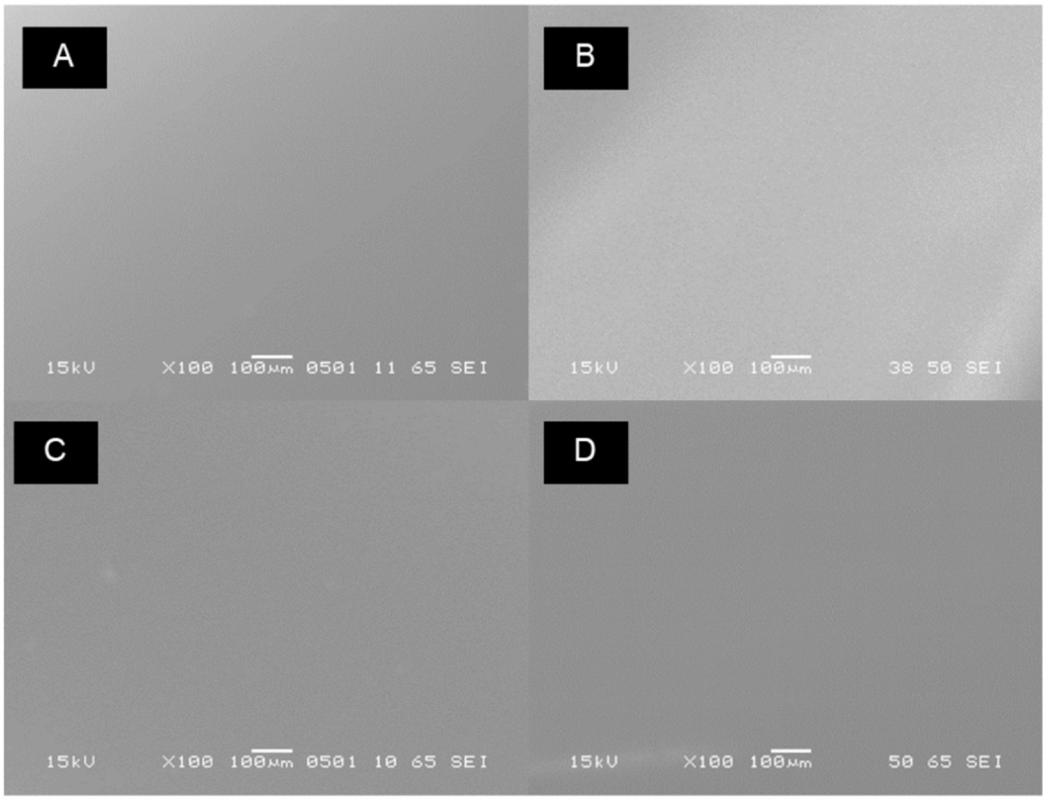

Figure 2.4 Representative scanning electron microscopy images of original SR cannula (A), SR-Si (B), SR-SNAP (C) SR-SNAP-Si cannula (D).

2.4.3 Evaluation of Sliding Angle and Lifetime of Antifouling Properties

The longevity of the liquid-infused interface will determine the antifouling lifetime of cannulas. The sliding angle of water on the surface of the cannula over 21 d was evaluated to establish the SLIP lifetime. The control SR experienced no sliding at angles < 90 ° throughout the duration of the experiment. In contrast, the SR-SNAP-Si exhibited an initial sliding angle of 12.33 ± 0.99 °. The sliding angle of Si infused surface remained < 20 ° over the duration of the

experiment (**Figure 2.5**). These results demonstrate the ability of the liquid-infused cannula to retain the antifouling interface to resist protein and bacterial adhesion for at least 21 d.

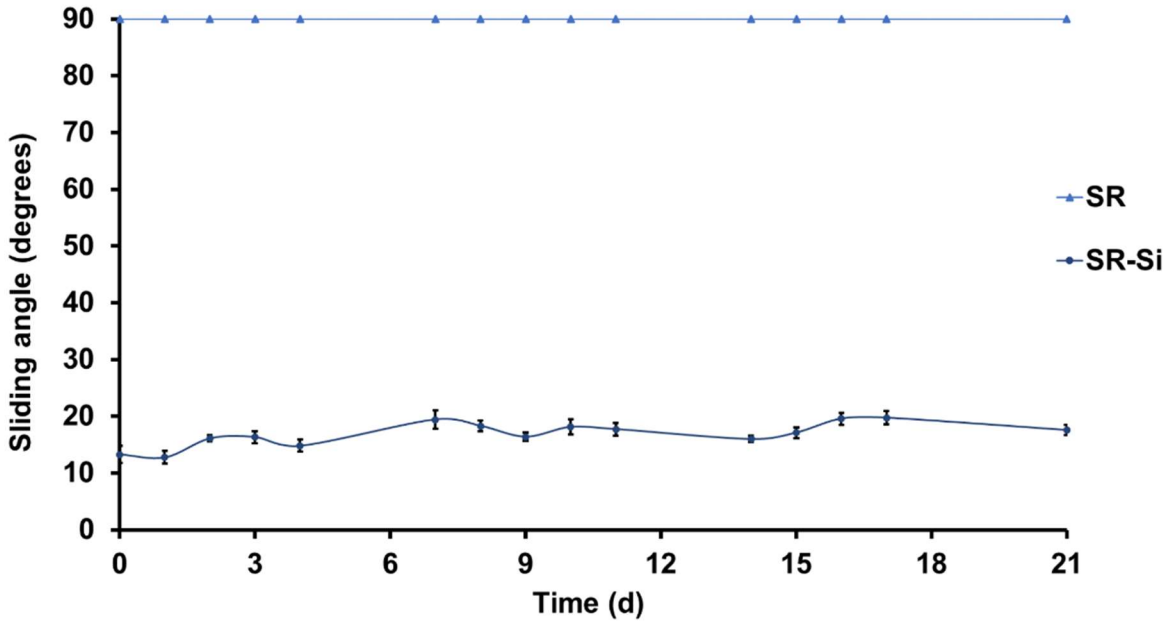

Figure 2.5 Sliding angle of original SR cannula and SR-SNAP-Si cannula over the period of 21 d when soaked in PBS at 37 °C.

2.4.4 Characterization of Antifouling Properties via *In Vitro* Fibrinogen Adsorption Assay

The adsorption of protein to the SR-SNAP-Si cannula and controls was evaluated both quantitatively and qualitatively after 2 h exposure to fibrinogen (**Figure 2.6**). The SR and SR-SNAP cannulas exhibited an increased amount of fibrinogen adsorption, similar to previously reported studies.[21, 50] The infusion of silicone oil and development of an antifouling surface in SR-Si and SR-SNAP-Si showed ca. 71.21% and 66.40% reduction in the amount of fibrinogen adsorbed on the cannula surface, respectively ($p < 0.05$ SR vs. SR-Si and SR-SNAP-Si). The results from the sliding angle experiment (**Figure 2.5**) demonstrate that the Si-infused interface can retain the antifouling property for at least 21 d, indicating the potential for the cannulas to exhibit long-term resistance to biofouling.

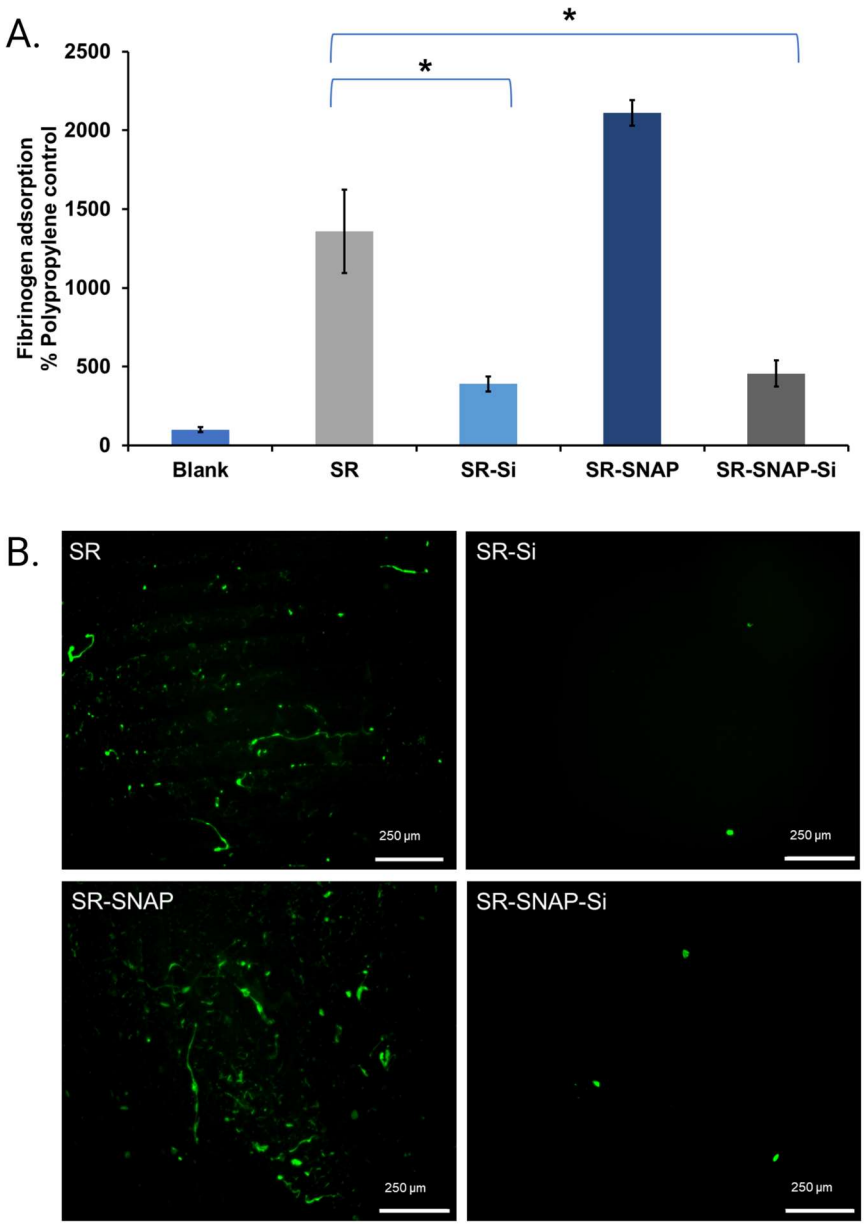

Figure 2.6 Assessment of fibrinogen adsorption on insulin cannula. (A) Fluorescence intensities recorded for fibrinogen adsorption after 2 h of exposure. Data represented as normalized values of % polypropylene control (mean ± standard error of mean, n ≥ 3; * represents $p < 0.05$, SR vs. SR-Si and SR-SNAP-Si) (B) Fluorescent images of cannula surface were captured after 2 h of protein exposure. All the images were captured with the same light exposure using Keyence Fluorescence Microscope BZ-X800 and processed using ImageJ software.

2.4.5 Characterization of SNAP-impregnated Insulin Cannula for Enhanced NO-releasing Properties

2.4.6 Determination of SNAP Impregnation in Insulin Cannula

After silicone oil infusion in the SNAP-impregnated SR, an absorbance-based extraction method was used to quantify the wt% SNAP impregnated in the cannula. Each sample was soaked in THF due to the excellent solubility of SNAP and the ability to extract all the impregnated SNAP for quantitative analysis via UV-vis spectroscopy. The SNAP-impregnation-solvent (125 mg mL^{-1}) resulted in a loading of 5.77 ± 0.14 wt% SNAP in the SR cannulas.

2.4.7 Real-time Nitric Oxide Release

The NO release measured from the SR-SNAP-Si cannulas under physiological conditions using chemiluminescence exhibited a consistent release at physiologically relevant levels of NO

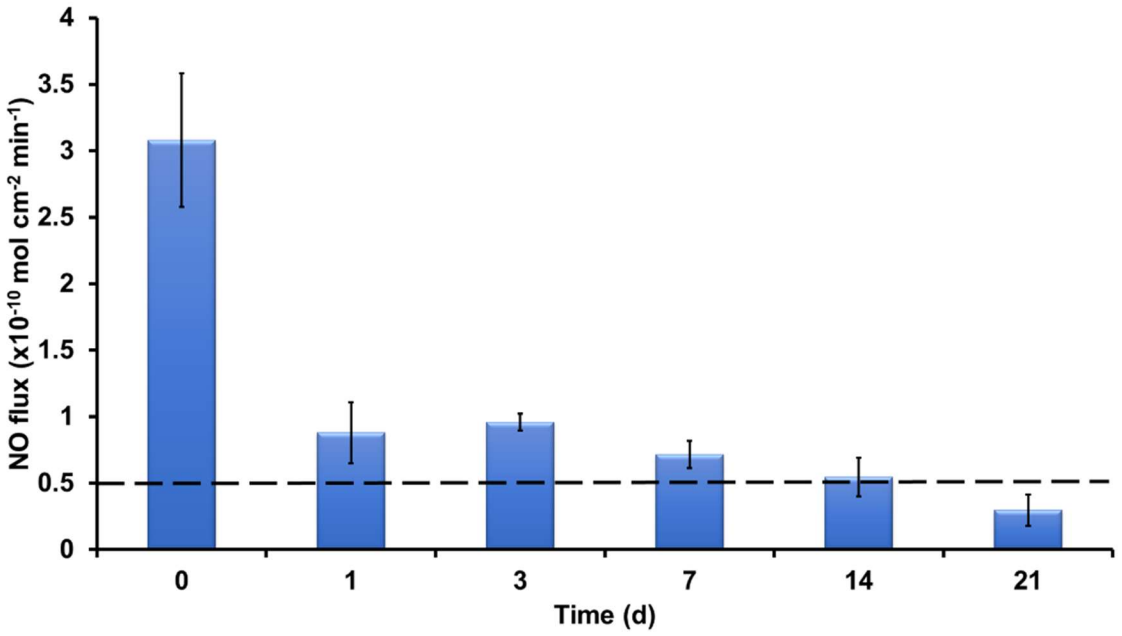

Figure 2.7 Measurement of real-time NO release from 5.7 wt% SR-SNAP-Si using a Chemiluminescence Nitric Oxide Analyzer. The NO flux levels were measured at physiological conditions in PBS with 100 µM EDTA for 21 d. Data represents mean ± standard error of mean, n≥3, dashed line represents physiological levels of NO release.

(0.5−4 × 10^{-10} mol cm^{-2} min^{-1}) over a 3-week period, with initial and final release rates of ca. 3.08 ± 0.50 × 10^{-10} mol cm^{-2} min^{-1} and 0.29 ± 0.11 × 10^{-10} mol cm^{-2} min^{-1}, respectively (**Figure 2.7**). The initial burst of NO flux levels was likely due to the presence of SNAP located in the water-rich layer of the polymer interface, which can more rapidly diffuse into the soaking buffer. The NO flux of the cannula then stabilizes over time and remains constant for > 14 d. It is important to note that the longevity of the NO release can be modulated by altering the SNAP concentration in the impregnating solution to control the wt% of SNAP incorporated in the polymer. However, this step was limited by the solubility of SNAP in THF. This tiny insulin cannula can remarkably release NO at physiological levels for > 14 d.

2.4.8 Shelf-Life of Insulin Cannula at Room Temperature

The cannulas were tested for their NO release under physiological conditions and the results from this study showed NO-releasing cannula are stable at room temperature for up to 30

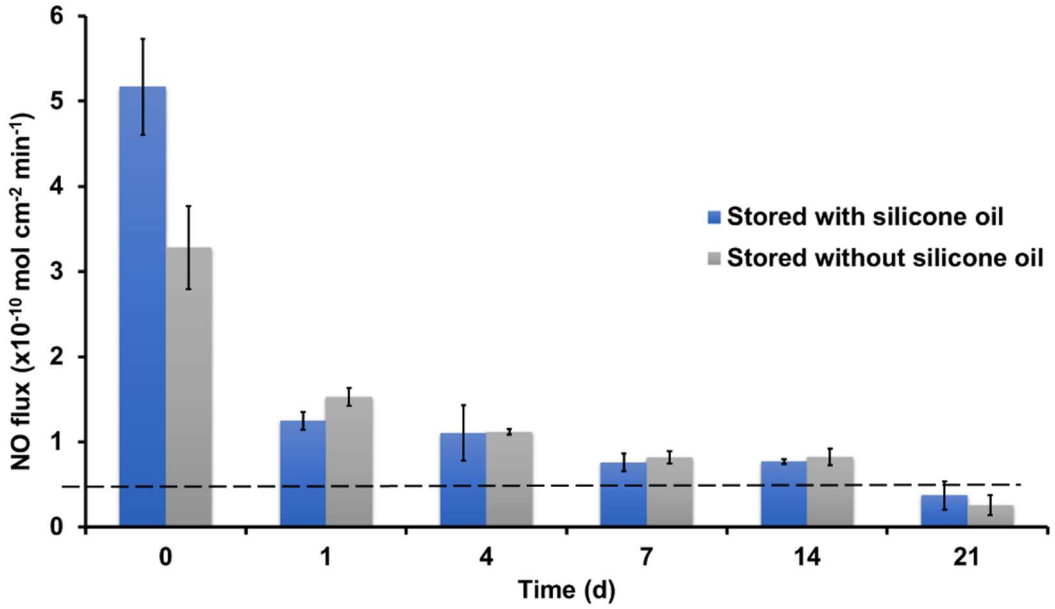

Figure 2.8. Measurement of real-time NO release from cannula stored at room temperature for 30 d. The NO flux levels were measured from SNAP impregnated cannulas infused with silicone oil before and after the storage. Data represents mean ± standard error of mean, n=3. Dashed line represents physiological levels of NO release.

d with and without the Si infusion. The cannulas stored with and without Si oil exhibited a NO release profile similar to fresh samples (**Figure 2.7**) and released NO at physiological levels for > 14 d (**Figure 2.8**). The results obtained from the shelf-life study validate that SNAP impregnation within the SR matrix exhibits SNAP stability and permits long-term storage of SNAP-impregnated silicone cannulas.

2.4.9 Determination of SNAP Leaching

To evaluate the amount of SNAP leached from the SR-SNAP-Si cannula, each sample was soaked in PBS at 37 °C for 7 d. The buffer was collected each day and the absorbance was measured using UV-vis spectroscopy. After 24 h, 35.26 ± 3.01 and 60.32 ± 5.74 μg cm^{-2} SNAP leached from SR-SNAP-Si and SR-SNAP, respectively (**Figure 2.9**). While the largest amount of leaching was after 24 h, the amount of leaching decreased with each successive day. The results indicated that after 7 d, a total of 128.40 ± 5.90 and 190.35 ± 11.90 μg cm^{-2} SNAP leached from

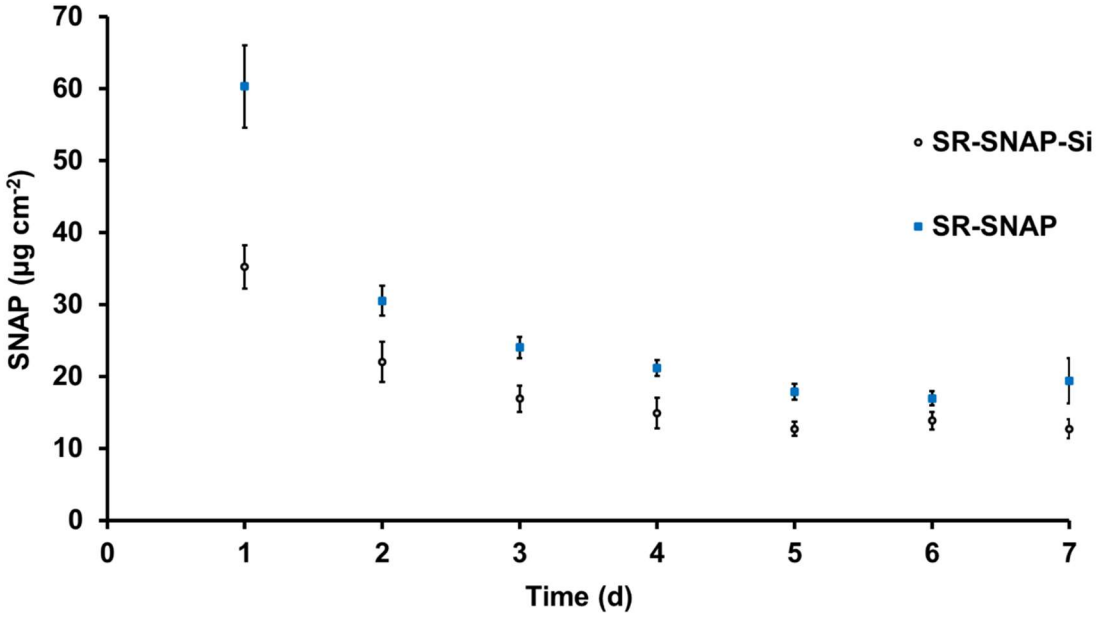

Figure 2.9 Mass of SNAP leaching per surface area of SR-SNAP cannula and SR-SNAP-Si cannula. Data represents mean ± standard error of mean, n ≥ 3.

SR-SNAP-Si and SR-SNAP, respectively. The incorporation of the silicone oil reduced SNAP leaching by 32.54%.

2.4.10 Evaluating the Antibacterial Efficacy of Insulin Cannula with 24 h Bacterial Adhesion *In Vitro*

The numerous biological roles of NO, including the antibacterial and anti-inflammatory properties, inspire the development of cannula with enhanced biocompatibility. Strategies to reduce bacterial adhesion and proliferation have included either modifying the physical or chemical characteristics of the material itself and/or incorporating of antibacterial agent. The SR-SNAP-Si cannula utilizes the combinational method of two strategies: (i) modifying the surface by infusion of silicone oil in the polymer and (ii) impregnating the NO donor for an active release of antibacterial agent (NO). Infusion of silicone oil offers a slippery, hydrophobic surface for reducing bacterial adhesion on the polymer surface to prevent the formation of biofilm, and NO as a free gas radical which provides a bactericidal activity through DNA deamination and membranal damage via lipid peroxidation and denaturation of enzymes.[51] In order the evaluate the antimicrobial properties of the SR-SNAP-Si cannula, the cannulas were exposed to *S. aureus* or *S. epidermidis* for 24 h followed by determining the viable bacterial cells adhered on the cannula surface to obtain viable CFU cm^{-2} (**Figure 2.10**). *S. aureus* adhesion (**Figure 2.10A**) on the SR-SNAP-Si exhibited a ca. 99.77% reduction compared to the SR control ($p < 0.01$). The SR-Si and SR-SNAP were observed to have ca. 89.92% and 99.04% reduction of viable adhered cells, respectively, ($p < 0.01$) due to the individual action of NO release and antifouling interface. The viable cell count of *S. epidermidis* adhered on the SR-SNAP-Si exhibited a ca. 94.89% reduction compared to SR control ($p < 0.05$), while the SR-Si and SR-SNAP cannula showed a ca. 35.34% and an 80.45% reduction in viable bacterial cells, respectively ($p > 0.05$) (**Figure 2.10B**). The integration of Si oil infusion with the bactericidal activity of NO exhibited a synergistic antimicrobial

action leading to the most significant reduction of viable bacteria on the SR-SNAP-Si cannula surfaces.

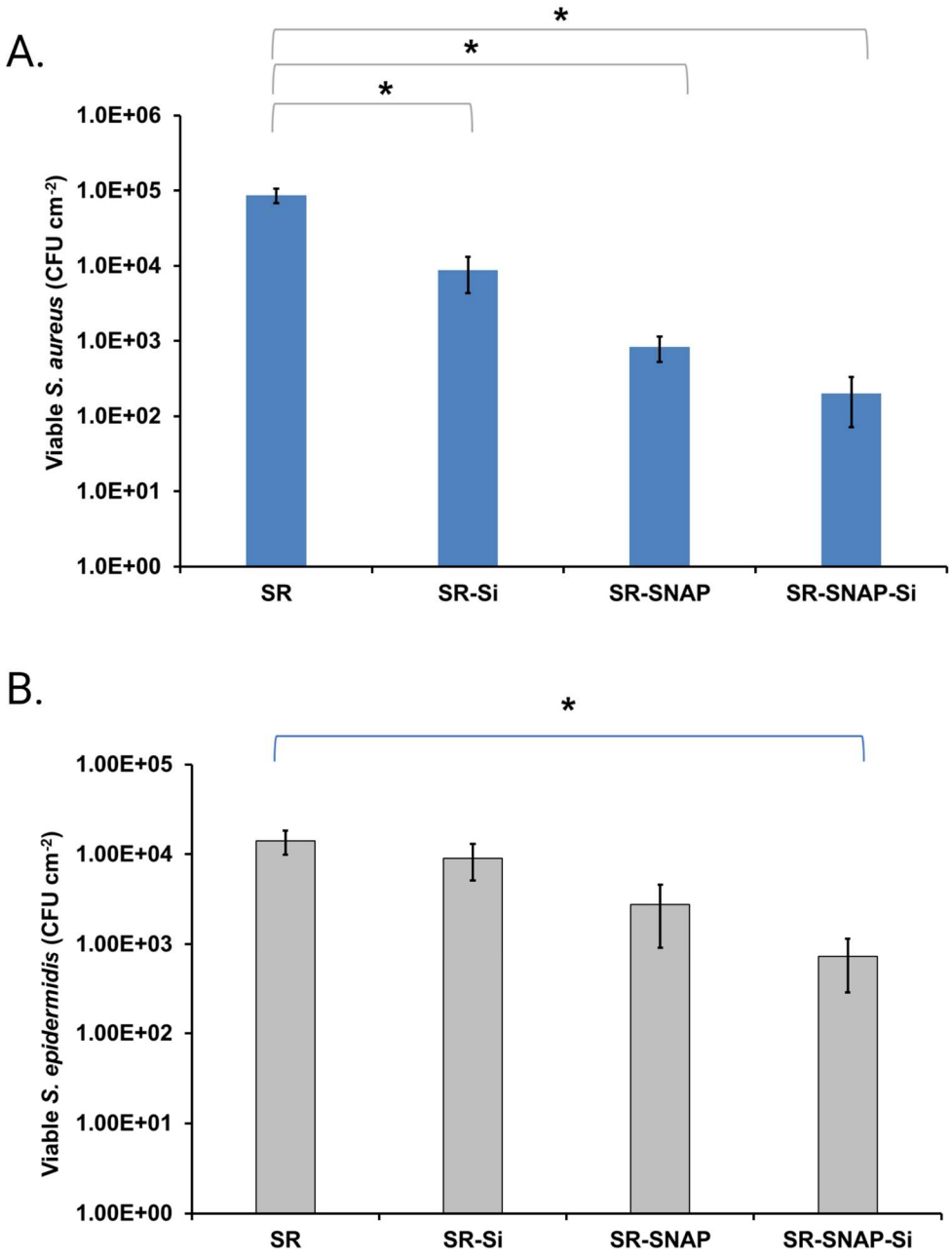

Figure 2.10 Antibacterial activity of insulin cannula calculated as a log of the colony forming units (CFU) cm^{-2} of surface area against (A) *Staphyloccocus aureus;* data represents mean ± standard error of mean (n≥3, * represents $p < 0.01$ SR vs. SR-Si, SR-SNAP, SR-SNAP-Si; and (B) *Staphylococcus epidermidis*; data represents mean ± standard error of mean (n≥3), * represents $p < 0.05$ SR-SNAP-Si.

2.5 Discussion

Silicone rubber has been extensively utilized in developing medical devices such as urinary catheters, shunts, and intravenous catheters. Silicone rubber polymer offers improved elasticity and endurance to fracture and distortion that can help prevent surface cracking during insertion or use. Regardless of the exceptional material characteristics, SR still suffers from biofouling and biofilm formation. In this work, a liquid-infused slippery surface was combined with NO-releasing capabilities through the infusion of Si oil and the impregnation of the NO donor SNAP into commercial medical-grade SR cannula tubing. The surface properties of a medical device play a key role in the adsorption of bacteria and proteins, which may lead to the pathogenesis of disease and device failure.[52] The SEM images showed no observable changes in the surface morphology of the SR-SNAP-Si cannula (**Figure 2.4**) which is consistent with previously reported SEM of SNAP-impregnated SR that showed no significant changes of the surface compared to the original SR.[34]

In addition, surface properties such as wettability affect device performance by altering biofouling.[53] Slippery liquid-infused porous surfaces (SLIPs) are effective at reducing biofouling by utilizing capillary forces to generate a low adhesion liquid layer between the device surface and the external physiological environment.[20] Characterization of antifouling interface durability was evaluated via sliding angle measurements of the SR-SNAP-Si cannula surface. The sliding angle of Si infused surface remained < 20 ° over 21 d (**Figure 2.5**). This result is supported by Goudie et al. which demonstrated the initial sliding angle of LI-SR was 10.8 ± 2.4 ° and remained < 20 ° after 7 d and also showed no significant difference between SNAP containing LINOrel-SR versus LI-SR.[21]

Protein adsorption is the first response of the host to the implanted biomaterials, where adsorbed proteins act as an attractant to activate various phagocytic cells of the immune defense system through ligand-receptor interactions.[18] Fibrinogen, a key protein molecule, has been

recognized as an initiator of inflammatory pathways in many diseased conditions[54] There has been a persistent rise in scientific investigation to derive the conspicuous role of fibrinogen and its degradation products in regulating the inflammatory response in various tissues.[54] The interaction of fibrinogen protein with the CD11b/CD18 integrin receptor has been recognized as a critical regulator of innate immune cell activation upon implantation of biomaterials. Fibrinogen signaling through CD11b/CD18 has been shown to activate proinflammatory pathways, such as NF-κB, which results in a local production of cell signaling protein (inflammatory cytokines), such as Tumor Necrosis Factor-alpha (TNFα) and Inter Leukin-1 (IL-1).[55-57] The immune cells activated by the protein molecules interact with proteins and other macromolecules to phagocytose the implanted material. The process of foreign body response activates the immune cells and can lead to the encapsulation of the cannula, which impairs the effective delivery of insulin to the bloodstream. Although, NO-releasing materials exhibit attenuation of inflammation, they have no mechanism to prevent the adsorption of proteins on the surface.[21, 50] Protein adsorption initiates an inflammatory response to indwelling medical devices. The series of reactions leading to a proinflammation state can be attenuated by modifying the surface chemistry of the cannula to avert the adsorption proteins. The infusion of Si in the SR-SNAP-Si cannulas significantly reduced fibrinogen adsorption by 66.40% as compared to the controls (**Figure 2.6**).

The amount of SNAP impregnated in the SR-SNAP-Si was quantified via UV-vis spectroscopy.[58] The SNAP impregnation method lead to loading of 5.77 ± 0.14 wt% SNAP in SR, which is consistent with previously reported SNAP impregnation of SR that achieved ca. 5 wt% when using a 125 mg mL^{-1} SNAP-impregnation-solvent.[44] Although in the previous report, the wt% SNAP loading was quantified using chemiluminescent detection, the similarity of these results demonstrated the THF extraction was a viable method for quantification of SNAP loading in SR.[43]

The SR-SNAP-Si cannulas released NO for > 14 d, with the initial and final release rates of 3.08 ± 0.50 × 10^{-10} mol cm^{-2} min^{-1} and 0.29 ± 0.11 × 10^{-10} mol cm^{-2} min^{-1}, respectively **(Figure 2.7)**. The NO-releasing cannula was stable during storage at room temperature for up to 30 d with and without Si incubation **(Figure 2.8).** Samples stored without Si during storage were infused with Si prior to the NOA test. The difference in the NO release levels of the two sets of samples could be due to the loss in the small amount of NO during the Si infusion process. After day 0, the NO release gradually lowers due to the slow diffusion of water into the hydrophobic polymeric matrix. Storage of the cannula had minimal effects on the NO release profile as compared to freshly prepared cannula samples **(Figure 2.7)**. The NO flux released from 5.7 wt% SR-SNAP-Si reported in this study mimics the range of endogenous NO flux from endothelial cells.[25] Previous reports have demonstrated that the infusion of Si in the crosslinked SR elastomer does not significantly alter the NO release profile.[21] Comparable reports of SNAP stability during storage were seen in the different polymeric matrices that showed the stability of SNAP for up to 8 months.[35, 59] The excellent storage stability can be attributed to the intramolecular hydrogen bonding between the SNAP crystals within the polymer-crystal composite.[35, 37] Overall, the NO release in the shelf-life studies remained within physiological levels throughout the 14 d period very similar to the freshly prepared cannula.

Leaching of SNAP from the SR matrix may reduce the NO release longevity of the device and cause nonlocalized NO-mediated responses.[60] Reports have shown that SNAP stability was enhanced by hydrophobic polymers, which increased the lifetime of NO release due to intramolecular hydrogen bonding among SNAP crystals and the low water uptake of hydrophobic polymers, which slows SNAP dissolution and diffusion out of the polymer.[37, 48] In addition, reports have demonstrated that hemocompatibility and biocompatibility of medical devices can be significantly improved by preventing fouling of proteins and bacteria on the surface via NO release and liquid-infused surfaces.[20, 21, 43] The overall leaching of NO donor SNAP in the soaking buffer

was reduced by 32.54% with the Si infusion compared to the controls (**Figure 2.9**). This result was consistent with previously reported LINORel-UC and LINORel-SR that found a ca. 38% and 45% reduction of SNAP leaching compared to samples without Si.[21, 43] The higher levels of SNAP leaching and higher initial NO flux levels during the first 24 h of incubation are a result of SNAP within the water-rich layer of the polymer. Low amounts of SNAP near the polymer-liquid interface may leach; however, the degradation products of SNAP are a non-toxic FDA-approved drug, *N*-acetyl-*D*-penicillamine (NAP), and NAP-dimer.[42] Previous reports have shown that low concentrations of SNAP were benign during *in vivo* testing of SR-SNAP.[61]

Chemical modification in the DNA by reactive nitrogen species is one of the leading processes of NO-facilitated antibacterial action.[23] Nitric oxide exhibits antimicrobial characteristics resultant of a combination of nitrosative and oxidative mechanisms which results in the deamination of DNA base pairs cytosine, adenine, and guanine.[62] The NO derivative molecules such as peroxynitrite and nitrogen dioxide alter and destruct the base pairs leading to the breakage of DNA strands and facilitating lipid peroxidation and membranal damage.[23, 51, 62, 63] Over the evolutionary process, eukaryotic cells have developed ways to scavenge these reactive oxygen and nitrogen species thereby placating their influence; however, bacterial cells remain susceptible.[64] The NO-releasing properties of the SR-SNAP-Si cannulas reduced the viable bacterial cell adhesion of *S. epidermidis* and *S. aureus* after 24 h by 94.89% and 99.77%, respectively, as compared to SR controls (**Figure 2.10**). These results are analogous to previous reports that characterized silicone rubber, polyurethane, and SNAP-E2A polymers, polyvinyl chloride which release similar levels of NO over a 24 h period.[33, 43, 65]

Surface modifications (physical surface properties) or chemical active release (nitric oxide) have both been individually demonstrated to be efficient approaches that inhibit the development of biofilm on medical devices. Liquid-infused porous surfaces generate a low-adhesion interface between the base polymer and the contacting liquid. This interface is established by the infusion

of the permeated liquid into the polymeric substrate where the fluid is influenced by the capillary forces and the existent chemical affinity between the infused liquid and the core polymer. The capability of the liquid-infused surface has been formerly validated with the infusion of biocompatible silicone oil in preventing biofouling on urinary catheters and blood-contacting devices.[21, 43] Although, liquid-infused surfaces can passively prevent device infections by inhibiting the attachment of microorganisms, there is still a concern regarding the capability of microorganisms to violate the oil surface and inhabit the base polymeric surface. Similarly, NO alone can kill the bacteria, but it does not prevent fouling of the surface and in fact, has been shown to exhibit high protein adsorption on catheters. For insulin cannulas to be successfully implanted long-term, both NO and antifouling properties are essential to address these issues. Here, two methods were combined to generate an insulin infusion cannula with a dual-operational surface that has significant benefits from a clinical translation perspective. The idea of utilizing these two methods comes from the antifouling nature of Si-infused surfaces that can prevent the attachment of protein and bacteria and the antimicrobial activity of NO. Unlike the current Teflon and steel cannula that need to be replaced every 2-3 days, SR-SNAP-Si has shown antifouling and NO-releasing properties that can help in increasing the lifetime of insulin cannula up to 21 d. It was observed that the combined approach in the SR-SNAP-Si cannulas provides a synergistic decline in the attachment of fibrinogen protein and *S. aureus* and *S. epidermidis* bacteria, implying that the new combination surface can generate a noticeably improved antifouling and antibacterial efficacy compared to either approach alone. The broad-spectrum antibacterial activity of NO can be applied to other pathogenic microorganisms often involved in catheter-related infections. The antibacterial activity of the SR-SNAP-Si can be enhanced by modulating the levels of NO release to further reduce viable bacterial attachment.

This methodology of SNAP impregnation in the commercial medical grade silicone rubber used in this study, not only addressed the problems associated with cannula-related infections

and biofouling but also addressed the concerns of developing NO-releasing polymers by conventional polymer engineering methods, that utilize high temperature possessing (i.e., polymer extrusion), which threatens the stability of SNAP and other NO donors. The novel insulin cannula exhibited an impressive ability to reduce biofouling due to the antifouling Si oil-infused surface and long-term NO release via SNAP impregnation for up to 3 weeks. These properties are significantly advantageous over the current commercially available insulin cannulas and demonstrate a promising method to fabricate insulin cannulas with enhanced long-term biocompatibility.

2.6 Conclusions

In this work, a liquid-infused slippery surface was combined with NO-releasing capabilities in commercial medical-grade silicone rubber tubing through the infusion of silicone oil and the impregnation of the NO donor SNAP. The SR-SNAP-Si cannulas were impregnated with 5.77 ± 0.14 wt% SNAP, which resulted in cannulas that release NO for > 14 d and also an antifouling surface for at least 21 d. The NO-releasing cannulas were stable during storage at room temperature both with and without Si oil for up to 30 d and showed NO flux values consistent with the cannula that was immediately tested after fabrication. The overall leaching of NO donor SNAP in the soaking buffer was reduced by 32.54% with the silicone oil infusion compared to the controls. The SR-SNAP-Si insulin cannula exhibited enhanced biocompatibility by displaying potent biocidal activity of NO (> 94 % reduction in viable *S. aureus* and *S. epidermidis*) as well as reduced biofouling via silicone oil infusion. These studies demonstrate the efficacy of the novel SR-SNAP-Si insulin cannula in reducing the challenges that impact the lifetime of the cannula used by Type 1 Diabetes patients. The novel insulin cannula can be easily combined with the continuous subcutaneous insulin infusion pump to expand the lifetime of the cannula from 3 days to 3 weeks. This work will help to further define the significance of the synergistic antibacterial, anti-inflammatory, and anti-fouling effects of NO and liquid-infused surfaces in the design of

insulin delivery systems. These new biomaterial interfaces can be utilized to provide antimicrobial and antifouling properties when applied to other indwelling medical devices, ultimately leading to improved biocompatibility of medical device interfaces and patient care.

2.7 References

1. Control, C. F. D.; Prevention, New CDC Report: More Than 100 Million Americans Have Diabetes Or Prediabetes. *Last Modified July* **2017,** *18*, 2017.

2. Association, A. D., Economic Costs Of Diabetes In The US In 2017. *Diabetes Care* **2018,** *41* (5), 917-928.

3. Umpierrez, G. E.; Klonoff, D. C., Diabetes Technology Update: Use Of Insulin Pumps And Continuous Glucose Monitoring In The Hospital. *Diabetes Care* **2018,** *41* (8), 1579-1589.

4. Lenhard, M. J.; Reeves, G. D., Continuous Subcutaneous Insulin Infusion: A Comprehensive Review Of Insulin Pump Therapy. *Archives Of Internal Medicine* **2001,** *161* (19), 2293-2300.

5. Bergenstal, R. M.; Tamborlane, W. V.; Ahmann, A.; Buse, J. B.; Dailey, G.; Davis, S. N.; Joyce, C.; Peoples, T.; Perkins, B. A.; Welsh, J. B., Effectiveness Of Sensor-Augmented Insulin-Pump Therapy In Type 1 Diabetes. *N. Engl. J. Med.* **2010,** *363* (4), 311-320.

6. Saboo, B. D.; Talaviya, P. A., Continuous Subcutaneous Insulin Infusion: Practical Issues. *Indian J. Endocrinol. Metabol.* **2012,** *16* (Suppl 2), S259.

7. Guinn, T. S.; Bailey, G. J.; Mecklenburg, R. S., Factors Related To Discontinuation Of Continuous Subcutaneous Insulin-Infusion Therapy. *Diabetes Care* **1988,** *11* (1), 46-51.

8. Mecklenburg, R. S.; Benson, E. A.; Benson, J. W.; Fredlund, P. N.; Guinn, T.; Metz, R. J.; Nielsen, R. L.; Sannar, C. A., Acute Complications Associated With Insulin Infusion Pump Therapy: Report Of Experience With 161 Patients. *JAMA* **1984,** *252* (23), 3265-3269.

9. Guenego, A.; Bouzillé, G.; Breitel, S.; Esvant, A.; Poirier, J. Y.; Bonnet, F.; Guilhem, I., Insulin Pump Failures: Has There Been An Improvement? Update Of A Prospective Observational Study. *Diabetes Technology & Therapeutics* **2016,** *18* (12), 820-824.

10. Heinemann, L.; Krinelke, L., Insulin Infusion Set: The Achilles Heel Of Continuous Subcutaneous Insulin Infusion. *J Diabetes Sci Technol* **2012,** *6* (4), 954-964.

11. Oliveira, W.; Silva, P.; Silva, R.; Silva, G.; Machado, G.; Coelho, L.; Correia, M., Staphylococcus Aureus And Staphylococcus Epidermidis Infections On Implants. *J. Hosp. Infect.* **2018,** *98* (2), 111-117.

12. Donlan, R. M., Biofilm Formation: A Clinically Relevant Microbiological Process. *Clin. Infect. Dis.* **2001,** *33* (8), 1387-1392.

13. Rupp, M. E.; Ulphani, J. S.; Fey, P. D.; Bartscht, K.; Mack, D., Characterization Of The Importance Of Polysaccharide Intercellular Adhesin/Hemagglutinin Of Staphylococcus Epidermidis In The Pathogenesis Of Biomaterial-Based Infection In A Mouse Foreign Body Infection Model. *Infection And Immunity* **1999,** *67* (5), 2627-2632.

14. Thammavongsa, V.; Missiakas, D. M.; Schneewind, O., Staphylococcus Aureus Degrades Neutrophil Extracellular Traps To Promote Immune Cell Death. *Science* **2013,** *342* (6160), 863-866.

15. Schmid, V.; Hohberg, C.; Borchert, M.; Forst, T.; Pfützner, A., Pilot Study For Assessment Of Optimal Frequency For Changing Catheters In Insulin Pump Therapy-Trouble Starts On Day 3. *J Diabetes Sci Technol* **2010,** *4* (4), 976-982.

16. Jamal, M. A.; Garoge, K.; Rosenblatt, J. S.; Hachem, R. Y.; Raad, I. I., Development Of Gendine-Coated Cannula For Continuous Subcutaneous Insulin Infusion For Extended Use. *Antimicrob. Agents Chemother.* **2015,** *59* (8), 4397-4402.

17. Kiedrowski, M. R.; Horswill, A. R., New Approaches For Treating Staphylococcal Biofilm Infections. *Annals Of The New York Academy Of Sciences* **2011,** *1241* (1), 104-121.

18. Anderson, J. M.; Rodriguez, A.; Chang, D. T. In *Foreign Body Reaction To Biomaterials*, Seminars In Immunology, Elsevier: 2008; Pp 86-100.

19. Hauzenberger, J. R.; Münzker, J.; Kotzbeck, P.; Asslaber, M.; Bubalo, V.; Joseph, J. I.; Pieber, T. R., Systematic In Vivo Evaluation Of The Time-Dependent Inflammatory Response To Steel And Teflon Insulin Infusion Catheters. *Sci Rep* **2018,** *8* (1), 1132.

20. Maccallum, N.; Howell, C.; Kim, P.; Sun, D.; Friedlander, R.; Ranisau, J.; Ahanotu, O.; Lin, J. J.; Vena, A.; Hatton, B., Liquid-Infused Silicone As A Biofouling-Free Medical Material. *ACS Biomater Sci. Eng.* **2014,** *1* (1), 43-51.

21. Goudie, M. J.; Pant, J.; Handa, H., Liquid-Infused Nitric Oxide-Releasing (Linorel) Silicone For Decreased Fouling, Thrombosis, And Infection Of Medical Devices. *Sci. Rep.* **2017,** *7* (1), 13623.

22. Leslie, D. C.; Waterhouse, A.; Berthet, J. B.; Valentin, T. M.; Watters, A. L.; Jain, A.; Kim, P.; Hatton, B. D.; Nedder, A.; Donovan, K., A Bioinspired Omniphobic Surface Coating On Medical Devices Prevents Thrombosis And Biofouling. *Nat Biotechnol* **2014,** *32* (11), 1134.

23. Schairer, D. O.; Chouake, J. S.; Nosanchuk, J. D.; Friedman, A. J., The Potential Of Nitric Oxide Releasing Therapies As Antimicrobial Agents. *Virulence* **2012,** *3* (3), 271-279.

24. Hibbs Jr, J.; Taintor, R.; Vavrin, Z., Macrophage Cytotoxicity: Role For L-Arginine Deiminase And Imino Nitrogen Oxidation To Nitrite. *Science* **1987**, *235* (4787), 473− 476.

25. Vaughn, M. W.; Kuo, L.; Liao, J. C., Estimation Of Nitric Oxide Production And Reactionrates In Tissue By Use Of A Mathematical Model. *Am. J. Physiol. Heart Circ. Physiol.* **1998,** *274* (6), H2163-H2176.

26. Weinberg, J.; Misukonis, M.; Shami, P.; Mason, S.; Sauls, D.; Dittman, W.; Wood, E.; Smith, G.; Mcdonald, B.; Bachus, K., Human Mononuclear Phagocyte Inducible Nitric Oxide Synthase (Inos): Analysis Of Inos Mrna, Inos Protein, Biopterin, And Nitric Oxide Production By Blood Monocytes And Peritoneal Macrophages. *Blood* **1995,** *86* (3), 1184-1195.

27. Carpenter, A. W.; Schoenfisch, M. H., Nitric Oxide Release: Part II. Therapeutic Applications. *Chem. Soc. Rev.* **2012,** *41* (10), 3742-3752.

28. Radomski, M. W.; Palmer, R.; Moncada, S., The Anti-Aggregating Properties Of Vascular Endothelium: Interactions Between Prostacyclin And Nitric Oxide. *Br. J. Pharmacol.* **1987,** *92* (3), 639-646.

29. Thomas, D. D.; Liu, X.; Kantrow, S. P.; Lancaster, J. R., Jr., The Biological Lifetime Of Nitric Oxide: Implications For The Perivascular Dynamics Of NO And O2. *Proc. Natl. Acad. Sci. U. S. A.* **2001,** *98* (1), 355-360.

30. Frost, M. C.; Reynolds, M. M.; Meyerhoff, M. E., Polymers Incorporating Nitric Oxide Releasing/Generating Substances For Improved Biocompatibility Of Blood-Contacting Medical Devices. *Biomaterials* **2005,** *26* (14), 1685-1693.

31. Soto, R. J.; Merricks, E. P.; Bellinger, D. A.; Nichols, T. C.; Schoenfisch, M. H., Influence Of Diabetes On The Foreign Body Response To Nitric Oxide-Releasing Implants. *Biomaterials* **2018,** *157*, 76-85.

32. Malone-Povolny, M. J.; Maloney, S. E.; Schoenfisch, M. H., Nitric Oxide Therapy For Diabetic Wound Healing. *Adv. Healthcare Mater.* **2019,** *8* (12), 1801210.

33. Singha, P.; Pant, J.; Goudie, M. J.; Workman, C. D.; Handa, H., Enhanced Antibacterial Efficacy Of Nitric Oxide Releasing Thermoplastic Polyurethanes With Antifouling Hydrophilic Topcoats. *Biomater. Sci.* **2017,** *5* (7), 1246-1255.

34. Brisbois, E. J.; Major, T. C.; Goudie, M. J.; Bartlett, R. H.; Meyerhoff, M. E.; Handa, H., Improved Hemocompatibility Of Silicone Rubber Extracorporeal Tubing Via Solvent Swelling-Impregnation Of S-Nitroso-N-Acetylpenicillamine (SNAP) And Evaluation In Rabbit Thrombogenicity Model. *Acta Biomater.* **2016,** *37*, 111-119.

35. Goudie, M. J.; Brisbois, E. J.; Pant, J.; Thompson, A.; Potkay, J. A.; Handa, H., Characterization Of An S-Nitroso-N-Acetylpenicillamine–Based Nitric Oxide Releasing Polymer From A Translational Perspective. *Int. J. Polym. Mater. Polym. Biomater.* **2016,** *65* (15), 769-778.

36. Pant, J.; Gao, J.; Goudie, M. J.; Hopkins, S. P.; Locklin, J.; Handa, H., A Multi-Defense Strategy: Enhancing Bactericidal Activity Of A Medical Grade Polymer With A Nitric Oxide Donor And Surface-Immobilized Quaternary Ammonium Compound. *Acta Biomater.* **2017,** *58*, 421-431.

37. Wo, Y.; Li, Z.; Brisbois, E. J.; Colletta, A.; Wu, J.; Major, T. C.; Xi, C.; Bartlett, R. H.; Matzger, A. J.; Meyerhoff, M. E., Origin Of Long-Term Storage Stability And Nitric Oxide Release

Behavior Of Carbosil Polymer Doped With S-Nitroso-N-Acetyl-D-Penicillamine. *ACS Appl. Mater. Interfaces* **2015,** *7* (40), 22218-22227.

38. Williams, D. L. H., The Chemistry Of S-Nitrosothiols. *Accounts Of Chemical Research* **1999,** *32* (10), 869-876.

39. Parameshvara, V., Mercury Poisoning And Its Treatment With N-Acetyl-D, L-Penicillamine. *Occup. Environ. Med.* **1967,** *24* (1), 73-76.

40. Agocs, M.; Clarkson, T., Mercury Toxicity. *Am. Fam Physician* **1992,** *46* (6), 1731– 1744.

41. Kark, R. P.; Poskanzer, D. C.; Bullock, J. D.; Boylen, G., Mercury Poisoning And Its Treatment With N-Acetyl-D, L-Penicillamine. *N. Engl. J. Med.* **1971,** *285* (1), 10-16.

42. Jones, M.; Weaver, A.; Weller, W., The Relative Effectiveness Of Some Chelating Agents As Antidotes In Acute Cadmium Poisoning. *Res. Commun. Mol. Pathol Pharmacol* **1978,** *22* (3), 581-588.

43. Homeyer, K. H.; Goudie, M. J.; Singha, P.; Handa, H., Liquid-Infused Nitric-Oxide-Releasing Silicone Foley Urinary Catheters For Prevention Of Catheter-Associated Urinary Tract Infections. *ACS Biomater. Sci. Eng.* **2019,** *5* (4), 2021-2029.

44. Colletta, A.; Wu, J.; Wo, Y.; Kappler, M.; Chen, H.; Xi, C.; Meyerhoff, M. E., S-Nitroso-N-Acetylpenicillamine (SNAP) Impregnated Silicone Foley Catheters: A Potential Biomaterial/Device To Prevent Catheter-Associated Urinary Tract Infections. *ACS Biomater. Sci. Eng.* **2015,** *1* (6), 416-424.

45. Hopkins, S. P.; Pant, J.; Goudie, M. J.; Schmiedt, C.; Handa, H., Achieving Long-Term Biocompatible Silicone Via Covalently Immobilized S-Nitroso-N-Acetylpenicillamine (SNAP) That Exhibits 4 Months Of Sustained Nitric Oxide Release. *ACS Appl. Mater. Interfaces* **2018**, 10 (32), pp. 27316-27325.

46. Zhang, H.; Cloud, A. In *The Permeability Characteristics Of Silicone Rubber*, Proceedings Of 2006 SAMPE Fall Technical Conference, 2006; Pp 72-75.

47. Chipinda, I.; Simoyi, R. H., Formation And Stability Of A Nitric Oxide Donor: S-Nitroso-N-Acetylpenicillamine. *J. Phys. Chem. B* **2006,** *110* (10), 5052-5061.

48. Wo, Y.; Brisbois, E. J.; Wu, J.; Li, Z.; Major, T. C.; Mohammed, A.; Wang, X.; Colletta, A.; Bull, J. L.; Matzger, A. J.; Xi, C.; Bartlett, R. H.; Meyerhoff, M. E., Reduction Of Thrombosis And Bacterial Infection Via Controlled Nitric Oxide (NO) Release From S-Nitroso-N-Acetylpenicillamine (SNAP) Impregnated Carbosil Intravascular Catheters. *ACS Biomater. Sci. Eng.* **2017,** *3* (3), 349-359.

49. Sivaraman, B.; Latour, R. A., The Relationship Between Platelet Adhesion On Surfaces And The Structure Versus The Amount Of Adsorbed Fibrinogen. *Biomaterials* **2010,** *31* (5), 832-839.

50. Lantvit, S. M.; Barrett, B. J.; Reynolds, M. M., Nitric Oxide Releasing Material Adsorbs More Fibrinogen. *J. Biomed. Mater. Res. A* **2013,** (11), 3201.

51. Fang, F. C., Antimicrobial Reactive Oxygen And Nitrogen Species: Concepts And Controversies. *Nat. Rev. Microbiol.* **2004,** *2* (10), 820.

52. Wang, Y.-X.; Robertson, J. L.; Spillman, W. B.; Claus, R. O., Effects Of The Chemical Structure And The Surface Properties Of Polymeric Biomaterials On Their Biocompatibility. *Pharm. Res.* **2004,** *21* (8), 1362-1373.

53. Van Loosdrecht, M.; Lyklema, J.; Norde, W.; Schraa, G.; Zehnder, A., The Role Of Bacterial Cell Wall Hydrophobicity In Adhesion. *Appl. Environ. Microbiol.* **1987,** *53* (8), 1893-1897.

54. Adams, R.; Schachtrup, C.; Davalos, D.; Tsigelny, I.; Akassoglou, K., Fibrinogen Signal Transduction As A Mediator And Therapeutic Target In Inflammation: Lessons From Multiple Sclerosis. *Curr. Med. Chem.* **2007,** *14* (27), 2925-2936.

55. Perez, R. L.; Ritzenthaler, J. D.; Roman, J., Transcriptional Regulation Of The Interleukin-1 B Promoter Via Fibrinogen Engagement Of The CD18 Integrin Receptor. *Am. J. Respir. Cell Mol. Biol.* **1999,** *20* (5), 1059-1066.

56. Perez, R. L.; Roman, J., Fibrin Enhances The Expression Of IL-1 Beta By Human Peripheral Blood Mononuclear Cells. Implications In Pulmonary Inflammation. *J. Immunol.* **1995,** *154* (4), 1879-1887.

57. Fan, S.T.; Edgington, T. S., Integrin Regulation Of Leukocyte Inflammatory Functions. CD11b/CD18 Enhancement Of The Tumor Necrosis Factor-Alpha Responses Of Monocytes. *J. Immunol.* **1993,** *150* (7), 2972-2980.

58. Lee, J. N.; Park, C.; Whitesides, G. M., Solvent Compatibility Of Poly (Dimethylsiloxane)-Based Microfluidic Devices. *Anal. Chem.* **2003,** *75* (23), 6544-6554.

59. Brisbois, E. J.; Handa, H.; Major, T. C.; Bartlett, R. H.; Meyerhoff, M. E., Long-Term Nitric Oxide Release And Elevated Temperature Stability With S-Nitroso-N-Acetylpenicillamine (SNAP)-Doped Elast-Eon E2As Polymer. *Biomaterials* **2013,** *34* (28), 6957-6966.

60. Scatena, R.; Bottoni, P.; Pontoglio, A.; Giardina, B., Pharmacological Modulation Of Nitric Oxide Release: New Pharmacological Perspectives, Potential Benefits And Risks. *Curr. Med. Chem.* **2010,** *17* (1), 61-73.

61. Brisbois, E. J.; Kim, M.; Wang, X.; Mohammed, A.; Major, T. C.; Wu, J.; Brownstein, J.; Xi, C.; Handa, H.; Bartlett, R. H.; Meyerhoff, M. E., Improved Hemocompatibility Of Multilumen Catheters Via Nitric Oxide (NO) Release From S-Nitroso-N-Acetylpenicillamine (SNAP) Composite Filled Lumen. *ACS Appl. Mater. Interfaces* **2016,** *8* (43), 29270-29279.

62. Wink, D. A.; Mitchell, J. B., Chemical Biology Of Nitric Oxide: Insights Into Regulatory, Cytotoxic, And Cytoprotective Mechanisms Of Nitric Oxide. *Free Radical Biol. Med.* **1998,** *25* (4-5), 434-456.

63. Fang, F. C., Perspectives Series: Host/Pathogen Interactions. Mechanisms Of Nitric Oxide-Related Antimicrobial Activity. *J. Clin. Invest.* **1997,** *99* (12), 2818-2825.

64. Fang, F. C., Antimicrobial Actions Of Reactive Oxygen Species. *Mbio* **2011, 2011**, *2* (5), E00141–11.

65. Pant, J.; Goudie, M. J.; Chaji, S. M.; Johnson, B. W.; Handa, H., Nitric Oxide Releasing Vascular Catheters For Eradicating Bacterial Infection. *J. Biomed. Mater. Res. B* **2018,** *106* (8), 2849-2857.

CHAPTER 3:

PREVENTION OF MEDICAL DEVICE INFECTIONS VIA MULTI-ACTION NITRIC OXIDE AND CHLORHEXIDINE DIACETATE RELEASING MEDICAL GRADE SILICONE BIOINTERFACES

Chug, M. K., Massoumi, H., Wu, Y., & Brisbois, E. J. (2022). Prevention of Medical Device Infections via Multi-Action Nitric Oxide and Chlorhexidine Diacetate Releasing Medical Grade Silicone Biointerfaces. *Journal of Biomedical Materials Research Part A*, *110*(6), 1263-1277.

3.1 Abstract

The presence of bacteria and biofilm buildup on medical device surfaces has been linked to serious infections, increased health care costs, and the failure of medical devices. Therefore, antimicrobial devices that can thwart microbial attachment and subsequent biofilm development have become an active research area, specifically for therapeutic applications. Both nitric oxide (NO) and chlorhexidine diacetate (CHXD) are known to possess broad-spectrum antibacterial properties. In the past, individual polymer release systems of CHXD and NO donor *S*-nitroso-*N*-acetylpenicillamine (SNAP) incorporated polymer platforms have attracted considerable attention for biomedical/therapeutic applications. However, the combination of the two surfaces has not been explored yet. Herein, the synergy of NO and CHXD was evaluated to create an antimicrobial medical-grade silicone rubber (SR) polymer. A 10 wt% SNAP incorporated films were fabricated using a solvent-evaporation process with a topcoat of CHXD (1, 3, and 5 wt%) to generate a dual-active antibacterial interface. Chemiluminescence studies confirmed the NO release from SNAP-CHXD films at physiologically relevant levels ($0.5 – 4 \times 10^{-10}$ mol min^{-1} cm^{-2}) of NO for at least 3 weeks and CHXD release for at least 7 d. Further characterization of the films via SEM-EDS confirmed uniform distribution of SNAP and presence of CHXD within the polymer films without substantial morphological changes, as confirmed by contact angle hysteresis. Moreover, the dual-active SNAP-CHXD films were able to significantly reduce *E. coli* and *S. aureus* bacteria (> 3-log reduction) compared to controls with no explicit toxicity towards mouse fibroblast cells. The synergy between the two potent antimicrobial agents will help combat bacterial contamination on biointerfaces and enhance the longevity of medical devices.

Keywords: Nitric oxide, Chlorhexidine, Antibacterial, Medical devices, Hospital-acquired infections

3.2 Introduction

Indwelling medical devices, like intravascular and urinary catheters, are the major source of catheter-associated bloodstream infections. Biomedical devices provide a suitable surface for bacterial adhesion which can eventually lead to biofilm formation. Devices that succumb to biofilm buildup on the surfaces often tend to have compromised functionality with reduced durability that can extend hospital stays and increase the financial burden on patients. In the US alone, a total of 250,000 cases of device-associated infections are reported every year.[1] When bacteria from the surrounding environment encounter a medical device, the first step of the multifaceted process is attachment to the surface. The attachment of bacteria is followed by uninhibited proliferation on the surface which then leads to the production of extracellular polymeric substances (EPS) comprising eDNA, genes, polysaccharides, lipids, enzymes, proteins, etc. The protective EPS matrix not only provides nutrients to growing bacteria but also protects embedded bacteria from the action of traditional antibiotics that fail to penetrate the defensive layer. Over time, bacteria protected within the biofilm can shift from a sessile state to a planktonic and use these indwelling medical devices as a port of entry into the body, leading to many chronic, nosocomial, and medical device-related infections.[2-6]

When it comes to bacterial pathogenesis, both Gram-positive and Gram-negative bacterial species have been seen to form biofilms on medical device surfaces. Despite keeping the surroundings clean and sterilization of medical devices, a lot of medical implants and prosthetic devices can succumb to bacterial contamination in both short- and long-term applications. This situation has become worse due to the emergence of antibiotic resistance in bacteria. It is estimated that >1000 times the dosage of antibiotic is required to eradicate bacteria encapsulated within the biofilm as opposed to free-floating bacteria.[7, 8] Therefore, there is a dire need for broad-spectrum antimicrobial approaches that can act upon the pathogenesis of microorganisms. Due to the shift in efforts of managing cases, the COVID-19 emergency has diverted the focus of

conventional infection control tactics which has resulted in a >50% increase in central line-associated bloodstream infections (CLABSI) rates.[9, 10]

Infections arising from medical devices can be modulated by developing infection-controlling strategies that can inhibit catheter-related infections and radically lower the instances of morbidity, mortality, and associated medical care costs. Previous studies have reported bactericidal or bacteria-resistant approaches to reduce the microbial burden on medical devices. These strategies include impregnation of antimicrobial agents such as silver, zinc [11, 12] in silicone-based polymers[13, 14], anti-fouling mechanisms (e.g., SLIPs, zwitterions) [14-17], antibiotic and antimicrobial coated/impregnated catheters (chlorhexidine (CHXD), silver sulfadiazine, rifampicin, auranofin, etc.)[18-21], and nitric oxide (NO)-releasing therapeutic approaches.[22, 23]

Chlorhexidine is an extensively used antimicrobial agent in hospital-based settings for skin disinfection and as well as prevention of bacterial contamination on common surfaces.[24] The positively charged CHXD binds to the negatively charged bacterial cell wall. The strong binding of moieties leads to loss of membrane integrity and malfunctioning of proteins and enzymes that causes cellular damage and cytoplasmic leakage resulting in microbial death. [25-28] The broad-spectrum antibacterial properties of CHXD have been widely studied for long-term antibacterial applications. Several researchers have reported sustained release from CHXD-impregnated, incorporated, and coated surfaces for the use of medical devices such as dental implants, vascular catheters, and antimicrobial dressings. [29-33] Some of these techniques have also made it to pre-clinical stages and are currently being used to treat catheter-associated infections in patients.[19] For example, CHXD and silver sulfadiazine-impregnated catheters are commercially available. However, infections on medical devices persist and are continuing to rise.[34] One solution to avoid using higher concentrations of CHXD that are toxic to mammalian cells is to combine CHXD with other antibacterial agents that can augment antibacterial properties and as well as enhance the biocompatibility of medical devices.

NO is an endogenous gas molecule responsible for several regulatory functions such as vasodilation and inhibition of platelet activation. Immune cells such as macrophages and neutrophils utilize NO to fight the invading pathogen by exhibiting antimicrobial and anti-inflammatory properties. [35] To exogenously mimic the innate functions of NO, several NO donors have been synthesized and integrated with medical-grade polymers to develop antimicrobial, hemocompatible, and biocompatible surfaces. Synthetic and endogenous *S*-nitrosothiols, such as *S*-nitroso-*N*-acetyl-penicillamine (SNAP) and *S*-nitrosoglutathione (GSNO), NO donors have demonstrated improved stability when incorporated within polymer matrices for the use of medical device application.[36] These polymers also have been shown to release NO at physiologically relevant levels by the means of a catalyst (heat, light, or metal ion).[37] Nitric oxide released from the polymer systems can emulate NO release from endothelial cells at a surface flux of 0.5 - 4 x 10^{-10} mol cm^{-2} min^{-1}, to prevent platelet activation and adhesion.[38] SNAP-incorporated polymers utilizing medical-grade polyurethane-based silicone elastomers (CarboSil, ChronoSil, silicone rubber) have been extensively studied to generate NO-releasing medical devices with prolonged and regulated NO release.[39-42] However, the levels of NO emitted from these matrices can eventually drop as the NO payload is depleted, which might restrict their ability to fully eradicate the bacteria in long-term applications. Therefore, combining NO-releasing materials with other broad-spectrum antibacterial agents, such as CHXD, that can elevate long-term applications is one possible solution to bacterial colonization on biomaterials.

Previously, both SNAP and CHXD have been individually incorporated/impregnated within polymer systems. However, the combination of these two compounds as an infection control strategy has not been studied until now. This study aims to combine SNAP and CHXD in a single polymer matrix to achieve amplified antibacterial properties for the use of potential biomedical applications. This technique can also be applied to other polymer-based medical device interfaces such as endotracheal tubes, insulin cannulas, and hemodialysis catheters that face the

challenges of bacterial contamination. In this study, commercial-grade silicone rubber (SR) polymer was used to fabricate SR films with dual antibacterial properties comprising of NO donor SNAP and CHXD using the solvent evaporation and dip-coating method. Varying concentrations of CHXD were optimized on the SNAP-incorporated SR and tested for cytocompatibility towards NIH 3T3 mouse fibroblast films. Examination of the surface characteristics of films was carried out via contact angle, scanning electron microscopy, and elemental mapping of modified and unmodified films. NO release from the samples was tested over 4 weeks using a chemiluminescence method and the leaching of NO donor and CHXD in the soaking buffer was assessed using the UV-vis spectroscopy technique. Finally, the antibacterial potential of the films was investigated in a 24 h bacterial adhesion assay against *E. coli* (Gram-negative) and *S. aureus* (Gram-positive) bacteria, two major bacterial strains frequently linked to infections arising from medical devices.

3.3 Materials and Methods

3.3.1 Materials

Ethylenediaminetetraacetic acid (EDTA), tetrahydrofuran (THF), and sterile phosphate buffer saline powder with 0.01 M, pH 7.4, containing 0.138 M NaCl, 2.7 mM KCl, were purchased from Sigma Aldrich (St. Louis, MO). *S*-nitroso-*N*-acetylpenicillamine was purchased from PharmaBlock (Hatfield, PA). Chlorhexidine diacetate hydrate and glutaraldehyde solution (50%/Certified/BioReagent) were obtained from Fisher Scientific (Hampton, NH). All aqueous solutions were prepared using deionized water. Phosphate buffer saline (PBS) 0.01M with 100 µM EDTA was used for all material characterization and NO analyzer studies. Dulbecco's modified Eagle's medium (DMEM) and trypsin-EDTA were purchased from Corning (Manassas, VA20109). The Cell Counting Kit-8 (CCK-8) was purchased from Sigma-Aldrich (St. Louis, MO). Antibiotics penicillin-streptomycin (Pen-Strep) and fetal bovine serum (FBS) were obtained from Gibco-Life Technologies (Grand Island, NY). The bacterial strain *S. aureus* (ATCC 6538), *E. coli*

(ATCC 25922), and 3T3 mouse fibroblast cells (ATCC 1658) for cytotoxicity studies were obtained from American Type Culture Collection (ATCC). All the buffers and media used in microbial and tissue culture were sterilized in an autoclave at 121 °C, 100 kPa (15 psi) for 30 minutes prior to use.

3.3.2 Preparation of SR-SNAP-CHXD Polymer Films

DOWSIL™ 3-1944 RTV silicone rubber with or without 10 wt% of SNAP was prepared by a solvent evaporation method. Films were prepared to fabricate four test groups (SR, SR-CHXD, SR-SNAP, and SR-SNAP-CHXD) (**Figure 3.1**). To prepare the polymer solution for the base films, 270 mg of SR was weighed out and dissolved in 1 mL of THF and 30 mg of SNAP was added to achieve 10wt% (w/w) as the final concentration of SNAP. The solution was vortexed until all the SNAP crystals were dissolved completely and then cast into the circular Teflon molds of 2.5 cm diameter. The polymer films in the mold were cured overnight in a fume hood initially and then for 24 h in the vacuum desiccator enabling the solvent to evaporate completely. For the corresponding controls without SNAP, 300 mg of SR was dissolved in 1 mL of THF and cast resulting in blank SR films. Once all the films were dried, smaller disks of diameter 0.65 cm were cut from the parent base film. **Table 3.1** describes all the sample types fabricated for this study and highlights the methodology followed to fabricate films. All the base films (SR and SR-SNAP) were first top-coated with 3 topcoats of a plain SR topcoat solution (1 mL SR-THF solution at 300 mg mL^{-1} concentration) at a 15 min interval. The films were allowed to dry for 2 h at room temperature. To generate 1, 3, and 5 wt% CHXD coated films, the SR and SR-SNAP films were top coated with 2 topcoats of the CHXD solution at 15 min intervals, resulting in SR-CHXD and SR-SNAP-CHXD films. To prepare the polymer solution for the CHXD topcoat, 297, 291, and 285 mg of SR were weighed out and dissolved in 1 mL of THF with 3, 9, and 15 mg of CHXD to achieve 1, 3, and 5 wt% (w/w) as the final CHXD concentration, respectively. For corresponding SR and SR-SNAP controls without CHXD, films were top-coated with 1 mL of SR dissolved in

THF (2 topcoats at 15 min intervals) at 300 mg mL^{-1} concentration to result in SR and SR-SNAP films. The small disks were dried overnight and then dried under vacuum for an additional 24 hours. This was done to remove any residual THF and ensure the polymers were cured. The weights and thickness of the final films were recorded using a Mettler Toledo analytical balance and a Mitutoyo micrometer. The prepared polymer samples were kept in the freezer (−20 °C) in the dark to retain their NO-releasing properties before further analysis.

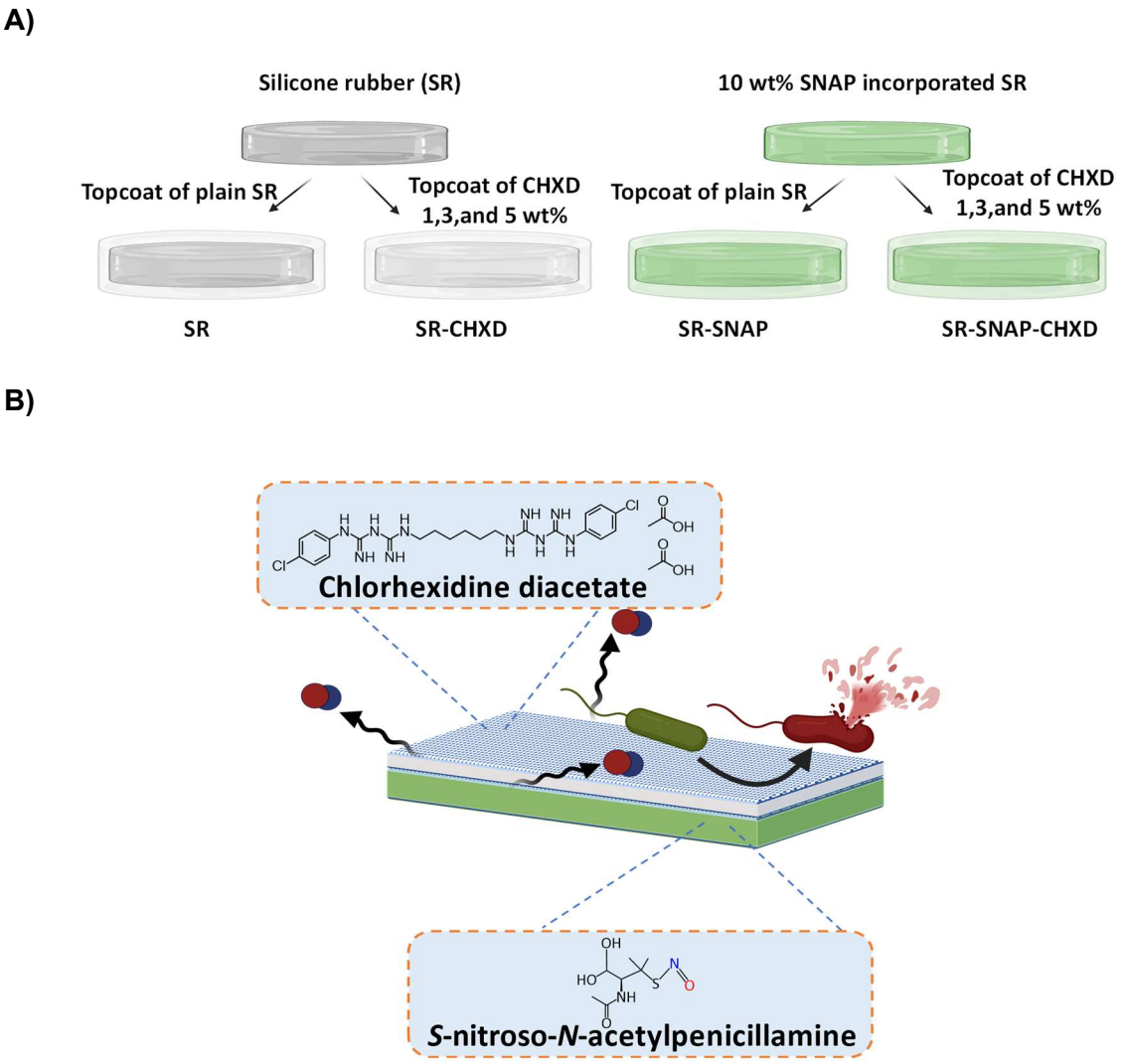

Figure 3.1 A) Methodology to fabricate SR, SR-SNAP, SR-CHXD and SR-SNAP-CHXD films. B) Schematic representation of SR-SNAP-CHXD films to combat medical device infections. SR-SNAP films are top coated with SR-CHXD to generate dual-active antimicrobial surfaces.

Table 3.1 Composition of SNAP-CHXD samples used in the study

Sample type	Base film	Topcoat
SR	300 mg mL^{-1} SR	5 topcoats of 300 mg mL^{-1} SR
SR-SNAP	300 mg mL^{-1} SR with 10 wt% SNAP	5 topcoats of 300 mg mL^{-1} SR
SR-CHXD	300 mg mL^{-1} SR	3 topcoats of 300 mg mL^{-1} SR, 2 topcoats of 300 mg mL^{-1} SR with 1,3,5 wt% CHXD
SR-SNAP-CHXD	300 mg mL^{-1} SR with 10 wt% SNAP	3 topcoats of 300 mg mL^{-1} SR, 2 topcoats of 300 mg/mL SR with 1,3,5 wt% CHXD

3.3.3 Characterization of SNAP-CHXD Films for Optimized NO-Releasing Polymers

3.3.3.1 NO-Release Measurements

NO release kinetics from the films was evaluated using Zysense chemiluminescence Nitric Oxide Analyzer (NOA) 280i (Zysense, Frederick, CO). For this, samples were submerged in NOA samples cell with Phosphate Buffer Saline (PBS) substituted with 100 μM EDTA (pH 7.4). EDTA was added to the buffer to quench the metal ion activity from water that can non-specifically catalyze NO from SNAP. The temperature of the system was maintained at 37 °C to emulate the physiological conditions. The NO released from the polymer films in the NOA cell was constantly carried into the reaction chamber via highly purified nitrogen gas at a continuous flow rate of 200 mL min^{-1}. The cell pressure of the NOA cell ranged from 8.9 to 9.7 torr with a supply pressure between 6.4-6.6 psi. All experiments were performed in triplicates protected from ambient light.

To quantitate the real-time NO release under physiological conditions, SR-SNAP and SR-SNAP-CHXD films (n=3) were each placed in 2 mL of PBS-EDTA in an NOA sample cell. The samples were tested until the steady state of NO release was attained. The films were incubated

in PBS-EDTA at 37 °C and the NO release from the films was recorded at various time points. The amount of NO released from the samples (ppb/ppm) was normalized with the surface areas of the samples to obtain the NO flux levels with mol cm^{-2} min^{-1} units. For evaluating the effect on the presence of CHXD, films were tested in a short-term experiment for up to 24 h with all different CHXD concentrations (1, 3, and 5 wt% CHXD topcoat). To understand the full potential of films, optimized concentrations of SR-SNAP-CHXD (5 wt%) were compared to SR-SNAP films in a long-term NO release study for up to 4 weeks. For the long-term study, the soaking buffer was replaced on each testing day during the incubation to prevent the saturation of SNAP leaching in the soaking buffer.

3.3.3.2 Effect of Sterilization on NO Release

To test the sterilization compatibility of SR-SNAP-CHXD films, samples were exposed to the EO sterilization process under AN 74i Anprolene EO gas sterilizer (Anderson Sterilizers). For this, SR-SNAP-CHXD films were packaged in a peel pouch and sterilized under EO gas under 24 h cycle followed by 2 h of air purging. To maintain a minimum of 35% humidity, a Humidichip was added to the sterilization bag and the whole process was done at room temperature. To test the influence of UV-light on the SNAP stability and corresponding NO release, SR-SNAP-CHXD films were exposed to UV-light under a biosafety cabinet administered by REDISHIP Purifier® Logic®+ Class II A2 Biosafety Cabinets, Labconco® for 30 min. NO release from the sterilized samples was measured using the same methodology as Section 3.3.3.1. Samples were tested for their NO release on day 0 and day 1 and compared to freshly prepared samples that were not exposed to any sterilization process.

3.3.4 Evaluation of SNAP and CHXD Release from Polymer Films

The amount of SNAP and CHXD released from the polymer films into the soaking buffer was measured by recording the absorbance of buffer solutions for up to 1 week. Three samples

for each type of film were prepared and weighed before initiating the study. These films were then soaked in PBS (with EDTA) at 37 °C. A UV-vis spectrophotometer (Cary 360, Agilent Technologies) was used to measure the absorbance of the buffer solutions every day. The absorbance of solutions was measured using a Quartz cuvette at 340 and 255 nm which is the maxima in the UV-Vis absorbance spectra for SNAP and CHXD, respectively. [43] The calibration graph of SNAP and CHXD in PBS with EDTA was used to interpolate the absorbance measurements recorded from the study and convert them to concentrations of the compound in the measured sample. Care was taken to make sure that the buffer solution amount for each sample was maintained at the same amount throughout the experiment to avoid any inconsistent readings and three replicates were used for each measurement.

3.3.5 Characterization of Films

3.3.5.1 Static Contact Angle Measurement

Polymer films that were compatible with the goniometer instrument were prepared by spin coating enabling the reproducible evaluation of any effects of SNAP or CHXD on the surface wettability of the samples. To measure the static water contact angle, thin films were prepared by spin coating SR, SR-SNAP, and SR-CHXD solutions on 15 mm Deckgläser Cover Glasses using a programmable MTI VTC-100A spin coater. The static contact angle measurement for the SR, SR-SNAP, SR-CHXD and SR-SNAP-CHXD polymer matrixes were conducted using Ossila Contact Angle Goniometer with sessile drop method with deionized water. A 10 µL of deionized water was dropped on different locations on film and the droplet was allowed to sit for 10 seconds before recording the values. Four replicates were used for each measurement, and the average of left and right contact angles was measured via the Ossila software.

3.3.5.2 Scanning Electron Microscopy Equipped with Elemental Mapping

Surface morphology and composition of SR, SR-SNAP, SR-CHXD, and SR-SNAP-CHXD were evaluated using a scanning electron microscope and elemental mapping techniques,

respectively. All the films were sputter-coated with a 10 nm gold-palladium mixture using a sputter coater (Leica Microsystems). Field emission scanning electron microscopy (FESEM) instrument (FEI Teneo, FEI, Inc., Hillsboro, OR USA) with an accelerating voltage of 5 kV at a working distance of 10 mm was utilized to obtain surface morphology images. Energy-dispersive X-ray spectroscopy (EDS –Oxford instruments) with an accelerating voltage of 20 kV, was used to evaluate the dispersion of chlorine (Cl) on the surface of CHXD-coated films and sulfur (S) in the cross-section of SNAP-incorporated samples as the characteristic element of SNAP composition.

3.3.6 Antibacterial Efficacy of Dual-Active SNAP-CHXD Polymer Films

3.3.6.1 24 h Bacterial Adhesion Assay

To assess the antibacterial efficacy of the polymer films, a 24 h antibacterial adhesion assay was used. All the samples SR, SR-SNAP, SR-CHXD, and SR-SNAP-CHXD were tested against two strains of bacteria *E. coli* and *S. aureus*. Bacterial cultures were prepared by inoculating single isolated colonies in LB media that were incubated and grown for 5 h at 120 rpm at 37 °C. Bacteria from the stock were extracted at the mid-log phase and washed in PBS at 3500 rpm, for 7 min to remove the dead cells and debris. Samples were exposed to a bacterial solution with adjusted optical density (O.D) of 0.5 measured at 600 nm wavelength corresponding to a final concentration of bacteria ~ 10^7 colony forming units (CFU) mL^{-1}. Polymer films with bacteria were incubated at physiological conditions (pH 7.4, 37 °C) for 24 h at 120 rpm. To evaluate the viable colonies adhered on the surface of films, polymer films were transferred into fresh PBS buffer, homogenized, and vortexed for 60 sec each. Diluted samples were then plated on the L.B agar media using a bacteria Spiral Plater (Eddy Jet 2W, IUL Instruments) (Log mode 100 uL). Results were recorded based on the growth of viable colonies on the agar plate after overnight incubation at 37 °C utilizing an automated bacteria colony counter (Sphere Flash, IUL Instruments). The results obtained from the study were normalized by the surface area of the films and represented as the percent reduction in the adherence of viable bacteria on the test surface

(SR-CHXD, SR-SNAP, and SR-SNAP-CHXD) with respect to the control surface (SR) determined by **Equation 3.1**.

$$\%\ bacterial\ reduction = \frac{(SR\ control) - (Test) \times 100}{(SR\ control)} \quad \textbf{(Equation 3.1)}$$

3.3.7 Bacteria Morphological Analysis

S. aureus and *E. coli* adhered on the surface were visualized using SEM to analyze the effect of CHXD and SNAP on morphological changes of Gram–positive and –negative bacteria strains. The SEM analysis was carried out using the previously reported method with slight modifications.[44] Bacteria cultured in LB media overnight were diluted to 10^7 CFU mL^{-1} concentrations and samples cut into disks with 0.65 cm diameter were placed in 2 mL microcentrifuge tubes. Each sample (SR, SR-CHXD, SR-SNAP, SR-SNAP-CHXD) was exposed to 1 mL bacteria culture in a shaker incubator at 37 °C and 120 rpm. After 24 h of incubation, samples were gently taken out and rinsed with fresh sterilized PBS to detach the loosely adhered bacteria from the surface and immersed in 3% glutaraldehyde in 0.1 M PBS solution overnight to fix the samples. Samples were dehydrated with an increasing amount of ethanol at 20 min intervals (50, 60, 70, 80, 90, and 100% v/v in DI water). Finally, samples were left at ambient temperature to dry completely in the fume hood, protected from light. Samples were mounted on double-sided carbon tape on an SEM specimen mount and sputter-coated with a 10 nm thick gold-palladium mixture using Leica EM ACE600 coater (Leica Microsystems, Wetzlar Germany). Microscope images of bacteria on the surface of different samples were obtained using a FESEM instrument (FEI Teneo, FEI, Inc., Hillsboro, OR, USA) with an accelerating voltage of 5 kV at a working distance of 10 mm.

3.3.8 *In Vitro* Cytocompatibility Study

The compatibility of films with mammalian cells was assessed by following the ISO standards (ISO10993-5:2009 Test for evaluating the compatibility of medical devices *in vitro*).

This was done as per the previously reported protocol with slight modifications.[45] All test and control group SR, SR-SNAP, SR-CHXD, and SR-SNAP-CHXD samples (n = 3) each were cleansed with 70% ethanol and sterilized under UV-light in a biosafety cabinet for 15 mins on each side. Each sample was submerged in complete DMEM media supplemented with 10% FBS and 1% Penicillin-streptomycin mixture (2 mL) and incubated for 24 h at 37 °C, 5% CO_2. The leachate of the samples was then used for exposure to the cells and further analysis.

NIH 3T3 mouse fibroblast cell line was used to test the cytocompatibility of the films. Cells at 5000 cells/ well were seeded into a cell-culture treated 96-well plate and incubated for 24 h at 37 °C, 5% CO_2 in humidified conditions. After 24 h, the old media from the wells was aspirated out and substituted with an equivalent volume of leachates and exposed to the confluent cells for each specific sample type. Cells exposed to leachates were then incubated for an additional 24 h to allow the leachates to act out on cells. All experiments were done in triplicates. After 24 h, CCK-8 was added to the cells and incubated for 2 h (10 µL). The absorbance of the cells was measured at 450 nm wavelength using a micro well-plate reader (Cytation 5 imaging multi-mode reader, BioTek). Results from the study are represented as cell viability of the test group (SR, SR-SNAP, SR-CHXD 1,3, and 5 wt%, and SR-SNAP-CHXD 1,3, and 5 wt%) relative to control 3T3 fibroblast cells in media alone that received no treatment (**Equation 3.2**).

$$Relative\ cell\ viability\ (\%) = \frac{absorbance\ \ treatment\ group}{absorbance\ cells\ in\ media\ without\ treatment}\ x\ 100 \quad \textbf{(Equation 3.2)}$$

3.3.9 Statistical Analysis

All experimentations in this study were conducted with a sample size n ≥ 3. Data obtained from the study are presented as mean ± standard error of the mean (SEM). To ascertain the statistical significance between the test (SR-SNAP-CHXD) and control group (SR, SR-SNAP, SR-CHXD), an unpaired Student's *t*-test was used with an assumption of unequal variance. *p* values of < 0.05 were considered statistically significant.

3.4 Results

3.4.1 NO Release Kinetics

The physical attributes of the sample weight and dimensions of the polymer films were recorded using an analytical balance (Mettler Toledo™ XS105DU, Columbus, OH) and a micrometer. The weights of the films before and after top coating were found to be 9.38 ± 0.53 and 19.55 ± 1.21 mg, respectively. All the films synthesized in the study (SR, SR-SNAP, SR-CHXD, and SR-SNAP-CHXD) were of uniform weight and thickness. The addition of five topcoats on the base films resulted in a corresponding increase in the thickness of the disks before and after topcoats from 0.36 ± 0.01 to 0.85 ± 0.08 mm, respectively. To understand if the addition of CHXD on the SNAP-loaded polymer affects the NO release, the SR-SNAP and SR-SNAP-CHXD films were tested for the NO release kinetics using the chemiluminescence method under physiological conditions (**Figure 3.2A**). While the SR-SNAP control films exhibited an initial flux of 5.46 x 10^{-10} mol min^{-1} cm^{-2}, SR-SNAP-CHXD with 1, 3, and 5 wt% CHXD exhibited 6.54, 6.06, and 5.67 x 10^{-10} mol min^{-1} cm^{-2}, respectively (**Figure 3.2B**). NO release from the study demonstrated no significant differences in the release kinetics with the presence of CHXD on the surface irrespective of CHXD concentration. In a longer-term study, SR-SNAP and SR-SNAP-CHXD with 5 wt% CHXD were tested over 4 weeks (**Figure 3.2C**). Results from the long-term study demonstrated similar NO release levels for samples with and without CHXD present in the topcoat. The initial and final NO release levels from samples are reported in **Table 3.2**.

3.4.2 Ethylene Oxide (EO) and Ultraviolet (UV) Light Sterilization

To determine the stability of SR-SNAP-CHXD (5 wt%) films to withstand clinically relevant sterilization processes, in this study ethylene oxide and ultraviolet light sterilization were utilized to determine the suitable sterilization method for the SNAP and CHXD-containing polymer films. Samples were first synthesized using the dip-coating method followed by EO and UV light sterilization for 24 h and 30 min, respectively. After exposure, the NO release from the samples

was quantified and compared to the NO release from fresh samples (**Figure 3.2D**). While the freshly prepared samples released NO at 5.67 ± 0.31 x 10^{-10} mol min^{-1} cm^{-2} NO flux, both EO and UV-light exposed samples exhibited 4.87 ± 0.41 and 4.90 ± 0.33 x 10^{-10} mol min^{-1} cm^{-2} NO flux, respectively on day 0. There was a slight reduction observed in the level of NO release from sterilized samples compared to freshly prepared samples on day 0. However, the difference between the NO release of fresh and sterilized samples was not statistically significant *(p* > 0.05) and the levels of NO continued to be at physiologically relevant levels post-sterilization for at least 24 h following the same trend as freshly prepared samples.

3.4.3 *In Vitro* Analysis of SNAP and CHXD Release in Soaking Buffer

Diffusion of SNAP and CHXD from polymer films into the PBS buffer was analyzed over a 7-d period using UV-vis spectroscopy. For this, SR-SNAP and SR-CHXD films were soaked in PBS-EDTA at 37 °C. At each time point, the soaking buffer was collected and analyzed to examine the amount of CHXD and SNAP that diffused out of the polymer films. To quantify the amount of SNAP and CHXD leached into the solution, a standard curve of both SNAP and CHXD was prepared in PBS-EDTA and plotted. The molar extinction coefficient of CHXD and SNAP in PBS-

Table 3.2 Initial and final NO release kinetics from SR-SNAP and SR-SNAP-CHXD (5wt%)

	NO release (x 10^{-10} mol min^{-1} cm^{-2})	
Sample type	**Initial (Day 0)**	**Final (Day 29)**
SR-SNAP	5.46 ± 0.64	0.28 ± 0.03
SR-SNAP-CHXD (5 wt%)	5.67 ± 0.31	0.41 ± 0.15

EDTA at room temperature was determined to be 2670 M^{-1} cm^{-1} and 999 M^{-1} cm^{-1} at 255 and 340 nm, respectively (**Figure 3.3A-D**).

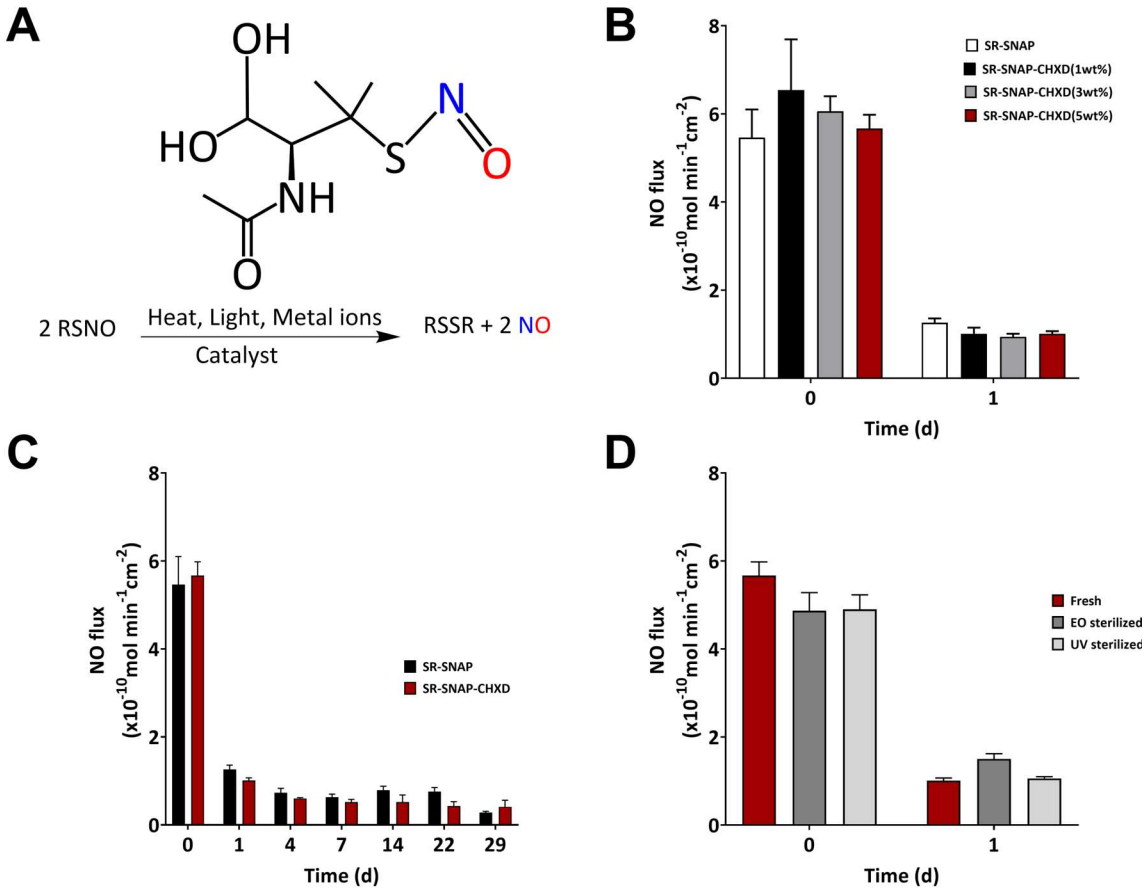

Figure 3.2 (A) Chemical structure of NO donor *S*-nitroso-*N*-acetylpenicillamine (SNAP). RSNOs have the capacity to be triggered by heat, light, or metal ions to cleave the S-N bond and release NO. (B) NO release levels from SR-SNAP and SR-SNAP-CHXD with 1, 3, and 5 wt% CHXD top coated films tested using Nitric oxide analyzer for up to 24 h. (C) Long-term NO release quantification from SR-SNAP and SR-SNAP-CHXD 5wt%. (D) Effect of ethylene oxide and UV-sterilization process on NO releasing SR-SNAP and SR-SNAP-CHXD 5wt% films. All NO release studies were performed at physiological conditions of pH 7.4 and 37 °C. Data represents mean ± SEM (n ≥ 3).

After 24 h, 0.27 ± 0.01 μg CHXD and 0.48 ± 0.03 μg of SNAP mg^{-1} of total film mass were detected in the buffer. In both cases, CHXD and SNAP diffusion was observed to be higher on the initial days due to the water-rich polymer layer that enables more rapid diffusion of these species into the buffer. However, the diffusion of the compounds stabilized with each testing day

(**Figure 3.3E**). The results indicated that a total of 0.47 ± 0.02 µg CHXD mg^{-1} and 2.06 ± 0.08 µg SNAP mg^{-1} polymer diffused out of the polymer films after 7 d of soaking.

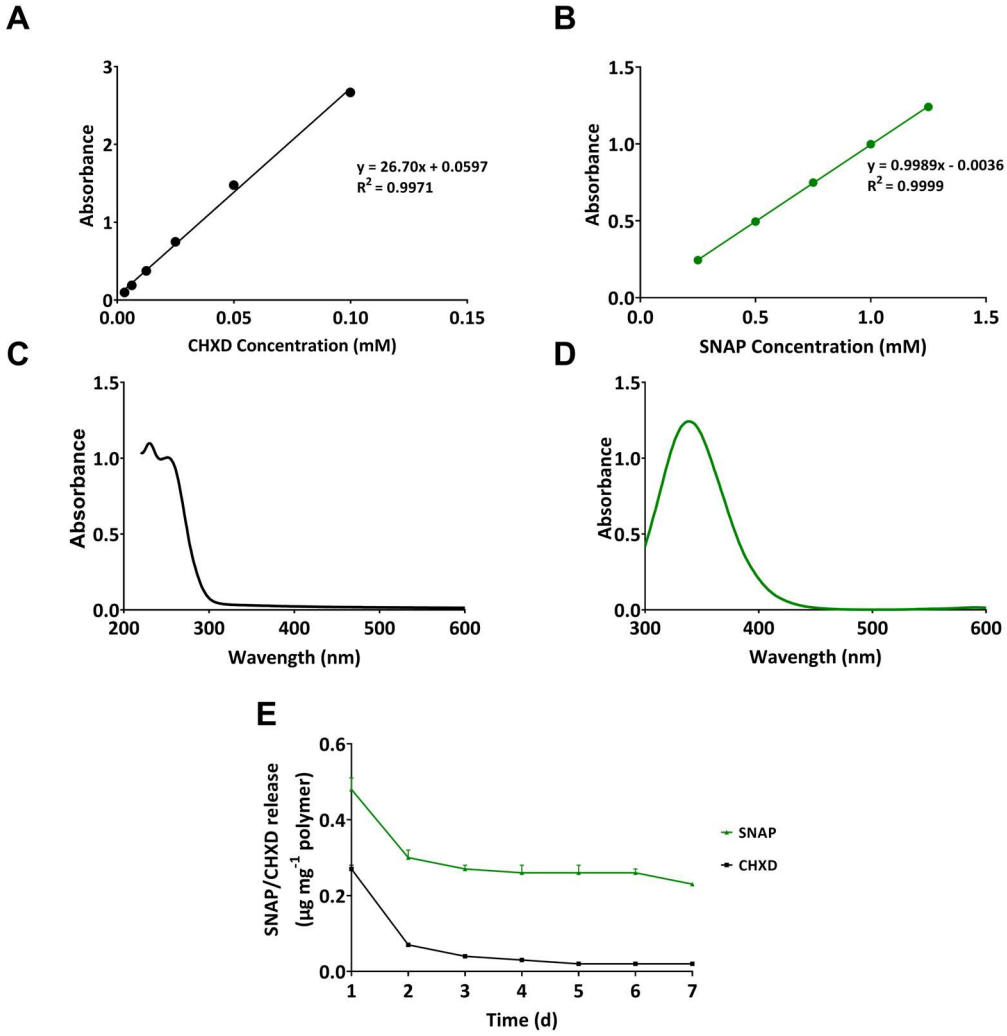

Figure 3.3. UV-vis calibration curve of (A) CHXD and (B) SNAP in PBS-EDTA buffer. The characteristic peak of (C) CHXD was observed at 255 nm and (D) SNAP at 340 nm wavelength. (E) Using the standard curve at 255 and 340 nm wavelength, the amount of SNAP and CHXD released from the polymer films was assessed for 7d at physiological conditions of pH 7.4 and 37 °C in PBS buffer. Data represents mean ± SEM (n ≥ 3).

3.4.4 Surface Characterization

3.4.4.1 Characterization of Polymer Surface via Contact Angle

Static contact angle measurements provide insights into the surface wettability of the polymers by determining the hydrophobicity or hydrophilicity of the surface, where materials at or

above 90° are classified as hydrophobic. To analyze how the modification of the surface through the incorporation of SNAP or top coating with CHXD altered the surface wettability, the static contact angle of water on the surface of the films was evaluated (**Figure 3.4**). The unmodified surface (SR) showed an initial water contact angle of 92.47 ± 2.14°. Both SR-SNAP and SR-CHXD exhibited a water contact angle of 96.16 ± 2.69° and 90.66 ± 1.80°, respectively, indicating that the surface hydrophobicity was not significantly affected by the inclusion of the SNAP and CHXD.

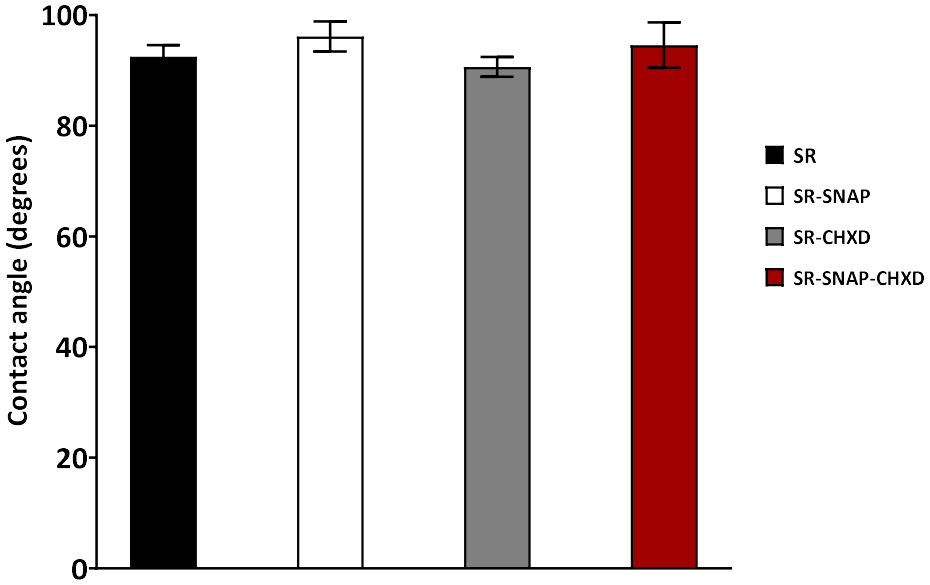

Figure 3.4. Surface wettability of polymer surfaces determined by static water contact angle. No significant difference was observed between the sample groups. Data represents mean ± SEM (n ≥ 3).

Similarly, the results from SR-SNAP-CHXD films showed 94.59 ± 4.09°. When comparing the SR-CHXD film to the SR control, a slightly lower average contact angle was observed in SR-SR-CHXD (90.67 ± 1.80°). This result is expected as an increase in CHXD concentration will increase the surface hydrophilicity.[46] Overall, all the films exhibited hydrophobicity and remained statistically insignificant after modification. In summary, film preparation through the incorporation of CHXD and SNAP did not alter the surface hydrophobicity significantly compared to the

unmodified SR surface and no statistical differences in wettability were observed between the sample types.

3.4.4.2 Surface Morphology and Elemental Mapping

Surface morphology and elemental mapping analysis were carried out to evaluate the surface of the samples and the dispersion of CHXD and SNAP in the structure (**Figure 3.5**). The surface of each sample observed by SEM imaging exhibited a relatively smooth surface, and no significant changes were observed on the surface compared to unmodified SR. The cross-sectional view of films clearly showed the presence of SNAP crystals which was confirmed by the EDS mapping of the sulfur element present in the S-NO bond of SNAP moiety (**Figure 3.5A-B**). Furthermore, the SEM-EDS showed dispersed CHXD within the topcoat layer via mapping of the Chlorine element in the CHXD structure confirming its presence on films (**Figure 3.5C-D**).

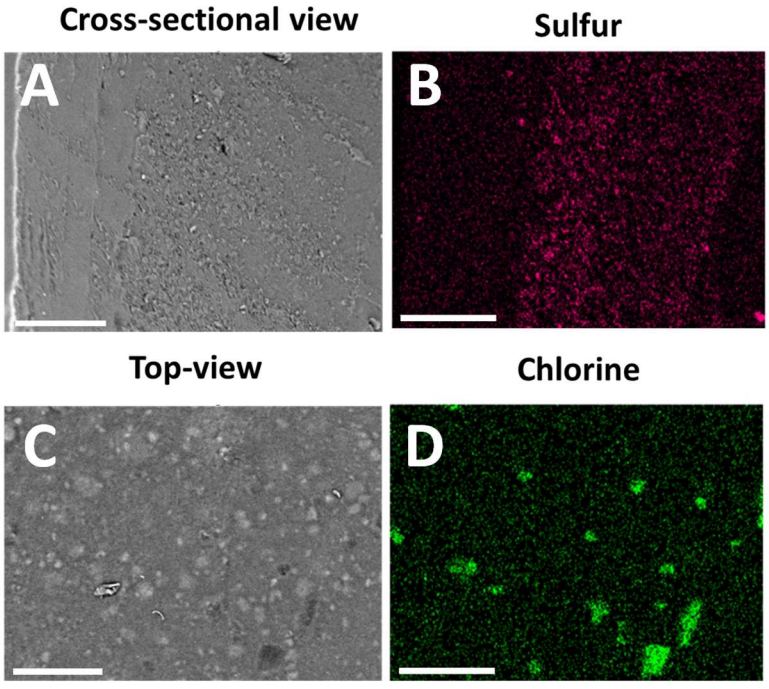

Figure 3.5 Surface SEM-EDS images of SR-SNAP-CHXD films. (A) SEM of cross-section of SR-SNAP-CHXD films. (B) Elemental mapping of SNAP to evaluate distribution in polymer films via mapping of sulfur group (depicted by red color) as the representative element of SNAP. (C) SEM image of films (top view). (D) Elemental mapping of chlorine (depicted with green color) dispersion on the surface of samples representing characteristic element of CHXD. Scale bar represents 100 μM.

3.4.5 Antibacterial Efficacy of SR-SNAP-CHXD Films

3.4.5.1 *In Vitro* Antibacterial Adhesion Assay

The antibacterial activity of the multi-active films was evaluated using 24 h bacterial adhesion assay against *S. aureus* and *E. coli* bacteria. Both SR-SNAP and SR-CHXD (5 wt%) resulted in 0.74 and 2.75 log reductions in *E. coli* bacteria viability, respectively ($p < 0.05$). However, the combinational effect of SNAP and CHXD into SR-SNAP-CHXD(5wt%) films resulted in the highest *E. coli* bacterial inhibition with 3.41 log bacterial reduction compared to SR control ($p < 0.05$) (**Figure 3.6A**). The synergy of SNAP and CHXD in SR-SNAP-CHXD also reduced the viable CFU of *S. aureus* bacteria on the film surface by 3.79-log reduction compared to SR control ($p < 0.05$), demonstrating the broad-spectrum antibacterial activity. While SR-SNAP and SR-CHXD also individually reduced the *S. aureus* adhesion by 0.91 and 2.76 log reductions, respectively ($p < 0.05$) (**Figure 3.6B**), the synergy of both SNAP-CHXD exhibited maximum reduction.

3.4.5.2 Bacteria Morphological Analysis

FESEM analysis of bacteria on the surface of films revealed the effect of individual CHXD and SNAP as well as their synergy through SR-SNAP-CHXD in bacterial eradication (**Figure 3.7**). Bacterial clusters with intact membranes on the SR surface were evident in SEM images (**Figure 3.7A and E**) that showed smooth outer membranes confirming the viability of adhered bacteria after 24 h. However, SR-SNAP, SR-CHXD, and SR-SNAP-CHXD (**Figure 3.7B-D,** and **F-H**), exhibited a significant reduction in bacteria colonization due to their inherent antibacterial properties. The bactericidal effect was enhanced with the synergy of SNAP-CHXD. SEM analysis showed disrupted, wrinkled, and indented bacterial cell walls with blisters indicating the antimicrobial action of CHXD.[47] Cellular debris from dead cells was also evident in samples with bactericidal capacities.

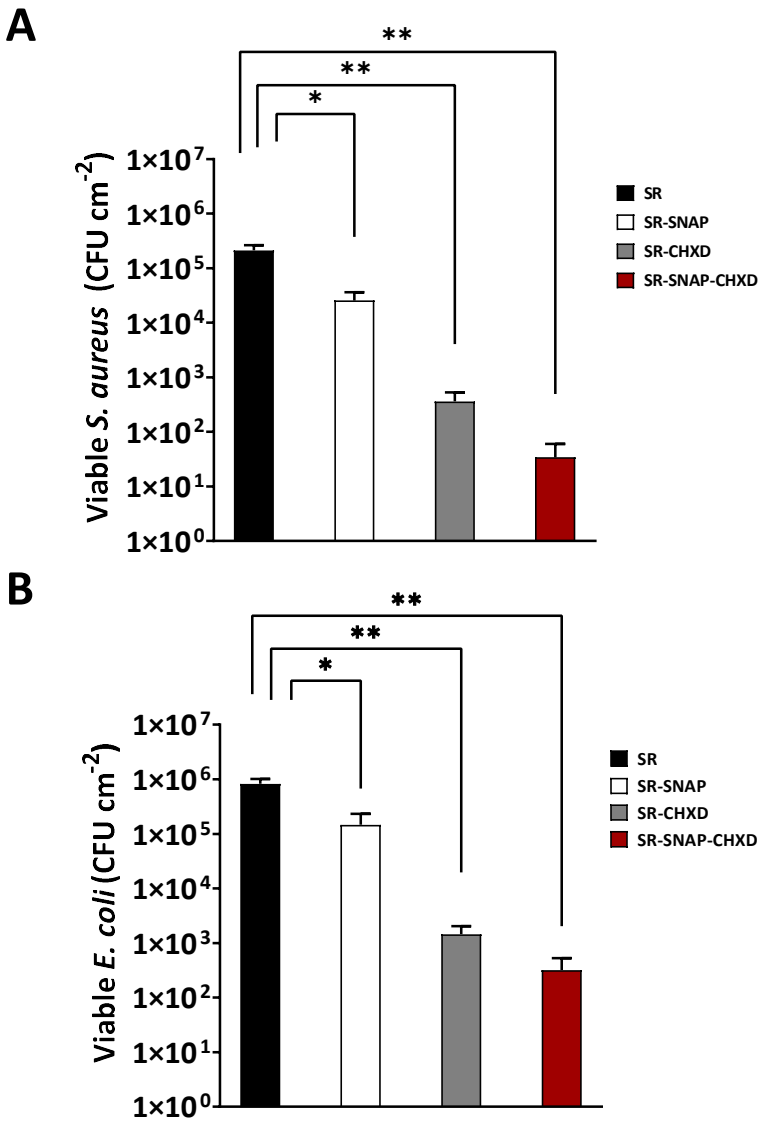

Figure 3.6 Antibacterial activity of polymer films calculated as a log of the colony forming units (CFU) cm^{-2} of surface area against (A) *S. aureus* (B) *E. coli* using a 24 h bacterial adhesion assay. Data represents mean ± standard error of mean (n≥3), * represents $p < 0.05$, ** $p < 0.01$ SR vs. SR-SNAP, SR-CHXD and SR-SNAP-CHXD.

3.4.6 Cytocompatibility of Films Towards Mammalian Cells

To assess the compatibility of SR-SNAP-CHXD films, mammalian NIH 3T3 fibroblast cells were exposed to leachates obtained from films over 24 h and tested for viability using a CCK-8 cell viability kit. The results from this study demonstrated that all the samples SR, SR-SNAP, SR-

CHXD, and SR-SNAP-CHXD at 1, 3, and 5 wt% CHXD exhibited more than 70% cell viability threshold (**Figure 3.8**). There was a slight variation in all the tested groups due to certain experimental variations, however, none of the results were significantly different. Polymer samples top-coated with concentrations greater than 5 wt% CHXD resulted in a reduction of cell viability (data not shown). Therefore, 5 wt% CHXD top-coated samples were utilized in all experiments.

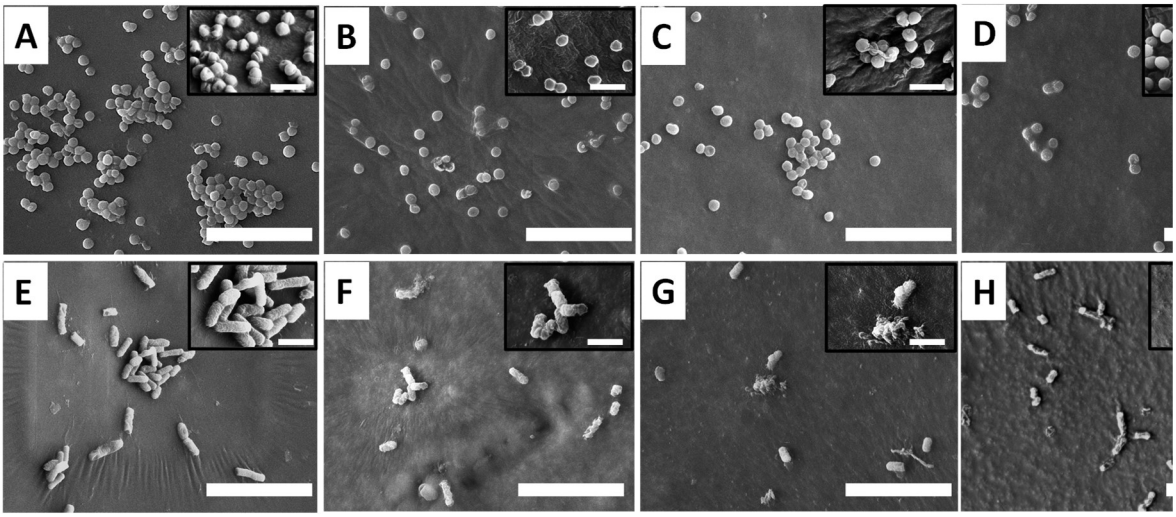

Figure 3.7 Representative images of *S. aureus* (A-D), and *E. coli* (E-H) adhesion on SR (A and E), SR-CHXD (B and F), SR-SNAP (C and G), and SR-SNAP-CHXD (D and H) samples after 24 h of incubation at 37 °C. Bacteria cell morphology was depicted in magnified insets within each image. Blisters appeared on bacteria cell walls on surface containing CHXD (B, D, F, and H). Bacteria cell wall destruction was also observed on the surface of the NO releasing samples (C, D, G, and H). The extended white scale bar represents 10 μm and the scale bar in the insets represent 2 μm.

3.5 Discussion

Medical devices coated/impregnated with CHXD are currently clinically used to combat catheter-related bloodstream infections. However, despite these efforts, the rate of infections is continuing to rise. To overcome the challenges associated with bacterial contamination, various surface strategies have been developed in the literature. SNAP-incorporated NO-releasing materials have been widely studied for antimicrobial and blood-contacting biomedical device applications.[17, 48, 49] These polymer systems provide excellent antimicrobial properties that can

prolong the lifetime and augment the biocompatibility of medical devices. However, over time the levels of NO may decrease due to the depletion of the NO reservoir within the material, which limits the ability of these materials to eradicate all bacteria.

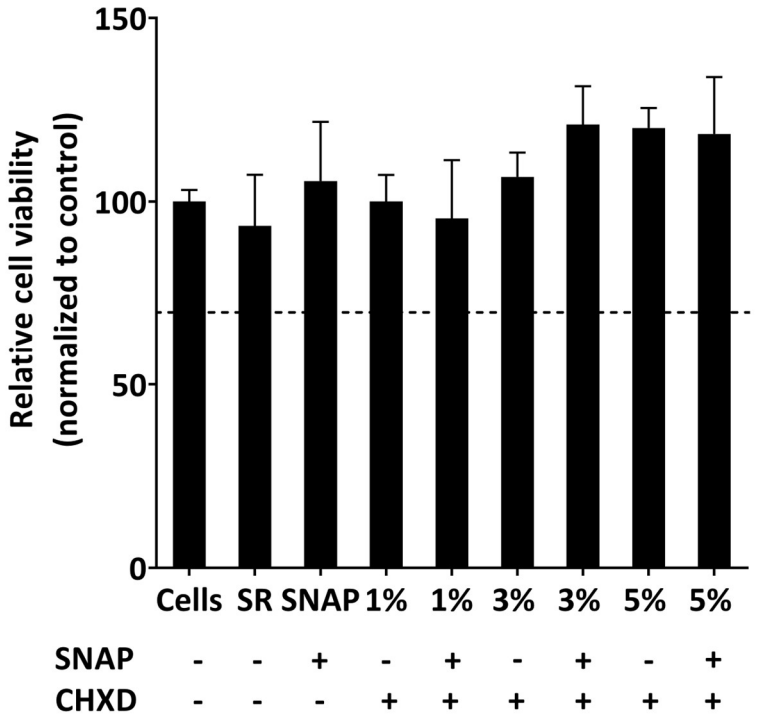

Figure 3.8. Cytocompatibility of polymer films tested against NIH 3T3 mouse fibroblast cells using a 24 h leachate exposure study. All samples exhibited >70% cell viability threshold (indicated by dashed line). Results are calculated as relative cell viability normalized to control cells that received no treatment. Data represents mean ± SEM (n ≥ 3).

Although NO holds great potential in conquering bacteria and associated issues, NO-releasing materials have not been commercialized yet. Therefore, combining NO-releasing materials with other clinically available broad-spectrum antibacterial agents, such as CHXD, can be one possible solution to bacterial colonization on biomaterials and provide multiple mechanisms at the medical device interfaces to ensure microbial eradication. Since the initial timepoint during the implantation or insertion of a medical device is considered extremely critical in determining the fate of the device, the synergy of two antimicrobial interfaces is expected to

lower the degree of bacterial adhesion at this potential early onslaught of infection. The subsequent physiological levels of NO from the samples can then provide prolonged antibacterial action against pathogens and continue to inhibit biofilm formation.

To combine NO-releasing SR polymer with CHXD, a facile and easy method is proposed in this study. Medical grade SR polymer was incorporated with 10 wt% of SNAP and top-coated with CHXD to combine two antibacterial strategies into one system for potential biomedical device application. Previous studies using SNAP have shown that polymeric materials retain their mechanical properties up to 10 wt% SNAP.[41] Beyond 10 wt% materials tend to demonstrate a sharp decline in ultimate tensile strength.[41] Therefore, a 10 wt% SNAP was chosen for this study. To optimize the concentration of CHXD, three different wt% of CHXD in SR-THF solution (1, 3, and 5 wt%) were dip-coated on SNAP incorporated SR (**Figure 3.1**). NO release kinetics from varying amounts of CHXD on SR-SNAP samples were measured using a nitric oxide analyzer. The levels of NO released from polymer films were observed to be above physiologically relevant levels (0.5 – 4 x 10^{-10} mol min^{-1} cm^{-2}) up to 24 h (**Figure 3.2B**). Since results from the study showed no significant difference between the release levels, the highest concentration of CHXD top-coated films (5 wt%) was chosen for further evaluation to maximize the antimicrobial potential of these materials. To analyze the long-term release levels of NO from SR-SNAP-CHXD as compared to SR-SNAP samples, the films were tested over 4 weeks at physiological conditions (**Figure 3.2C**). The data revealed similar levels of NO and duration from both SR-SNAP and SR-SNAP-CHXD films with initial levels of NO 5.46 ± 0.64 and 5.67 ± 0.31 x 10^{-10} mol min^{-1} cm^{-2} on day 0. The final NO release values tested from films on day 29 were 0.28 ± 0.03 and 0.41 ± 0.15 x 10^{-10} mol min^{-1} cm^{-2} for SR-SNAP and SR-SNAP-CHXD films, respectively (**Table 3.2**). Values obtained in this study align with previously reported NO flux from SNAP-incorporated RTV polymer at the same initial SNAP loading (10 wt%) that showed 5.34 ± 0.91 x 10^{-10} mol cm^{-2} min^{-1} of NO release on day 0.[39]

To evaluate the translational properties of these surfaces for medical device application, the SR-SNAP-CHXD films were also tested for their compatibility with conventional ethylene oxide and UV sterilization methods used in hospital settings. Bioactive materials that contain NO donor compounds can lose their functions during sterilization due to their thermal and moisture sensitivity. However, the results obtained in this study confirmed that the NO levels from the sterilized samples continued to stay above physiological levels similar to that of freshly fabricated films (**Figure 3.2D**). Similar results have been reported about both SNAP and CHXD compatibility with various sterilization methods.[41, 50] These studies have presented the ability of SNAP-incorporated films (10 wt%) in retaining more than 90% of initial SNAP loaded into Elast-eon E2As (a copolymer of combined soft portions of polydimethylsiloxane and poly(hexamethylene oxide)) polymer matrix after UV and EO sterilization.[41] Similarly, Sherertz *et al*. have reported the compatibility of CHXD-coated triple-lumen polyurethane catheters with an EO sterilization method which were also able to preserve their antibacterial efficacies against *S. aureus* pathogen in an *in vivo* rabbit model.[50] Overall, the results obtained from this study confirm that both ethylene oxide and UV-light sterilization methods are viable options with the combinational films highlighting the potential of this material for clinical translation.

The amount of SNAP and CHXD released from polymer films into the PBS buffer under physiological conditions was also analyzed over 7-d using UV-vis spectroscopy. The data were extrapolated using the standard curve and characteristic peak of SNAP and CHXD compounds at 255 and 340 nm wavelength, respectively (**Figure 3.3A-D**). After 24 h, 0.27 ± 0.01 μg CHXD and 0.48 ± 0.03 μg of SNAP mg^{-1} of total film mass was detected in the buffer which translates to 53.98 and 4.80% of the initial SNAP and CHXD loaded in the polymer, respectively. In both cases, CHXD and SNAP diffusion was observed to be higher on the initial days. However, the diffusion of the compounds stabilized with each testing day (**Figure 3.3E**). It was found that after 7 d of testing, 95.04 and 20.63% of CHXD and SNAP leached into the soaking buffer, respectively. The

higher amount of CHXD leaching from the polymer samples can be beneficial at the onset of infection in the initial days. The corresponding slow NO release from polymer would then help in the prevention of biofilm development on medical device surfaces over relatively long durations. The cross-linked nature of silicone polymer with very low water uptake properties makes it a suitable choice for long-term antibacterial applications since it slows the release of both SNAP and CHXD from the polymer matrix.

This data is consistent with NO release flux from SNAP films that showed higher levels of initial NO flux during the 24 h incubation (**Figure 3.2B**). The high levels of SNAP leaching and NO flux can be attributed to the SNAP present in the water-rich layer of the polymer matrix. Leaching of SNAP and its byproducts is not a concern as SNAP is synthesized from its parent thiol, *N*-acetyl-*D*-penicillamine (NAP), which is an FDA-approved drug used to treat heavy metal poisoning.[51] In fact, several studies have been reported in the past using rabbit and sheep animal models that confirmed the safety of SNAP-incorporated materials during *in vivo* testing of SR-SNAP.[52, 53] Overall, results obtained from NO release and CHXD diffusion confirm the longevity of the polymer films.

The hydrophobicity of the drug and polymer both can dictate the drug release kinetics. Therefore, the release behavior of drugs from polymers can be altered by changing the parameters such as initial drug loading, polymer substrate (hydrophobic vs. hydrophilic), and thickness of topcoat (diffusion) based on the type and duration of application. The surface wettability of polymers can play a critical role in regulating the NO release from polymers by prolonging or preventing moisture from reaching the embedded SNAP molecule in the polymer matrix to stimulate NO release. Therefore, SNAP was integrated with silicone rubber polymer which is known to exhibit hydrophobic characteristics. These properties of silicone rubber make it an excellent choice for catheter-related applications. In order to analyze the effect of modification on SR polymer, surface characterization of polymer films was carried out using

contact angle measurement (**Figure 3.4**). Contact angle measurements on the samples revealed no significant difference between unmodified SR and modified surfaces (SR-SNAP, SR-CHXD, and SR-SNAP-CHXD) and all the samples remained hydrophobic with contact angle > 90º (**Figure 3.4**). Results from this study corroborate with previously published reports that showed no significant difference in water contact angles of thermoplastic polyurethane polymers with and without SNAP incorporation (10 wt%) assuming that the interface between blood proteins and film surface will stay unaltered with the addition of SNAP.[39, 41] In addition, using scanning electron microscopy and EDS mapping results confirmed the homogenous distribution of SNAP and CHXD in the polymers (**Figure 3.5**). These results demonstrate that SNAP incorporation through solvent evaporation and dip coating CHXD on the top of films is a facile and reliable technique to generate these dual-active antimicrobial surfaces.

Bacterial colonization on biomedical devices leads to ca. 90% of all hospital-acquired infections.[54] Bacteria like *S. aureus* and *E. coli* are a part of the group of ESKAPE pathogens that are the leading cause of nosocomial infections around the globe. Overuse of antibiotics and their abuse has triggered antimicrobial resistance in these opportunistic pathogens making them even harder to eradicate. Moreover, the altered gene expression of bacteria encapsulated within biofilm guards them against the host immune response. In these scenarios, it will be beneficial to have strategies that can help potentially thwart the progression of bacterial colonization on medical devices. Both NO and CHXD are known to exhibit broad-spectrum antimicrobial effects. Previous studies have reported the use of NO and CHXD in medical device applications such as dental implants, sutures, vascular catheters, antimicrobial dressings, antibiotic lock solutions, etc. to combat bacterial infections [26, 55-58]. However, to date, no study has been reported that combined NO and CHXD within polymer materials for developing dual-active antibacterial interfaces. The antibacterial activity of the films was analyzed against *S. aureus* (Gram-positive) and *E. coli* (Gram-negative) bacteria using a 24 h antibacterial adhesion assay and imaged using FESEM.

Results from the study showed the highest bacterial killing with SR-SNAP-CHXD against both *S. aureus* and *E. coli* bacteria with >3-log reduction in just 24 h (**Figure 3.6**). Although individual SR-SNAP and SR-CHXD films did exhibit antibacterial properties, the method of combining the two seemed more potent. The results from SR-SNAP films are equivalent to previous studies that utilized polyurethane-based polymers to incorporate or impregnate SNAP that released similar NO levels over a 24 h period.[39, 59, 60] NO can damage bacterial cell membranes by the means of lipid peroxidation that disrupts the outer membrane of cells.[61-63] Notably, the majority of antibacterial effects were found to be through antiseptic CHXD as opposed to SNAP in both *S. aureus* and *E. coli* 24 h antibacterial studies. It was also observed that SR-SNAP-CHXD was more potent against *S. aureus* bacteria which is a Gram-positive strain as opposed to *E. coli*. These results are analogous to previous reports that showed differential actions of CHXD on Gram-positive vs. Gram-negative bacteria.[64] This can be explained by the high binding efficiency of CHXD to the Gram-positive bacteria cell wall. To visualize the morphology of bacteria on the films scanning electron microscopy was utilized (**Figure 3.7**). The reduction of bacteria on the bactericidal surface was very evident and it was observed that CHXD-coated surfaces caused blisters on *S. aureus* (**Figure 3.7B and D**) and wrinkles on *E. coli* bacteria (**Figure 3.7F and H**) which aligns with previously studied effects of CHXD on bacteria.[64, 65] The cationic nature of the CHXD structure attracts the negatively charged bacteria membrane with strong adsorption to phosphate-containing groups. This binding results in loss of integrity in the cell membrane and malfunctioning of proteins and enzymes that lead to cell damage and intracellular compound leakage. [25-28] Similar to the results from the plate counting method, SEM imaging validated the highest reduction of bacteria on SR-SNAP-CHXD films.

While the films demonstrated excellent antibacterial properties, it was important to determine the safety of films towards mammalian cells. NO-releasing materials have been observed to carry enhanced biocompatibility *in vitro* due to the inherent endogenous regulatory functions of NO.

The NO donor SNAP is easy to synthesize and a well-characterized NO donor with enhanced biocompatibility. For this reason, SNAP-loaded materials are extensively studied both *in vitro* and *in vivo*. Previous studies have shown polymeric medical devices with NO-releasing capacity for the use of endotracheal tubes, insulin cannula, catheters, extracorporeal circulation, etc.[17, 49, 52] Results obtained in this study align with previously published articles that emphasize the compatibility of SNAP-loaded polymers for biomedical applications.[59, 66] Cell compatibility studies confirmed >70% cell survival rate with all samples (**Figure 3.8**). Results from the cytotoxicity study were in alignment with previously published reports where higher concentrations of CHXD were seen to trend toward cytotoxicity (data not shown). For example, higher concentrations of CHXD have previously been reported to damage skin cells.[67-69] Therefore, 5 wt% samples were selected for this study which showed excellent compatibility towards mouse fibroblast cells. The approach of combining both SNAP and CHXD can moderate CHXD-mediated toxicity and add potential benefits of SNAP to medical devices. The combination of the two compounds can amplify the antibacterial efficacy of medical devices without causing adverse effects on native cells and tissues in the body.

The results from the bacteria studies highlight the success of combining the two bioactive approaches. Both SNAP and CHXD have previously been used individually to incorporate the bactericidal properties into various other polymeric medical devices such as polyurethane, E2As, PVC, etc. [10, 17, 22, 56] To reduce the cytotoxicity induced by higher concentrations of CHXD, CHXD materials can be combined with NO (second antibacterial agent). Because NO possess several other regulatory functions such as wound healing, anti-inflammatory, and anti-thrombotic properties, the combination of a dual-functional surface can be one collective solution to several medical device-related issues.[70] Moreover, due to the short half-life of NO, there have been no reported cases of resistance in microorganisms which makes it a superior therapeutic as opposed to conventional antibiotic therapy for overcoming antimicrobial resistance.[71, 72] Together the

results from cytocompatibility and antibacterial studies underscore the necessity for bringing two antimicrobial surface strategies into one polymer system to effectively tackle bacteria and device-associated infections.

3.6 Conclusions

To utilize the antibacterial effects of both NO and CHXD, a CHXD salt and NO donor SNAP were incorporated in medical-grade silicone rubber (SR) polymer for biomedical/therapeutic applications. The 10 wt% SNAP incorporated films were fabricated using a solvent-evaporation process with a topcoat of CHXD (1, 3, and 5 wt%) to generate a dual-active antibacterial interface. Chemiluminescence studies confirmed the NO release from SR-SNAP-CHXD films at physiologically relevant levels ($0.5 – 4 \times 10^{-10}$ mol min^{-1} cm^{-2}) of NO for at least 4 weeks with a minimal amount of leaching. Further characterization of the films via SEM-EDS confirmed uniform distribution of SNAP and the presence of CHXD within the polymer films without substantial morphological changes confirmed by contact angle hysteresis. Moreover, the dual-active SNAP-CHXD films were able to significantly reduce *E. coli* and *S. aureus* bacteria (> 3-log reduction) compared to plain SR and individual SNAP and CHXD controls with no explicit toxicity towards NIH 3T3 mouse fibroblast cells. The synergy between the two systems can reduce bacterial contamination on the surface and enhance the durability of medical devices with a potential application for a wide range of biointerfaces (e.g., urinary catheters, blood catheters, insulin cannulas).

3.7 References

1. O'grady, N. P.; Alexander, M.; Burns, L. A.; Dellinger, E. P.; Garland, J.; Heard, S. O.; Lipsett, P. A.; Masur, H.; Mermel, L. A.; Pearson, M. L., Guidelines For The Prevention Of Intravascular Catheter-Related Infections. *Clin Infect Dis.* **2011,** *52* (9), e162-e193.

2. Zhu, L.; Gong, T.; Wood, T. L.; Yamasaki, R.; Wood, T. K., σ54-Dependent Regulator DVU2956 Switches Desulfovibrio Vulgaris From Biofilm Formation To Planktonic Growth And Regulates Hydrogen Sulfide Production. *Environ Microbiol.* **2019,** *21* (10), 3564-3576.

3. Bryers, J. D., Medical Biofilms. *Biotechnol Bioeng.* **2008,** *100* (1), 1-18.

4. Percival, S. L.; Suleman, L.; Vuotto, C.; Donelli, G., Healthcare-Associated Infections, Medical Devices and Biofilms: Risk, Tolerance and Control. *J. Med. Microbiol.* **2015,** *64* (4), 323-334.

5. Donlan, R. M., Biofilms: Microbial Life On Surfaces. *Emerg Infect Dis.* **2002,** *8* (9), 881.

6. Donlan, R. M., Biofilm formation: a clinically relevant microbiological process. *Clin Infect Dis.* **2001,** *33* (8), 1387-1392.

7. Stewart, P. S.; William Costerton, J., Antibiotic Resistance of Bacteria in Biofilms. *Lancet* **2001,** *358* (9276), 135-138.

8. Dincer, S.; Uslu, F. M.; Delik, A., *Bacterial biofilms*, IntechOpen: 2020.

9. Fakih, M. G.; Bufalino, A.; Sturm, L.; Huang, R.-H.; Ottenbacher, A.; Saake, K.; Winegar, A.; Fogel, R.; Cacchione, J., Coronavirus disease 2019 (COVID-19) Pandemic, Central-Line–Associated Bloodstream Infection (CLABSI), And Catheter-Associated Urinary Tract Infection (CAUTI): The Urgent Need To Refocus On Hardwiring Prevention Efforts. *Infect. Control Hosp. Epidemiol.* **2021**, 1-6.

10. Baccolini, V.; Migliara, G.; Isonne, C.; Dorelli, B.; Barone, L.; Giannini, D.; Marotta, D.; Marte, M.; Mazzalai, E.; Alessandri, F., The Impact Of The COVID-19 Pandemic On Healthcare-

Associated Infections In Intensive Care Unit Patients: A Retrospective Cohort Study. *Antimicrob Resist Infect Control* **2021,** *10* (1), 1-9.

11. Liedberg D, L. T., Silver Alloy Coated Catherters Reduce Catheter-Associated Bacteriuria. *BJU Int.* **1990,** *65* (4), 379-381.

12. Redfern, J.; Geerts, L.; Seo, J. W.; Verran, J.; Tosheva, L.; Wee, L. H., Toxicity And Antimicrobial Properties Of Zno@ ZIF-8 Embedded Silicone Against Planktonic And Biofilm Catheter-Associated Pathogens. *ACS Appl Nano Mater.* **2018,** *1* (4), 1657-1665.

13. Armugam, A.; Teong, S. P.; Lim, D. S.; Chan, S. P.; Yi, G.; Yew, D. S.; Beh, C. W.; Zhang, Y., Broad Spectrum Antimicrobial PDMS-Based Biomaterial For Catheter Fabrication. *Biomater Res.* **2021,** *25* (1), 1-13.

14. Liu, F.; Qu, W.; Zhang, J.; Liu, J.; Zhu, Q.; Yue, T.; Xu, X.; Ma, N.; Ma, J.; Sun, Y., Cationic Alternating Polypeptide Fixed on Polyurethane at Multiple Sites for Excellent Antibacterial and Antifouling Properties. *Langmuir* **2021,** *37* (36), 10657-10667.

15. Xie, D.; Howard, L.; Almousa, R., Surface Modification Of Polyurethane With A Hydrophilic, Antibacterial Polymer For Improved Antifouling And Antibacterial Function. *J Biomater Appl.* **2018,** *33* (3), 340-351.

16. Zeng, Q.; Zhu, Y.; Yu, B.; Sun, Y.; Ding, X.; Xu, C.; Wu, Y.-W.; Tang, Z.; Xu, F.J., Antimicrobial And Antifouling Polymeric Agents For Surface Functionalization Of Medical Implants. *Biomacromolecules* **2018,** *19* (7), 2805-2811.

17. Chug, M. K.; Feit, C.; Brisbois, E. J., Increasing the Lifetime of Insulin Cannula with Antifouling and Nitric Oxide Releasing Properties. *ACS Appl Bio Mater.* **2019**, *2*(12), Pp.5965-5975.

18. Salim, N.; Silikas, N.; Satterthwaite, J.; Moore, C.; Ramage, G.; Rautemaa, R., Chlorhexidine-impregnated PEM/THFM Polymer Exhibits Superior Activity To Fluconazole-Impregnated Polymer Against Candida Albicans Biofilm Formation. *Int J Antimicrob Agents* **2013,** *41* (2), 193-196.

19. Wassil, S. K.; Crill, C. M.; Phelps, S. J., Antimicrobial Impregnated Catheters In The Prevention Of Catheter-Related Bloodstream Infection In Hospitalized Patients. *J Pediatr Pharmacol Therapeut.* **2007,** *12* (2), 77-90.

20. Belfield, K.; Chen, X.; Smith, E. F.; Ashraf, W.; Bayston, R., An Antimicrobial Impregnated Urinary Catheter That Reduces Mineral Encrustation And Prevents Colonisation By Multi-Drug Resistant Organisms For Up To 12 Weeks. *Acta Biomater.* **2019,** *90*, 157-168.

21. Liu, H.; Shukla, S.; Vera-González, N.; Tharmalingam, N.; Mylonakis, E.; Fuchs, B. B.; Shukla, A., Auranofin Releasing Antibacterial And Antibiofilm Polyurethane Intravascular Catheter Coatings. *Front Cell Infect Microbiol* **2019,** *9*, 37.

22. Feit, C.; Chug, M. K.; Brisbois, E. J., Development of S-Nitroso-N-Acetylpenicillamine (SNAP) Impregnated Medical Grade Polyvinyl Chloride for Antimicrobial Medical Device Interfaces. *ACS Appl Bio Mater* **2019**, *2*(10), 4335-4345.

23. Chug, M. K.; Bachtiar, E.; Narwold, N.; Gall, K.; Brisbois, E. J., Tailoring Nitric Oxide Release With Additive Manufacturing To Create Antimicrobial Surfaces. *Biomater. Sci.* **2021**. 9 (8), 3100– 3111.

24. Wang, E. W.; Layon, A. J., Chlorhexidine Gluconate Use To Prevent Hospital Acquired Infections—A Useful Tool, Not A Panacea. *Ann Transl Med.* **2017,** *5* (1).

25. Cieplik, F.; Jakubovics, N. S.; Buchalla, W.; Maisch, T.; Hellwig, E.; Al-Ahmad, A., Resistance Toward Chlorhexidine in Oral Bacteria – Is There Cause for Concern? *Front Microbiol.* **2019,** *10* (587).

26. Łukomska-Szymańska, M.; Sokołowski, J.; Łapińska, B., Chlorhexidine – Mechanism Of Action And Its Application To Dentistry. *J. Stomatol.* **2017,** *70* (4), 405-417.

27. Kuyyakanond, T.; Quesnel, L. B., The Mechanism Of Action Of Chlorhexidine. *FEMS Microbiol Lett.* **1992,** *100* (1-3), 211-215.

28. Russell, A.; Path, F., Chlorhexidine: Antibacterial Action And Bacterial Resistance. *Infection* **1986,** *14* (5), 212-215.

29. Obermeier, A.; Schneider, J.; Harrasser, N.; Tübel, J.; Mühlhofer, H.; Pförringer, D.; Deimling, C. V.; Foehr, P.; Kiefel, B.; Krämer, C.; Stemberger, A.; Schieker, M.; Burgkart, R.; Von Eisenhart-Rothe, R., Viable adhered Staphylococcus Aureus Highly Reduced On Novel Antimicrobial Sutures Using Chlorhexidine And Octenidine To Avoid Surgical Site Infection (SSI). *PLOS ONE* **2018,** *13* (1), e0190912.

30. Zhi, X.; Wang, Y.; Li, P.; Yuan, J.; Shen, J., Preparation Of Keratin/Chlorhexidine Complex Nanoparticles For Long-Term And Dual Stimuli-Responsive Release. *RSC Adv.* **2015,** *5* (100), 82334-82341.

31. Ji, Q. X.; Zhao, Q. S.; Deng, J.; Lü, R., A Novel Injectable Chlorhexidine Thermosensitive Hydrogel For Periodontal Application: Preparation, Antibacterial Activity And Toxicity Evaluation. *J Mater Sci Mater Med.* **2010,** *21* (8), 2435-2442.

32. Moritz, M.; Geszke-Moritz, M., Mesoporous Silica Materials With Different Structures As The Carriers For Antimicrobial Agent. Modeling Of Chlorhexidine Adsorption And Release. *Appl Surf Sci.* **2015,** *356*, 1327-1340.

33. Anusavice, K.; Zhang, N.-Z.; Shen, C., Controlled Release Of Chlorhexidine From UDMA-TEGDMA Resin. *J Dent Res.* **2006,** *85* (10), 950-954.

34. Wang, H.; Tong, H.; Liu, H.; Wang, Y.; Wang, R.; Gao, H.; Yu, P.; Lv, Y.; Chen, S.; Wang, G., Effectiveness Of Antimicrobial-Coated Central Venous Catheters For Preventing Catheter-Related Blood-Stream Infections With The Implementation Of Bundles: A Systematic Review And Network Meta-Analysis. *Annals of intensive care* **2018,** *8* (1), 1-12.

35. Weinberg, J.; Misukonis, M.; Shami, P.; Mason, S.; Sauls, D.; Dittman, W.; Wood, E.; Smith, G.; McDonald, B.; Bachus, K., Human Mononuclear Phagocyte Inducible Nitric Oxide Synthase (Inos): Analysis Of Inos Mrna, Inos Protein, Biopterin, And Nitric Oxide Production By Blood Monocytes And Peritoneal Macrophages. *Blood* **1995,** *86* (3), 1184-1195.

36. Frost, M. C.; Reynolds, M. M.; Meyerhoff, M. E., Polymers Incorporating Nitric Oxide Releasing/Generating Substances for Improved Biocompatibility of Blood-contacting Medical Devices. *Biomaterials* **2005,** *26* (14), 1685-1693.

37. Chipinda, I.; Simoyi, R. H., Formation and Stability of a Nitric Oxide Donor: S-nitroso-N-acetylpenicillamine. *J. Phys. Chem. B* **2006,** *110* (10), 5052-5061.

38. Vaughn, M. W.; Kuo, L.; Liao, J. C., Estimation of Nitric Oxide Production and Reactionrates in Tissue by Use of a Mathematical Model. *Am. J. Physiol. Heart Circ. Physiol.* **1998,** *274* (6), H2163-H2176.

39. Singha, P.; Pant, J.; Goudie, M. J.; Workman, C. D.; Handa, H., Enhanced Antibacterial Efficacy of Nitric Oxide Releasing Thermoplastic Polyurethanes with Antifouling Hydrophilic Topcoats. *Biomater. Sci.* **2017,** *5* (7), 1246-1255.

40. Brisbois, E. J.; Major, T. C.; Goudie, M. J.; Bartlett, R. H.; Meyerhoff, M. E.; Handa, H., Improved Hemocompatibility Of Silicone Rubber Extracorporeal Tubing Via Solvent Swelling-Impregnation Of S-Nitroso-N-Acetylpenicillamine (SNAP) And Evaluation In Rabbit Thrombogenicity Model. *Acta Biomater.* **2016,** *37*, 111-119.

41. Goudie, M. J.; Brisbois, E. J.; Pant, J.; Thompson, A.; Potkay, J. A.; Handa, H., Characterization of an S-nitroso-N-acetylpenicillamine–Based Nitric Oxide Releasing Polymer from a Translational Perspective. *Int. J. Polym. Mater. Polym. Biomater.* **2016,** *65* (15), 769-778.

42. Pant, J.; Gao, J.; Goudie, M. J.; Hopkins, S. P.; Locklin, J.; Handa, H., A Multi-Defense Strategy: Enhancing Bactericidal Activity of a Medical Grade Polymer with a Nitric Oxide Donor and Surface-immobilized Quaternary Ammonium Compound. *Acta Biomater.* **2017,** *58*, 421-431.

43. Al-Obaidy, S. S.; Greenway, G. M.; Paunov, V. N., Enhanced Antimicrobial Action of Chlorhexidine Loaded in Shellac Nanoparticles with Cationic Surface Functionality. *Pharmaceutics* **2021,** *13* (9), 1389.

44. Mondal, A.; Devine, R.; Estes, L.; Manuel, J.; Singha, P.; Mancha, J.; Palmer, M.; Handa, H., Highly Hydrophobic Polytetrafluoroethylene Particle Immobilization Via Polydopamine

Anchor Layer On Nitric Oxide Releasing Polymer For Biomedical Applications. *J Colloid Interface Sci.* **2021,** *585*, 716-728.

45. Grommersch, B. M.; Pant, J.; Hopkins, S. P.; Goudie, M. J.; Handa, H., Biotemplated Synthesis and Characterization of Mesoporous Nitric Oxide-Releasing Diatomaceous Earth Silica Particles. *ACS Appl. Mater. Interfaces* **2018,** *10* (3), 2291-2301.

46. Wang, S.; Yang, Y.; Li, W.; Wu, Z.; Li, J.; Xu, K.; Zhang, W.; Zheng, X.; Chen, J., Study of the Relationship Between Chlorhexidine-Grafted Amount and Biological Performances of Micro/Nanoporous Titanium Surfaces. *ACS Omega* **2019,** *4* (19), 18370-18380.

47. Tattawasart, U.; Hann, A.; Maillard, J.-Y.; Furr, J.; Russell, A., Cytological Changes In Chlorhexidine-Resistant Isolates Of Pseudomonas Stutzeri. *J Antimicrob Chemother.* **2000,** *45* (2), 145-152.

48. Colletta, A.; Wu, J.; Wo, Y.; Kappler, M.; Chen, H.; Xi, C.; Meyerhoff, M. E., S-Nitroso-N-acetylpenicillamine (SNAP) Impregnated Silicone Foley Catheters: A Potential Biomaterial/Device to Prevent Catheter-Associated Urinary Tract Infections. *ACS Biomater. Sci. Eng.* **2015,** *1* (6), 416-424.

49. Homeyer, K. H.; Singha, P.; Goudie, M. J.; Handa, H., S-Nitroso-N-acetylpenicillamine Impregnated Endotracheal Tubes For Prevention Of Ventilator-Associated Pneumonia. *Biotechnol Bioeng. 2020;* ***117****(7): 2237- 2246.*

50. Sherertz, R. J.; Heard, S. O.; Raad, I. I.; Gentry, L.; Bowton, D.; Scuderi, P.; Hu, J.; Carruth, W.; Satishchandra, B.; Pepe, J., Gamma Radiation-Sterilized, Triple-Lumen Catheters Coated With A Low Concentration Of Chlorhexidine Were Not Efficacious At Preventing Catheter Infections In Intensive Care Unit Patients. *Antimicrob Agents Chemother.* **1996,** *40* (9), 1995-1997.

51. Jones, M.; Weaver, A.; Weller, W., The Relative Effectiveness Of Some Chelating Agents As Antidotes In Acute Cadmium Poisoning. *Res Commun Chem Pathol Pharmacol.* **1978,** *22* (3), 581-588.

52. Brisbois, E. J.; Kim, M.; Wang, X.; Mohammed, A.; Major, T. C.; Wu, J.; Brownstein, J.; Xi, C.; Handa, H.; Bartlett, R. H.; Meyerhoff, M. E., Improved Hemocompatibility of Multilumen Catheters via Nitric Oxide (NO) Release from S-nitroso-N-acetylpenicillamine (SNAP) Composite Filled Lumen. *ACS Appl. Mater. Interfaces* **2016,** *8* (43), 29270-29279.

53. Brisbois, E. J.; Davis, R. P.; Jones, A. M.; Major, T. C.; Bartlett, R. H.; Meyerhoff, M. E.; Handa, H., Reduction in Thrombosis and Bacterial Adhesion with 7 Day Implantation of S-nitroso-N-acetylpenicillamine (SNAP)-Doped Elast-eon E2As Catheters in Sheep. *J. Mater. Chem. B* **2015,** *3* (8), 1639-1645.

54. Richards, M. J.; Edwards, J. R.; Culver, D. H.; Gaynes, R. P., Nosocomial Infections in Medical Intensive Care Units in the United States. *Crit. Care Med.* **1999,** *27* (5), 887-892.

55. Balagopal, S.; Arjunkumar, R., Chlorhexidine: the Gold Standard Antiplaque Agent. *J Pharm Sci Res.* **2013,** *5* (12), 270.

56. Brisbois, E. J.; Handa, H.; Major, T. C.; Bartlett, R. H.; Meyerhoff, M. E., Long-term nitric oxide release and elevated temperature stability with S-nitroso-N-acetylpenicillamine (SNAP)-doped Elast-eon E2As Polymer. *Biomaterials* **2013,** *34* (28), 6957-6966.

57. Brisbois, E. J.; Bayliss, J.; Wu, J.; Major, T. C.; Xi, C.; Wang, S. C.; Bartlett, R. H.; Handa, H.; Meyerhoff, M. E., Optimized Polymeric Film-based Nitric Oxide Delivery Inhibits Bacterial Growth in a Mouse Burn Wound Model. *Acta Biomater.* **2014,** *10* (10), 4136-4142.

58. Kumar, R.; Massoumi, H.; Chug, M. K.; Brisbois, E. J., S-Nitroso-N-acetyl-l-cysteine Ethyl Ester (SNACET) Catheter Lock Solution to Reduce Catheter-Associated Infections. *ACS Appl. Mater. Interfaces* **2021**.

59. Pant, J.; Goudie, M. J.; Chaji, S. M.; Johnson, B. W.; Handa, H., Nitric Oxide Releasing Vascular Catheters for Eradicating Bacterial Infection. *J. Biomed. Mater. Res. B* **2018,** *106* (8), 2849-2857.

60. Homeyer, K. H.; Goudie, M. J.; Singha, P.; Handa, H., Liquid-Infused Nitric-Oxide-Releasing Silicone Foley Urinary Catheters for Prevention of Catheter-Associated Urinary Tract Infections. *ACS Biomater. Sci. Eng.* **2019,** *5* (4), 2021-2029.

61. Deupree, S. M.; Schoenfisch, M. H., Morphological Analysis Of The Antimicrobial Action Of Nitric Oxide On Gram-Negative Pathogens Using Atomic Force Microscopy. *Acta Biomater.* **2009,** *5* (5), 1405-1415.

62. Gao, Q.; Zhang, X.; Yin, W.; Ma, D.; Xie, C.; Zheng, L.; Dong, X.; Mei, L.; Yu, J.; Wang, C., Functionalized Mos2 Nanovehicle With Near-Infrared Laser-Mediated Nitric Oxide Release And Photothermal Activities For Advanced Bacteria-Infected Wound Therapy. *Small* **2018,** *14* (45), 1802290.

63. Rong, F.; Tang, Y.; Wang, T.; Feng, T.; Song, J.; Li, P.; Huang, W., Nitric Oxide-Releasing Polymeric Materials for Antimicrobial Applications: A Review. *Antioxidants* **2019,** *8* (11), 556.

64. Cheung, H.-Y.; Wong, M. M.-K.; Cheung, S.-H.; Liang, L. Y.; Lam, Y.-W.; Chiu, S.-K., Differential Actions Of Chlorhexidine On The Cell Wall Of Bacillus Subtilis and Escherichia Coli. *PLoS One* **2012,** *7* (5), e36659.

65. Shalamanov, D., Chlorhexidine Gluconate-Induced Morphological Changes In Gram Negative Microorganisms. *Biotechnol Biotechnol Equip.* **2005,** *19* (1), 121-124.

66. Singha, P.; Workman, C. D.; Pant, J.; Hopkins, S. P.; Handa, H., Zinc-oxide Nanoparticles Act Catalytically and Synergistically with Nitric Oxide Donors to Enhance Antimicrobial Efficacy. *J. Biomed. Mater. Res. A* **2019**.

67. Liu, J. X.; Werner, J.; Kirsch, T.; Zuckerman, J. D.; Virk, M. S., Cytotoxicity Evaluation Of Chlorhexidine Gluconate On Human Fibroblasts, Myoblasts, And Osteoblasts. *J Bone Joint Infect.* **2018,** *3* (4), 165-172.

68. Lang, N. P.; Ramseier-Grossmann, K., Optimal Dosage Of Chlorhexidine Digluconate In Chemical Plaque Control When Applied By The Oral Irrigator. *J Clin Periodontol.* **1981,** *8* (3), 189-202.

69. Hidalgo, E.; Dominguez, C., Mechanisms Underlying Chlorhexidine-Induced Cytotoxicity. *Toxicol in Vitro.* **2001,** *15* (4-5), 271-276.

70. Hetrick, E. M.; Prichard, H. L.; Klitzman, B.; Schoenfisch, M. H., Reduced Foreign Body Response At Nitric Oxide-Releasing Subcutaneous Implants. *Biomaterials* **2007,** *28* (31), 4571-80.

71. Friedman, A.; Blecher, K.; Sanchez, D.; Tuckman-Vernon, C.; Gialanella, P.; Friedman, J. M.; Martinez, L. R.; Nosanchuk, J. D., Susceptibility of Gram-positive and -Negative bacteria To Novel Nitric Oxide-Releasing Nanoparticle Technology. *Virulence* **2011,** *2* (3), 217-21.

72. Hetrick, E. M.; Shin, J. H.; Paul, H. S.; Schoenfisch, M. H., Anti-biofilm Efficacy Of Nitric Oxide-Releasing Silica Nanoparticles. *Biomaterials* **2009,** *30* (14), 2782-9.

CHAPTER 4:

TAILORING NITRIC OXIDE RELEASE WITH ADDITIVE MANUFACTURING TO CREATE ANTIMICROBIAL SURFACES

Chug, M. K., Bachtiar, E., Narwold, N., Gall, K., & Brisbois, E. J. (2021). Tailoring Nitric Oxide Release with Additive Manufacturing to Create Antimicrobial Surfaces. *Biomaterials Science*, *9*(8), 3100-3111.

4.1 Abstract

Current use of implantable and indwelling medical devices have restricted life due to potential microbial colonization leading to severe ailments. The aim of this work is to develop bioactive polymers that can be customized based on patient needs and help prevent bacterial infection. Potential benefits of additive manufacturing technology are integrated with the antimicrobial properties of nitric oxide (NO) to develop NO-releasing biocompatible polymer interfaces for treating bacterial infections. Using filament-based additive manufacturing, polycarbonateurethane-Silicone (PCU-Sil) a range of films possessing unique porosities (Disk-60, Disk-40, Solid, Capped) were fabricated. The films were impregnated with S-nitroso-N-acetyl-penicillamine (SNAP) using a solvent-swelling process. The Disk-60 porous films had the greatest amount of SNAP (19.59 wt%) as measured by UV-vis spectroscopy. Scanning electron microscopy and energy-dispersive X-ray spectroscopy confirmed an even distribution of SNAP throughout the polymer. The films exhibited a structure-based tunable NO-release at physiological levels ranging from 7-14 days for solid and porous films, as measured by chemiluminescence. The antibacterial efficacy of the films was studied against Staphylococcus aureus using a 24 h in vitro bacterial adhesion assay. The results demonstrated a >99% reduction of viable bacteria on the surface of all the NO-releasing films compared to unmodified PCU-Sil controls. The combination of 3D-printing technology with NO-releasing properties represents a promising technique to developing customized medical devices, such as 3D scaffolds, catheters, etc. with distinct NO-release levels, providing antimicrobial properties and enhanced biocompatibility.

Keywords: Nitric oxide, Additive manufacturing, Antibacterial, Impregnation, Medical device

4.2 Introduction

In recent years, additive manufacturing has emerged as a powerful and useful method for polymer fabrication. Major advantages of additive manufacturing include capabilities for rapid iteration and fabrication of the geometrically complex object.[1] In turn, this allows tuning the structures of an object to modulate specific properties, such as mechanical behavior [2] and drug release.[3] Applications of 3D-printing have a wide range of applications including stereolithography, fused deposition modeling (FDM), direct ink writing, and inkjet printing. The FDM printing utilized in this study is a 3D-printing technique wherein filaments of thermoplastic polymer are melted and extruded through a nozzle to build 3-D objects one horizontal layer at a time. Although FDM printing has some limitations in terms of geometrical complexity, it can print a large variety of biocompatible materials at a low-cost and in relatively simple manner.[4] With the modern developments in both degradable and non-degradable materials, the application of additive manufacturing in therapeutic and pharmacological disciplines has surged.[3,5,6] Three-dimensional printing has the potential to transform the healthcare system by personalizing implantable and insertable medical devices with porous and non-porous morphology for the use of catheters, drug delivery vehicles, tissue engineering scaffolds, and bioprinted organs.[7] Additionally, 3-D printing has also been employed for high-tech applications like structuring biomedical prototypes and anatomical surgical aids customized to the patient.[8, 9]

The biomedical field has made advances in medical device technology and materials, but a significant number of nosocomial infections originating from medical devices still exist. In 2002, the Centers for Disease Control and Prevention (CDC) reported 99,000 deaths occurred from hospital-acquired infections among 1.7 million hospitalized patients in the United States alone.[10] Infections transpiring from catheter-associated urinary tract infection (CAUTI), central line-associated bloodstream infections (CLABSI), and ventilator-associated pneumonia (VAP) are primarily associated with indwelling medical devices.[11-13] The lifetime of medical devices is limited

by infections related to such medical devices which are a result of microbial colonization and biofilm formation leading to delayed recovery and a large therapeutic and financial burden among infected patients.[14] Bacterial cells protected under the extracellular polymeric substances (EPS) matrix or 'slime' grow highly resistant to most effective antibiotics and as well as host immune response.[15] Moreover, these bacteria can withstand the action of bactericidal agents and can disintegrate the polymer material that the device is made of.[16, 17] The pathogenesis of device-related infections involves a multidimensional interface between the pathogen, the device, and the host. Medical device-related infections have spurred the development of new effective biocompatible and antimicrobial materials. Common strategies to inhibit biofilm colonization consist of physical and chemical alteration of the biomaterial surface to generate anti-adhesive surfaces (e.g. slippery liquid infused porous surfaces to reduce the fouling of the surface) [18], incorporation of bactericidal agents (e.g. silver) [19], or release of one or more types of antibacterial agents.[20] These strategies have been widely employed to prevent bacterial contamination of medical device surfaces. Nonetheless, the success of these options has been fairly limited in clinical applications.[21, 22]

In the last few decades, nitric oxide (NO) based materials have surfaced as a prospective biocidal and antithrombotic alternative to current strategies for medical device interfaces. Nitric oxide is an endogenous free radical gas molecule that is synthesized in mammalians via NO synthase (NOS) enzymes that converts L-arginine into citrulline and NO.[23, 24] NO is also a crucial antimicrobial and antioxidant agent. Immune cells, such as macrophages, utilize NO produced via inducible nitric oxide synthase (iNOS) at > 1 μM NO concentration during phagocytosis that functions as a bactericidal agent and promotes biofilm dispersion.[25] Furthermore, endothelial cells exhibit NO release in the range of 0.5 - 4 x 10^{-10} mol cm^{-2} min^{-1}.[26] Multiple classes of NO donors have been synthesized and used in polymers to mimic the endogenous properties of NO and enhance biocompatibility.[27, 28] Polymers that mimic this NO release level have also

demonstrated potent antimicrobial activity.[29-32] *S*-Nitroso-*N*-acetylpenicillamine (SNAP) is a well-characterized S-nitrosothiol (RSNO) NO donor with high stability, low cost, and long-term NO release under physiological conditions (37 °C, pH 7.4). It has been incorporated in a variety of medical-grade polymers to create NO-releasing materials for hemocompatibility and antimicrobial applications.[33]

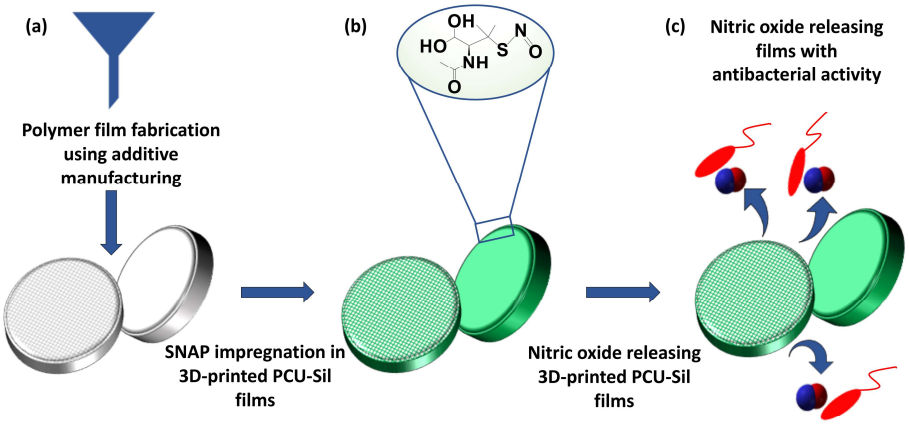

Figure 4.1. Schematic representation of methodology to develop 3D-printed NO-releasing PCU-Sil films. (a) Films are printed using an FFF 3D printer (Lulzbot Taz 6, Aleph Objects). (b) Post-fabrication, NO donor SNAP (*S*-nitroso-*N*-acetylpenicillamine) is impregnated in the polymer via a solvent-impregnation process. (c) The SNAP impregnated films can release NO at physiological conditions or in the presence of heat, light, and metal ions to exhibit broad-spectrum antimicrobial properties.

Previous studies have utilized 3D printing for fabricating antimicrobial thermoplastic polymers doped with antibiotics, silver nanoparticles, and antimicrobial drugs to overcome medical device infections.[34, 35] However, antibiotic and silver-based therapies possess several disadvantages because of their inability to penetrate the EPS matrix of the biofilm.[36] Furthermore, high concentrations of these compounds can be toxic to mammalian cells.[37] Nitric oxide-releasing materials are advantageous because NO is a potent gasotransmitter with the ability to penetrate and disperse the biofilm kill the planktonic cells that carry the threat to re-colonize surfaces, and

has a short half-life (seconds) preventing the emergence of resistance in the microbes, thereby thwarting the reoccurrence of biofilm.[38 39]

Herein, for the first time, 3-D printing of polycarbonate-based silicone elastomer (PCU-Sil, ChronoSil) with various geometries is impregnated with NO donor chemistry (**Figure 4.1**). This study presents a new additively manufactured PCU-Sil strategy to create tunable NO release for biomedical applications. Four different porosity designs of the PCU-Sil were additively manufactured and then impregnated with the NO donor SNAP. The NO-releasing properties and leaching of SNAP from the polymer matrix were quantified and correlated to the various geometric porosities. Scanning electron microscopy with energy-dispersive X-ray spectroscopy was utilized to perform morphological and elemental analysis of the SNAP in the polymer to evaluate the impregnation process, stability, and duration of NO release kinetics. Finally, the SNAP-based PCU-Sil polymers were evaluated for their efficacy in reducing microbial adhesion after 24 h of exposure to *S. aureus*, a common bacterial strain often associated with medical device infections.

4.3 Materials and Methods

4.3.1 Materials

N-Acetyl-*D*-penicillamine (NAP), sodium nitrite, *L*-cysteine, sodium chloride, potassium chloride, sodium phosphate dibasic, potassium phosphate monobasic, copper (II) chloride, ethylenediaminetetraacetic acid (EDTA), *N, N*-Dimethylacetamide (DMAc), methyl ethyl ketone (MEK), and sterile phosphate buffer saline powder with 0.01 M, pH 7.4, containing 0.138 M NaCl, 2.7 mM KCl, were purchased from Sigma Aldrich (St. Louis, MO). Methanol, hydrochloric acid, and sulfuric acid were obtained from Fisher Scientific (Hampton, NH). All aqueous solutions were prepared using deionized water. Phosphate buffer saline (PBS) 0.01 M with 100 μM EDTA was used for all material characterization and NO analyzer studies. The bacterial strain *Staphylococcus aureus* (ATCC 6538) was obtained from American Type Culture Collection (ATCC). All the buffers and media were sterilized in an autoclave at 121 °C, 100 kPa (15 psi)

above atmospheric pressure for 20 minutes prior to the biocompatibility experiments. Polycarbonate-urethane-silicone (PCU-Sil) copolymer with 10% silicone content and 85A Shore hardness was obtained from Advansource Biomaterials in pellet form. The PCU-Sil pellet was processed as received without any further modifications.

4.3.2 Fabrication of PCU-Sil Disks

The PCU-Sil pellets were dried at 85 °C over 24 h and then extruded through a 1.75 mm nozzle with a single-stage single-screw extruder (Filabot EX2, Triex LLC.) at 210 °C. The resulting filament diameter was measured at 10 different locations and determined to be 1.63 +- 0.11 mm (mean ± standard deviation). The filaments were stored in a desiccator box after processing and dried at 80 °C for 24 h before characterization and 3D printing to prevent moisture absorption and the creation of undesired porosity in 3D printed samples. PCU-Sil filaments were printed using an FFF 3D printer (Lulzbot Taz 6, Aleph Objects) equipped with a custom flexible filament extruder (Flexion, Diabase Engineering) and a 0.40 mm nozzle. The nozzle temperature was set at 260 °C, the printing speed at 3 mm/s, and the layer height at 0.30 mm. Further details on the printing parameters for 3D printed films used in the study are provided in (**Table 4.1**). Four disk varieties

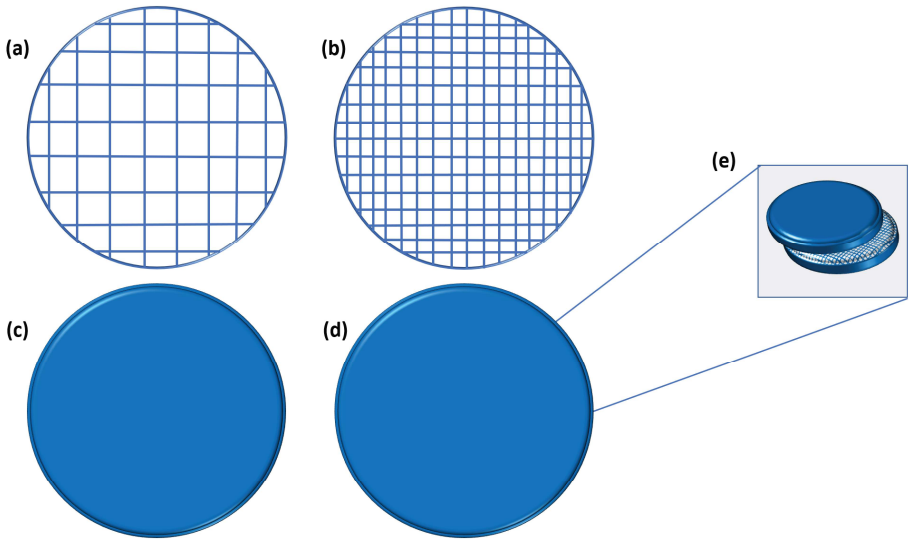

Figure 4.2 Schematic representation of 3D-printed PCU-Sil films. (a) Disk-60 (b) Disk-40 (c) Solid (d) Capped (e). Internal structure of capped films showing solid on top and bottom with 40% porous structure in the interior.

were printed with different porosity: Disk-60 (60% porosity), Disk-40 (40% porosity), Solid (0% porosity), and a Capped (solid on top and bottom with 40% porous structure in the interior) (**Figure 4.2**). Infills were printed with a 45º/45º crosshatch pattern.

Table 4.1 Printing parameters used for fabricating PCU-Sil disks

3D Printing Parameters	Values
Nozzle Size	0.40 mm
Printing Speed	480 mm/min
Nozzle Temperature	260 ºC
Bed Temperature	70 ºC
Extrusion Multiplier	0.55
Layer Height	0.30 mm
Layer Width	0.30 mm
Raster Angle	45º/-45º
Infill	(Dependent upon desired porosity)
Perimeter Overlap	70%
Shell	0.3 mm x 1

4.3.3 *S*-nitroso-*N*-acetylpenicillamine Synthesis

S-nitroso-*N*-acetylpenicillamine was synthesized using an altered version of a previously reported protocol.[40] *N*-Acetyl-*D*-penicillamine and sodium nitrite were dissolved in an equimolar

proportion in 2:3 parts of water and methanol. Next, concentrated H_2SO_4 and HCl were added to the above reaction such that the final concentration of acids in the mixture was 0.7 and 1.6 M, respectively. The reaction solution was stirred for 10 min, blown with gentle air, and placed on ice until crystals formed (6-8 h). The precipitated SNAP crystals were collected into a Buchner funnel using suction filtration, rinsed with ice-cold DI water, and dried overnight in a vacuum desiccator protected from light. The purity of synthesized SNAP crystals (> 90%) was verified using the chemiluminescence NO analyzer and a standard UV-vis calibration curve.

4.3.4 Preparation of NO-releasing PCU-Sil Films

To establish the solvent impregnation time for optimal SNAP impregnation into PCU-Sil, wt % of SNAP in the films was determined by the solvent impregnation method based on a previously reported protocol [41]. Briefly, methyl ethyl ketone (MEK) and methanol (MeOH) in a 40:60 ratio were optimized to impregnate the films. All four types of blank films (Disk-60, Disk-40, Solid, and Capped; n ≥ 3) were soaked in SNAP solution (100 mg mL^{-1}) dissolved in MEK-MeOH mixture at three different time points (0.5, 1, 2 h). The resultant SNAP-impregnated films were air dried first in the dark overnight and then dried in the desiccator for 24 h under ambient conditions. Finally, films were rinsed with water and methanol to wash away the surface crystals of SNAP and used for further analysis.

4.3.5 Scanning Electron Microscopy and Energy-dispersive X-ray Spectroscopy

Scanning electron microscopy images of the 3D printed PCU-Sil films were obtained using an Apreo S (ThermoFisher Scientific) in OptiPlan mode using a 2.00 kV accelerating voltage, 25 pA current, and 10.7 mm working distance. Images were taken at magnification ranges of 46x-500x. Two images were acquired for each disk sample: a top surface view and a transverse cross-sectional view. Transverse cross-section images of the disks were obtained by cutting the disk along the diameter of the circular face of the disk gently with a razor blade. Prior to SEM observation, the samples were sputtered with a thin Au layer (~8 nm) using a Denton Desk IV

vacuum sputter coater. Elemental composition analysis and mapping of the materials were done using Oxford Instruments X-Max-N 150 SDD (Oxford Instruments) and AZtec analysis software (Oxford Instruments). Data acquisition was done at 350x magnification and an accelerating voltage of 20kV.

4.3.6 Micro-CT Imaging of PCU-Sil Films

Micro-computed tomography (micro-CT) was done to evaluate the internal structure of the PCU-Sil 3D-printed films before and after SNAP impregnation. Micro-CT analysis was carried out on a Nikon XTH 225 ST at 108 kV/88 μA. Exposure time was set at 708 ms and 2 frames are averaged for each image. Voxel sizes are maintained at 14.9 μm. CT data was processed into cross-sections using CT Agent. 3D rendering and porosity analysis of micro-CT scans was carried out using Avizo (FEI Visualization Sciences Group).

4.3.7 Characterization of SNAP-Impregnated 3D-PCU-Sil Films for NO-Releasing Properties

4.3.7.1 Characterization of SNAP Impregnation

The amount of SNAP (wt%) in the final films was analyzed to obtain the time needed to achieve maximum SNAP impregnation into the polymer films. To do this, the weights of the samples were recorded using an analytical balance (Mettler Toledo™ XS105DU, Columbus, OH). To quantify the impregnated SNAP, the samples were dissolved in DMAc for 1 h on a magnetic stirrer at room temperature and protected from light. The solution was analyzed by UV-vis spectroscopy (Cary 60, Agilent Technologies) at 340 nm to measure the milligrams of SNAP loaded in the films. The molar absorptivity of SNAP in DMAc at 22 °C was determined to be 1008 M^{-1} cm^{-1} at 340 nm. The weight percentage (wt%) of SNAP loaded was determined using **Equation 4.1**.

$$wt\ \%\ SNAP = \frac{milligrams\ of\ SNAP}{milligrams\ of\ film} \times 100$$ (**Equation 4.1**)

4.3.7.2 Real-time Nitric Oxide Release Kinetics

The real-time NO release from the films was quantified by a gold standard chemiluminescence method using a Zysense chemiluminescence Nitric Oxide Analyzer (NOA) 280i (Frederick, CO). The cell pressure of the NOA cell was at 9.8 Torr with an oxygen pressure of 6.7 psi. The nitric oxide analyzer was calibrated for baseline using zero NO gas (baseline) and then with the calibration standard NO gas (46.6 ppm). To quantify the NO release, each disk was placed in 2 mL of PBS buffer with EDTA pH 7.4 in the NOA sample cell at 37 °C. Samples were tested in the NOA until the release reached the steady state using a nitrogen sweep gas [42]. The ppm/ppb of NO release levels measured by the NOA were normalized with the polymer volume of films (excluding any air spaces) to obtain the NO flux levels with units of mol cm^{-3} min^{-1}. Samples were incubated in PBS at 37 °C and the NO release from the samples was quantified at different time points during the 14 d of the experiment. Fresh PBS was replaced daily during the incubation of the samples to avoid the inundation of leached SNAP in the buffer.

4.3.8 Characterization of SNAP Leaching

The amount of SNAP leached from Disk-60, Disk-40, Solid, and Capped films was determined by a UV-vis spectrophotometer. The mass of films was recorded to normalize the SNAP leaching of each sample. Each sample was incubated in 10 mM PBS, pH 7.4, with 100 μM EDTA at 37 °C for 14 d. The amount of SNAP leached per mg of samples was determined by evaluating the amount of SNAP present in the soaking buffer over a 14-d period. The molar absorptivity of SNAP in 10 mM PBS, pH 7.4, with 100 μM EDTA at 37 °C was verified as 1072 M^{-1} cm^{-1} at 340 nm and was used to calculate the SNAP leaching. The soaking buffer was replenished with fresh buffer after each measurement and samples were continually incubated at 37 °C.

4.3.9 Evaluating the Antibacterial Efficacy of PCU-Sil with an *In Vitro* 24 h Bacterial Adhesion Assay

4.3.9.1 Preparation of Bacterial Suspension

All the protocols pertaining to the usage of bacterial strains were used in a Biosafety level (BSL-2) protocol following the university guidelines. The antibacterial activity of films was examined in terms of viable bacterial adhesion on the surface of the films using a 24 h bacterial adhesion assay. A single isolated colony of the bacterial strain *Staphylococcus aureus* (ATCC 6538) was inoculated in LB medium for 5 h at 120 rpm (revolutions per minute) at 37 °C in a shaking incubator. The optical density (OD) was measured at 600nm (OD_{600}) using a UV-vis spectrophotometer. All samples (Disk-60, Disk-40, Solid, and Capped; n ≥ 3 each) both NO-releasing and controls were first soaked in PBS for 5 h at 37 °C to remove any remaining surface SNAP crystals from NO-releasing films. Samples were cleaned with 70% ethanol and then sterilized with UV irradiation under a Biosafety Cabinet (BSC) for 15 min. Each film was exposed to the bacterial solution, with the final OD_{600} of bacteria ranging between 10^6 – 10^8 CFU mL^{-1}, 24 h at 120 rpm in the shaking incubator at 37 °C to maintain chronic infection conditions.

4.3.9.2 Quantitating the Viable Bacteria Adhered on NO-releasing 3D-PCU-Sil Films

After 24 h of bacterial exposure, samples were gently rinsed with PBS to eliminate any lightly attached bacterial cells. Films were then transferred to a fresh tube with sterile PBS and homogenized for 60 s using an OmniTip THb tissue homogenizer (Omni International, Inc.), and vortexed for 60 s to isolate the attached bacterial cells from the film into the PBS solution. The bacterial cells collected in the PBS buffer were serially diluted (10^{-1} to 10^{-4}) and 30 µL of bacterial culture was spread onto an LB agar plate using a sterile L-shape spreader. The plates were incubated overnight at 37 °C and viable colonies were enumerated to determine the antibacterial activity of the NO-releasing PCU-Sil films (C_{Test}) compared to the blank PCU-Sil films (C_{Blank}) using **Equation 4.2** and presented as CFU cm^{-2}.

$$\% \, Bacterial \, reduction = \frac{C_{Blank} - C_{Test}}{C_{Blank}} \times 100 \quad \textbf{(Equation 4.2)}$$

4.4. Statistical Analysis

All the experiments were performed with a sample size n ≥ 3. Data are all reported as mean ± standard error of the mean (SEM). Student's *t*-test was used to determine the statistical significance between SNAP-impregnated films and blank PCU-Sil films with an assumption of unequal variance. To demonstrate the significance of the results, $\alpha = 0.05$ was used for comparison between the test and control samples.

4.5 Results and Discussion

4.5.1 Characterization of SNAP Impregnation in 3D-PCU-Sil Films

The optimum soaking time to achieve maximum SNAP impregnation into 4 types of PCU-Sil films (Disk-60, Disk-40, Solid, and Capped) was verified by confirming the wt% of SNAP in the films by solvent impregnation method. Two important aspects were considered for this process: (1) optimal solvent ratio for solubility of SNAP in the solvent mix, and (2) maximum capacity to impregnate the SNAP in the PCU-Sil matrix without causing physical distortion to the structure of the films. The solvent mixture utilized in these studies consists of methyl ethyl ketone (MEK) to facilitate easier impregnation of SNAP and methanol (MeOH) to achieve greater SNAP solubility (MeOH) based on previously reported studies.[41]

The SNAP impregnation kinetics as a function of polymer structure was studied by first impregnating the film with SNAP, and then dissolving the films in DMAc to quantify the amount of SNAP impregnated via UV-vis. Further analysis of the SNAP-impregnation duration revealed an increased SNAP amount upon extending the duration of swelling from 0.5 to 2 h (**Figure 4.3**). The maximum amount of SNAP was seen at a 2 h timepoint. At the end of 2 h, Disk-60 and Disk-40 films had ca. 19.59 and 13.95 wt% SNAP loaded, respectively, and Solid and Capped films had ca. 8.76 and 11.90 wt% SNAP loaded, respectively. The higher amount of SNAP in the porous films (Disk-60 and Disk-40) is due to their porous structure.

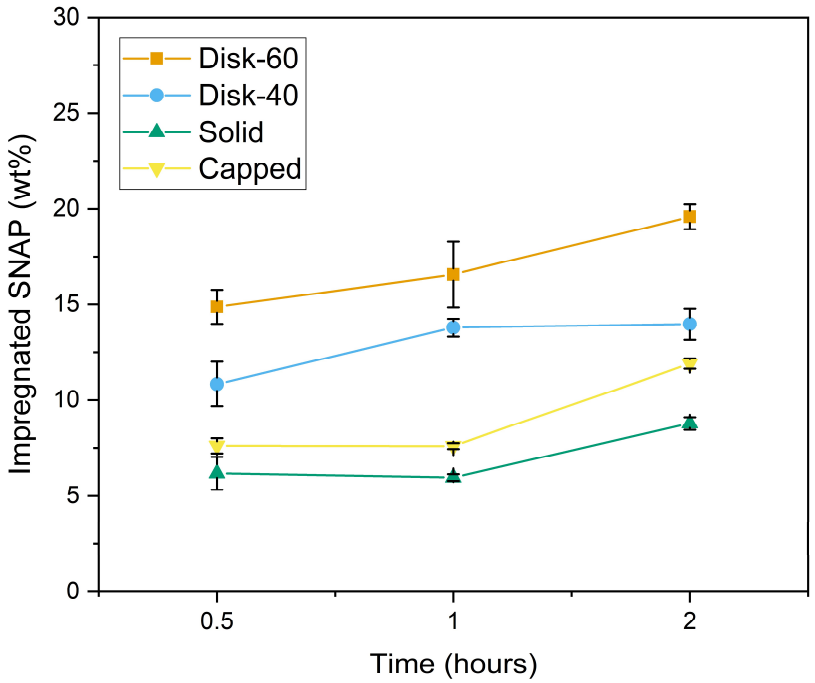

Figure 4.3 SNAP impregnated (wt%) in 3D-printed PCU-Sil films. Kinetics of SNAP impregnation in PCU-Sil films using 100 mg mL^{-1} SNAP in swelling solution (40% MEK and 60% MeOH), with respect to swelling time and different structures of films. The results indicate that maximum SNAP incorporation is achieved at 2 h of swelling in all types of films without significant changes.

Porous films have SNAP quantified from the residual SNAP crystals remaining in the pores of the polymer films in addition to the SNAP impregnated in the polymer matrix, contributing to higher overall SNAP content as characterized in the later sections. Moreover, porous films had a larger surface area exposed to MEK-MeOH solution thus facilitating higher SNAP loading. A swelling timepoint of 2 h was chosen for all the films due to the largest amount of SNAP loading without distortion to the structure of the films. It was important for the films to retain their shape after the SNAP impregnation process. Therefore, any further timepoint or different ratio of solvents were not selected due to the distortion of porous films at elevated time points.

The results obtained are consistent with previously reported SNAP-impregnated polyurethane CarboSil (2.5−15.7 wt% loaded with 5.5−120 mg mL^{-1} SNAP), that controlled the SNAP impregnation by altering the impregnation time in the solvent.[41] Previous studies have

verified up to 8 months of shelf-life stability of SNAP in post-fabricated elastomers and polyurethane medical devices with the solvent-impregnation process.[33, 41, 43, 44] Solvent-swelling-impregnation of SNAP provides an advantage over previous methods of casting the SNAP and polymer as a blend, especially in already fabricated devices. This process of impregnation will utilize solvents that can penetrate deep into the polymer matrix, thus allowing SNAP molecules to diffuse into the bulk polymer and crystallize to attain better stability in crystal form after solvent evaporation.

4.5.2 Scanning Electron Microscopy (SEM) and Energy-Dispersive X-ray Spectroscopy (EDS)

SEM and EDS were used to investigate the morphology and elemental composition of the films before and after SNAP impregnation (**Figure 4.4**). To detect SNAP, the presence of sulfur located in the S-NO bond of the SNAP molecules were mapped via EDS. All impregnated samples were observed to contain detectable sulfur content, whereas the pristine samples were Sulphur free, indicating a successful SNAP impregnation. The top surface of the Solid and Capped films were observed to be smooth with an even distribution of sulfur throughout, whereas crystal aggregates were observed on the surface the of porous films (Disk-60 and Disk-40). The transverse cross-section of the solid films exhibited a smooth surface as well, whereas the porous films showed crystal aggregates of about 5 μm in size and capped films showed larger, but fewer crystal aggregates of about 25 μm in size. This can perhaps be attributed to the slower solvent evaporation that results in relatively larger SNAP crystals in the capped films as compared to porous and solid films. Past studies have shown that above a solubility limit, SNAP crystals start to form in the polymer matrix beyond its solubility limit in the polymer.[45] This correlates with data shown in (Figure 3), where the porous films were found to be of higher SNAP wt% compared to the capped and solid films.[46]

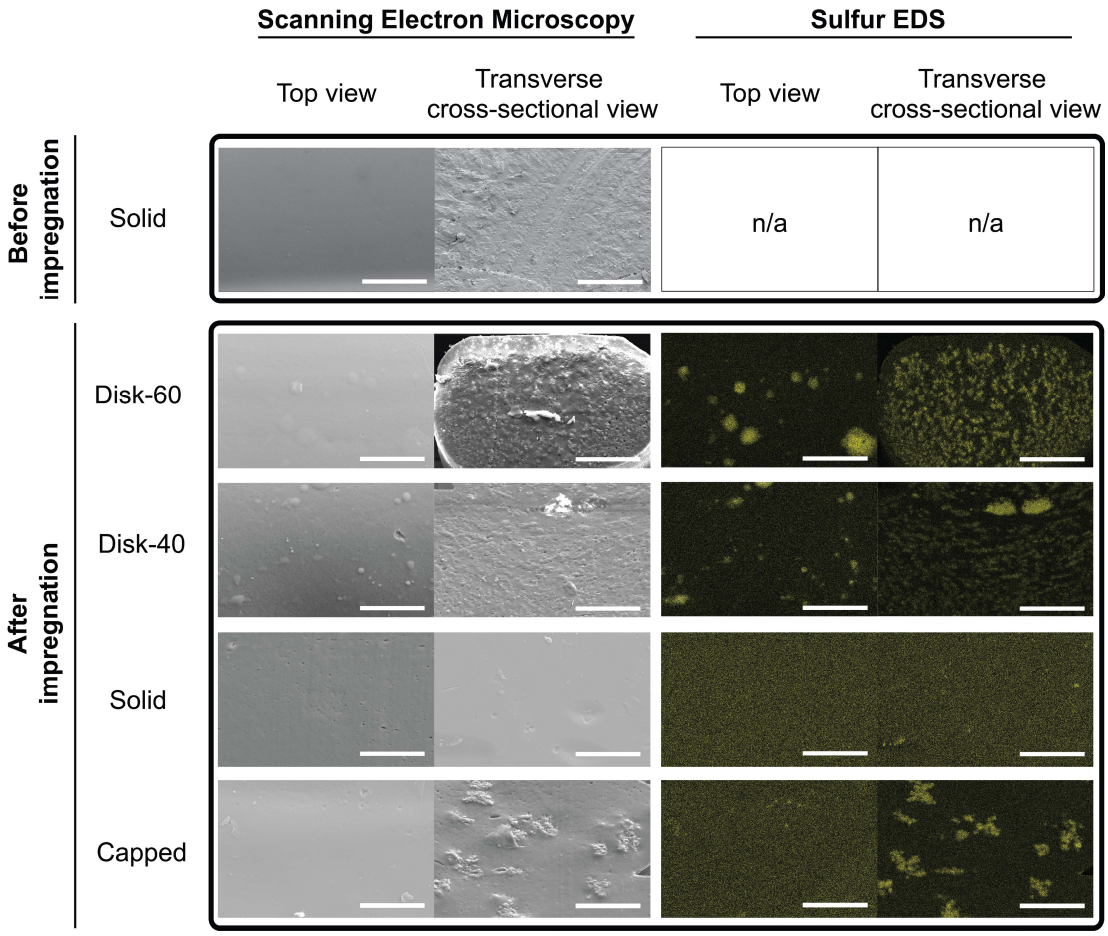

Figure 4.4 SEM and EDS analysis of PCU-Sil films before and after SNAP impregnation. Scale bar represents 100 μm. SNAP was identified by the presence of sulfur (S) located in the S−NO bond.

4.5.3 Micro-CT image of 3D-printed PCU-Sil Films

Micro-CT images were acquired to ascertain dimensional changes caused by the impregnation process. Images of the films before and after impregnation are shown in (**Figure 4.5**). The films were found to be composed of circular struts with a 330 μm diameter forming a crosshatch pattern. The originally designed porosities for printing and the final true porosities are listed in (**Table 4.2**). The true porosities of both porous films were measured to be 51.68% for Disk-60 and 23.67% for Disk-40. Capped disks were found to possess a true porosity of 11.72%

and solid disks were found to be slightly porous with a true porosity of 1.65%. After the impregnation process, slight deformations of the struts are observed for the more porous films.

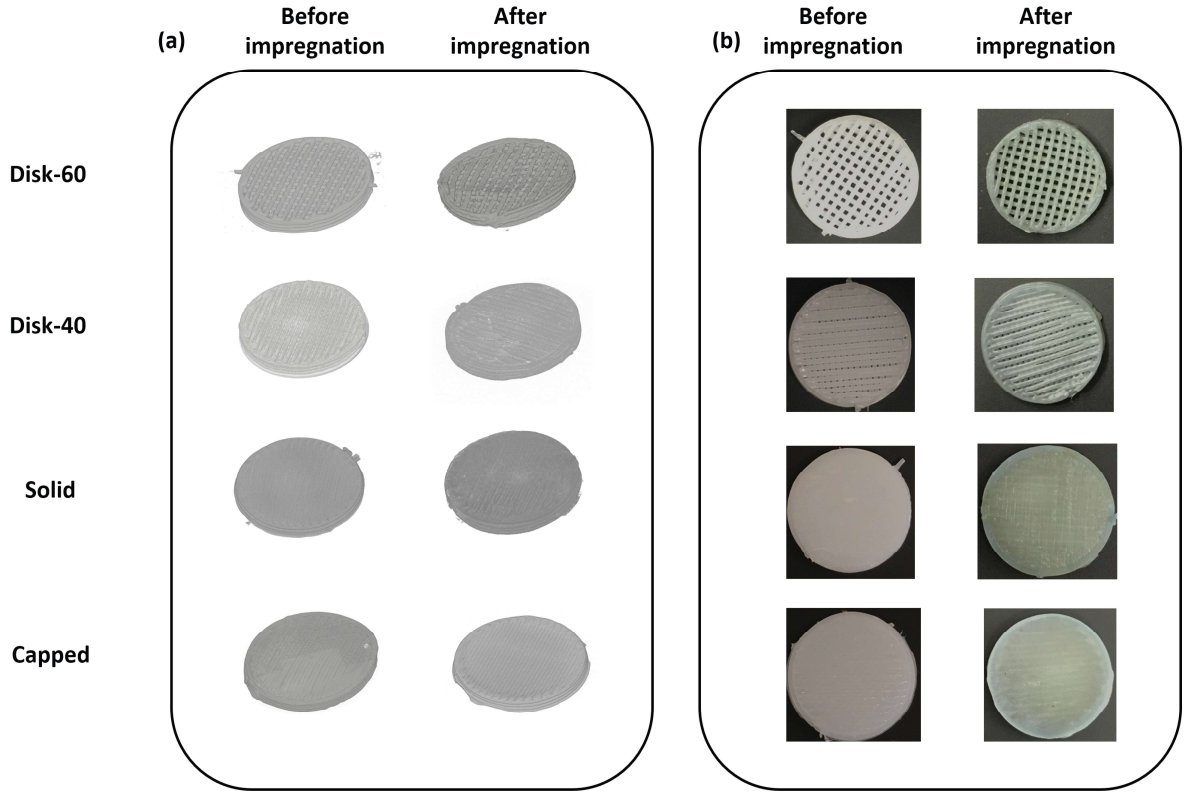

Figure 4.5 (a) Rendering of CT images of 3D-printed PCU-Sil films before (left) and after (right) SNAP impregnation. (b) Optical images of 3D-printed PCU-Sil films before (left) and after (right) SNAP impregnation.

Table 4.2 Original designed porosities and true porosities of PCU-Sil films.

	Film Porosity	
	Designed porosity	**True porosity**
Disk-60	60%	51.69%
Disk-40	40%	23.67%
Solid	0%	1.65%
Capped	0% top and bottom, 40% in centre	11.72%

4.5.4 Quantification of NO Release

The NO release was measured from the Disk-60, Disk-40, Solid, and Capped films under physiological conditions using the chemiluminescence method (**Figure 4.6a**). The initial and final release from the samples recorded on day 0 and day 14 are reported in (**Table 4.3**). All the samples exhibited higher release at the initial time points which can be attributed to the presence of SNAP on the water-contacting surfaces and in the water-rich region of the polymer matrix which can more quickly solubilize and release its NO payload. After exhaustion of the SNAP reservoir in the outmost layer, the NO release rate gradually drops over the duration of the 14-d experiment. On day 14, > 85% of the SNAP in the bulk of the polymer is decomposed in Disk-60 and Disk-40 films. As studied in SEM studies and also reported previously, the majority of the SNAP molecules impregnated in the PCU-Sil films are in their crystallized form and it takes time for the crystalline SNAP impregnated in the bulk of the polymer matrix to solubilize and release its NO.[45] The gradual dissolution of the crystalline SNAP leads to the long-lasting release of NO from the 3D-printed PCU-Sil films.

Table 4.3 The NO release levels obtained on Day 0 and Day 14 of the study from 3D-printed PCU-Sil films. Data represents mean ± standard error of mean, n≥3.

Film Type	**NO Flux (x 10^{-10} mol min^{-1} cm^{-3})**	
	Day 0	**Day 14**
Disk-60	4.095 ± 0.305	0.107 ± 0.024
Disk-40	4.331 ± 0.013	0.198 ± 0.080
Solid	3.625 ± 0.482	0.005 ± 0.002
Capped	2.634 ± 0.242	0.022 ± 0.004

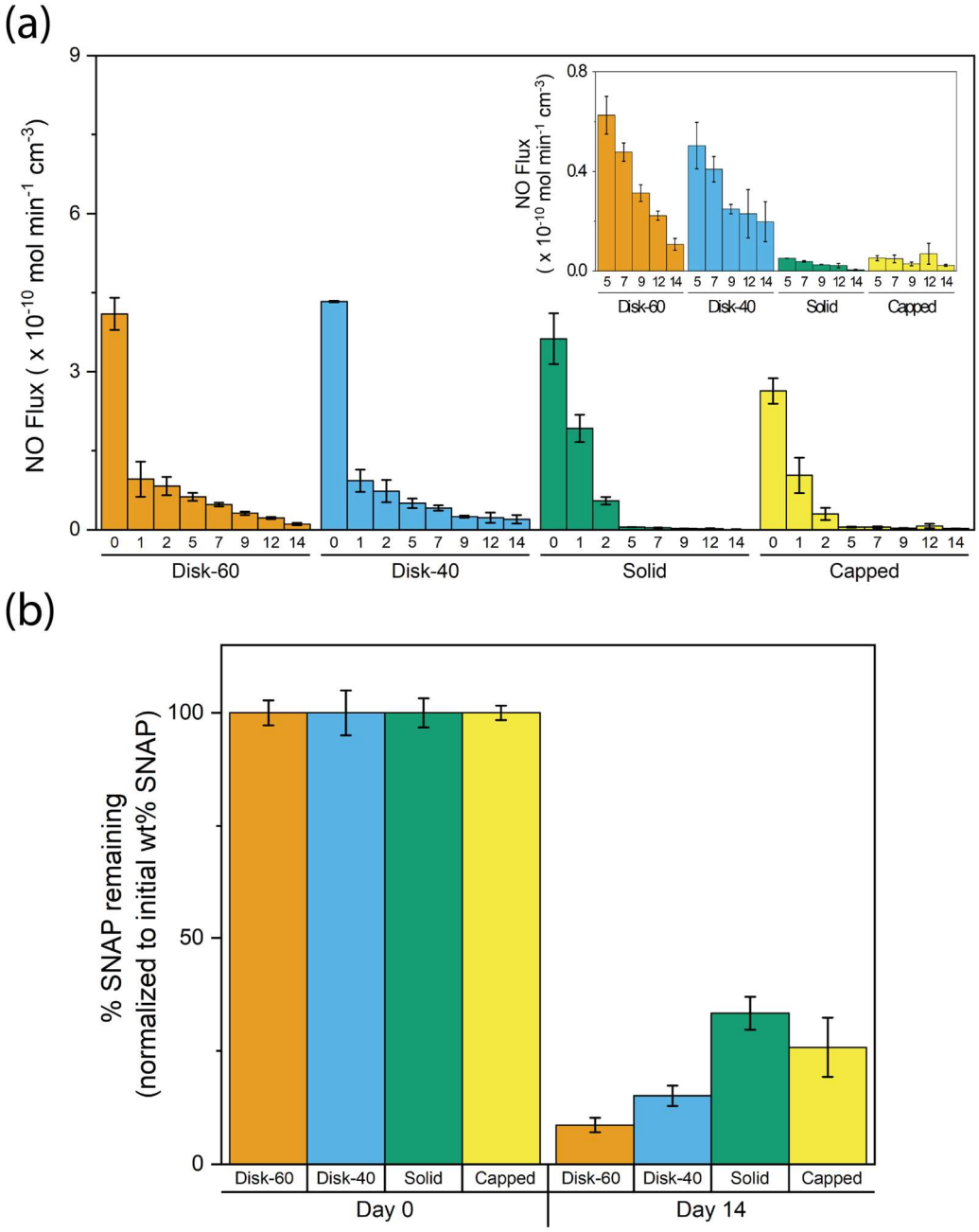

Figure 4.6 (a) Measurement of real-time NO release using a Chemiluminescence Nitric Oxide Analyzer. The NO flux levels were measured at physiological conditions in PBS with 100 μM EDTA for 14 d. Data represents mean ± standard error of mean, n≥3. (b) The wt% SNAP remaining in the films after 14 d of incubation at 37 °C is determined and normalized with the initial level of SNAP loading. Data are represented as mean ± standard error of mean (n = 3).

Nitric oxide release kinetics demonstrated porous samples with continued NO release at a relatively longer duration and higher levels than solid and capped films. The difference in the

levels of NO release between the sample types can be attributed to the variance in the amount of SNAP impregnated into the polymer and could also be likely due to the structure of the films that restricts the penetration of water to the deep-embedded SNAP into the polymer matrix. This information is supported by the wt% of SNAP determined in the samples in UV-vis studies which demonstrated a lower wt% of SNAP present in solid and capped samples as opposed to the porous samples (**Figure 4.3**). Although the NO release levels began to decrease by day 14, the films still appeared slightly green indicating the presence of SNAP crystals impregnated in the polymer. To confirm this, the films were dissolved in DMAc at the end of day 14 to analyze the wt% of SNAP remaining in the films compared to the wt% SNAP obtained in freshly impregnated samples (**Figure 4.6b**). It was found at the end of day 14, Disk-60 and Disk-40 had 8.66% and 15.11% SNAP remaining, respectively. On the contrary, Solid and Capped samples had 33.35% and 25.83% SNAP still present in the films, respectively. While there was a significant amount of SNAP present in these types of films, the NO release from these films was observed to be at the lowest level. The closed design and low water-contacting surface area of the films limit the rate of crystallized SNAP to dissolve and release NO. On the other hand, porous samples have a higher water-contacting surface area, which helps maintain higher NO levels on days 5-14 which leads to more complete depletion of the SNAP reservoir in the material. Wo et al. have shown the ability of CarboSil films impregnated with SNAP to release NO at physiological levels for 14 d.[41] The difference in the wt% SNAP impregnated and NO release can be due to the polymer source, the thickness of the films, varying percentage of silicone in the polymer structure, and the difference of water-contacting polymer surface area exposed to buffer (in this case increased porosity).[41, 46] Moreover, these films had an extra layer of topcoat that prevented the leaching of SNAP and helped in prolonging the NO release for a longer duration of time. However, the process of topcoat is not a viable option for all the 3D-printed PCU-Sil films reported here due to the presence of porous structures. The longevity of the NO release can be modulated by altering the film thickness, structure of the films, and SNAP concentration in the impregnating solution.

4.5.5 SNAP Leaching

A SNAP leaching study was performed to determine the ability of PCU-Sil films to retain a significant amount of SNAP in them after soaking in PBS. High-level SNAP preservation in the polymer is ideal since it translates to prolong NO release from the polymer system and reduction of possible risks (if any) linked to SNAP leaching. After 24 h, 21.82 ± 0.59, 25.35 ± 2.80, 5.10 ± 0.45, and 5.30 ± 0.76 μg/mg of SNAP leached from Disk-60, Disk-40, Solid and Capped films, respectively (**Figure 4.7**).

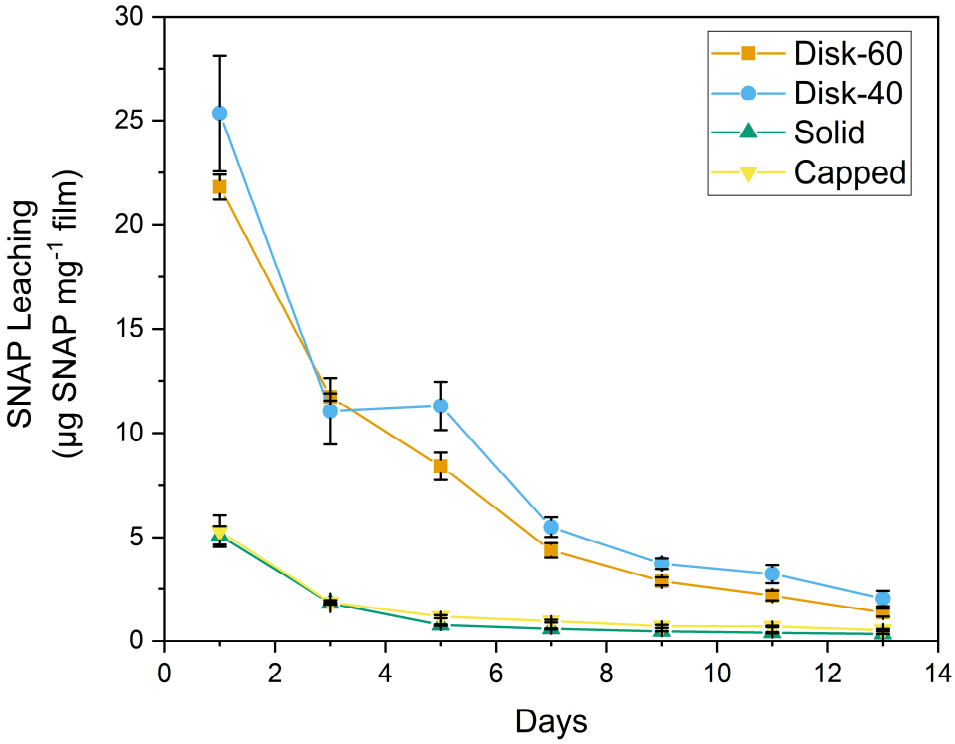

Figure 4.7 Quantitation of amount of SNAP leached into 2 mL of PBS (soaking buffer) from 3D-printed SNAP-impregnated PCU-Sil films over a period of 14 days, at 37 °C in the dark. Data represented as mean ± standard error of mean (n = 3).

Of all the four types of films tested, Disk-60 and Disk-40 porous samples had the highest amount of SNAP leaching. Solid and Capped samples were observed to have similar amounts of leaching throughout the duration of the experiment. Due to the residual surface crystals and larger water-contacting polymer surface area exposed to the test solution, the rate of SNAP leaching is higher in the porous films for the first few days, and then significantly lower amounts

of SNAP continue to diffuse into the PBS over sequential days. With this initial high rate of leaching from the polymer, it was expected that the samples would leach a significant amount of SNAP within 24 h. The results indicated that at the end of 14 days a cumulative total of ~ 18%, 35%, 22%, and 19% of the initial SNAP diffuses out of the Disk-60, Disk-40, Solid and Capped films into the incubation buffer, respectively. While the largest amount of leaching was at 24 h timepoint, prolonged incubation of the films showed a diminishing amount of SNAP leaching with each successive day.

This characteristic of a hydrophobic polymer such as PCU-Sil makes it suitable for integrating with NO donors to sustain a regulated release of NO for an extended period. Quantifying the levels of SNAP leaching is critical to understanding the antimicrobial effects observed as SNAP possesses the capability to release its antimicrobial payload, which its degradation products of NAP and NAP disulfide do not. Prior literature has quantified the leaching of SNAP, NAP, and NAP dimers from a similar silicone-based polyurethane, CarboSil via mass spectrometry.[41] At the end of 2- a week period, a total of ca. 12% SNAP, ca. 2% NAP, and ca. 14% NAP disulfide were measured in the buffer.[41] Leaching of SNAP, or its parent molecule NAP and its dimers, eventually leave penicillamine as a degraded product. Penicillamine is an FDA-approved drug and is broadly employed for treating heavy metal poising in humans, as per the FDA recommendation.[47-50] Thus, NAP and NAP disulfide leaching from the SNAP films into the soaking buffer or physiological environment are deemed safe at these levels and unlikely to instigate any sort of adverse consequence in potential clinical applications.

4.5.6 Antibacterial Activity of NO-releasing PCU-Sil Films

There is an urgent need for efficacious and harmless approaches that can not only handle the emergence but also the propagation of pathogenic microorganisms. Due to the antibacterial properties of NO, the active release of NO from the donor molecule incorporated in the hydrophobic polymer films can reduce the chances of biomedical device-related infections or

hospital-associated infections. NO as a free gas radical offers bactericidal properties by means of DNA deamination and membranal damage via lipid peroxidation and denaturation of enzymes in bacterial cells.[51] In order to evaluate the antimicrobial properties, the 3D printed PCU-Sil films were exposed to *S. aureus*, for 24 h followed by quantitating the viable bacterial cells adhered onto the films' surface to obtain viable CFU cm^{-2} (**Figure 4.8**).

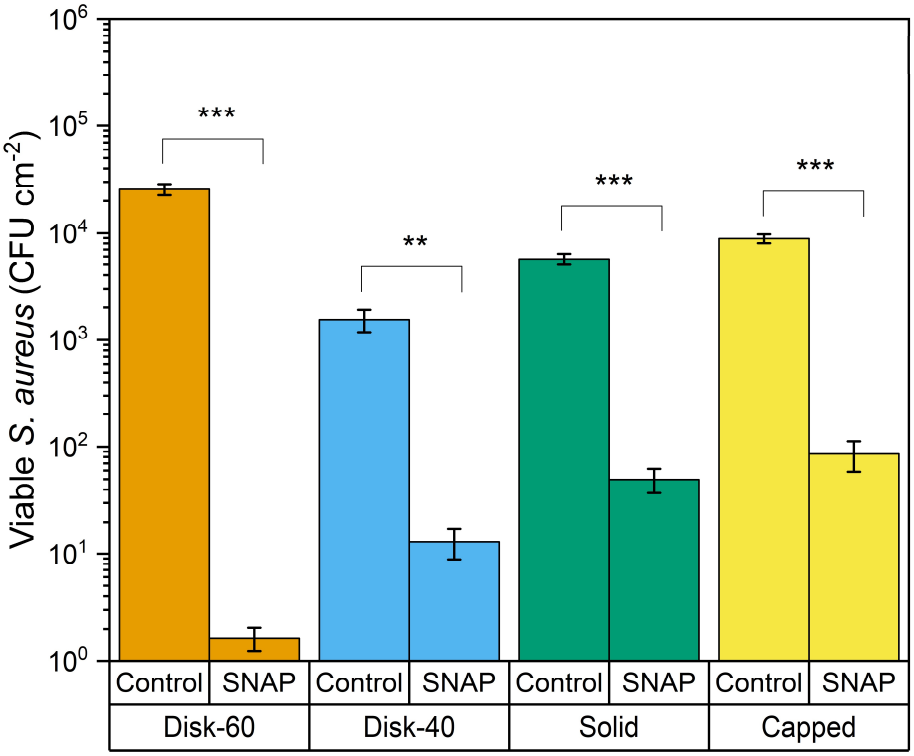

Figure 4.8 Antibacterial activity of SNAP impregnated 3D-printed PCU-Sil films calculated as a log of the colony forming unit (CFU) cm^{-2} of surface area against *Staphylococcus aureus;* data represents mean ± standard error of mean (n≥3, ** = p ≤ 0.01, *** = p ≤ 0.001, calculated for SNAP impregnated PCU-Sil films against individual blank PCU-Sil control films.

S. aureus adhesion on the Disk-60 exhibited a ca. 99.99% reduction compared to the blank control ($p \leq 0.001$), while the Disk-40 exhibited a ca. 99.16% reduction ($p \leq 0.01$). The solid and capped were observed to have ca. 99.13% and 99.04% reduction of viable adhered cells, respectively ($p \leq 0.001$). The results obtained from the bacterial adhesion test correlate with the higher amount of SNAP impregnated (**Figure 4.3**), higher SNAP leaching levels (**Figure 4.7**), and higher NO release profiles (**Figure 4.6a**) for the porous Disk-60 and Disk-40 films as compared

to the Solid and Capped samples. This helps explain the difference in the biocidal activity of each sample type, where the killing efficiency is proportional to the SNAP impregnation and leaching, and NO release levels determined by the UV-vis and NOA studies. Overall, all 4 types of porous and non-porous films with NO-releasing properties exhibited statistically fewer bacteria than controls (> 99% reduction). The difference in the bacteria on the surface of control films is due to the variance in the design of struts of polymer structure and the slight variance in the starting concentration of bacteria (10^6 – 10^8 CFU mL^{-1}). These results are analogous to previous reports that characterized polyurethane CarboSil, with equivalent levels of NO over a 24 h period [46]. The ability to design and 3D-print the PCU-Sil films with the bactericidal activity of NO demonstrated an enhanced antimicrobial action leading to the most significant reduction of viable bacteria on the films.

PCU-Sil polymers are an attractive choice for developing medical devices due to the benefits of polycarbonate-based urethanes, including high-pressure resistance, and tensile strength combined with silicone's biostability and superior elongation. Until now PCU-Sil-based polymers such as CarboSil, ChronoSil, etc. have been used in implants/devices fabricated through traditional polymer processing methods. Unlike thermoplastic aliphatic polyesters such as Poly Lactic Acid (PLA), NO-releasing PCU-Sil can inhibit bacterial adhesion without being susceptible to degradation *in vivo*. Design and fabrication of user bioimplants with tuned internal and external porosity are possible with 3D-printing technology. For this reason, Kabirian et. al has recently reported SNAP-coated 3D-printed vascular grafts made from polylactic acid (PLA) with a polycaprolactone topcoat.[52, 53] The PLA composites are, however, degradable which can alter their physicochemical traits and their performance *in vivo* (NO release profile, interface with neighboring tissues, etc.) and require an application where degradation is desired. In addition, the lower fracture resistance can restrict their usage for catheter-like applications.[54] Nitric oxide can effectively inhibit platelet activation and aggregation at the blood-biomaterial interface.[41, 55-57] It is well-understood that the characteristic hemocompatibility of the polymer that contacts blood

can greatly influence its ultimate efficacy in preventing thrombus formation. ChronoSil, belongs to a family of polycarbonate-based silicone elastomers very similar to the Elast-eon E2As and CarboSil. Incorporation of RSNOs and NO release from these polymers in non-printed form have been previously reported to reduce the platelet activation and thrombus formation in an *in vivo* rabbit model.[41, 58]

In the current study, we demonstrate a proof-of-concept for combining additively manufactured surfaces with NO-releasing chemistry. The 3D-printing method has the advantage over typical polymer device fabrication methods (e.g., high-temperature extrusion) due to its cost-effectiveness, fast processing time, and capacity to customize geometries with high accuracy. This study demonstrates the ability to fabricate 3D-printed PCU-Sil-based polymers and incorporate NO donor chemistry, resulting in materials with potent antimicrobial properties. The 3D printing fabrication enabled a study comparing the tunability of NO release properties to various material geometries. Integrating the benefits of additive manufacturing with the SNAP impregnation method opens an array of opportunities to further customize and optimize NO-release polymers for a wider range of medical devices and scaffold applications. The results of this study present a promising biomaterial specifically designed to integrate properties of both additive manufacturing and NO release to achieve localized NO at polymer interfaces to overcome both acute and chronic biocompatibility and microbial challenges associated with indwelling medical devices. Further evaluation using *in vivo* models for long-term clinical application is underway.

4.6 Conclusions

Polycarbonate-based silicone elastomer (PCU-Sil) polymers are well-characterized as biocompatible and biostable. This work illustrates the ability to 3D-print custom-designed scaffolds made of PCU-Sil and impregnate them with a NO donor for potentially preventing device-related infections. Generation of NO from these 3D-printed medical devices can be

extremely powerful in thwarting the biofilm establishment and thrombus formation on a device surface. In this study, four different 3D-printed PCU-Sil film structures (Disk-60, Disk-40, Solid, and Capped) were impregnated with the NO donor SNAP and tested for their NO-releasing properties. Scanning electron microscopy accompanied by an energy-dispersive X-ray spectroscopy system revealed an even distribution of SNAP in the polymer composite, demonstrating the presence of SNAP embedded within the polymer. The studies showed tunable properties of NO release from the four types of films with minimal amounts of leaching. Owing to their designs, films with more porosity (Disk-60 and Disk-40) were capable of enhanced storage of SNAP in the polymer matrix and releasing NO for a longer duration as compared to Solid and Capped designs. All the NO-releasing PCU-Sil films exhibited substantial efficacy in reducing microbial adhesion on the films after 24 h of exposure to *S. aureus* (>99% reduction) as compared to blank PCU-Sil films. The antibacterial activity of SNAP-doped PCU-Sil films is expected to reduce the incidences of infections occurring from medical devices in a hospital-based setting. This method holds the potential to impart enhanced biocompatibility and antimicrobial properties to 3-D printed biomedical surfaces and devices to improve their efficacy in the patient care setting.

4.7 References

1. Ngo, T. D.; Kashani, A.; Imbalzano, G.; Nguyen, K. T.; Hui, D., Additive Manufacturing (3D Printing): A Review Of Materials, Methods, Applications And Challenges. *Composites, Part B* **2018,** *143*, 172-196.

2. Miller, A. T.; Safranski, D. L.; Wood, C.; Guldberg, R. E.; Gall, K., Deformation And Fatigue Of Tough 3D Printed Elastomer Scaffolds Processed By Fused Deposition Modeling And Continuous Liquid Interface Production. *J. Mech. Behav. Biomed. Mater.* **2017,** *75*, 1-13.

3. Maniruzzaman, M., *3D And 4D Printing In Biomedical Applications: Process Engineering And Additive Manufacturing*. John Wiley & Sons: 2019.

4. Giannatsis, J.; Dedoussis, V., Additive Fabrication Technologies Applied To Medicine And Health Care: A Review. *J. Adv Manu.Technol.* **2009,** *40* (1-2), 116-127.

5. Jamróz, W.; Szafraniec, J.; Kurek, M.; Jachowicz, R., 3D Printing In Pharmaceutical And Medical Applications–Recent Achievements And Challenges. *Pharm. Res.* **2018,** *35* (9), 176.

6. Trivedi, M.; Jee, J.; Silva, S.; Blomgren, C.; Pontinha, V. M.; Dixon, D. L.; Van Tassel, B.; Bortner, M. J.; Williams, C.; Gilmer, E., Additive Manufacturing Of Pharmaceuticals For Precision Medicine Applications: A Review Of The Promises And Perils In Implementation. *Addit Manuf.* **2018,** *23*, 319-328.

7. Bernards, D. A.; Desai, T. A., Nanoscale Porosity In Polymer Films: Fabrication And Therapeutic Applications. *Soft Matter* **2010,** *6* (8), 1621-1631.

8. Tappa, K.; Jammalamadaka, U., Novel Biomaterials Used In Medical 3D Printing Techniques. *J. Funct. Biomater.* **2018,** *9* (1), 17.

9. Aimar, A.; Palermo, A.; Innocenti, B., The Role Of 3D Printing In Medical Applications: A State Of The Art. *J. Healthcare Eng.,* **2019,** *2019*.

10. Klevens, R. M.; Jonathan, R. E.; Chesley, L. R., Jr.; Teresa, C. H.; Robert, P. G.; Daniel, A. P.; Denise, M. C., Estimating Health Care-Associated Infections and Deaths in U.S. Hospitals, 2002. *Public Health Rep. (122)* **2007,** (2), 160-166.

11. Weiner, L. M.; Webb, A. K.; Limbago, B.; Dudeck, M. A.; Patel, J.; Kallen, A. J.; Edwards, J. R.; Sievert, D. M., Antimicrobial-Resistant Pathogens Associated With Healthcare-Associated Infections: Summary of Data Reported to the National Healthcare Safety Network at the Centers for Disease Control and Prevention, 2011–2014. *Infect. Control Hosp. Epidemiol.* **2016,** *37* (11), 1288-1301.

12. Mermel, L. A., Short-Term Peripheral Venous Catheter–Related Bloodstream Infections: A Systematic Review. *Clin. Infect. Dis,* **2017,** *65* (10), 1757-1762.

13. Boev, C.; Kiss, E., Hospital-Acquired Infections: Current Trends And Prevention. *Crit. Care Clin.* **2017,** *29* (1), 51-65.

14. Khatoon, Z.; McTiernan, C. D.; Suuronen, E. J.; Mah, T. F.; Alarcon, E. I., Bacterial Biofilm Formation On Implantable Devices And Approaches To Its Treatment And Prevention. *Heliyon* **2018,** *4* (12), e01067.

15. Oliveira, W.; Silva, P.; Silva, R.; Silva, G.; Machado, G.; Coelho, L.; Correia, M., Staphylococcus Aureus And Staphylococcus Epidermidis Infections On Implants. *J. Hosp. Infect.* **2018,** *98* (2), 111-117.

16. O'Gara, J. P., Ica And Beyond: Biofilm Mechanisms And Regulation In Staphylococcus Epidermidis And Staphylococcus Aureus. *FEMS Microbiol. Lett.,* **2007,** *270* (2), 179-188.

17. O'GARA, J. P.; Humphreys, H., Staphylococcus epidermidis biofilms: importance and implications. *J. Med. Microbiol.* **2001,** *50* (7), 582-587.

18. Chug, M. K.; Feit, C.; Brisbois, E. J., Increasing the Lifetime of Insulin Cannula with Antifouling and Nitric Oxide Releasing Properties. *ACS Appl. Bio Mater.,* **2019**, 5965-5975.

19. Schierholz, J.; Lucas, L.; Rump, A.; Pulverer, G., Efficacy Of Silver-Coated Medical Devices. *J. Hosp. Infect.* **1998,** *40* (4), 257-262.

20. Shahverdi, A. R.; Fakhimi, A.; Shahverdi, H. R.; Minaian, S., Synthesis And Effect Of Silver Nanoparticles On The Antibacterial Activity Of Different Antibiotics Against Staphylococcus Aureus And Escherichia Coli. *Nanomedicine,* **2007,** *3* (2), 168-171.

21. Donlan, R. M., Biofilms: Microbial Life On Surfaces. *Emerging Infect. Dis.* **2002,** *8* (9), 881.

22. Lansdown, A.; Williams, A., Bacterial Resistance To Silver-Based Antibiotics. *Nursing Times* **2007,** *103* (9), 48-49.

23. Schairer, D. O.; Chouake, J. S.; Nosanchuk, J. D.; Friedman, A. J., The Potential of Nitric Oxide Releasing Therapies as Antimicrobial Agents. *Virulence* **2012,** *3* (3), 271-279.

24. Hibbs Jr, J.; Taintor, R.; Vavrin, Z., Macrophage Cytotoxicity: Role For L-Arginine Deiminase And Imino Nitrogen Oxidation To Nitrite, *Science*, 1987, **235** , 473 —476

25. Weinberg, J.; Misukonis, M.; Shami, P.; Mason, S.; Sauls, D.; Dittman, W.; Wood, E.; Smith, G.; McDonald, B.; Bachus, K., Human Mononuclear Phagocyte Inducible Nitric Oxide Synthase (Inos): Analysis Of Inos Mrna, Inos Protein, Biopterin, And Nitric Oxide Production By Blood Monocytes And Peritoneal Macrophages. *Blood* **1995,** *86* (3), 1184-1195.

26. Vaughn, M. W.; Kuo, L.; Liao, J. C., Estimation of Nitric Oxide Production and Reactionrates in Tissue by Use of a Mathematical Model. *Am. J. Physiol. Heart Circ. Physiol.* **1998,** *274* (6), H2163-H2176.

27. Yang, L.; Feura, E. S.; Ahonen, M. J. R.; Schoenfisch, M. H., Nitric Oxide–Releasing Macromolecular Scaffolds For Antibacterial Applications. *Adv. Healthcare Mater.,* **2018,** *7* (13), 1800155.

28. Carpenter, A. W.; Schoenfisch, M. H., Nitric Oxide Release: Part II. Therapeutic Applications. *Chem. Soc. Rev.* **2012,** *41* (10), 3742-3752.

29. Hopkins, S. P.; Pant, J.; Goudie, M. J.; Schmiedt, C.; Handa, H., Achieving Long-term Biocompatible Silicone via Covalently Immobilized S-nitroso-N-acetylpenicillamine (SNAP) that Exhibits 4 Months of Sustained Nitric Oxide Release. *ACS Appl. Mater. Interfaces* **2018**, 10 (32), pp. 27316-27325.

30. Xu, L.-C.; Wo, Y.; Meyerhoff, M. E.; Siedlecki, C. A., Inhibition of Bacterial Adhesion and Biofilm Formation by Dual Functional Textured and Nitric Oxide Releasing Surfaces. *Acta Biomater.* **2017,** *51*, 53-65.

31. Sundaram, J.; Pant, J.; Goudie, M. J.; Mani, S.; Handa, H., Antimicrobial and Physicochemical Characterization of Biodegradable, Nitric Oxide-Releasing Nanocellulose–Chitosan Packaging Membranes. *J. Agric. Food Chem.,* **2016,** *64* (25), 5260-5266.

32. Feit, C.; Chug, M. K.; Brisbois, E. J., Development of S-Nitroso-N-Acetylpenicillamine (SNAP) Impregnated Medical Grade Polyvinyl Chloride for Antimicrobial Medical Device Interfaces. *ACS Appl. Bio Mater.,* **2019***,* 2(10) , 4335-4345.

33. Goudie, M. J.; Brisbois, E. J.; Pant, J.; Thompson, A.; Potkay, J. A.; Handa, H., Characterization of an S-nitroso-N-acetylpenicillamine–Based Nitric Oxide Releasing Polymer from a Translational Perspective. *Int. J. Polym. Mater. Polym. Biomater.* **2016,** *65* (15), 769-778.

34. Xue, C.; Song, X.; Liu, M.; Ai, F.; Liu, M.; Shang, Q.; Shi, X.; Li, F.; He, X.; Xie, L., A Highly Efficient, Low-Toxic, Wide-Spectrum Antibacterial Coating Designed For 3D Printed Implants With Tailorable Release Properties. *J. Mater. Chem. B* **2017,** *5* (22), 4128-4136.

35. González-Henríquez, C. M.; Sarabia-Vallejos, M. A.; Rodríguez Hernandez, J., Antimicrobial Polymers For Additive Manufacturing. *Int. J. Mol. Sci.* **2019,** *20* (5), 1210.

36. Dincer, S.; Uslu, F. M.; Delik, A., *Bacterial Biofilms*, IntechOpen: 2020.

37. de Lima, R.; Seabra, A. B.; Durán, N., Silver Nanoparticles: A Brief Review of Cytotoxicity and Genotoxicity of Chemically and Biogenically Synthesized Nanoparticles. *J. Appl. Toxicol.,* **2012,** *32* (11), 867-879.

38. Barraud, N.; J Kelso, M.; A Rice, S.; Kjelleberg, S., Nitric Oxide: A Key Mediator of Biofilm Dispersal with Applications in Infectious Diseases. *Curr. Pharm. Des.* **2015,** *21* (1), 31-42.

39. Privett, B. J.; Deupree, S. M.; Backlund, C. J.; Rao, K. S.; Johnson, C. B.; Coneski, P. N.; Schoenfisch, M. H., Synergy Of Nitric Oxide And Silver Sulfadiazine Against Gram-Negative, Gram-Positive, And Antibiotic-Resistant Pathogens. *Mol. Pharmaceutics.* **2010,** *7* (6), 2289-2296.

40. Chipinda, I.; Simoyi, R. H., Formation and Stability of a Nitric Oxide Donor: S-nitroso-N-acetylpenicillamine. *J. Phys. Chem. B* **2006,** *110* (10), 5052-5061.

41. Wo, Y.; Brisbois, E. J.; Wu, J.; Li, Z.; Major, T. C.; Mohammed, A.; Wang, X.; Colletta, A.; Bull, J. L.; Matzger, A. J.; Xi, C.; Bartlett, R. H.; Meyerhoff, M. E., Reduction of Thrombosis and Bacterial Infection via Controlled Nitric Oxide (NO) Release from S-nitroso-N-acetylpenicillamine (SNAP) Impregnated CarboSil Intravascular Catheters. *ACS Biomater. Sci. Eng.* **2017,** *3* (3), 349-359.

42. Coneski, P. N.; Schoenfisch, M. H., Nitric Oxide Release: Part III. Measurement and Reporting. *Chem. Soc. Rev.* **2012,** *41* (10), 3753-3758.

43. Brisbois, E. J.; Handa, H.; Major, T. C.; Bartlett, R. H.; Meyerhoff, M. E., Long-term nitric oxide release and elevated temperature stability with S-nitroso-N-acetylpenicillamine (SNAP)-doped Elast-eon E2As polymer. *Biomaterials* **2013,** *34* (28), 6957-6966.

44. Colletta, A.; Wu, J.; Wo, Y.; Kappler, M.; Chen, H.; Xi, C.; Meyerhoff, M. E., S-Nitroso-N-acetylpenicillamine (SNAP) Impregnated Silicone Foley Catheters: A Potential Biomaterial/Device to Prevent Catheter-Associated Urinary Tract Infections. *ACS Biomater. Sci. Eng.* **2015,** *1* (6), 416-424.

45. Wo, Y.; Li, Z.; Colletta, A.; Wu, J.; Xi, C.; Matzger, A. J.; Brisbois, E. J.; Bartlett, R. H.; Meyerhoff, M. E., Study of Crystal Formation and Nitric Oxide (NO) Release Mechanism from S-nitroso-N-acetylpenicillamine (SNAP)-doped CarboSil Polymer Composites for Potential Antimicrobial Applications. *Composites, Part B* **2017,** *121*, 23-33.

46. Wo, Y.; Li, Z.; Brisbois, E. J.; Colletta, A.; Wu, J.; Major, T. C.; Xi, C.; Bartlett, R. H.; Matzger, A. J.; Meyerhoff, M. E., Origin of Long-Term Storage Stability and Nitric Oxide Release Behavior of CarboSil Polymer Doped with S-nitroso-N-acetyl-D-penicillamine. *ACS Appl. Mater. Interfaces* **2015,** *7* (40), 22218-22227.

47. Parameshvara, V., Mercury Poisoning and its Treatment with N-acetyl-D, L-penicillamine. *Occup. Environ. Med.* **1967,** *24* (1), 73-76.

48. Agocs, M.; Clarkson, T., Mercury Toxicity. *Am. Fam Physician* **1992,** *46* (6), 1731– 1744.

49. Kark, R. P.; Poskanzer, D. C.; Bullock, J. D.; Boylen, G., Mercury Poisoning and its Treatment with N-acetyl-D, L-penicillamine. *N. Engl. J. Med.* **1971,** *285* (1), 10-16.

50. Jones, M.; Weaver, A.; Weller, W., The Relative Effectiveness Of Some Chelating Agents As Antidotes In Acute Cadmium Poisoning. *Res. Commun. Chem. Pathol. Pharmacol.,* **1978,** *22* (3), 581-588.

51. Fang, F. C., Antimicrobial Reactive Oxygen And Nitrogen Species: Concepts And Controversies. *Nat. Rev. Microbiol.,* **2004,** *2* (10), 820.

52. Kabirian, F.; Brouki Milan, P.; Zamanian, A.; Heying, R.; Mozafari, M., Additively Manufactured Small-Diameter Vascular Grafts With Improved Tissue Healing Using A Novel SNAP Impregnation Method. *J. Biomed. Mater. Res. B* **2019,** 108, 1322-1331.

53. Kabirian, F.; Brouki, P.; Zamanian, A.; Heying, R.; Mozafari, M., Nitric Oxide-Releasing Vascular Grafts: A Therapeutic Strategy To Promote Angiogenic Activity And Endothelium Regeneration. *Acta Biomater.* **2019,** 82-91.

54. Baran, E. H.; Erbil, H. Y., Surface Modification of 3D Printed PLA Objects by Fused Deposition Modeling: A Review. *Colloids and Interfaces* **2019,** *3* (2), 43.

55. Major, T. C.; Brant, D. O.; Reynolds, M. M.; Bartlett, R. H.; Meyerhoff, M. E.; Handa, H.; Annich, G. M., The Attenuation of Platelet and Monocyte Activation in a Rabbit Model of Extracorporeal Circulation by a Nitric Oxide Releasing Polymer. *Biomaterials* **2010,** *31* (10), 2736-2745.

56. Brisbois, E. J.; Major, T. C.; Goudie, M. J.; Meyerhoff, M. E.; Bartlett, R. H.; Handa, H., Attenuation of Thrombosis and Bacterial Infection Using Dual Function Nitric Oxide Releasing Central Venous Catheters in a 9 Day Rabbit Model. *Acta Biomater.* **2016,** *44*, 304-312.

57. Brisbois, E. J.; Davis, R. P.; Jones, A. M.; Major, T. C.; Bartlett, R. H.; Meyerhoff, M. E.; Handa, H., Reduction in Thrombosis and Bacterial Adhesion with 7 Day Implantation of S-

nitroso-N-acetylpenicillamine (SNAP)-Doped Elast-eon E2As Catheters in Sheep. *J. Mater. Chem. B* **2015,** *3* (8), 1639-1645.

58. Handa, H.; Major, T. C.; Brisbois, E. J.; Amoako, K. A.; Meyerhoff, M. E.; Bartlett, R. H., Hemocompatibility Comparison of Biomedical Grade Polymers Using Rabbit Thrombogenicity Model for Preparing Nonthrombogenic Nitric Oxide Releasing Surfaces. *J. Mater. Chem. B* **2014,** *2* (8), 1059-1067.

CHAPTER 5:

SMARTPHONE COMPATIBLE NITRIC OXIDE RELEASING INSERT TO PREVENT CATHETER-ASSOCIATED INFECTIONS

Chug, M. K., & Brisbois, E. J. (2022). Smartphone Compatible Nitric Oxide Releasing Insert to Prevent Catheter-Associated Infections. *Journal of Controlled Release*, *349*, 227-240.

5.1 Abstract

A large fraction of nosocomial infections is associated with medical devices that are deemed life-threatening in immunocompromised patients. Medical device-related infections are a result of bacterial colonization and biofilm formation on the device surface that affects > 1 million people anually in the US alone. Over the past few years, light-based antimicrobial therapy has made substantial advances in tackling microbial colonization. Taking the advantage of light and antibacterial properties of nitric oxide (NO), for the first time, a robust, biocompatible, anti-infective approach to design a universal disposable catheter disinfection insert (DCDI) that can both prevent bacterial adhesion and disinfect indwelling catheters *in situ* is reported. The DCDI is engineered using a photo-initiated NO donor molecule, incorporated in polymer tubing that is mounted on side glow fiber optic connected to an LED light source. Using a smartphone application, the NO release from DCDI is photoactivated via white light resulting in tunable physiological levels of NO for up to 24 h. When challenged with microorganisms *S. aureus* and *E. coli*, the NO-releasing DCDI statistically reduced microbial attachment by >99% versus the controls with just 4 h of exposure. The DCDI also eradicated ~97% of pre-colonized bacteria on the CVC catheter model demonstrating the ability to exterminate an established catheter infection. The smart, mobile-operated novel universal antibacterial device can be used to both prevent catheter infections or inserted within an infected catheter to eradicate the bacteria without complex surgical interventions. The therapeutic levels of NO generated via illuminating fiber optic can be the next generation biocompatible solution for catheter-related blood-stream infections.

Keywords: Antibacterial, *In situ* disinfection, Fiber optic, Nitric oxide, Catheter infections

5.2 Introduction

Intravascular (IV) catheters are fundamental to contemporary hospital practices and are frequently implanted in critically ill patients for the administration of drugs, fluids, blood transfusion, dietary solutions, and for hemodynamic monitoring. Approximately, 90% of all the patients admitted to the hospital encounter some sort of intravenous therapy during their hospital stay.[1] The typical duration of a catheter used in clinical settings like emergency rooms, operating theaters, and intensive care units (ICUs) ranges from minutes to months. While the acute catheters are used for shorter periods (weeks), longer insertion periods of a catheter, like those used in hemodialysis, may be used from several months to years.[2] Among all the medical devices used in a hospital setting, IV catheters account for an increased risk of device-related infections compared to any other medical device categories. The infection causing bacteria can adhere to the catheter surface and colonize to develop biofilms. The primary contact of the bacterial cells on the surface of the catheter can emanate from the patient's own skin flora which can colonize the catheter lumen triggering the bacteria to travel from the catheter insertion site into the vascular.[3, 4]Furthermore, hematogenous seeding from a different contaminated site can become a source of infection in catheters. In rare occasions, catheter lumen contamination occurs when the infusate is contaminated.[5] These are the predominant source of morbidity and mortality in patients contributing to conditions like catheter-related bloodstream infections (CRBSIs) (e.g., bacteremia and sepsis). Each year the occurrence of CRBSIs in the United States alone is estimated to be more than 250,000 incidences with a mortality rate of approximately 35%, and an annual medical care outlay of approximately $2.3 billion.[6, 7]

Catheter-related infections have escalated especially due to the formation of biofilms.[8] As per the reports, over 1 million cases of hospital-acquired infections are reported every year.[9] About 60-70% of these infections are identified to arise from bacterial contamination and biofilm formation on the surface of the medical device which severely compromises the durability of the

medical devices.[10] The steps to address a catheter infection typically include irrigation of infection site with antibiotics, removal of catheter and initiation of antibiotic lock therapy.[11] Bacteria protected within biofilms require up to 1,000 times more dosage of antibiotics than their free-floating (planktonic) counterparts.[12] This high dosage can increase the possibility of antibiotic resistance across the bacterial species, engender a great deal of economic burden, and is a threat to native beneficial bacteria and other healthy organs of the body.[13, 14] Therefore, there is an urgent need for the efficacious and harmless approaches that can not only handle the emergence but also the propagation of pathogenic microorganisms. To overcome this issue and enhance the bactericidal effect of medical devices, several antimicrobial strategies including silver doping catheters, incorporation of antibiotics, or antimicrobial peptide coatings are employed to thwart the replication of bacteria or increase the susceptibility of antibiotics.[15-19] Likewise, IV line devices with potent antibacterial activity against various bacterial and fungal strains via alcohol impregnation have been reported in the literature.[20-23] Of these approaches that have been extensively tested and evaluated *in vivo* have reached clinical stages and are commercially available; however, while many of these approaches are effective against planktonic bacteria, they remain ineffective in reducing biofilms.[24] Similarly, even the most robust antibiotics are growing ineffective against biofilm-forming microorganisms. Current clinical guidelines oppose the idea of prolonged use of antibiotic impregnated catheters mainly due to the problem of uncontrolled leaching of antibiotic species from implanted devices, related toxicity, and emergence of antibiotic resistance.[25] Despite all these efforts, CRBSIs still remain one of the most significant concerns pertaining to biomedical devices as there is no definite solution for resisting biofilm that meets the prerequisite of clinically suitable catheter sizes.

Nitric oxide (NO) based therapy is emerging as a potential antibacterial treatment due to its bacteria-killing and biofilm dispersing abilities.[26, 27] Nitric oxide (NO) is an innate signaling diatomic molecule utilized by the body's defense system for fighting the infection-causing

microorganisms, preventing platelet activation, reducing localized and chronic inflammations, and enhancing wound healing.[28] The endogenous synthesis of NO in the body happens via NO synthase (NOS) enzymes which convert the amino acid L-arginine into citrulline and NO.[29, 30] Macrophages and neutrophils utilize NO synthesized via the inducible nitric oxide synthase (iNOS) to eradicate the invading pathogens in the body by promoting biofilm dispersal and preventing the adherence of planktonic bacteria. Nitric oxide donor molecules, like *S*-nitrosothiols (RSNO), incorporated into a polymer substrate can mimic endogenous NO release levels, such as endothelial cells that release NO at a surface flux of 0.5 - 4 x 10^{-10} mol cm^{-2} min^{-1} to prevent platelet activation and adhesion and exhibit broad-spectrum antimicrobial properties.[31, 32] Considering the potential benefits of endogenous NO, various studies have been designed that can utilize these benefits synthetically by either incorporating or impregnating the NO donors in the polymer matrix that will release their NO payload [33-35] or using a generation mechanism to stimulate the release of endogenous NO in blood.[36]

The release of NO from polymeric substrate has been tremendously explored in the past two decades demonstrating its wide range of tunable properties for achieving controlled NO release depending on the trigger mechanism. Therefore, to enhance the NO payload and extend the lifetime of NO release, several distinct frameworks have been designed with NO-releasing mechanisms at the polymer interface. Such engineered polymer surfaces that can release NO have been comprised of physical dispersal of NO donors into the polymer substrate, or covalent conjugation of NO donor onto polymer backbone.[37-40] The RSNO donors, like *S*-nitroso-*N*-acetylpenicillamine (SNAP) have been recognized to have extended storage capacity in crystallized form and can emit NO either photochemically, thermally by heat, light, or metal ions (Cu^{2+}, Se, Zn, etc.). Photocatalytic release of NO from RSNOs and RSNO-based polymers has been extensively explored.[41, 42]

The characteristic absorption maxima for the RSNOs occurs at wavelengths 340 nm and 520-590 nm with corresponding to n → π* electronic transition of the S-NO functional group that has been primarily associated with their decomposition.[43]

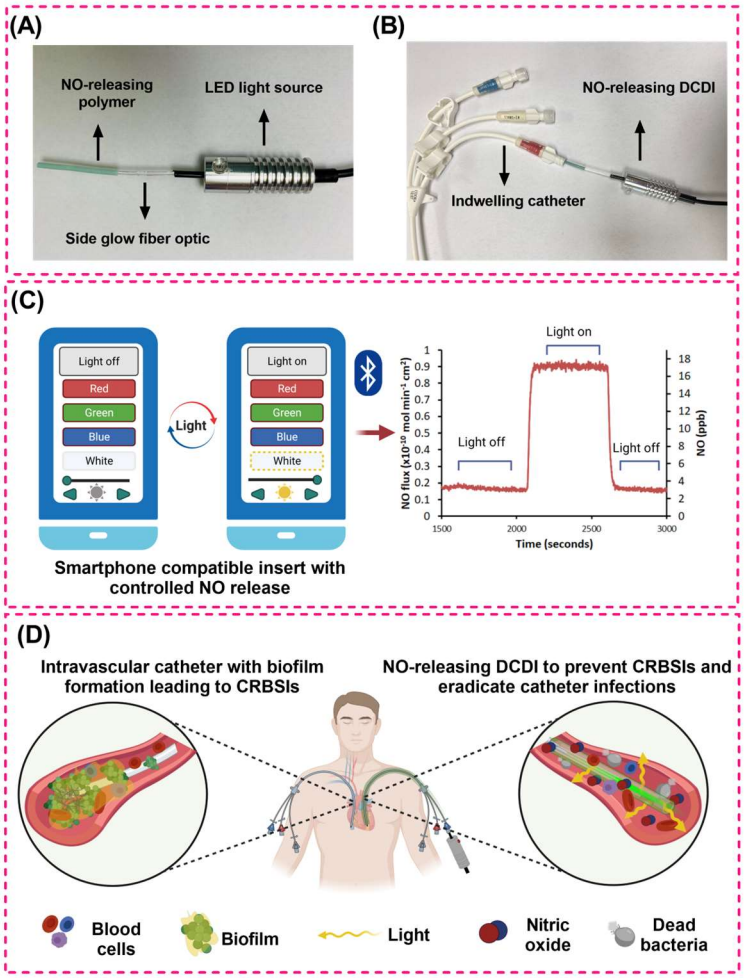

Figure 5.1 Design and functional use of the NO-releasing Disposable Catheter Disinfection Insert (DCDI). **(A)** NO-releasing SR is mounted on a side glow fiber optic and connected to a LED light source to develop the DCDI device. **(B)** The DCDI device can then easily be integrated with indwelling catheter (intravascular, urinary, etc.) for decontamination in between clinical uses. **(C)** The DCDI is engineered using a light-sensitive NO donor molecule, *S*-nitroso-*N*-acetylpenicillamine (SNAP), incorporated in polymer tubing mounted on side glow fiber optic. The photosensitivity of SNAP can be exploited using an LED light source that can illuminate the side glow fiber optic using a simple mobile phone application which activates and enables real-time control of the NO release levels. **(D)** The DCDI can both eradicate catheter infections and prevent Catheter-related bloodstream infections (CRBSIs) thereby extending the usage lifetime of medical devices and drastically reducing associated treatment cost.

Encouraged by the promising capabilities of NO and light-mediated microbe killing, a novel smartphone-based Disposable Catheter Disinfection Insert (DCDI) is engineered in this study which, for the first time, combines NO-releasing polymer and side glowing fiber optic. The NO-release polymer tubing was prepared by impregnating commercial silicone tubing with a light activated NO donor molecule.[2] The NO-releasing polymer tubing is mounted on a side glowing fiber optic to illuminate the full length of the NO-releasing tubing and is connected to a light source (**Figure 5.1A**). To activate the NO release and eradicate the viable pathogenic bacteria, the antimicrobial DCDI can be inserted within the lumen of IV catheters (**Figure 5.1B**) that can be the Bluetooth using a smartphone application. When the DCDI is powered by Bluetooth connected light source, the side glow fiber optic will illuminate, and the degradation of SNAP can be triggered under irradiation by LED with a wavelength of 450 – 650 nm to generate NO (**Figure 5.1C**). Taking this into consideration, NO release kinetics from the DCDI using LED source in dark and with different nominal lights and intensities was evaluated using the chemiluminescence detection method. Using the UV-vis spectroscopy method, the amount of NO donor impregnated in the SR polymer, leaching from the device with and without light, and stability with various sterilization methods was investigated. The antibacterial efficacy of DCDI was studied using a 4 h bacterial adhesion assay against two prominent bacterial strains associated with CRBSIs, Gram-positive (*S. aureus*) and Gram-negative (*E. coli*). The DCDI was also evaluated in a more challenging *in vitro* infection model to evaluate its ability to disinfect an *S. aureus* infected catheter, which closely mimics the end-use clinical application of the DCDI device. The small DCDI is envisioned to be a part of the catheter lumen cap and inserted within the lumen of IV catheters between clinical use of the IV catheters (when not in use by clinicians for blood draws, infusion, and other fluid administration). Once the NO release is depleted, a new DCDI can easily be replaced which extends the NO release capability at the catheter interface to the entire indwelling lifetime of the IV catheter. It is expected that light as a catalyst from the fiber optic combined with the NO-

releasing SR will enhance the antimicrobial activity of NO released from the catheter by both disinfecting the catheter *in situ* and preventing the impending infections (**Figure 5.1D**).

5.3 Experimental Section

5.3.1 Materials

N-Acetyl-D-penicillamine (NAP), sodium nitrite, L-cysteine, sodium chloride, potassium chloride, sodium phosphate dibasic, potassium phosphate monobasic, copper (II) chloride, ethylenediaminetetraacetic acid (EDTA), tetrahydrofuran (THF), and sterile phosphate buffer saline powder with 0.01 M, pH 7.4, containing 0.138 M NaCl, 2.7 mM KCl, were purchased from Sigma Aldrich (St. Louis, MO). Methanol, hydrochloric acid, and sulfuric acid were obtained from Fisher Scientific (Hampton, NH). Helixmark® silicone tubing (60-011-06 and 60—011-09) was purchased from VWR (Radnor, PA). PMMA side glow optical fiber (Huaxi, Amazon.com), 12V 1.5W LED light source (Rayauto, Amazon.com), and LED BLE Bluetooth 4.0 software were used for the light studies. All aqueous solutions were prepared using deionized water. Phosphate buffer saline (PBS) 0.01M with 100 μM EDTA was used for all material characterization and NO analyzer studies. Dulbecco's modified Eagle's medium (DMEM) and trypsin-EDTA were purchased from Corning (Manassas, VA20109). The Cell Counting Kit-8 (CCK-8) was purchased from Sigma-Aldrich (St. Louis, MO). Penicillin-Streptomycin (Pen-Strep) and fetal bovine serum (FBS) were obtained from Gibco-Life Technologies (Grand Island, NY). The bacterial strain *S. aureus* (ATCC 6538), *E. coli* (ATCC 25922), and 3T3 mouse fibroblast cells (ATCC 1658) for cell compatibility experiments were obtained from American Type Culture Collection (ATCC). All the buffers and media were sterilized in an autoclave at 121 °C, 100 kPa (15 psi) for 30 minutes.

5.3.2 *S*-nitroso-*N*-acetylpenicillamine Synthesis

S-nitroso-*N*-acetylpenicillamine (SNAP) synthesis procedure was adapted from a previously published report with a slight modification.[40] Briefly, NAP was dissolved in a 2:3 ratio

of water and methanol. To this mixture, 0.7 and 1.6 M of H_2SO_4 and HCl were added, respectively followed by dropwise addition of sodium nitrite dissolved in water and stirring for 10 min at room temperature. The beaker was shielded from ambient light and incubated in an ice bucket with continuous nitrogen purging for 8 h. After incubation, the filter paper was used to collect the SNAP crystals into a Buchner funnel using suction filtration. SNAP was then rinsed with ice-cold DI water and placed in a vacuum desiccator overnight allowing the product to dry. Care was taken throughout the process to shield the samples from light. Each batch of synthesized SNAP was tested for its purity using the chemiluminescence NOA and UV-vis calibration curve with a characteristic spectrum of SNAP molecule at 340 nm. All batches used in the study had recorded purity levels of >90%.

5.3.3 Preparation of NO-Releasing Polymer

The NO-releasing polymer was prepared by impregnating the silicone rubber (SR) tubing with SNAP, a stock solution of SNAP and THF (125 mg mL^{-1}) was prepared based on previously reported methods.[2] A 3 cm long Helix Silastic SR tubing with an inner diameter of 0.058" was incubated in SNAP-THF solution for 24 h in dark at room temperature. After 24 h, the SNAP impregnated NO-releasing SR (SR-NO) was removed from the solution and dried overnight in a vacuum desiccator protected from light. All samples were rinsed with PBS to remove excess SNAP crystals from the outer surface and lumen of the impregnated tubing before conducting any further experiments.

5.3.4 Determining wt% SNAP using UV-vis Spectroscopy

The amount of SNAP impregnated in the SR-NO tubing was quantified using a UV-vis spectrophotometer (Cary 60, Agilent Technologies). For this, first, the mass of each SR-NO sample was recorded using an analytical balance (Mettler Toledo™ XS105DU, Columbus, OH). Each SR-NO sample was soaked in THF for 30 min to extract all the impregnated SNAP from the

SR tubing. The tubing appeared clear after incubation in the THF, indicating all SNAP had been extracted into the THF. The SNAP extracted solution was evaluated by UV-vis spectroscopy at 340 nm wavelength. The molar absorptivity of SNAP in THF at 340 nm was determined to be 909 M^{-1} cm^{-1}. The weight percentage (wt%) of SNAP loaded is reported as milligrams of SNAP loaded per milligram of tubing.

5.3.5 Fabrication of Disposable Catheter Disinfection Insert (DCDI)

The Disposable Catheter Disinfection Insert (DCDI) was produced using a 2.9 cm SR-NO tubing mounted on a 7 cm segment of 1.5 mm diameter PMMA side glow optical fiber (Huaxi, Amazon.com). The SR-NO-Light DCDI samples were connected to a 12V 1.5W LED light source and controlled via Bluetooth using a smartphone application. For controls, either unmodified SR or SR-NO were mounted on the fiber optic and operated with or without light, resulting in the SR, SR-Light, and SR-NO control groups.

5.3.6 Light Emission Spectroscopy Measurements

To determine the wavelength of light emitted by the LED light source, a wireless spectrophotometer (PS-2600, PASCO Scientific) with a detection range of 380–950 nm was utilized. The light detecting fiber optic cable was held in place with a clamp and the DCDI samples were exposed to the detector and the wavelength of light was recorded with four different colors (red, blue, green, and white). Studies with light were done in the absence of ambient light to ensure only desired lights were being characterized.

5.3.7 Photoinitiated NO Release

The NO release from samples with light (SR-NO-Light) and without light (SR-NO) was quantified using the gold standard Zysense chemiluminescence Nitric Oxide Analyzer (NOA) 280i (Frederick, CO) under nitrogen atmosphere under physiological conditions. The NO release from the samples is normalized to the surface area of the DCDI and is presented as moles min^{-1} cm^{-2}.

5.3.8 NO Release vs. Light Color

In order to optimize the light from DCDI, samples were placed in an NOA sample cell at 37 °C connected to the LED light source (SR-NO-Light). To avoid the interference of leached SNAP in buffer conditions, a dry state at physiological conditions was used to study the influence of white light on DCDI at different light intensities. Using the mobile phone application, the LED light source was set to emit light at 100% intensity, and the NO flux was recorded as the light color was adjusted. Four different light colors (white, blue, green, and red) were tested for their NO release.

5.3.9 Tunable Photoinitiated NO Release

The SR-NO-Light samples were placed in an NOA sample cell under a dry state at 37 °C protected from ambient light. The LED light source was set to emit white light from the connected fiber optic and the NO flux from samples was recorded as the light intensity was adjusted using the smartphone application. Starting without light (in dark), the intensity of light was increased in 25% increments until 100% intensity was reached. The light intensity was then decreased by 25% to 0% to demonstrate control over NO levels.

5.3.10 24 Hour NO Release

The samples were immersed in PBS with EDTA (7.4 pH) at the physiological temperature of 37 °C in an amber NOA sample cell. For the SR-NO-light samples, the LED light source was set to emit white light at 100% intensity. The 24 h NO release profiles for the DCDI samples were recorded using 0% (light off) and 100% white light intensity from SR-NO and SR-NO-Light samples, respectively.

5.3.11 Determination of SNAP Diffusion

The amount of SNAP leached from samples in the presence (100% light intensity) and absence of light (0% light intensity) was determined by a UV-vis spectrophotometric method. Each sample SR-NO and SR-NO-Light was incubated in 10 mM PBS, pH 7.4, with 100 μM EDTA

at 37 °C for 24 h. The soaking buffer was evaluated for SNAP concentration at 2, 4, 6, 8, and 24 h timepoints. The molar absorptivity of SNAP in 10 mM PBS, pH 7.4, with 100 μM EDTA at 37 °C was determined to be 1072 M^{-1} cm^{-1} at 340 nm. Samples were incubated at 37 °C in PBS throughout the duration of the experiment. Results were analyzed by calculating SNAP concentration from each sample, normalized by the surface area of DCDI.

5.3.12 Sterilization of NO-Releasing Tubing

Sterilization of medical devices is an important process for decontaminating the surfaces before *in vivo* application. Therefore, it is very critical for medical devices to withstand the sterilization process without compromising the desired properties. In this study, two common sterilization methods ethylene oxide (EO) and ultraviolet (UV) light were compared to identify the most compatible method with the NO-releasing polymer. For EO sterilization, the NO-releasing DCDI inserts were packaged into the sterilization pouch and exposed to EO under AN 74i Anprolene EO gas sterilizer (Anderson Sterilizers). The sterilizer was operated at room temperature (between 68 - 91 °F) with a Humidichip to ensure at least 35% humidity was achieved. Samples were sterilized for 12 h with 2 h of purging with ambient air. Similarly, for UV sterilization, SR-NO samples were sterilized with UV-light under biosafety cabinet administered by REDISHIP Purifier® Logic®+ Class II A2 Biosafety Cabinets, Labconco® for 30 min. Upon sterilization, all the samples (n =4) were weighed and then suspended in THF (30 min) to fully extract the SNAP from the polymer.

The amount of SNAP remaining in the SR-NO tubing after the sterilization process was compared to fresh samples using UV-vis spectroscopy by measuring the absorbance of SNAP extracted in THF at 340 nm wavelength. The results of the study are reported as normalized values to initial wt% of SNAP (weight of SNAP/weight of polymer). The confirm the activity of SNAP in the SR-NO samples, the samples were also tested for their NO release levels using the same methodology as Section 5.3.10 before and after sterilization.

5.3.13 Shelf-life Storage of DCDI

To evaluate the long-term stability of DCDI at various storage conditions, SNAP-impregnated SR were stored at -20 °C, 4 °C and RT for 30 d in a tighly closed vial in dark with desiccant to protect the insert from moisture. After 30 d, the SNAP-SR tubing was mounted on fiber optic, connected to light-source and NO release from the samples before and after storage was evaluated using chemiluminescence NOA at 37 °C. The NO release from samples was recorded in the absence (0%) and presence of light (100% white light) at physiological conditions.

5.3.14 *In Vitro* Antibacterial Evaluation

5.3.14.1 Antibacterial Activity of DCDI using 4 h Bacterial Adhesion Assay

Studies were conducted to determine the efficacy of DCDI to prevent bacterial adhesion on the surface. The antibacterial activity of DCDI was examined against *S. aureus* (ATCC 6538) *and E. coli* (ATCC 25922) in terms of viable bacterial adhesion on the catheter surface. Individual colonies of *S. aureus* and *E. coli* were inoculated in LB media and grown until mid-log phase on a shaking incubator at 120 rpm, at 37 °C for 5 h. All DCDI samples (SR, SR-Light, SR-NO, and SR-NO-Light; n = 3 each) were exposed to the bacterial solution with the final OD_{600} of bacteria ranging between 10^6 – 10^8 CFU mL^{-1} for 4 h at 150 rpm at 37 °C to maintain the chronic infection conditions. After 4 h incubation, bacteria adhered on the DCDI surface were homogenized to detach, diluted, and plated using a spiral plater (Eddy Jet 2, IUL Instruments). Viable colony forming units (CFU) were determined after 24 h of incubation at 37 °C using an automated bacteria colony counter (Sphere Flash, IUL Instruments). The CFUs on the samples and individual controls were normalized by the surface area of the samples and the percentage of reduction in bacterial viability was determined by the following **equation 5.1** with respect to SR control. C represents the concentration of viable bacteria in CFU cm^{-2}.

$$\%\ Bacterial\ reduction = \frac{(C_{SR}) - (C_{Test}) \times 100}{(C_{SR})} \quad \textbf{(Equation 5.1)}$$

5.3.15 *In Situ* Catheter Disinfection using Catheter Infection Model

To evaluate the efficacy of DCDI in disinfecting an infected model medical catheter (Helixmark® silicone tubing 60-011-09) with an ID of 0.078" and OD of 0.125" was used to develop an *in vitro* assay using *S. aureus* bacteria (ATCC 6538). *S. aureus* was grown overnight in an LB media following the same procedure as 5.3.14.1 Then, 3 mL of bacterial suspension (0.1 optical density) was added to the model CVC catheter (Helix-09 tubing; 3 cm long) such that both inner lumen and external surface were exposed to bacteria. Samples were incubated for 24 h in LB medium under stagnant conditions at 37 °C. Nutrient media in the tubes was changed periodically to keep the supply of nutrients stable. After 24 h, catheter samples were taken out from media containing bacteria and briefly rinsed to remove any unadhered cells on the catheter tubing. Then the DCDI (SR-NO-Light) and control (SR) devices were inserted into the infected catheter tubing and incubated in PBS for 4 h at 37 °C under static conditions. The control samples contained no NO-releasing DCDI, just an unmodified SR tubing mounted on fiber optic inserted into the bacteria-infected catheter. Samples were taken out after incubation and bacteria remaining on the catheter tubing (both insider and outside) were enumerated using the same CFU counting protocol described in Section 5.3.14.1.

5.3.16 *In Vitro* Cytocompatibility Study

5.3.16.1 Leachate Preparation

All test and control groups (SR, SR-NO, SR-Light, and SR-NO-Light samples; n = 3) each were first cleaned with ethanol and UV-sterilized for 30 mins. Next, DCDI samples were incubated in complete DMEM media (1 mL) to collect the leachates in the solution by following the ISO standards (ISO10993-5:2009 Test for *in vitro* cytotoxicity assessment of biomedical devices). All the vials were covered in aluminum foil to prevent the effect of ambient light and incubated for 24 h at 37 °C. After 24 h, the samples were removed, and the leachates were used for further analysis.

5.3.16.2 Cytocompatibility of DCDI

A cell culture treated 96-well plate was used to seed 3T3 mouse fibroblast cells (10,000 cells/mL) in each well and incubated in a humidified incubator at 37 °C, 5% CO_2 for 24 h. Later, leachate samples were exposed to the cells (100 µL) and incubated for another 24 h to let the leachates act on the cells. The cytocompatibility of samples was analyzed using a CCK-8 cell viability kit following the manufacturer's instructions (Sigma Aldrich). To each of the wells, CCK-8 solution was added (10 µL) and incubated for 1 h. The absorbance (abs) of the samples was recorded at 450 nm wavelength using a microplate reader (Cytation 5 imaging multi-mode reader, BioTek). Results from the experiment are reported as relative cell viability of test group normalized to control (cells in media) using the **equation 5.2**:

$$Relative\ cell\ viability = \frac{absorbance\ \ test\ group}{absorbance\ cells\ control} \quad \textbf{(Equation 5.2)}$$

5.4 Statistical Analysis

All results in the study are presented with a sample size n ≥ 3. Data are all reported as mean ± standard error of the mean (SEM). Statistical significance between the sample types was determined using a student's *t*-test. To ascertain the significance of the results, a value of p <0.05 was used to evaluate statistical differences between the test (SR-Light, SR-NO, SR-NO-Light) and control groups (SR).

5.5 Results and Discussion

5.5.1 Fabrication of the DCDI

To generate the NO-releasing DCDI insert, segments of SR tubing were soaked in the SNAP-THF impregnation solution for 24 h (125 mg mL^{-1}) (**Figure 5.2A**). The solvent impregnation process is one of the simple and effective ways to incorporate NO donors in the polymer matrix. It has been previously reported that SNAP incorporation/impregnation into various polymers, like polyurethanes and silicone elastomers, and studied for their clinical applications for devices

including intravascular catheters, urinary catheters, insulin cannulas, extracorporeal circuit tubing.[34, 44-46] These polymers have exhibited uniform SNAP impregnation[45, 47] long-lasting and controlled NO release,[47-50] with enhanced shelf-life[46,51] and sterilization[32, 49] stability, ability to withstand low rates of SNAP leaching, and photosensitivity.[52] This impregnation approach helps conquer challenges with the typical style of polymer manufacturing procedures that use elevated temperature possessing (i.e., polymer extrusion), which could negatively influence the thermally sensitive NO donors, like SNAP. In this study, the amount of SNAP impregnated into SR was confirmed by the UV-vis spectroscopy method which revealed 4.66 ± 0.16 wt% of SNAP impregnated into the SR-NO samples (**Figure 5.2B**). The values obtained in this study are consistent with the previously reported values for SNAP impregnation of SR that accomplished ca. 5 wt% with the same concentration of SNAP-impregnation-solvent (125 mg mL^{-1}).[45, 46]

5.5.2 Quantification and Control of Real-time NO Release

5.5.2.1 NO release vs. Light Wavelength

To confirm the wavelength of light emitted by the LED source, a PASCO wireless spectrometer optical probe was utilized. The wavelength of light was determined at four different colors of light (**Figure 5.2C**). Results confirmed that the red, green, and blue light had emissions ranging from 570 – 650 nm, 475 – 575 nm, 450 – 500 nm, respectively (**Figure 5.2 D-F**). Furthermore, the study confirmed the white light provided by the light source is comprised of red, blue, and green wavelengths of light (**Figure 5.2G)**.

The NO donor SNAP can catalytically release NO upon exposure to heat, light, or metal ions (**Figure 5.3A**). The small side glow fiber optic used in this study enable compatible application with the IV catheter. Fiber optics are used in clinical applications such as sterilization of medical device surfaces. The illuminating light has been shown to be compatible with endoscopes, respiratory devices, catheters (endotracheal tube, urinary catheters), and bandages for wound healing.[53] The thin, flexible nature and a tubular scattering factor make the light from

fiber optic cable of uniform light dissemination. Therefore, a side glow fiber optic is utilized in the DCDI due to its significant advantages over end glow fiber optics in order to illuminate the full length of SNAP tubing for catheter applications. The DCDI can be inserted within the vascular catheters to disinfect the entire length of the catheter tubing (**Figure 5.3B**).

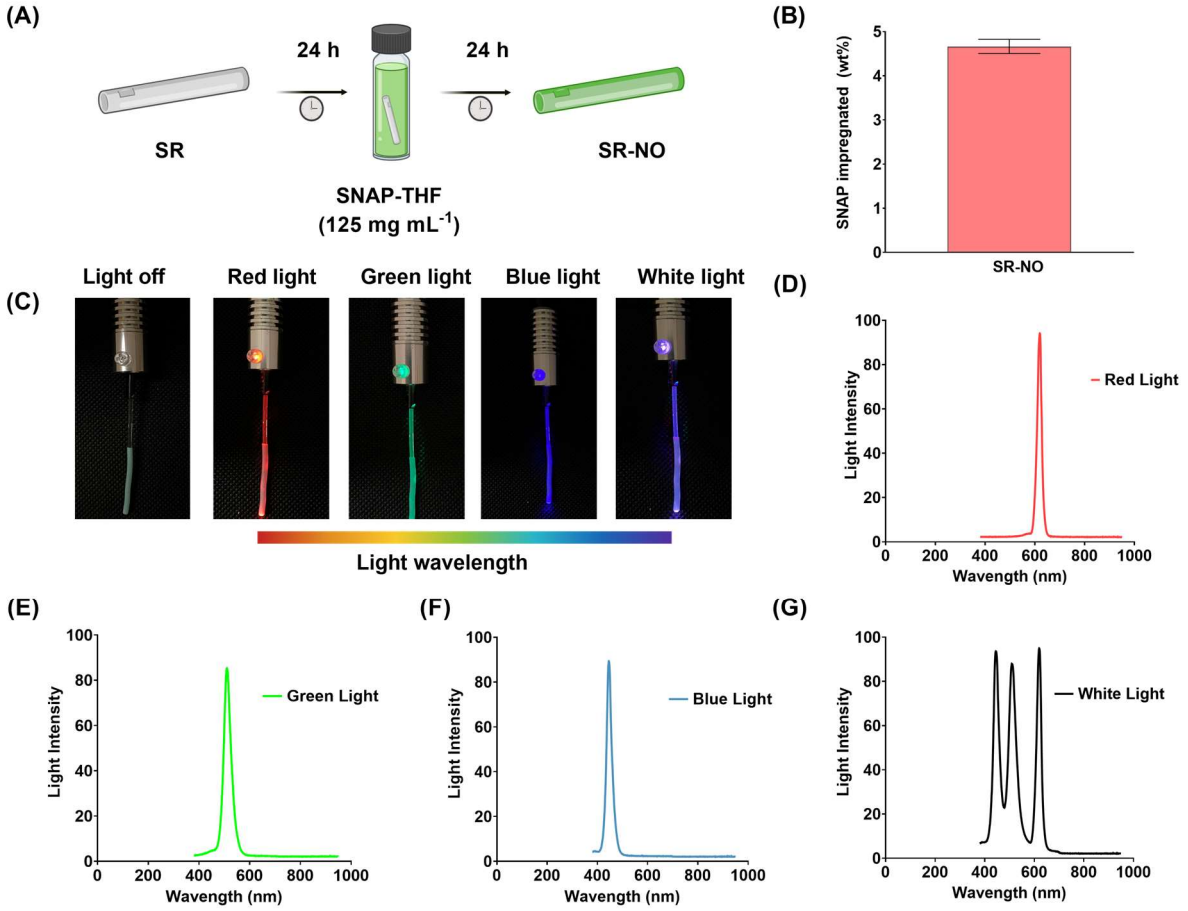

Figure 5.2 (A) NO-releasing tubing is fabricated by soaking the SR tubing in SNAP-THF solution (125 mg mL^{-1}) for 24 h followed by drying in vacuum desiccator for 24 h. **(B)** Quantification of SNAP impregnation in SR-NO samples is determined by UV-vis spectroscopy. Data represents mean ± SEM for n ≥ 3. **(C)** To develop nitric oxide releasing Disposable Catheter Disinfection Insert (DCDI), SR-NO tubing is mounted on a side glow fiber optic and connected to a LED Light source. DCDI with different nominal lights from left to right: light off, red, green, blue, and white light. Verification of wavelength of light emitted by LED light source **(D)** red (621 nm) **(E)** green (512 nm), **(F)** blue (447 nm), and **(G)** white (mixture of red, green, and blue) set at 100% light intensity.

To optimize the light color for the study, NO release from the DCDI was tested against various colors of light red (620 nm), green (530 nm), blue (450 nm), and white (mixture of red, green, and blue) at 100% light intensity (n≥3). DCDI samples were inserted in the amber NOA sample cell to protect the samples from ambient light. First, the NO release from the samples was recorded in the absence of light (dark) and then the color of the light was changed, and the intensity was adjusted using the mobile phone application. The NO release in dark was 0.09 x 10^{-10} mol cm^{-2} min^{-1} flux, and the red, green, blue, and white light at 100% light intensity triggered 0.14, 0.17, 1.23, and 1.69 x 10^{-10} mol cm^{-2} min^{-1} of NO from DCDI, respectively (**Figure 5.3C**). The hemolytic cleavage of S-N bond of *S*-nitrosothiols has been well-established in the visible light spectrum. Once the results were confirmed with white light resulting in the maximum levels of NO, all the further studies were conducted with white light. These results are consistent with previously published reports that utilized white light to maximize the NO release from NO donating compound.[54, 55]

5.5.2.2 Real-Time Control of NO Release

NO-releasing materials hold a huge potential in clinical applications. However, it is crucial to gain the ability to dynamically control the NO levels depending on the biomedical application. For instance, at the time of implantation, the catheter may require a higher level of NO to prevent bacterial colonization on the device surface. However, over time the same device may need lower levels of NO to maintain the biofilm-free state of the device. Similarly, a significantly contaminated device surface may require very high levels of NO to disinfect and eradicate the pre-established biofilm on the catheter surface. This modulatory capacity of NO release can be achieved by exploiting the photosensitivity of NO donating compounds that can tune the NO release in response to the intensity and wavelength of light. Based on this, other RSNOs like GSNO, *N*-nitrosoamine-based NO donors with a combination of antibiotics, or even modified RSNOs have been studied for their light-sensitive properties.[56-59]

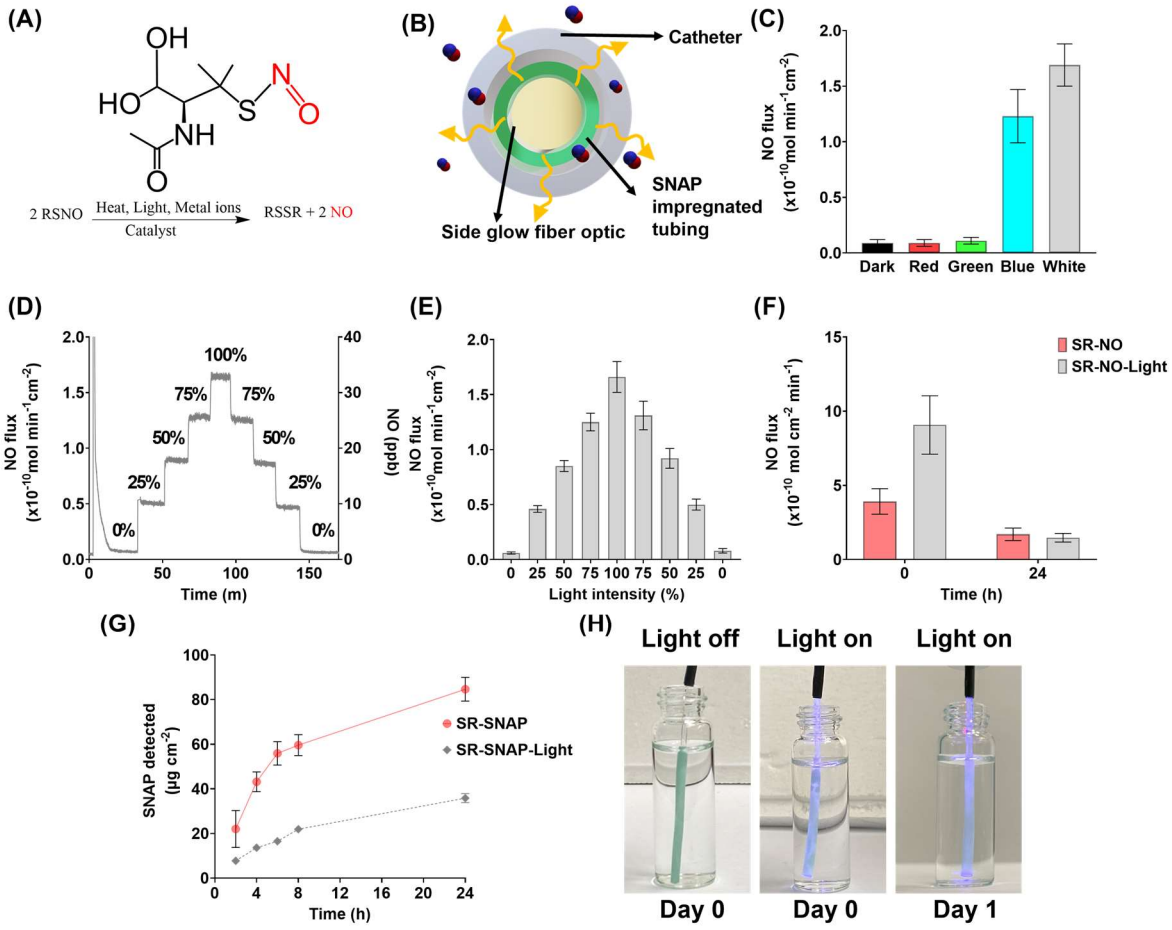

Figure 5.3 (A) Chemical structure of the NO donor *S*-nitroso-*N*-acetylpenicillamine (SNAP). RSNOs like SNAP can be triggered by the stimulus of heat, light, or metal ions to cleave the S-N bond and release NO. **(B)** Cross-section of the Disposable Catheter Disinfection Insert (DCDI) device comprised of SNAP impregnated SR tubing mounted on a side glow fiber optic. **(C)** Comparison of steady-state NO release from DCDI at physiological temperature (37 °C) in dark and photoinitiated at 100% light intensity of red (620 nm), green (530 nm), blue (450 nm), and white (mixture of red, green, and blue) light. **(D)** Representative example of tunable NO release via increasing and decreasing intensities of light (between 0% and 100%). **(E)** Quantification of NO release using chemiluminescence measured with the trigger of different light intensities at 37 °C (n ≥ 3). **(F)** Determination of real-time NO release from NO (dark) and SR-NO-Light (100% light intensity) using a chemiluminescence NO analyzer. The NO flux levels were measured at physiological conditions in PBS with 100 µM EDTA up to 24 h. **(G)** Quantitation of amount of SNAP present in the PBS (soaking buffer) from SR-NO and SR-NO-light samples at 37 °C in dark and 100% white light intensity conditions, respectively. Data normalized to surface area of the polymer. All data are reported as mean ± standard error of mean (n ≥ 3). **(H)** DCDI soaked in PBS-EDTA from left to right: DCDI without light on day 0, DCDI with 100% white light on day 0 and day 1 (24 h).

The ability to control the release of NO by changing the light intensity was assessed by increasing and decreasing the white light intensity in 25% intervals (**Figure 5.3D**). These results demonstrate that each degree of light intensity can modulate the NO release levels from the DCDI in real-time (**Figure 5.3E**). The NO release levels at each light intensity are tabulated in **Table 5.1**. The advantage of the DCDI design is that the NO release levels can be controlled via adjusting the intensity of the light source connected to the fiber optic. This data demonstrates that using light as a trigger to potentiate the NO release enables accurate modulation of the NO levels as required to achieve antibacterial properties.

Table 5.1 NO release levels measured from SR-NO-Light DCDI at different intensities of white light at 37 °C using chemiluminescence nitric oxide analyzer. Data represents mean ± SEM (n ≥ 3).

Light intensity	NO flux ($\times 10^{-10}$ mol min^{-1} cm^{-2})
0%	0.06 ± 0.01
25%	0.46 ± 0.03
50%	0.85 ± 0.05
75%	1.25 ± 0.08
100%	1.66 ± 0.14
75%	1.31 ± 0.13
50%	0.92 ± 0.09
25%	0.50 ± 0.05
0%	0.08 ± 0.02

5.5.2.3 Real-Time NO Release

The NO release from the DCDI was measured under physiological conditions (37°C in PBS buffer) using chemiluminescence for 24 h at 0% (dark), and 100% white light intensity. NO release from the samples was investigated over 24 h with the idea that the DCDI device could be replaced daily during clinical catheter applications. The average initial NO flux for 0% and 100% light intensity was found to be 3.92×10^{-10} mol cm^{-2} min^{-1} and 9.01×10^{-10} mol cm^{-2} min^{-1}, respectively, demonstrating that the light intensity is directly proportional to the level of NO

released from DCDI on day 0 (**Figure 5.3F**). However, all samples ultimately reach an equivalent NO release level at 24 h timepoint as the SNAP payload becomes depleted. The SR-NO-Light DCDI samples have a fixed amount of NO and will exhaust over time as NO is constantly discharged. The 100% light intensity significantly increases the rate at which NO is depleted from the samples early in the experiment which explains the decrease in the NO flux level at the 24 h time point. Overall, the DCDI with and without light are able to closely mimic the levels of NO released by endothelium ($0.5{-}4 \times 10^{-10}$ mol cm^{-2} min^{-1}) even after 24 h. These levels of NO are known to exhibit important biological functions such as reducing inflammation and fibrosis, killing various microbial species (bacteria, fungus, viruses), inhibiting disrupting and dispersing microbial biofilm formation, preventing platelet activation, reducing clotting and thrombosis.[31] Once the NO flux is below physiological levels, a new DCDI could be easily replaced within the catheter periodically (e.g. daily).

5.5.3 Quantification of SNAP in Soaking Buffer

To quantify the amount of SNAP leached from NO-releasing samples, both SR-NO (0% light) and SR-NO-Light (100% white light) DCDI samples were incubated in PBS-EDTA at 37 °C for 24 h. The soaking buffer was collected at various timepoints, and the absorbance was recorded using UV-vis spectroscopy. After 24 h, 84.61 ± 5.32 and 35.83 ± 2.04 μg cm^{-2} of SNAP were detected from SR-NO and SR-NO-light samples, respectively (**Figure 5.3G).** The introduction of light to the SR-NO-Light significantly enhanced the catalysis rate to release NO, resulting in a lower concentration of SNAP in the soaking buffer as compared to the SR-NO samples. Overall, the low SNAP leaching results observed in this experiment demonstrate that the NO released is localized at the DCDI polymer interface. The fiber optic also showed the ability to be illuminated in buffer even after a day of soaking (**Figure 5.3H**).

Impregnating the NO donor SNAP into hydrophobic polymers like SR has been reported to significantly reduce leaching which consequently prolongs the NO release from the polymer.[47,

[60] Due to the intramolecular hydrogen bonding between SNAP molecules and the low water uptake of hydrophobic polymers, SNAP dissolution and dissemination out of the polymer is significantly contained.[2, 51] The SNAP leaches out of the polymer and eventually degrade into *N*-acetyl-*D*-penicillamine (NAP), and NAP-dimer. It is anticipated that the levels of SNAP detected in the buffer are observed to be lower when the fiber optic is illuminated due to the relatively faster light-mediated conversion of SNAP to NAP disulfide.[34] These degradation products of SNAP are non-toxic and an FDA approved drug utilized to treat heavy metal poisoning.[61, 62]

5.5.4 Sterilization of SNAP Impregnated SR

Infection-causing pathogens can easily adhere to the polymer surfaces in a hospital-based setting. If left untreated, these pathogens can migrate into the patient's body and can lead to blood-stream infections in severe scenarios, increase healthcare costs and prolong the patient treatment time. Therefore, sterilization of medical devices is an important process for decontaminating the surfaces before clinical application.[63] It is extremely critical for medical devices to withstand the sterilization process without compromising the desired properties. NO donating compounds, such as RSNOs, are known to degrade due to their sensitivity to temperature and thermal degradation.[64] To investigate their stability during the sterilization process, samples were exposed to clinically relevant UV-light and EO sterilization methods commonly used in thermally sensitive medical devices.[65, 66] The SR-NO DCDI retained 99.06 ± 2.26% and 99.33 ± 1.08% SNAP after UV and EO sterilization, respectively, compared to the initial wt% of SNAP in freshly prepared DCDI samples (**Figure 5.4A**). In order to evaluate and confirm the activity of insert in terms of NO-releasing characteristics, NO release from samples was measured in the absence (0% light) and presence of light (100%) before and after sterilization (ethylene oxide and UV-light), respectively. The results from the study revealed no significant difference between NO-release kinetics from freshly prepared samples vs. sterilized samples. Data suggests that while the freshly prepared samples had $1.740 \pm 0.092 \times 10^{-10}$ mol min^{-1} cm^{-2}

of NO flux, EO and UV sterilized samples showed 1.707 ± 0.083 x 10^{-10} mol min^{-1} cm^{-2} and 1.689 ± 0.078 x 10^{-10} mol min^{-1} cm^{-2}, respectively with 100% white light stimulation (**Figure 5.4B**). These results indicate that both sterilization methods are compatible with the SR-NO polymeric device without significant losses in the amount of NO payload in the device, critical for clinical translation.

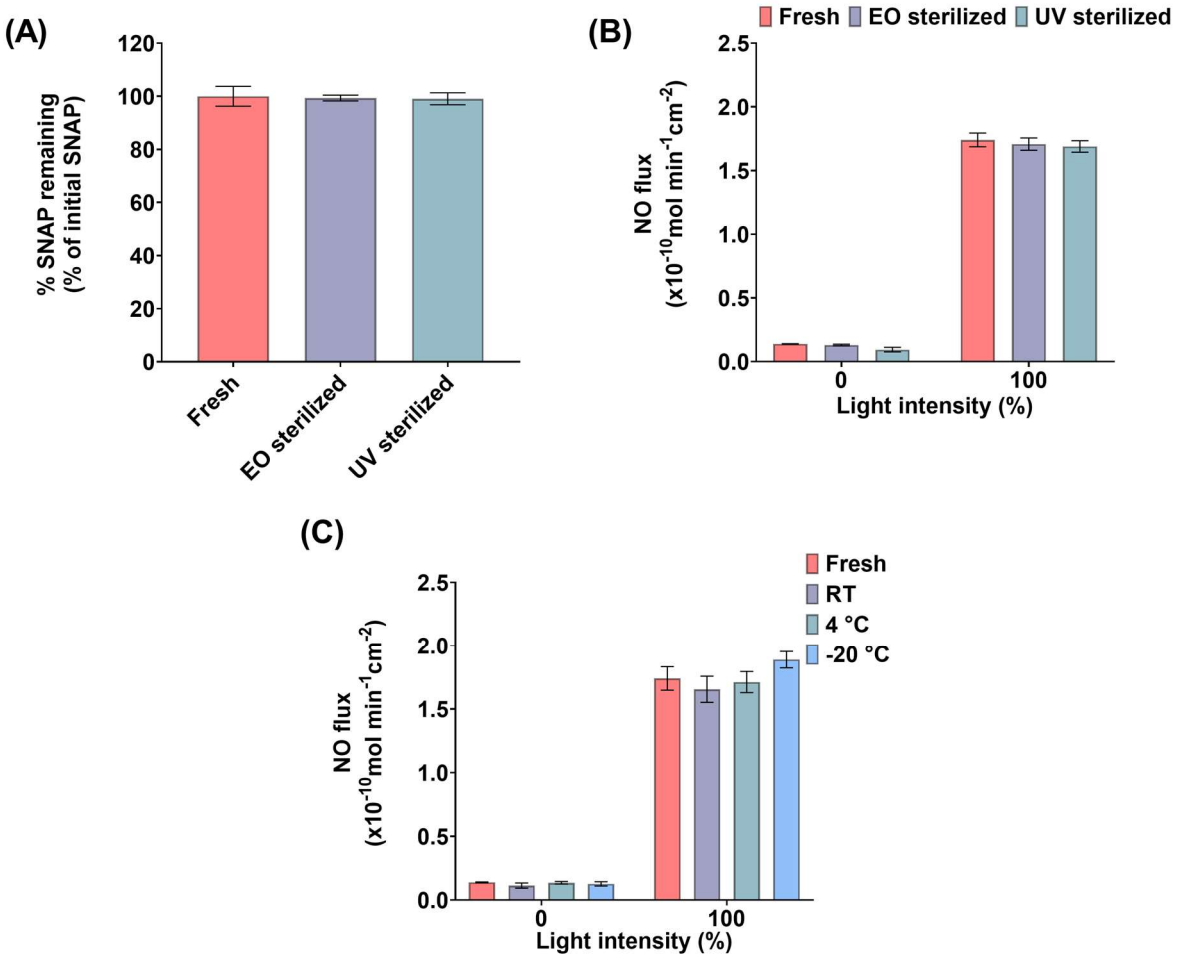

Figure 5.4. Impact of storage and sterilization on NO-releasing SR. **(A)** The retention of SNAP in the polymer after sterilization process was analyzed by extracting the SNAP remaining in the polymer in THF solvent and measuring the absorbance of SNAP at 340 nm using UV-vis. Data represents mean ± SEM normalized to initial wt% of SNAP in freshly prepared samples (n ≥ 3). Measurement of NO release from SR-NO samples after **(B)** sterilization with ethylene oxide and UV-light, and **(C)** 30 d of storage at room temperature (RT), -20 °C and 4 °C. Data represents mean ± SEM normalized to initial wt% of SNAP in freshly prepared samples (n ≥ 3).

5.5.5 Shelf-life Storage of DCDI

The success of biomedical devices is highly dependent on their ability to retain their function for a prolonged period. To evaluate the potential of DCDI to be stored at various storage conditions, SR-NO samples were stored for 30 d at clinically relevant storage conditions ie., -20 °C, 4 °C and RT for 30 d in a tighly closed vial in dark with desiccant to protect the insert from moisture. After 30 d, the SNAP-SR tubing was mounted on fiber optic, connected to light-source and NO release from the samples was recorded with and without light before and after storage using chemiluminescence NOA at 37 °C. Results from the storage stability experiment confirmed the stability of samples at different storage conditions for at least 30 d with no significant difference in the NO release levels (**Figure 5.4C**). These results are in agreement with previously reported studies that confirm the stability of SNAP loaded polymer for upto 8 months.[49, 51]

5.5.6 Antibacterial Activity of DCDI using 4 h Bacterial Adhesion Assay

5.5.6.1 Evaluating the Antibacterial Efficacy of DCDI

Various nosocomial infections in hospitalized patients are frequently linked with biomedical devices. While these devices are expected to offer life-saving protection, they are reported to be a primary source of device-associated infections in many instances.[67] A recent study reported an upsurge in the rate of hospital-acquired infections in COVID-19 patients due to longer lengths of hospital stay.[68] In times like these when conventional antimicrobial therapies are failing to contain the infection rates, alternative strategies are critically needed. For this reason, novel antimicrobial approaches have been proposed as an alternative to traditional methods. Light-based antimicrobial therapy is one such strategy heavily being employed for combating biofilms on medical implants.[69] Clinical pathogens such as S*. aureus* and *E. coli* have been proven to be vulnerable to photodynamic inactivation by the wavelengths of the visible spectrum of light (400–800 nm).[70-72] Similarly, photoactivation of silver and gold nanoparticles has also been explored for bactericidal efficacy; however, the metal-dependent killing is distinct for Gram-

positive than for Gram-negative bacteria and often exhibits cytotoxicity towards mammalian cells.[73, 74] For this reason, a broad-spectrum, biocompatible disinfecting device was developed in this study for eradicating both Gram-positive and Gram-negative bacteria.

The bactericidal efficiency of the DCDI device was evaluated against *S. aureus* (ATCC 6538) *and E. coli* (ATCC 25922) bacteria using a 4 h bacterial adhesion assay. The bacterial cells adhered to the DCDI were enumerated and normalized to the surface area of the DCDI to obtain viable CFU cm^{-2}. Results from *S. aureus* adhesion on the synergy of SR-NO-Light unveiled a 99.45% reduction compared to the SR control ($p < 0.05$). The SR-Light and SR-NO samples also had a significant reduction in viable adhered cells as compared to SR control ($p < 0.05$) due to the action of the NO release (93.05% reduction) and light-mediated interface (41.30% reduction), respectively (**Figure 5.5A**). A similar trend was observed after exposure to *E. coli,* where the SR-Light and SR-NO controls resulted in an 85.01% and 92.89% reduction in viable cells, respectively. The highest reduction in viable *E. coli* adhesion on the surface occurred with the SR-NO-light DCDI resulting in a 99.36% reduction compared to SR control ($p < 0.05$) (**Figure 5.5B**). These results align with the NO release levels obtained from SR-NO and SR-NO-Light samples, where both samples exhibit physiological levels of NO that are increased via the photoinitiated catalysis with the white light (**Figure 5.3F**). Overall, the synergistic effect of NO and light resulted in broad-spectrum antimicrobial activity on the DCDI surface and significant inhibition of both *S. aureus* and *E. coli* bacteria. Mutations in the DNA sequence via reactive nitrogen species (RNS) is one of the major mechanism by which NO exhibits antimicrobial activity.[29] NO's reaction with oxygen and peroxides leads to the formation of a range of free radical antimicrobial species such as peroxynitrite and nitrogen dioxide that can modify and destroy the DNA base pairs using oxidative and nitrosative mechanisms. The damage of DNA strands facilitates lipid peroxidation, constrains enzyme functions, and results in eventual membrane loss in microorganisms.[29, 75-77]

5.5.6.2 *In Situ* Surface Disinfection using Catheter Infection Model

The ability of DCDI to disinfect the catheter surface was characterized against *S. aureus,* one of the most common bacteria associated with biofilm-related infections. The *S. aureus* bacteria were grown in LB media until the mid-log phase and exposed to model CVC catheters for 24 h at 37 °C in order to develop a pre-established infection/biofilm on the CVC catheter surface. After 24 h, the DCDI and the corresponding SR control were then inserted into the infected catheter to investigate the disinfecting ability (**Figure 5.5C**). After 4 h exposure to the DCDI device, the viable bacteria remaining on the surface of the catheter were enumerated using the plate counting method (**Figure 5.5D**). The study demonstrates the ability of the SR-NO-Light DCDI to eradicate a pre-established *S. aureus* infection on the CVC catheter surfaces by ca. 96.99% compared to the unmodified SR control ($p < 0.05$) (**Figure 5.5E**). Nitric oxide is known to induce biofilm dispersal across many bacterial strains, which led to its importance in emerging as a therapeutic for biofilm-related infections. NO is a reactive gas with a very short half-life with the ability to diffuse through the cell membranes spontaneously. Previous reports have shown that NO at lower concentrations can trigger the switch of sessile cells to free-floating planktonic phenotype in bacterial cells enclosed within the biofilm.[78] It is understood that the control of intracellular secondary messenger such as cyclic di-GMP by NO imitates the effectors which can hamper the biofilm buildup and disperse the mature biofilm. [79] The reactive nitrogen species from NO and the superoxide ions lower the extracellular polysaccharide production which is an important intermediary component for bacterial attachment on a substratum. The role of NO in facilitating biofilm dispersion is maintained across a wide range of bacterial species. [80] Activation of NO release from SNAP and other photo-responsive NO-releasing composite materials have been previously reported using visible and near-infrared LED lights.[81, 82 52] The advantage of RSNO's sensitivity to light can be exploited to control the amounts of NO released by modifying irradiation time and intensity of light from NO-releasing biocompatible polymer.

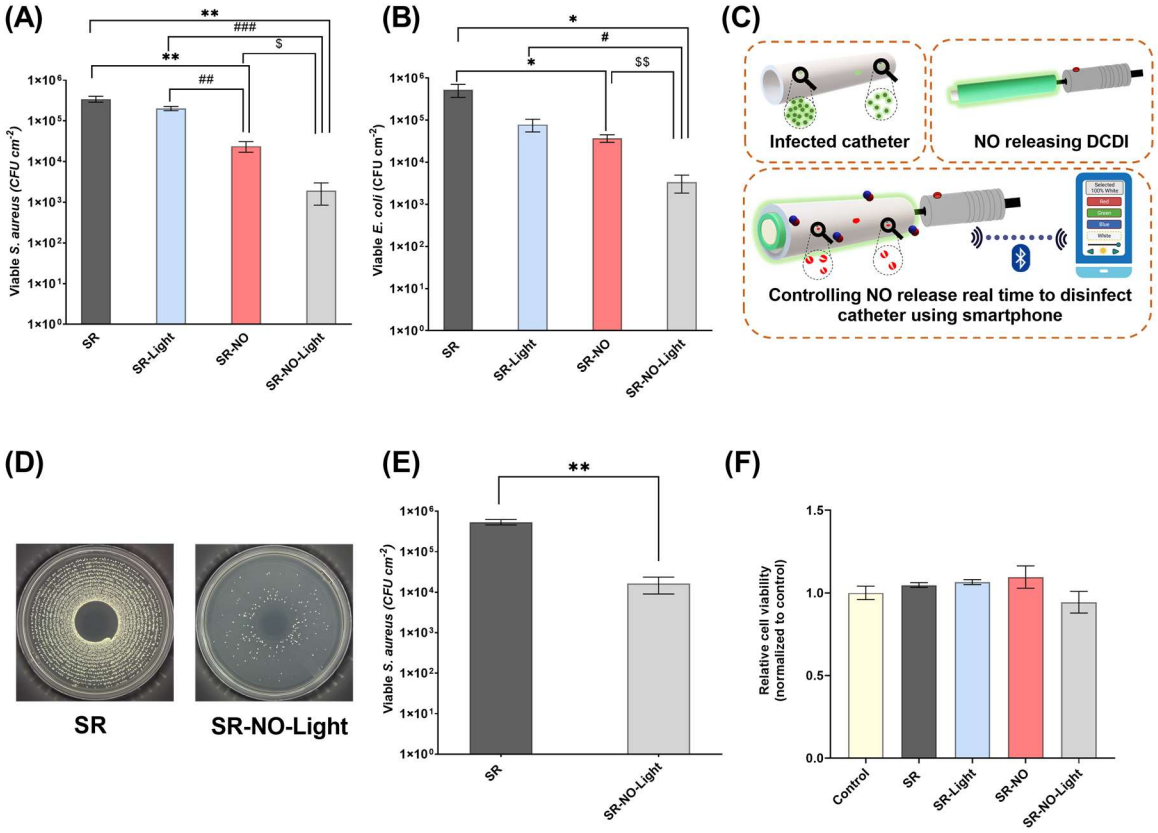

Figure 5.5. Antibacterial activity of the DCDI device calculated as a log of the colony forming units (CFU) cm^{-2} of surface area against: **(A)** *S. aureus;* ** represents $p \leq 0.01$, calculated for SR-NO, SR-NO-Light vs. SR, ## represents $p \leq 0.01$, calculated for SR-NO vs. SR-Light, ### represents $p \leq 0.001$, calculated for SR-NO-Light vs. Light, $ represents $p \leq 0.05$ calculated for SR-NO-Light vs. SR-NO; and **(B)** *E. coli;* * represents $p \leq 0.05$, calculated for SR-NO, SR-NO-light vs. SR, # represents $p \leq 0.05$, calculated for SR-NO-light vs. light, $$ represents $p \leq 0.01$ calculated for SR-NO-Light vs. SR-NO. **(C)** Design of *in situ* catheter disinfection experimental model. A model catheter is exposed to *S. aureus* bacteria for 24 h allowing the bacteria to adhere and proliferate, creating the pre-infected catheter surface. The DCDI is inserted within the catheter lumen and the adhered bacteria are dispersed via the photoinitiated NO release. **(D)** Representative images of LB agar plates with viable *S. aureus* bacteria CFU after 4 h of exposure to SR control and SR-NO-Light DCDI in the *in situ* catheter disinfection model. **(E)** *In situ* disinfection of a contaminated model catheter *with* DCDI calculated as a log of CFU cm^{-1} of catheter length against *S. aureus.* **(F)** Cytocompatibility of DCDI evaluated against 3T3 mouse fibroblast cell line relative to cell control in a 24 h cell viability assay using CCK-8 cell viability kit. All data are represented as mean ± SEM (n≥3).

The influence of light instantly releases NO from the polymer matrix proving the sensitivity of RSNOs to the photolytic feedback. Although, previous studies demonstrated the advantages of having strong control over the NO release levels,[83, 84] this work on development of the DCDI

device validates a practical and functional method to take advantage of the tunable photo-release properties of RSNOs for clinical catheter infection applications. The significant results from both the prevention of bacterial adhesion and *in situ* disinfection of pre-infected catheter surfaces support the significance of DCDI in reducing bacterial contamination on medical devices in clinical settings. The photoinitiated NO release from the DCDI is a potent and locally acting antimicrobial device that is biocompatible, low cost, shelf-stable, and easy to apply. These characteristics make it an ideal choice for integrating with medical devices such as catheters, where the disposable nature of the DCDI device will enable long-term applications of NO to the catheter surfaces both to prevent viable microbial adhesion on catheter surfaces and eradicate biofilms on catheter surfaces to reduce instances of CRBSIs. Therefore, the development of DCDI is expected to be a significant step towards preventing microbial contamination in both short- and long-term indwelling catheters that are regularly at a higher risk of contracting an infection (intravenous catheters, urinary catheters, insulin cannulas, peritoneal dialysis catheters, hemodialysis catheter, etc.), resulting in reduced morbidity, mortality, and associated healthcare costs.[85-87]

5.5.7 Cytocompatibility of DCDI

Over the years, eukaryotic cells have established mechanisms for scavenging the reactive oxygen and nitrogen species-mediated by NO which enables them to negate their influence; however, various microorganisms (bacteria and virus) remain vulnerable.[88] The combination of SNAP and light emitted from the DCDI provides broad-spectrum antimicrobial activity as described above. Nonetheless, it was crucial to determine the compatibility of engineered disinfection devices towards mammalian cells for effective *in vivo* application. To investigate this, the leachates collected over 24 h in DMEM media from the SR, SR-NO, SR-Light, and SR-NO-Light DCDI samples were added and incubated with NIH 3T3 mouse fibroblast cells for 24 h at 37 °C. The cell cytotoxicity assay was quantified using the CCK-8 cell viability kit. All the samples exhibited > 90% viability in the cells over 24 h (**Figure 5.5F)**. Experimental designs based on the

ISO standards have been previously used to demonstrate the biocompatibility of medical devices.[89] This data is consistent with prior studies that confirmed the biocompatibility of SNAP-based NO-releasing polymer both *in vitro* and *in vivo*.[90, 91] Together the results from these cytocompatibility studies offers encouraging evidence toward the potential biocompatibility of the light-induced DCDI.

5.6 Conclusions

To address the challenges associated with catheter-related bloodstream infections (CRBSIs), a simple, effective, smartphone-compatible universal Disposable Catheter Disinfection Insert (DCDI) was fabricated in this study that can both prevent and disinfect indwelling catheters (intravascular, urinary, etc.). The novel DCDI is comprised of a light-sensitive NO donor molecule, SNAP, impregnated in medical-grade silicone rubber tubing that is mounted on side glow fiber optic. In clinical practice, the DCDI would be attached to the catheter lumen cap and inserted within the lumen of the indwelling catheter. Once the DCDI is inserted, a light source would illuminate the side glow fiber optic by using a simple mobile phone application, providing tunable photoactivated NO release levels in real-time via modulation of light intensity. The modulation of light-activated NO release from the DCDI device can then be used to prevent catheter infections or inserted within an infected catheter to eradicate the colonized bacteria. Among the wavelengths and intensity of light emitted from the side glow fiber optics, the maximum photocatalytic activity of the DCDI releasing physiological NO levels from the SR-NO polymer occurred with the white light (mixture of red (620 nm), green (530 nm), blue (450 nm)) at 100% intensity as measured using a chemiluminescence NO analyzer. The antibacterial activity and biocompatibility of the DCDI with real-time control of NO release at physiological levels were also evaluated *in vitro*. The SR-NO-Light DCDI demonstrated broad-spectrum antibacterial activity eradicating >99% viable *S. aureus* (Gram-positive) and *E. coli* (Gram-negative) on the DCDI surface with just 4 h of exposure. Additionally, the insertion of DCDI in an infected model catheter resulted in 97%

eradication of *S. aureus* bacteria *in situ* exhibiting the potential to eradicate an established catheter infection. The insert presented in this study offers widespread compatibility with broad class of catheters used for biomedical applications. In some cases, this can also be applied for other industrial applications that use polymer tubings and require bacteria-free state for efficient function. The capacity of DCDI to be tuned for its NO release, ease of synthesis, antibacterial efficacy, biocompatibility, smartphone compatibility, and ability to sustain conventional hospital sterilization processes and long-term shelf-life stability at various storage conditions makes the DCDI device a promising new solution for the prevention and eradication of catheter-related infections without the need of complicated surgical interventions.

5.7 References

1. Giuliano, K. K., Intravenous Smart Pumps: Usability Issues, Intravenous Medication Administration Error, And Patient Safety. *Critic. Care Nurs. Clin.* **2018,** *30* (2), 215-224.

2. Wo, Y.; Brisbois, E. J.; Wu, J.; Li, Z.; Major, T. C.; Mohammed, A.; Wang, X.; Colletta, A.; Bull, J. L.; Matzger, A. J.; Xi, C.; Bartlett, R. H.; Meyerhoff, M. E., Reduction Of Thrombosis And Bacterial Infection Via Controlled Nitric Oxide (NO) Release From S-Nitroso-N-Acetylpenicillamine (SNAP) Impregnated Carbosil Intravascular Catheters. *ACS Biomater. Sci. Eng.* **2017,** *3* (3), 349-359.

3. Raad, I. I.; Bodey, G. P., Infectious Complications Of Indwelling Vascular Catheters. *Clin. Infect. Dis.* **1992**, 197-208.

4. Crnich, C. J.; Maki, D. G., The Promise Of Novel Technology For The Prevention Of Intravascular Device—Related Bloodstream Infection. I. Pathogenesis And Short-Term Devices. *Clin. Infect. Dis.* **2002,** *34* (9), 1232-1242.

5. Stamm, W. E., Infections Related To Medical Devices. *Annals Of Internal Medicine* **1978,** *89*, 764-769.

6. O'grady, N. P.; Alexander, M.; Burns, L. A.; Dellinger, E. P.; Garland, J.; Heard, S. O.; Lipsett, P. A.; Masur, H.; Mermel, L. A.; Pearson, M. L., Guidelines For The Prevention Of Intravascular Catheter-Related Infections. *Clin. Infect. Dis.* **2011,** *52* (9), E162-E193.

7. Maki, D. G.; Kluger, D. M.; Crnich, C. J. In The Risk Of Bloodstream Infection In Adults With Different Intravascular Devices: A Systematic Review Of 200 Published Prospective Studies, Mayo Clinic Proceedings, Elsevier: 2006; Pp 1159-1171.

8. Anaissie, E.; Samonis, G.; Kontoyiannis, D.; Costerton, J.; Sabharwal, U.; Bodey, G.; Raad, I., Role Of Catheter Colonization And Infrequent Hematogenous Seeding In Catheter-Related Infections. *Eur. J. Clin. Microbiol. Infect.* **1995,** *14* (2), 134-137.

9. Klevens, R. M.; Jonathan, R. E.; Chesley, L. R., Jr.; Teresa, C. H.; Robert, P. G.; Daniel, A. P.; Denise, M. C., Estimating Health Care-Associated Infections And Deaths In U.S. Hospitals, 2002. *Public Health Rep. (122)* **2007,** (2), 160-166.

10. Bryers, J. D., Medical Biofilms. *Biotechnol. Bioeng.* **2008,** *100* (1), 1-18.

11. Mermel, L. A.; Farr, B. M.; Sherertz, R. J.; Raad, I. I.; O'Grady, N.; Harris, J. S.; Craven, D. E., Guidelines For The Management Of Intravascular Catheter-Related Infections. *Clin. Infect. Dis.* **2001,** *32* (9), 1249-1272.

12. Rasmussen, T. B.; Givskov, M., Quorum-Sensing Inhibitors As Anti-Pathogenic Drugs. *Int. J. Med. Microbiol.* **2006,** *296* (2-3), 149-161.

13. Stewart, P. S.; William Costerton, J., Antibiotic Resistance Of Bacteria In Biofilms. *The Lancet* **2001,** *358* (9276), 135-138.

14. Dincer, S.; Uslu, F. M.; Delik, A., Antibiotic Resistance In Biofilm. *Bacterial Biofilms*, Intechopen: 2020.

15. Veenstra, D. L.; Saint, S.; Saha, S.; Lumley, T.; Sullivan, S. D., Efficacy Of Antiseptic-Impregnated Central Venous Catheters In Preventing Catheter-Related Bloodstream Infection: A Meta-Analysis. *Jama* **1999,** *281* (3), 261-267.

16. Politano, A. D.; Campbell, K. T.; Rosenberger, L. H.; Sawyer, R. G., Use Of Silver In The Prevention And Treatment Of Infections: Silver Review. *Surg. Infect.* **2013,** *14* (1), 8-20.

17. Osma, S.; Kahveci, Ş.; Kaya, F.; Akalın, H.; Özakın, C.; Yılmaz, E.; Kutlay, O., Efficacy Of Antiseptic-Impregnated Catheters On Catheter Colonization And Catheter-Related Bloodstream Infections In Patients In An Intensive Care Unit. *J. Hosp. Infect.* **2006,** *62* (2), 156-162.

18. Yu, K.; Lo, J. C.; Yan, M.; Yang, X.; Brooks, D. E.; Hancock, R. E.; Lange, D.; Kizhakkedathu, J. N., Anti-Adhesive Antimicrobial Peptide Coating Prevents Catheter Associated Infection In A Mouse Urinary Infection Model. *Biomaterials* **2017,** *116*, 69-81.

19. Ivanova, K.; Fernandes, M. M.; Mendoza, E.; Tzanov, T., Enzyme Multilayer Coatings Inhibit Pseudomonas Aeruginosa Biofilm Formation On Urinary Catheters. *Appl. Microbiol. Biotechnol.* **2015,** *99* (10), 4373-4385.

20. Simon, A.; Fahrendorf, W.; Hitschmann, G., Preclinical Evaluation Of Passive Disinfection Caps With A Long-Term Catheter For The Prevention Of Catheter-Related Bloodstream Infection In Pediatric Cancer Patients. *GMS Hygiene Infect. Contr.* **2021,** *16*.

21. Sauron, C.; Jouvet, P.; Pinard, G.; Goudreault, D.; Martin, B.; Rival, B.; Moussa, A., Using Isopropyl Alcohol Impregnated Disinfection Caps In The Neonatal Intensive Care Unit Can Cause Isopropyl Alcohol Toxicity. *Acta Paediatr.* **2015,** *104* (11), E489-E493.

22. O'Connell, S.; Dale, M.; Morgan, H.; Carter, K.; Carolan-Rees, G., Curos™ Disinfection Caps For The Prevention Of Infection When Using Needleless Connectors: A NICE Medical Technologies Guidance. *Appl. Health Econ. Health Pol.* **2021,** *19* (2), 145-153.

23. Kumeria, T.; Wang, J.; Chan, N.; Harris, T. J.; Sailor, M. J., Visual Sensor For Sterilization Of Polymer Fixtures Using Embedded Mesoporous Silicon Photonic Crystals. *ACS Sensors* **2018,** *3* (1), 143-150.

24. Wassil, S. K.; Crill, C. M.; Phelps, S. J., Antimicrobial Impregnated Catheters In The Prevention Of Catheter-Related Bloodstream Infection In Hospitalized Patients. *J. Pediatric Pharmacol. Therap.* **2007,** *12* (2), 77-90.

25. Raad, I.; Costerton, W.; Sabharwal, U.; Sadlowski, M.; Anaissie, E.; Bodey, G. P., Ultrastructural Analysis Of Indwelling Vascular Catheters: A Quantitative Relationship Between Luminal Colonization And Duration Of Placement. *J. Infect. Dis,* **1993,** *168* (2), 400-407.

26. Barraud, N.; Hassett, D. J.; Hwang, S.-H.; Rice, S. A.; Kjelleberg, S.; Webb, J. S., Involvement Of Nitric Oxide In Biofilm Dispersal Of Pseudomonas Aeruginosa. *J. Bacteriol.* **2006,** *188* (21), 7344-7353.

27. Chug, M. K.; Bachtiar, E.; Narwold, N.; Gall, K.; Brisbois, E. J., Tailoring Nitric Oxide Release With Additive Manufacturing To Create Antimicrobial Surfaces. *Biomater. Sci.* **2021**, 9 (8), pp. 3100-3111.

28. Carpenter, A. W.; Schoenfisch, M. H., Nitric Oxide Release: Part II. Therapeutic Applications. *Chem. Soc. Rev.* **2012,** *41* (10), 3742-3752.

29. Schairer, D. O.; Chouake, J. S.; Nosanchuk, J. D.; Friedman, A. J., The Potential Of Nitric Oxide Releasing Therapies As Antimicrobial Agents. *Virulence* **2012,** *3* (3), 271-279.

30. Hibbs Jr, J.; Taintor, R.; Vavrin, Z., Science **1987**, 235, 473− 476.

31. Vaughn, M. W.; Kuo, L.; Liao, J. C., Estimation Of Nitric Oxide Production And Reactionrates In Tissue By Use Of A Mathematical Model. *Am. J. Physiol. Heart Circ. Physiol.* **1998,** *274* (6), H2163-H2176.

32. Brisbois, E. J.; Davis, R. P.; Jones, A. M.; Major, T. C.; Bartlett, R. H.; Meyerhoff, M. E.; Handa, H., Reduction In Thrombosis And Bacterial Adhesion With 7 Day Implantation Of S-Nitroso-N-Acetylpenicillamine (SNAP)-Doped Elast-Eon E2As Catheters In Sheep. *J. Mater. Chem. B* **2015,** *3* (8), 1639-1645.

33. Feit, C.; Chug, M. K.; Brisbois, E. J., Development Of S-Nitroso-N-Acetylpenicillamine (SNAP) Impregnated Medical Grade Polyvinyl Chloride For Antimicrobial Medical Device Interfaces. *ACS Appl. Bio. Mat.* **2019**, 2 (10), pp. 4335-4345

34. Brisbois, E. J.; Handa, H.; Major, T. C.; Bartlett, R. H.; Meyerhoff, M. E., Long-Term Nitric Oxide Release And Elevated Temperature Stability With S-Nitroso-N-Acetylpenicillamine (SNAP)-Doped Elast-Eon E2As Polymer. *Biomaterials* **2013,** *34* (28), 6957-6966.

35. Brisbois, E. J.; Major, T. C.; Goudie, M. J.; Meyerhoff, M. E.; Bartlett, R. H.; Handa, H., Attenuation Of Thrombosis And Bacterial Infection Using Dual Function Nitric Oxide Releasing Central Venous Catheters In A 9 Day Rabbit Model. *Acta Biomater.* **2016,** *44*, 304-312.

36. Bryan, N. S., Nitric Oxide Enhancement Strategies. *Future Science OA* **2015,** *1* (1).

37. Reynolds, M. M.; Frost, M. C.; Meyerhoff, M. E., Nitric Oxide-Releasing Hydrophobic Polymers: Preparation, Characterization, And Potential Biomedical Applications. *Free Radical Biol. Med.* **2004,** *37* (7), 926-936.

38. Wo, Y.; Li, Z.; Colletta, A.; Wu, J.; Xi, C.; Matzger, A. J.; Brisbois, E. J.; Bartlett, R. H.; Meyerhoff, M. E., Study Of Crystal Formation And Nitric Oxide (NO) Release Mechanism From S-Nitroso-N-Acetylpenicillamine (SNAP)-Doped Carbosil Polymer Composites For Potential Antimicrobial Applications. *Composites, Part B* **2017,** *121*, 23-33.

39. Wood, P. D.; Mutus, B.; Redmond, R. W., The Mechanism Of Photochemical Release Of Nitric Oxide From S-Nitrosoglutathione. *Photochem. Photobiol.* **1996,** *64* (3), 518-524.

40. Chipinda, I.; Simoyi, R. H., Formation And Stability Of A Nitric Oxide Donor: S-Nitroso-N-Acetylpenicillamine. *J. Phys. Chem. B* **2006,** *110* (10), 5052-5061.

41. Singh, R. J.; Hogg, N.; Joseph, J.; Kalyanaraman, B., Mechanism Of Nitric Oxide Release From S-Nitrosothiols. *J. Biol. Chem.* **1996,** *271* (31), 18596-18603.

42. Yang, T.; Zelikin, A. N.; Chandrawati, R., Progress And Promise Of Nitric Oxide-Releasing Platforms. *Adv. Sci.* **2018,** *5* (6), 1701043.

43. Marazzi, M.; López-Delgado, A.; Fernández-González, M. A.; Castaño, O.; Frutos, L. M.; Temprado, M., Modulating Nitric Oxide Release By S-Nitrosothiol Photocleavage: Mechanism And Substituent Effects. *J. Phys. Chem. A* **2012,** *116* (26), 7039-7049.

44. Homeyer, K. H.; Singha, P.; Goudie, M. J.; Handa, H., S-Nitroso-N-Acetylpenicillamine Impregnated Endotracheal Tubes For Prevention Of Ventilator-Associated Pneumonia. *Biotechnol. Bioeng.* **2020**.

45. Colletta, A.; Wu, J.; Wo, Y.; Kappler, M.; Chen, H.; Xi, C.; Meyerhoff, M. E., S-Nitroso-N-Acetylpenicillamine (SNAP) Impregnated Silicone Foley Catheters: A Potential Biomaterial/Device To Prevent Catheter-Associated Urinary Tract Infections. *ACS Biomater. Sci. Eng.* **2015,** *1* (6), 416-424.

46. Chug, M. K.; Feit, C.; Brisbois, E. J., Increasing The Lifetime Of Insulin Cannula With Antifouling And Nitric Oxide Releasing Properties. *ACS Appl. Bio. Mat.* **2019**, 2 (12), pp. 5965-5975.

47. Brisbois, E. J.; Major, T. C.; Goudie, M. J.; Bartlett, R. H.; Meyerhoff, M. E.; Handa, H., Improved Hemocompatibility Of Silicone Rubber Extracorporeal Tubing Via Solvent Swelling-Impregnation Of S-Nitroso-N-Acetylpenicillamine (SNAP) And Evaluation In Rabbit Thrombogenicity Model. *Acta Biomater.* **2016,** *37*, 111-119.

48. Singha, P.; Pant, J.; Goudie, M. J.; Workman, C. D.; Handa, H., Enhanced Antibacterial Efficacy Of Nitric Oxide Releasing Thermoplastic Polyurethanes With Antifouling Hydrophilic Topcoats. *Biomater. Sci.* **2017,** *5* (7), 1246-1255.

49. Goudie, M. J.; Brisbois, E. J.; Pant, J.; Thompson, A.; Potkay, J. A.; Handa, H., Characterization Of An S-Nitroso-N-Acetylpenicillamine–Based Nitric Oxide Releasing Polymer From A Translational Perspective. *Int. J. Polym. Mater. Polym. Biomater.* **2016,** *65* (15), 769-778.

50. Pant, J.; Gao, J.; Goudie, M. J.; Hopkins, S. P.; Locklin, J.; Handa, H., A Multi-Defense Strategy: Enhancing Bactericidal Activity Of A Medical Grade Polymer With A Nitric Oxide Donor And Surface-Immobilized Quaternary Ammonium Compound. *Acta Biomater.* **2017,** *58*, 421-431.

51. Wo, Y.; Li, Z.; Brisbois, E. J.; Colletta, A.; Wu, J.; Major, T. C.; Xi, C.; Bartlett, R. H.; Matzger, A. J.; Meyerhoff, M. E., Origin Of Long-Term Storage Stability And Nitric Oxide Release Behavior Of Carbosil Polymer Doped With S-Nitroso-N-Acetyl-D-Penicillamine. *ACS Appl. Mater. Interfaces* **2015,** *7* (40), 22218-22227.

52. Lautner, G.; Stringer, B.; Brisbois, E. J.; Meyerhoff, M. E.; Schwendeman, S. P., Controlled Light-Induced Gas Phase Nitric Oxide Release From S-Nitrosothiol-Doped Silicone Rubber Films. *Nitric Oxide* **2019**.

53. Klubben, W. S.; Logunov, S. L.; Fewkes, E. J.; Mooney, J.; Then, P. M.; Wigley, P. G.; Schreiber, H.; Matias, K.; Wilson, C. J.; Ocampo, M. In *Novel Light Diffusing Fiber For Use In*

Medical Applications, Optical Fibers And Sensors For Medical Diagnostics And Treatment Applications XVI, International Society For Optics And Photonics: 2016; P 970218.

54. Liu, J.; Duan, Q.; Wang, J.; Song, Z.; Qiao, X.; Wang, H., Photocontrolled Nitric Oxide Release From Two Nitrosylruthenium Isomer Complexes And Their Potential Biomedical Applications. *J. Biomed. Opt.* **2015,** *20* (1), 015004.

55. Kim, C.; Diring, S.; Furukawa, S.; Kitagawa, S., Light-Induced Nitric Oxide Release From Physiologically Stable Porous Coordination Polymers. *Dalton Transactions* **2015,** *44* (34), 15324-15333.

56. Shen, Z.; He, K.; Ding, Z.; Zhang, M.; Yu, Y.; Hu, J., Visible-Light-Triggered Self-Reporting Release Of Nitric Oxide (NO) For Bacterial Biofilm Dispersal. *Macromolecules* **2019,** *52* (20), 7668-7677.

57. De Souza, G. F.; Taladriz-Blanco, P.; Velloso, L. A.; De Oliveira, M. G., Nitric Oxide Released From Luminal S-Nitroso-N-Acetylcysteine Increases Gastric Mucosal Blood Flow. *Molecules* **2015,** *20* (3), 4109-4123.

58. Kumar, R.; Massoumi, H.; Chug, M. K.; Brisbois, E. J., S-Nitroso-N-Acetyl-L-Cysteine Ethyl Ester (SNACET) Catheter Lock Solution To Reduce Catheter-Associated Infections. *ACS Appl. Mater. Interfaces* **2021**, 13 (22), pp. 25813-25824.

59. Hunter, R. A.; Schoenfisch, M. H., S-Nitrosothiol Analysis Via Photolysis And Amperometric Nitric Oxide Detection In A Microfluidic Device. *Anal. Chem.,* **2015,** *87* (6), 3171-3176.

60. Wo, Y.; Xu, L.-C.; Li, Z.; Matzger, A. J.; Meyerhoff, M. E.; Siedlecki, C. A., Antimicrobial Nitric Oxide Releasing Surfaces Based On S-Nitroso-N-Acetylpenicillamine Impregnated Polymers Combined With Submicron-Textured Surface Topography. *Biomater. Sci.* **2017,** *5* (7), 1265-1278.

61. Jones, M.; Weaver, A.; Weller, W., The Relative Effectiveness Of Some Chelating Agents As Antidotes In Acute Cadmium Poisoning. *Res. Commun. Chem. Pathol. Pharmacol.* **1978,** *22* (3), 581-588.

62. Brisbois, E. J.; Kim, M.; Wang, X.; Mohammed, A.; Major, T. C.; Wu, J.; Brownstein, J.; Xi, C.; Handa, H.; Bartlett, R. H.; Meyerhoff, M. E., Improved Hemocompatibility Of Multilumen Catheters Via Nitric Oxide (NO) Release From S-Nitroso-N-Acetylpenicillamine (SNAP) Composite Filled Lumen. *ACS Appl. Mater. Interfaces* **2016,** *8* (43), 29270-29279.

63. Dempsey, D. J.; Thirucote, R. R., Sterilization Of Medical Devices: A Review. *J. Biomater. App.* **1988,** *3* (3), 454-523.

64. Haitham, A.-S. D.; Ferro, A., S-Nitrosothiols: A Class Of Nitric Oxide-Donor Drugs. *Clinic. Sci.* **2000,** *98* (5), 507-520.

65. Mubarak, M. T.; Ozsahin, I.; Ozsahin, D. U. In *Evaluation Of Sterilization Methods For Medical Devices*, 2019 Advances In Science And Engineering Technology International Conferences (ASET), IEEE: 2019; Pp 1-4.

66. Aljamali, N. M.; Abdullabass, H. K.; Jawad, A. M.; Alfatlawi, I. O.; Jawd, S. M., Review On Types Of Automatic Sterilization Systems In Hospitals. *Int. J. Industr. Biotechnol. Biomat.* **2020,** *6* (1), 15-21p.

67. Weinstein, R. A.; Darouiche, R. O., Device-Associated Infections: A Macroproblem That Starts With Microadherence. *Clin. Infect. Dis.* **2001,** *33* (9), 1567-1572.

68. Mcmullen, K. M.; Smith, B. A.; Rebmann, T., Impact Of SARS-Cov-2 On Hospital Acquired Infection Rates In The United States: Predictions And Early Results. *Am. J. Infect. Control* **2020,** *48* (11), 1409-1411.

69. Hu, X.; Huang, Y.-Y.; Wang, Y.; Wang, X.; Hamblin, M. R., Antimicrobial Photodynamic Therapy To Control Clinically Relevant Biofilm Infections. *Front Microbiol.* **2018,** *9*, 1299.

70. Gad, F.; Zahra, T.; Hasan, T.; Hamblin, M. R., Effects Of Growth Phase And Extracellular Slime On Photodynamic Inactivation Of Gram-Positive Pathogenic Bacteria. *Antimicrob. Agents Chemother.* **2004,** *48* (6), 2173-2178.

71. Enwemeka, C. S.; Williams, D.; Hollosi, S.; Yens, D.; Enwemeka, S. K., Visible 405 Nm SLD Light Photo-Destroys Methicillin-Resistant Staphylococcus Aureus (MRSA) In Vitro. *Lasers Surg. Med.* **2008,** *40* (10), 734-737.

72. Lipovsky, A.; Nitzan, Y.; Gedanken, A.; Lubart, R., Visible Light-Induced Killing Of Bacteria As A Function Of Wavelength: Implication For Wound Healing. *Lasers Surg. Med.* **2010,** *42* (6), 467-472.

73. Méndez-Pfeiffer, P. A.; Soto Urzúa, L.; Sánchez-Mora, E.; González, A. L.; Romo-Herrera, J. M.; Gervacio Arciniega, J. J.; Martínez Morales, L. J., Damage On Escherichia Coli And Staphylococcus Aureus Using White Light Photoactivation Of Au And Ag Nanoparticles. *J. Appl. Phys.* **2019,** *125* (21), 213102.

74. Kim YS, S. M., Park JD, Et Al., Subchronic Oral Toxicity Of Silver Nanoparticles. . *Particle And Fibre Toxicology* **2010,** (7), 20.

75. Fang, F. C., Perspectives Series: Host/Pathogen Interactions. Mechanisms Of Nitric Oxide-Related Antimicrobial Activity. *J. Clin. Invest.* **1997,** *99* (12), 2818-2825.

76. Fang, F. C., Antimicrobial Reactive Oxygen And Nitrogen Species: Concepts And Controversies. *Nat. Rev. Microbiol.* **2004,** *2* (10), 820.

77. Wink, D. A.; Mitchell, J. B., Chemical Biology Of Nitric Oxide: Insights Into Regulatory, Cytotoxic, And Cytoprotective Mechanisms Of Nitric Oxide. *Free Radic. Biol. Med.* **1998,** *25* (4-5), 434-456.

78. Howlin, R. P.; Cathie, K.; Hall-Stoodley, L.; Cornelius, V.; Duignan, C.; Allan, R. N.; Fernandez, B. O.; Barraud, N.; Bruce, K. D.; Jefferies, J., Low-Dose Nitric Oxide As Targeted Anti-Biofilm Adjunctive Therapy To Treat Chronic Pseudomonas Aeruginosa Infection In Cystic Fibrosis. *Mol. Ther.* **2017,** *25* (9), 2104-2116.

79. Barraud, N.; Schleheck, D.; Klebensberger, J.; Webb, J. S.; Hassett, D. J.; Rice, S. A.; Kjelleberg, S., Nitric Oxide Signaling In Pseudomonas Aeruginosa Biofilms Mediates Phosphodiesterase Activity, Decreased Cyclic Di-GMP Levels, And Enhanced Dispersal. *J. Bacteriol.* **2009,** *191* (23), 7333-7342.

80. Zhu, X.; Oh, H.-S.; Ng, Y. C. B.; Tang, P. Y. P.; Barraud, N.; Rice, S. A., Nitric Oxide-Mediated Induction Of Dispersal In Pseudomonas Aeruginosa Biofilms Is Inhibited By Flavohemoglobin Production And Is Enhanced By Imidazole. *Antimicrob. Agents Chemother.* **2018,** *62* (3), e01832-17.

81. Lautner, G.; Meyerhoff, M. E.; Schwendeman, S. P., Biodegradable Poly(Lactic-Co-Glycolic Acid) Microspheres Loaded With S-Nitroso-N-Acetyl-D-Penicillamine For Controlled Nitric Oxide Delivery. *J. Control. Release.* **2016,** *225*, 133-139.

82. Mase, J. D.; Razgoniaev, A. O.; Tschirhart, M. K.; Ostrowski, A. D., Light-Controlled Release Of Nitric Oxide From Solid Polymer Composite Materials Using Visible And Near Infra-Red Light. *Photochem. Photobiol. Sci.* **2015,** *14* (4), 775-785.

83. Hopkins, S.; Frost, M., Synthesis And Characterization Of Controlled Nitric Oxide Release From S-Nitroso-N-Acetyl-D-Penicillamine Covalently Linked To Polyvinyl Chloride (SNAP-PVC). *Bioengineering* **2018,** *5* (3), 72.

84. Frost, M. C.; Meyerhoff, M. E., Controlled Photoinitiated Release Of Nitric Oxide From Polymer Films Containing S-Nitroso-N-Acetyl-DL-Penicillamine Derivatized Fumed Silica Filler. *J. Am. Chem. Soc.* **2004,** *126* (5), 1348-1349.

85. Weiner, L. M.; Webb, A. K.; Limbago, B.; Dudeck, M. A.; Patel, J.; Kallen, A. J.; Edwards, J. R.; Sievert, D. M., Antimicrobial-Resistant Pathogens Associated With Healthcare-Associated Infections: Summary Of Data Reported To The National Healthcare Safety Network At The Centers For Disease Control And Prevention, 2011–2014. *Infect. Control Hosp. Epidemiol.* **2016,** *37* (11), 1288-1301.

86. Saboo, B. D.; Talaviya, P. A., Continuous Subcutaneous Insulin Infusion: Practical Issues. *Indian J. Endocrinol. Metabol.* **2012,** *16* (Suppl 2), S259.

87. Allon, M.; Sexton, D. J., Tunneled Hemodialysis Catheter-Related Bloodstream Infections a prospective multicenter cohort study from Spain." *The Journal of Vascular Access,* **2012**, 13(2), 239-245.

88. Fang, F. C., Antimicrobial Actions Of Reactive Oxygen Species. *Mbio* **2011,** *2* (5).

89. ISO, I., 10993–5: 2009 Biological Evaluation Of Medical Devices—Part 5: Tests For In Vitro Cytotoxicity. *International Organization For Standardization, Geneva* **2009**.

90. Pant, J.; Goudie, M. J.; Hopkins, S. P.; Brisbois, E. J.; Handa, H., Tunable Nitric Oxide Release From S-Nitroso-N-Acetylpenicillamine Via Catalytic Copper Nanoparticles For Biomedical Applications. *ACS Appl. Mater. Interfaces* **2017,** *9* (18), 15254-15264.

91. Hopkins, S. P.; Pant, J.; Goudie, M. J.; Schmiedt, C.; Handa, H., Achieving Long-Term Biocompatible Silicone Via Covalently Immobilized S-Nitroso-N-Acetylpenicillamine (SNAP) That Exhibits 4 Months Of Sustained Nitric Oxide Release. *ACS Appl. Mater. Interfaces* **2018,** 10 (32), pp. 27316-27325

CHAPTER 6:

CONCLUSIONS AND FUTURE DIRECTIONS

6.1 Conclusions

Despite the promising physiological roles of nitric oxide (NO) in combating bacteria and biofilm, NO-releasing materials have not reached the stage of commercialization yet. This challenge of clinical translation can be linked to a lack of control over NO release, premature loss of NO donors during the high-temperature polymer extrusion process, restricted shelf-life stability, and inability to thwart fouling on surfaces. To overcome these challenges associated with NO-releasing materials, two important strategies have been presented in this dissertation that can control the NO release from biomedical materials and prevent biofouling on the biomedical device surface. The work done in this dissertation is the proof-of-concept that validates the principles of enhancing the potential of NO-releasing materials for clinical translation that can be further investigated with animal studies. The portions of introduction chapter are published as a review article in *ACS Materials Au* journal and featured as a cover.[1]

The presence of dead bacteria debris and protein accumulation on the surfaces have been linked to reduced device functionality and eventual biofilm formation. In Chapter 2, the methodology to prevent biofouling on NO-releasing biomedical materials was investigated. To reduce biofouling on medical device surfaces, NO-releasing silicone rubber polymer was combined with a passive antifouling strategy involving slippery surface technology via slippery silicone oil infusion. This material was applied and studied for insulin cannula applications, where it provided continuous NO release and an antifouling interface for > 14 d which also exhibited a significant reduction in protein and bacterial adhesion. This method of developing dual-function NO-releasing and antifouling surfaces for subcutaneous insulin infusion cannulas holds immense potential to reduce infection and inflammation associated with insulin pump delivery systems. This work has been published in the journal *ACS Applied Bio Materials*.[2]

Chapter 3 in the dissertation presents a unique strategy for generating dual-active antimicrobial medical device interfaces using NO and a broad-spectrum antiseptic called chlorhexidine diacetate (CHXD). Through a series of optimization, the most potent CHXD concentration on NO-releasing SR was finalized that posed no toxicity to mammalian cells. The dual-active NO-CHXD films were able to significantly reduce *E. coli* and *S. aureus* bacteria (> 3-log reduction) compared to controls with no explicit toxicity towards mouse fibroblast cells. As the initial time during the insertion of a medical implant is considered very crucial in defining the fate of the device, and the combination of two antimicrobial agents delivered from the materials interface is anticipated to greatly reduce the attachment of bacteria on surfaces and inhibit the initiation of infection. In longer-term medical devices, the corresponding physiologically relevant levels of NO from the device surface can then offer persistent antimicrobial action against microorganisms and maintain a biofilm-free state. This work has been published in the *Journal of Biomedical Materials Research Part A* and featured as a cover for the journal.[3]

In Chapter 4, a method to tune NO release via additive manufacturing has been presented. Additive manufacturing offers flexibility to custom-fabricate polymeric devices. This chapter studied the effect of tuning surface porosities in tunable NO donor loading and NO release. To overcome the challenge of premature loss of NO donors in the additive manufacturing process, a strategy to incorporate NO donors into 3D printed films was introduced via the solvent evaporation method. With the help of various characterization techniques, the NO donor loading, NO release, leaching, and change in porosity after NO donor impregnation was studied. Porous films had higher amounts of SNAP loading and correspondingly higher NO release over relatively longer durations. On the other hand, solid and capped films exhibited lower amounts of SNAP loading and relatively lower NO release levels. This difference can be attributed to the structure of the films where porous films had higher surface area and more surface exposure to soaking solution. However, due to the closed structure of solid and capped films, these films had lower exposure

to soaking buffer and less surface porosity which restricted the impregnated SNAP in coming in contact with the solution. The antibacterial studies resulted in >99% reduction in viable *S. aureus* bacteria on the surface of all the NO-releasing films as compared to unmodified control films demonstrating the potential for generating customized additively manufactured medical devices such as 3D-scaffolds, catheters, etc. This work has been published in the journal *Biomaterials Science*.[4]

Chapter 5 focuses on regulating NO release from the polymer in real-time via light activation using side glow fiber optic. This chapter demonstrated that light can be used as a catalytic agent to modulate NO release levels from the polymer using a simple Bluetooth-operated mobile phone application. The catalytic property of light to release NO from NO donor was used to design a disposable catheter disinfection insert (DCDI) that can prevent >99% viable bacterial adhesion and exterminate 97% of existing bacteria on catheter surfaces. To demonstrate the potential of clinical translation, the DCDI was examined for its compatibility with various clinically relevant sterilization techniques such as ethylene oxide and UV-light. The catheter insert developed in this study can be considered a universal antimicrobial solution for both short- and long-term catheter applications which costs < $5 in material and supply costs and demonstrates enhanced biocompatibility compared to current clinical regimens. This work has been published in the *Journal of Controlled Release* and featured as a cover for the journal.[5]

6.2 Future Directions

6.2.1 Screening of Slippery Surfaces for Long-term Storage and Antifungal Studies

In this dissertation, the antibacterial efficacy of NO-releasing biomedical devices was augmented by integrating NO-releasing surfaces with other active and passive antimicrobial strategies. In addition, the methodology to generate 3D-printed NO-releasing materials was demonstrated via solvent impregnation technique and the use of fiber optics to design a universal catheter disinfection insert. Results obtained from these studies underscore the potential of NO-

releasing materials for antibacterial applications. The combination of antifouling and NO-releasing surfaces has the benefit of preventing bacterial fouling aided with continuous antimicrobial action from passive and active interfaces, respectively. This approach can be critical in maintaining long-term medical devices that are prone to getting seriously infected (e.g., heart valves) or in extending the usage time of medical devices (e.g., insulin cannula). Moreover, the liquid-infused surface strategy can be extended to the application of urinary catheters or extracorporeal circuits where the presence of proteins, electrolytes, and platelet adhesion and subsequent activation on the surface may occlude the efficient operation of the device. Great attention has been centered on assessing the function of liquid-infused NO-releasing surfaces against the attachment of Gram-positive and Gram-negative bacteria. However, in practical scenarios, the biofilm formation process may comprise microbial cells including algal, fungal, and bacterial species. Previous studies have shown that NO-releasing surfaces are relatively less effective against fungi (*C. albicans*) with ≈ 65% reduction in viability on PDMS surfaces as opposed to > 80% reduction in bacterial (*S. aureus* and *E. coli*) viability.[6] Therefore, it is noteworthy to evaluate the compatibility of liquid-infused NO-releasing surfaces with various fungal and clinically isolated antibiotic-resistant species to successfully translate these materials for clinical use in patients. Additionally, these materials are yet to be investigated for their long-term storage (6-12 months) at various temperatures and compatibility with different hospital-based sterilization methods before they could be used in patients.

6.2.2 Exploration of Long-term Dual-Active Antimicrobial Surfaces

Similarly, CHXD in combination with silver sulfadiazine is currently clinically used in indwelling catheters to eradicate bacterial infections originating from biomedical devices.[7] However, these commercial surfaces lack mechanisms to address other clinical challenges associated with medical devices, such as thrombosis and inflammation. Moreover, elevated concentrations of silver-based technologies can prove cytotoxic to local mammalian tissue and may fail to

exterminate bacteria encapsulated within the biofilm.[8, 9] The combination of CHXD and NO is a promising combinational approach not just pertaining to stronger antibacterial action and biofilm prevention on medical devices, but also to other biocompatibility challenges, including clotting and foreign body response (inflammation). Although, these types of approaches can prove highly beneficial to prevent an early onslaught of infection, the reservoir of both antimicrobials (NO and CHXD) is bound to deplete over time. Future studies focusing on dual-active surfaces should incorporate mechanisms of long-term NO-releasing/generating surfaces that deals with longevity limitations for prolonged usage. This can involve increasing the payload of CHXD/NO donor in the polymer matrix, conjugating antimicrobials to the polymer backbone that can reduce the untimely leaching and provide sustained release or incorporation of NO generating compounds (e.g., Cu, Se) that can generate NO from endogenous *S*-nitrosothiols (RSNO) present in the blood such as *S*-Nitrosoglutathione (GSNO). More importantly, this work can also be extended to fabricating dual-active medical devices involving various broad-spectrum antibiotics and antifungal agents that can eliminate the infection-causing bacterial and fungal species.

6.2.3 Development of Hemocompatible and Clinically Relevant Size 3D-Printed Medical Devices

In addition, the 3D-printing method can be used to tune surface porosities to fabricate customized medical devices with NO-releasing and antibacterial traits. RSNO-incorporated materials may face difficulties in potential clinical applications because of their thermal instability at elevated temperatures used during the polymer extrusion process. The solvent swelling technique used here provides a solution to incorporate NO donor into the device post-fabrication such that the donor is protected from premature loss upon exposure to higher temperatures during 3D printing. As a follow-up project to current work, polymer films with varying porosities presented in the study can be studied for their specific applications. For instance, more porous films can be used for stent, drug delivery or even 3D-scaffold applications. Future studies intending to use the

additively manufactured NO-releasing devices should investigate properties specific to the application of the device e.g., blood-compatibility, hemolysis, platelet adhesion and activation etc., for blood contacting materials. For solid and capped films involving catheter-like applications it is essential to investigate the mechanical properties of the material after NO donor incorporation, viability of adhered bacteria on the inside vs. outside the catheter surface under flow conditions for longer incubation hours that closely mimic the end-use application of the device and optimize the interior porous structures in capped films to increase the NO reservoir in the polymer. For effective clinical translation, catheters with clinically applicable length should be manufactured and evaluated for their efficacy *in vivo*. This work can be extended to utilizing other type of NO donors impregnated or immobilized on the variety of polymer surfaces or can also be studied with catalyzing agents and antifouling strategies. For the current study, ChronoSil was selected as a model polymer that demonstrated proof-of-concept, nevertheless, other polymer types commonly used in medical device fabrication can be studied for their compatibility with 3D-printing process and NO donor incorporation.

6.2.4 Optimization of DCDI for Portability and Controlled Leaching

Nitric oxide release from SNAP-incorporated materials can be enhanced using photocatalysis. Chapter 5 of the dissertation successfully demonstrates how light wavelength and intensity can be used to alter the NO release from SNAP-impregnated polymer. Results obtained from the UV-Vis characterization showed that the introduction of light to SNAP polymer enhances the rate of NO release from the donor in the soaking buffer (**Figure 5.4**). The DCDI presented in Chapter 5 is a first-generation antibacterial catheter insert that releases NO on-demand using a Bluetooth-operated device. This insert is, however, restricted in terms of the amount of SNAP impregnated into the polymer matrix, as well as the leaching of SNAP from polymer over time which directly impacts the duration of NO release. Blue light between 400–450 nm wavelength is widely known to cause irreversible damage to bacterial proteins and DNA.[10] A Versalume wearable module with

blue light can emit light in 450 nm wavelength spectra.[11] Therefore, future studies with DCDI can involve the use of covalently conjugated SNAP to PDMS polymer (**Figure 6.1**) as a coating for fiber optics connected to the commercial Versalume light module for generating battery-operated disposable catheter disinfection insert.[11] While the conjugated SNAP can provide control over leaching and higher initial SNAP content (as opposed to the impregnation process studied in this dissertation), the battery-operated module will enable the portability of disinfection insert in patients with short-and long-term catheter applications. Conjugating the NO donor SNAP with hydrophobic polymers like PDMS and PVC has been reported to significantly reduce leaching which consequently prolongs the NO release from the polymer.[12, 13] This covalent immobilization of SNAP on PDMS polymer can be achieved via conjugation to the aminosilane cross-linker in the PDMS polymer. Previous studies have shown the enhancement in the NO release levels *in vitro* longevity with a stable and exceptional NO release for 125 d under physiological conditions.[12] Due to the intramolecular hydrogen bonding between SNAP molecules, covalent conjugation of SNAP to polymer, and the low water uptake of hydrophobic polymers, SNAP dissolution and dissemination out of the PDMS polymer is significantly contained.[14]

The NO-releasing light insert proposed in this study can be used as a universally applicable catheter disinfection insert that can be employed across various catheters with varying lengths,

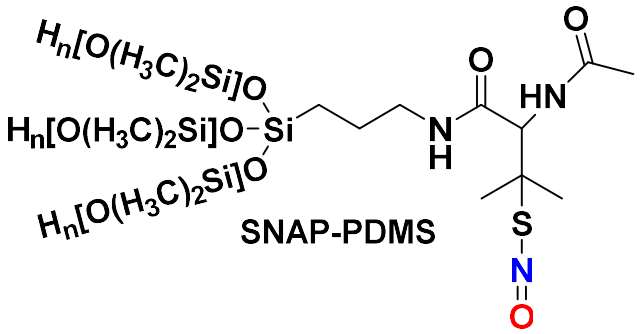

Figure 6.1 Structure of *S*-nitroso-*N*-acetyl-penicillamine covalently conjugated to hydroxy-terminated Polydimethylsiloxane (PDMS) polymer resulting in SNAP-PDMS molecule.

diameters, and/or materials. Chapter 5 confirmed the compatibility of the insert with the CVC catheter model where the insert can be a part of the catheter between the clinical administration of fluids and drugs. In this study, silicone rubber/PDMS was chosen as the platform to demonstrate the excellent capacity of the insert due to the inherent permeation of NO through silicone rubber catheter. Catheters come in varied sizes, with distinct diameters, wall lengths, and materials, future studies must assess the effect of materials (e.g., silicone rubber vs. other polyurethanes), diameters of commercial catheters vs. the size of DCDI in terms of NO transport to the interior and exterior of catheter surfaces, and optimization of the effective length of DCDI within the catheter lumen for clinical translation of this technology. Previous studies have shown the compatibility of NO chemistry with various polymers such as polyurethanes, E2As, polyvinyl chloride that release NO over extended period of time.[15-17] The diffusion of NO through extensive range of polymers inspires these studies to determine the broad effectiveness of DCDI on different catheters. Notably, Meyerhoff group has recently demonstrated even a short GSNO-based insert attached onto the hub region cap of catheters with localized NO release can dramatically reduce the bacteria on the full length of the catheter in a 14-d sheep model.[18] The versatility of the NO-releasing antibacterial DCDI is expected to lower the burden of catheter-related infections on biomedical devices that can also be applied to other industrial uses that involve polymer tubing and need clean surfaces for efficient operation.

6.2.5 Additional Fundamental Biocompatibility Studies

The role of NO in eradication of bacteria has been well understood with both *in vitro* and *in vivo* studies conducted over the past years. However, the challenge of determining the precise amounts of NO levels required to exterminate bacteria while maintaining therapeutic efficacy and biocompatibility is yet to be answered. The human body utilizes NO at > 1 μM concentration to tackle the invading pathogen via generating reactive oxygen and nitrogen species that destroy the DNA, thwart protein functions and lead to lipid peroxidation of membranes in bacteria.[19] Since

nitric oxide is a hydrophobic gas, it tends to be more attractive toward the lipid membranes and hydrophobic regions of membrane proteins.[20] Polymer surfaces with NO-releasing capacity have been shown to emulate NO levels similar to endothelial cells that release NO at a surface flux of 0.5 - 4 x 10^{-10} mol cm^{-2} min^{-1}, which can inhibit platelet adhesion and activation.[21] While materials at or above physiological levels of NO release have shown to exhibit broad-spectrum antibacterial properties (> 80% reduction in viability), materials with NO release levels below physiological levels (~0.1 x 10^{-10} mol cm^{-2} min^{-1}) have also been demonstrated to lower the viability of *S. aureus* adhesion on the surface by ~60%.[12] Moreover, bacterial biofilms when exposed to low amounts of NO can transition from biofilm to planktonic state which makes them significantly more susceptible to the action of antimicrobial agents.[22] Although many studies have focused on designing materials with physiologically-relevant levels of NO, not much has been researched on the influence of NO at higher flux levels. Moreover, the correlation of NO release levels on mammalian cell viability and antimicrobial action considerably above physiological levels is not fully understood. Nitric oxide can prove cytotoxic to the body at extremely high concentrations which makes it a critical component of designing NO releasing surfaces in the biomaterials field. Since, introduction of light to SNAP-PDMS is anticipated to elevate the levels of NO flux from insert, it is crucial to determine the threshold of NO needed for efficacy vs. toxicity which is essential for enhancing clinical value such that material exhibits potent antimicrobial properties while retaining its biocompatibility. Prior literature has demonstrated the success of NO-releasing biomedical materials in both short- and long-term animal models,[23, 24] however, the studies reported in this dissertation are yet to be evaluated for their *in vivo* performance. Furthermore, to efficiently translate these strategies for clinical use in patients, it is crucial to create scalable methods for clinically applicable size medical devices, which are commercially viable, easy to produce, well-prepared for the regulatory process, and solve microbial challenges.

To overcome the challenge of pathogen propagation on medical device surfaces and improve the antibacterial efficacy of medical devices, various antimicrobial approaches including silver-doped catheters, incorporation of antibiotics, or antimicrobial peptide coatings to inhibit the invasion of bacterial cells on materials have been explored in the literature.[25-29] Similarly, IV line devices with antimicrobial activity against broad strains of bacterial and fungal species via alcohol infusion have been reported in the literature.[30-33] Despite their progress to clinical translation and commercialization, many of these strategies are limited to acting against free-floating bacteria and tend to fail against mature biofilms. NO-based antibacterial therapy is considered superior and envisioned to eradicate bacteria present in both the planktonic phase and as well as biofilm phase, as the gaseous nature of NO allows deeper penetration of NO into the EPS matrix where many broad-spectrum antibiotics and metal ions fail to infiltrate.

Summary

In summary, this dissertation work demonstrates that having another active and passive mechanism to either prevent fouling (passive) or increase antimicrobial efficacy using other antimicrobial strategies (active) can synergistically enhance the antimicrobial properties of NO-releasing surfaces. While NO with other active strategies can prove a superior and well-suited solution for short-term medical device applications as the antimicrobial moieties will be exhausted over time, the presence of passive technology with NO can prevent the accumulation of biological debris and provide an antifouling and antibacterial interface for medical devices over longer durations. Alternatively, using additive manufacturing and light active NO release can help in modulating NO release from materials for improving biocompatibility and antimicrobial properties. The data presented in this dissertation suggest the promising potential of NO-releasing surfaces for the production of antibacterial and antifouling medical devices. For effective clinical translation, it is imperative to design commercially viable and scalable methods that can be applied to clinically

relevant size biomedical devices, avoid complexity, are relatively easy to manufacture, and most importantly should be able to satisfy the regulatory guidelines.

6.3 References

1. Chug, M. K.; Brisbois, E. J., Recent Developments In Multifunctional Antimicrobial Surfaces And Applications Toward Advanced Nitric Oxide-Based Biomaterials. *ACS Materials Au* **2022,** *2* (5), 525-551.

2. Chug, M. K.; Feit, C.; Brisbois, E. J., Increasing The Lifetime Of Insulin Cannula With Antifouling And Nitric Oxide Releasing Properties. *ACS Appl. Bio. Mat.* **2019**, *2*(12), Pp.5965-5975.

3. Chug, M. K.; Massoumi, H.; Wu, Y.; Brisbois, E. J., Prevention Of Medical Device Infections Via Multi-Action Nitric Oxide And Chlorhexidine Diacetate Releasing Medical Grade Silicone Biointerfaces. *J. Biomed. Mater. Res. A* **2022,** *110* (6), 1263-1277.

4. Chug, M. K.; Bachtiar, E.; Narwold, N.; Gall, K.; Brisbois, E. J., Tailoring Nitric Oxide Release With Additive Manufacturing To Create Antimicrobial Surfaces. *Biomater. Sci.* **2021**, 9 (8), 3100– 3111.

5. Chug, M. K.; Brisbois, E., Smartphone Compatible Nitric Oxide Releasing Insert To Prevent Catheter-Associated Infections. *J. Control. Release* **2022**, S0168-3659 (22) 00385.

6. Devine, R.; Douglass, M.; Ashcraft, M.; Tayag, N.; Handa, H., Development Of Novel Amphotericin B-Immobilized Nitric Oxide-Releasing Platform For The Prevention Of Broad-Spectrum Infections And Thrombosis. *ACS Appl. Mater. Interfaces* **2021,** *13* (17), 19613-19624.

7. Wassil, S. K.; Crill, C. M.; Phelps, S. J., Antimicrobial Impregnated Catheters In The Prevention Of Catheter-Related Bloodstream Infection In Hospitalized Patients. *J. Pediatric Pharmacol. Therap.* **2007,** *12* (2), 77-90.

8. De Lima, R.; Seabra, A. B.; Durán, N., Silver Nanoparticles: A Brief Review Of Cytotoxicity And Genotoxicity Of Chemically And Biogenically Synthesized Nanoparticles. *Journal Of Applied Toxicology* **2012,** *32* (11), 867-879.

9. Lansdown, A.; Williams, A., Bacterial Resistance To Silver-Based Antibiotics. *Nursing Times* **2007,** *103* (9), 48-49.

10. Gwynne, P. J.; Gallagher, M. P., Light As A Broad-Spectrum Antimicrobial. *Front Microbiol.* **2018,** *9*, 119.

11. Galatus, R. M.; Papara, R.; Buzura, L.; Roman, A.; Ursu, T. In *Wearable Multi-Sensor For Plant Monitoring, Based On Fluorescent Fibers*, Biophotonics In Point-Of-Care, Spie: 2020; Pp 40-45.

12. Hopkins, S. P.; Pant, J.; Goudie, M. J.; Schmiedt, C.; Handa, H., Achieving Long-Term Biocompatible Silicone Via Covalently Immobilized S-Nitroso-N-Acetylpenicillamine (SNAP) That Exhibits 4 Months Of Sustained Nitric Oxide Release. *ACS Appl. Mater. Interfaces* **2018,** 10 (32), pp. 27316-27325.

13. Hopkins, S.; Frost, M., Synthesis And Characterization Of Controlled Nitric Oxide Release From S-Nitroso-N-Acetyl-D-Penicillamine Covalently Linked To Polyvinyl Chloride (Snap-Pvc). *Bioengineering* **2018,** *5* (3), 72.

14. Wo, Y.; Li, Z.; Brisbois, E. J.; Colletta, A.; Wu, J.; Major, T. C.; Xi, C.; Bartlett, R. H.; Matzger, A. J.; Meyerhoff, M. E., Origin Of Long-Term Storage Stability And Nitric Oxide Release Behavior Of Carbosil Polymer Doped With S-Nitroso-N-Acetyl-D-Penicillamine. *ACS Appl. Mater. Interfaces* **2015,** *7* (40), 22218-22227.

15. Singha, P.; Pant, J.; Goudie, M. J.; Workman, C. D.; Handa, H., Enhanced Antibacterial Efficacy Of Nitric Oxide Releasing Thermoplastic Polyurethanes With Antifouling Hydrophilic Topcoats. *Biomater. Sci.* **2017,** *5* (7), 1246-1255.

16. Pant, J.; Goudie, M. J.; Chaji, S. M.; Johnson, B. W.; Handa, H., Nitric Oxide Releasing Vascular Catheters For Eradicating Bacterial Infection. *J. Biomed. Mater. Res. B* **2018,** *106* (8), 2849-2857.

17. Homeyer, K. H.; Goudie, M. J.; Singha, P.; Handa, H., Liquid-Infused Nitric-Oxide-Releasing Silicone Foley Urinary Catheters For Prevention Of Catheter-Associated Urinary Tract Infections. *ACS Biomater. Sci. Eng.* **2019,** *5* (4), 2021-2029.

18. Doverspike, J. C.; Mack, S. J.; Luo, A.; Stringer, B.; Reno, S.; Cornell, M. S.; Rojas-Pena, A.; Wu, J.; Xi, C.; Yevzlin, A., Nitric Oxide-Releasing Insert For Disinfecting The Hub Region Of Tunnel Dialysis Catheters. *ACS Appl. Mater. Interfaces* **2020,** *12* (40), 44475-44484.

19. Weinberg, J.; Misukonis, M.; Shami, P.; Mason, S.; Sauls, D.; Dittman, W.; Wood, E.; Smith, G.; Mcdonald, B.; Bachus, K., Human Mononuclear Phagocyte Inducible Nitric Oxide Synthase (Inos): Analysis Of Inos Mrna, Inos Protein, Biopterin, And Nitric Oxide Production By Blood Monocytes And Peritoneal Macrophages. *Blood* **1995,** *86* (3), 1184-1195.

20. Goss, S. P.; Singh, R. J.; Hogg, N.; Kalyanaraman, B., Reactions Of· No,· No2 And Peroxynitrite In Membranes: Physiological Implications. *Free Radical Research* **1999,** *31* (6), 597-606.

21. Vaughn, M. W.; Kuo, L.; Liao, J. C., Estimation Of Nitric Oxide Production And Reactionrates In Tissue By Use Of A Mathematical Model. *Am. J. Physiol. Heart Circ. Physiol.* **1998,** *274* (6), H2163-H2176.

22. Barraud, N.; Storey, M. V.; Moore, Z. P.; Webb, J. S.; Rice, S. A.; Kjelleberg, S., Nitric Oxide-Mediated Dispersal In Single-And Multi-Species Biofilms Of Clinically And Industrially Relevant Microorganisms. *Microbial Biotechnology* **2009,** *2* (3), 370-378.

23. Brisbois, E. J.; Davis, R. P.; Jones, A. M.; Major, T. C.; Bartlett, R. H.; Meyerhoff, M. E.; Handa, H., Reduction In Thrombosis And Bacterial Adhesion With 7 Day Implantation Of S-Nitroso-N-Acetylpenicillamine (Snap)-Doped Elast-Eon E2as Catheters In Sheep. *J. Mater. Chem. B* **2015,** *3* (8), 1639-1645.

24. Douglass, M.; Hopkins, S.; Chug, M. K.; Kim, G.; Garren, M. R.; Ashcraft, M.; Nguyen, D. T.; Tayag, N.; Handa, H.; Brisbois, E. J., Reduction In Foreign Body Response And Improved Antimicrobial Efficacy Via Silicone-Oil-Infused Nitric-Oxide-Releasing Medical-Grade Cannulas. *ACS Appl. Mater. Interfaces* **2021,** *13* (44), 52425-52434.

25. Veenstra, D. L.; Saint, S.; Saha, S.; Lumley, T.; Sullivan, S. D., Efficacy Of Antiseptic-Impregnated Central Venous Catheters In Preventing Catheter-Related Bloodstream Infection: A Meta-Analysis. *Jama* **1999,** *281* (3), 261-267.

26. Politano, A. D.; Campbell, K. T.; Rosenberger, L. H.; Sawyer, R. G., Use Of Silver In The Prevention And Treatment Of Infections: Silver Review. *Surg. Infect.* **2013,** *14* (1), 8-20.

27. Osma, S.; Kahveci, Ş.; Kaya, F.; Akalın, H.; Özakın, C.; Yılmaz, E.; Kutlay, O., Efficacy Of Antiseptic-Impregnated Catheters On Catheter Colonization And Catheter-Related Bloodstream Infections In Patients In An Intensive Care Unit. *J. Hosp. Infect.* **2006,** *62* (2), 156-162.

28. Yu, K.; Lo, J. C.; Yan, M.; Yang, X.; Brooks, D. E.; Hancock, R. E.; Lange, D.; Kizhakkedathu, J. N., Anti-Adhesive Antimicrobial Peptide Coating Prevents Catheter Associated Infection In A Mouse Urinary Infection Model. *Biomaterials* **2017,** *116*, 69-81.

29. Ivanova, K.; Fernandes, M. M.; Mendoza, E.; Tzanov, T., Enzyme Multilayer Coatings Inhibit Pseudomonas Aeruginosa Biofilm Formation On Urinary Catheters. *Appl. Microbiol. Biotechnol.* **2015,** *99* (10), 4373-4385.

30. Simon, A.; Fahrendorf, W.; Hitschmann, G., Preclinical Evaluation Of Passive Disinfection Caps With A Long-Term Catheter For The Prevention Of Catheter-Related Bloodstream Infection In Pediatric Cancer Patients. *GMS Hygiene And Infection Control* **2021,** *16*.

31. Sauron, C.; Jouvet, P.; Pinard, G.; Goudreault, D.; Martin, B.; Rival, B.; Moussa, A., Using Isopropyl Alcohol Impregnated Disinfection Caps In The Neonatal Intensive Care Unit Can Cause Isopropyl Alcohol Toxicity. *Acta Paediatr.* **2015,** *104* (11), E489-E493.

32. O'connell, S.; Dale, M.; Morgan, H.; Carter, K.; Carolan-Rees, G., Curos™ Disinfection Caps For The Prevention Of Infection When Using Needleless Connectors: A Nice Medical Technologies Guidance. *Appl. Health Econ. Health Pol.* **2021,** *19* (2), 145-153.

33. Kumeria, T.; Wang, J.; Chan, N.; Harris, T. J.; Sailor, M. J., Visual Sensor For Sterilization Of Polymer Fixtures Using Embedded Mesoporous Silicon Photonic Crystals. *ACS Sensors* **2018,** *3* (1), 143-150.